

University of Montana

ScholarWorks at University of Montana

Graduate Student Theses, Dissertations, &
Professional Papers

Graduate School

2002

Synthesis and reactivity of electron deficient benzoheterocycle triosmium complexes

Md. Joynal Abedin

The University of Montana

Follow this and additional works at: <https://scholarworks.umt.edu/etd>

Let us know how access to this document benefits you.

Recommended Citation

Abedin, Md. Joynal, "Synthesis and reactivity of electron deficient benzoheterocycle triosmium complexes" (2002). *Graduate Student Theses, Dissertations, & Professional Papers*. 9443.
<https://scholarworks.umt.edu/etd/9443>

This Dissertation is brought to you for free and open access by the Graduate School at ScholarWorks at University of Montana. It has been accepted for inclusion in Graduate Student Theses, Dissertations, & Professional Papers by an authorized administrator of ScholarWorks at University of Montana. For more information, please contact scholarworks@mso.umt.edu.

INFORMATION TO USERS

This manuscript has been reproduced from the microfilm master. UMI films the text directly from the original or copy submitted. Thus, some thesis and dissertation copies are in typewriter face, while others may be from any type of computer printer.

The quality of this reproduction is dependent upon the quality of the copy submitted. Broken or indistinct print, colored or poor quality illustrations and photographs, print bleedthrough, substandard margins, and improper alignment can adversely affect reproduction.

In the unlikely event that the author did not send UMI a complete manuscript and there are missing pages, these will be noted. Also, if unauthorized copyright material had to be removed, a note will indicate the deletion.

Oversize materials (e.g., maps, drawings, charts) are reproduced by sectioning the original, beginning at the upper left-hand corner and continuing from left to right in equal sections with small overlaps.

ProQuest Information and Learning
300 North Zeeb Road, Ann Arbor, MI 48106-1346 USA
800-521-0600

UMI[®]



**Maureen and Mike
MANSFIELD LIBRARY**

The University of

Montana

Permission is granted by the author to reproduce this material in its entirety, provided that this material is used for scholarly purposes and is properly cited in published works and reports.

****Please check "Yes" or "No" and provide signature****

Yes, I grant permission

Yes

No, I do not grant permission

Author's Signature: Med. Jamal Abedin

Date: 8/30/02

Any copying for commercial purposes or financial gain may be undertaken only with the author's explicit consent.

**Synthesis and Reactivity of Electron Deficient
Benzoheterocycle Triosmium Complexes**

By

Md. Joynal Abedin

M.Sc., Jahangirnagar University, Savar, Dhaka, Bangladesh

Presented in partial fulfillment of the requirements

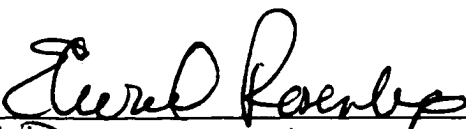
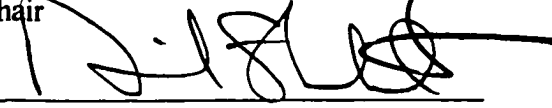
for the degree of Doctor of philosophy

Department of Chemistry

The University of Montana

2002

Approved by


Chair

Dean, Graduate School

9-5-02

Date

UMI Number: 3062636

Copyright 2002 by
Abedin, Md. Joynal

All rights reserved.

UMI[®]

UMI Microform 3062636

Copyright 2002 by ProQuest Information and Learning Company.
All rights reserved. This microform edition is protected against
unauthorized copying under Title 17, United States Code.

ProQuest Information and Learning Company
300 North Zeeb Road
P.O. Box 1346
Ann Arbor, MI 48106-1346

Synthesis and Reactivity of Electron Deficient Benzoheterocycle Triosmium Complexes

Director: Edward Rosenberg

Abstract



A series of electron deficient benzoheterocycle complexes, $\text{Os}_3(\text{CO})_9(\mu_3\text{-}\eta^2\text{-L-H})(\mu\text{-H})$ (L = Phenanthridine, **29**; 2-methylbenzimidazole, **32**; 2,3- dimethylbenzimidazole, **71**; 2-methylbenzotriazole, **33**, benzoxazole, **37**; 2-methylbenzoxazole, **38**; benzothiazole, **39**; 2-methylbenzothiazole, **40**; quinoxaline, **43** and 2-methylquinoxaline, **66**) of triosmium carbonyl were synthesized. These complexes possess a special $\mu_3\text{-}\eta^2$ - bonding mode at the C(7) or C(8)-position of the carbocyclic ring and a protective coordination of the nitrogen atom to the metal core which changes the normal reactivity of these benzoheterocycles. Sequential reactions of these complexes with H^-/H^+ have been studied. Complexes of phenanthridine and other benzoheterocycles with an alkyl group at the C(2) or C(3)-positions of the heterocyclic ring such as, 2-methylbenzimidazole, 2,3-dimethylbenzimidazole, 2-methylbenzothiazole, 2-methylbenzothiazole, 2-methylquinoxaline undergo regioselective nucleophilic addition reactions at the carbocyclic ring to form $\sigma\text{-}\pi$ vinyl complexes. For 2-methylbenzoxazole nucleophilic addition reaction occurs at the 2-position of the heterocyclic ring to give a ring opened $\sigma\text{-}\pi$ vinyl complex. Electron deficient complexes without an alkyl at the heterocyclic ring undergo hydride attack at the C(2)-position of the heterocyclic ring followed by protonation at the metal core to form dihydride complexes.

The studies of these complexes with relatively bulky carbon based nucleophiles show that complexes with or without an alkyl group at the heterocyclic ring all go regioselective nucleophilic addition reactions at the carbocyclic ring to give $\sigma\text{-}\pi$ vinyl complexes. These nucleophilic products have been rearomatized by facile oxidation of the intermediate anions without adding any deprotonating agent.

These complexes undergo ligand addition at the metal core with soft nucleophiles such as PPh_3 but with harder nucleophiles, both small (hydride) and relatively bulky carbon based carbanion (isobutyronitrile), nucleophilic attack occur at the benzoheterocycle ligands. In light of this diverse reactivity, a study of the reactivity of these complexes with n-butyl amine and carboxylic acid which are intermediate in nucleophilicity relative to phosphine and amine was carried out to define the stereodynamics of their coordination modes. The structural features of these coordinated complexes and the mechanistic implications of these transformations have been discussed and compared with the previously reported complexes with quinoxaline.

Acknowledgements

I would like to express my sincere gratitude to my advisor Dr. Edward Rosenberg for his valuable support and guidance during the entire period of this research. He proved to be an excellent mentor and a research collaborator in guiding students and sharing ideas with insight knowledge of the subject. His knowledge in the NMR impressed me and I especially enjoyed working with him learning the different NMR techniques. His friendship, generosity and understanding of the student's needs make him an exceptional person in general.

A special thanks goes to Dr. Kenneth Hardcastle and his group at the Emory University, Georgia for their meticulous work in performing all the solid state structures. I would like to thank my committee members for their valuable suggestions and concern about this work. I am also thankful to the entire Rosenberg group, especially Brian Bergman who obtained a Ph.D. working on this field for sharing his expertise with me. I appreciate the contributions of all the other members for their helping hands.

Finally, I express my gratitude to my parents, late Md. Motiur Rahman and Johura Khatun for their deepest love and support. I gratefully acknowledge their contribution. I want to thank my wife Dalia Rokhsana for her encouragement and patience during the course of work and preparation of this thesis. I also want express my deepest love to my daughter Wafa who stands as an inspiration to me.

To my parents
Md. Motiur Rahman and Johura Khatun
for their love and support

Table of Contents

| | Page |
|--|----------|
| Authorization to Submit Dissertation | i |
| Abstract | ii |
| Acknowledgements | iii |
| Dedication | iv |
| Table of Contents | v |
| List of Figures | xi |
| List of Tables | xiii |
| List of Compounds..... | xv |
| | |
| Introduction | 1 |
| | |
| Chapter 1. General Background for Transition Metal Activated | |
| Aromatic Heterocycles..... | 3 |
| Major Objectives..... | 19 |
| | |
| Chapter 2. The Synthesis of Electron Deficient Benzoheterocycles, | |
| Os ₃ (CO) ₉ (μ ₃ -η ² -benzoheterocycle-H)(μ-H). | |

| | | |
|-----|---|----|
| 2.1 | The Reactions of Benzoheterocycles with $\text{Os}_3(\text{CO})_9(\text{CH}_3\text{CN})_2$ | 20 |
| 2.2 | Results and Discussion..... | 20 |
| 2.2 | The Reactions of Functionalized Benzotheterocycles with $\text{Os}_3(\text{CO})_{10}(\text{CH}_3\text{CN})_2$ | 38 |
| 2.4 | Results and Discussion..... | 39 |
| 2.5 | Conclusions..... | 60 |
| 2.6 | Experimental Section for Synthesis of the Benzoheterocycle Complexes Materials and General Considerations Materials and General Considerations..... | 61 |
| | Preparation of Electron Deficient Benzoheterocycles, $\text{Os}_3(\text{CO})_9$ $(\mu_3\text{-}\eta^2\text{-benzohetero cycle})(\mu\text{-H})$ (29 , 32-33 , 37-40 , 43 , 56 , 65-66 and 71)..... | 62 |
| | Synthesis of 2-benzothiazolyl benzyl ether (50)..... | 63 |
| | Synthesis of 2-Benzyloxycarbamate benzothiazole (60) and 6-Ethoxy-2-benzyloxy carbamate benzothiazole (63)..... | 64 |
| | Synthesis of 1,2-Dimethylbenzimidazole (68)..... | 68 |
| | Preparation of other Benzoheterocycle Complexes (36 , 44-49 , 51-59 , 61-62 , 64 ,)..... | 65 |
| | Crystal Structure Analysis..... | 66 |
| | Analytical and Spectroscopic Data for Compounds 29 through 71 | 67 |

Chapter 3. Reactions of Electron Deficient Benzoheterocyclic Clusters,

**Os₃(CO)₉(μ₃-η²-heterocycle-H)(μ-H) with Heteroatom Nucleophiles
and Protic Acids.**

| | | |
|-------|--|-----|
| 3.1 | Introduction..... | 77 |
| 3.2 | Results and Discussion | |
| 3.2.1 | Reactions with Triphenylphosphine, Acetonitrile and n-Butylamine..... | 82 |
| 3.2.2 | Reactions with HBF ₄ and CF ₃ CO ₂ H..... | 99 |
| 3.3 | General Conclusions | 106 |
| 3.4 | Experimental Section | |
| | Materials and General Considerations..... | 107 |
| | Synthesis of the Phosphine Derivatives 75-77 | 108 |
| | Analytical and Spectroscopic Data of complexes 75 through 79 | 108 |
| | Synthesis of the Amine Adducts 78 and 79 | 109 |
| | Measurement of the Formation Constants for the Amine Adducts | 110 |
| | Crystal Structure Analysis of 78 | 110 |

Chapter 4. Reactivity of Electron Deficient Benzoheterocycles with H⁻/H⁺

| | | |
|-------|---|-----|
| 4.1 | Introduction | 112 |
| 4.2 | Results and discussion | |
| 4.2.1 | Reactions of Os ₃ (CO) ₉ (μ ₃ -η ² -C ₁₃ H ₈ N)(μ-H)(29) with LiEt ₃ BH and CF ₃ COOH | 115 |
| 4.2.2 | Reactions of Quinoxaline and 3- Methylquinoxaline Triosmium Carbonyl Clusters, Os ₃ (CO) ₉ (μ ₃ -η ² -C ₈ H ₄ (3-R)N ₂ (μ-H)(R = H, 43 ; R= CH ₃ , 66) with LiEt ₃ BX and CF ₃ COOX (X = H or D) | 117 |

| | | |
|-------|--|-----|
| 4.2.3 | Reactions of 2-Methylbenzotriazole Complex, $\text{Os}_3(\text{CO})_9(\mu_3\text{-}\eta^2\text{-C}_6\text{H}_3\text{N}_3(2\text{-CH}_3)(\mu\text{-H}))$ (33) with LiEt_3BH and CF_3COOH | 126 |
| 4.2.4 | Reactions of the 2-Methylbenzimidazole and 2,3-Dimethyl benzimidazole Complexes, $\text{Os}_3(\text{CO})_9(\mu_3\text{-}\eta^2\text{-C}_7\text{H}_3(2\text{-CH}_3)\text{N}_2(3\text{-R})(\mu\text{-H}))$ ($\text{R} = \text{H}$, 32 ; $\text{R} = \text{CH}_3$, 71) with LiEt_3BX and CF_3COOX ($\text{X} = \text{H}$ or D)..... | 127 |
| 4.2.5 | Reactions of $\text{Os}_3(\text{CO})_9(\mu_3\text{-}\eta^2\text{-C}_7\text{H}_3(2\text{-R})\text{NX})(\mu\text{-H})$ ($\text{R} = \text{H}$, $\text{X} = \text{S}$, 39 ; $\text{R} = \text{CH}_3$, $\text{X} = \text{S}$, 40 ; $\text{R} = \text{H}$, $\text{X} = \text{O}$, 37 ; $\text{R} = \text{CH}_3$, $\text{X} = \text{O}$, 38 ;) with LiEt_3BX ($\text{X} = \text{H}$ or D) and CF_3COOH | 131 |
| 4.3 | Conclusions | 147 |
| 4.4 | Experimental Section | |
| | Materials and general considerations | 147 |
| | Reactions of $\text{Os}_3(\text{CO})_9(\mu_3\text{-}\eta^2\text{-benzoheterocycle-H})(\mu\text{-H})$ (29 , 33 and 40) with LiEt_3BH and CF_3COOH | 148 |
| | Reactions of $\text{Os}_3(\text{CO})_9(\mu_3\text{-}\eta^2\text{-Quinoxaline(or 3-Methylquinoxaline)-H})(\mu\text{-H})$ (43 or 66) with LiEt_3BH and CF_3COOH | 149 |
| | Reactions of $\text{Os}_3(\text{CO})_9(\mu_3\text{-}\eta^2\text{-Quinoxaline-H})(\mu\text{-H})$ (43) with LiEt_3BD and CF_3COOD | 150 |
| | Reactions of $\text{Os}_3(\text{CO})_9(\mu_3\text{-}\eta^2\text{-2-Methyl (or 2,3-Dimethyl benzimidazole)-H})(\mu\text{-H})$ (32 or 71) with LiEt_3BH and CF_3COOH | 150 |
| | Reactions of $\text{Os}_3(\text{CO})_9(\mu_3\text{-}\eta^2\text{-2-Methyl(or 2, 3-Dimethyl)benzimidazole-H})(\mu\text{-H})$ (32 or 71) with LiEt_3BD and CF_3COOD | 151 |

| | |
|--|-----|
| Reactions of $\text{Os}_3(\text{CO})_9(\mu_3\text{-}\eta^2\text{-C}_7\text{H}_3(2\text{-R})\text{NX})(\mu\text{-H})$; (R= H, X= O, 37 ; R=CH ₃ , X= O, 38 ; R=H, X=S, 39) with LiEt_3BH and CF_3COOH | 151 |
| Evaluation of Equilibrium Constant (K_{eq}) for Complexes 8 and 99 , and 102 and 103 | 152 |
| Kinetics of Conversions of 98 to 99 and 102 to 103 | 153 |
| Analytical and Spectroscopic Data of Complexes 80 through 106 | 153 |

Chapter 5. Reactions of Electron Deficient Benzoheterocycles, $\text{Os}_3(\text{CO})_9(\mu_3\text{-}\eta^2\text{-}$
benzoheterocycle-H)($\mu\text{-H}$) with Carbanions.

| | |
|---|-----|
| 5.1 Results and Discussion | |
| 5.1.1 Reaction of Phenanthridine Complex, $\text{Os}_3(\text{CO})_9(\mu_3\text{-}\eta^2\text{-C}_{13}\text{H}_8\text{N})$ ($\mu\text{-H}$)(29) with the Isobutyronitrile Carbanion..... | 160 |
| 5.1.2 Reaction of 2-Methylbenzimidazole complex, $\text{Os}_3(\text{CO})_9(\mu_3\text{-}\eta^2\text{-C}_7\text{H}_4$ (2-CH ₃)N ₂)($\mu\text{-H}$) (32) with the Isobutyronitrile Carbanion. | 162 |
| 5.1.3 Reaction of 2,3-Dimethylbenzimidazole Complex, $\text{Os}_3(\text{CO})_9$ ($\mu_3\text{-}\eta^2\text{-C}_7\text{H}_3(2\text{-CH}_3)(3\text{-CH}_3)\text{N}_2$)($\mu\text{-H}$) (71) with the Isobutyronitrile Carbanion..... | 168 |
| 5.1.4 Reaction of 2-Methylquinoxaline Complex, $\text{Os}_3(\text{CO})_9(\mu_3\text{-}\eta^2\text{-}$ $\text{C}_8\text{H}_4(3\text{-CH}_3)\text{N}_2$)($\mu\text{-H}$) (66) with the Isobutyronitrile Carbanion. | 170 |
| 5.1.5 Reaction of 2-Methylbenzothiazole Complex, $\text{Os}_3(\text{CO})_9(\mu_3\text{-}\eta^2\text{-}$ $\text{C}_7\text{H}_3(2\text{-CH}_3)\text{NS}$) ($\mu\text{-H}$) (40) with the Isobutyronitrile Carbanion..... | 171 |

| | | |
|-------|---|-----|
| 5.1.6 | Reaction Benzothiazole Complex, $\text{Os}_3(\text{CO})_9(\mu_3\text{-}\eta^2\text{-C}_7\text{H}_4\text{NS})$ ($\mu\text{-H}$) (39) with the Isobutyronitrile Carbanion..... | 172 |
| 5.1.7 | Reaction of Quinoxaline Complex, $\text{Os}_3(\text{CO})_9(\mu_3\text{-}\eta^2\text{-C}_8\text{H}_5\text{N}_2)$ ($\mu\text{-H}$) (43) with the Isobutyronitrile Carbanion..... | 177 |
| 5.2 | Rearomatization of the Nucleophilic Addition Products..... | 178 |
| 5.3 | Conclusions and Future work | 180 |
| 5.3.1 | Cleavage of the Functionalized Benzoheterocycles from the Clusters..... | 181 |
| 5.3.2 | Reactions with other Carbanions. | 182 |
| 5.4 | Experimental Section | |
| | Materials and General Considerations..... | 183 |
| | Preparation of Isobutyronitrile Carbanion..... | 183 |
| | Preparation of $\text{Os}_3(\text{CO})_9(\mu_3\text{-}\eta^3\text{-C}_{13}\text{H}_9(5\text{-C}(\text{CH}_3)_2\text{CN})\text{N})(\mu\text{-H})$ (109)..... | 184 |
| | Preparation of $\text{Os}_3(\text{CO})_9(\mu_3\text{-}\eta^2\text{-C}_7\text{H}_3(2\text{-CH}_3)(4\text{-C}(\text{CH}_3)_2\text{CN})\text{N}_2)(\mu\text{-H})$ (110) and $\text{Os}_3(\text{CO})_9(\mu_3\text{-}\eta^3\text{-C}_7\text{H}_5(2\text{-CH}_3)(4\text{-C}(\text{CH}_3)_2\text{CN})\text{N}_2)(\mu\text{-H})$ (111)..... | 184 |
| | Preparation of $\text{Os}_3(\text{CO})_9(\mu_3\text{-}\eta^2\text{-C}_7\text{H}_2(2\text{-CH}_3)(3\text{-CH}_3)(4\text{-C}(\text{CH}_3)_2\text{CN})\text{N}_2)(\mu\text{-H})$ (114) and $\text{Os}_3(\text{CO})_9(\mu_3\text{-}\eta^3\text{-C}_7\text{H}_4(2\text{-CH}_3)(3\text{-CH}_3(4\text{-C}(\text{CH}_3)_2\text{CN})\text{N}_2)(\mu\text{-H})$ (115)..... | 185 |
| | Preparation of $\text{Os}_3(\text{CO})_9(\mu_3\text{-}\eta^3\text{-C}_8\text{H}_5(3\text{-CH}_3)(5\text{-C}(\text{CH}_3)_2\text{CN})\text{N}_2)(\mu\text{-H})$ (116)..... | 186 |
| | Preparation of $\text{Os}_3(\text{CO})_9(\mu_3\text{-}\eta^3\text{-C}_7\text{H}_4(2\text{-CH}_3)(4\text{-C}(\text{CH}_3)_2\text{CN})\text{NS})(\mu\text{-H})$ (118) and $\text{Os}_3(\text{CO})_9(\mu_3\text{-}\eta^3\text{-C}_7\text{H}_5(4\text{-C}(\text{CH}_3)_2\text{CN})\text{NS})(\mu\text{-H})$ (119)..... | 187 |
| | Preparation of $\text{Os}_3(\text{CO})_9(\mu_3\text{-}\eta^2\text{-C}_8\text{H}_4\text{N}_2)(5\text{-C}(\text{CH}_3)_2\text{CN})(\mu\text{-H})$ (120) | |

| | |
|--|-----|
| and Os ₃ (CO) ₉ (μ ₃ -η ³ -C ₈ H ₆ N ₂)(5-C(CH ₃) ₂ CN)(μ-H) (121)..... | 187 |
| X-Ray structures determination of 111 and 119 | 188 |
| Analytical and spectroscopic data of complexes 109 through 123 | 189 |
| References | 193 |

List of Figures

| | |
|--|----|
| Figure 2.1 Solid state structure of Os ₃ (CO) ₉ (μ ₃ -η ² -C ₁₃ H ₈ N)(μ-H) (29) showing the calculated position of the hydride..... | 25 |
| Figure 2.2 Solid state structure of Os ₃ (CO) ₉ (μ ₃ -η ² -C ₇ H ₄ N ₂ (2-CH ₃)(μ-H) (32) showing the calculated position of the hydride..... | 26 |
| Figure 2.3 Solid state structure of Os ₃ (CO) ₉ (μ ₃ -η ² -C ₆ H ₃ N ₃ (2-CH ₃)(μ-H) (33) showing the calculated position of the hydride..... | 27 |
| Figure 2.4 Solid state structure of Os ₃ (CO) ₁₀ (μ-η ² -C ₆ H ₃ N ₃ (3-CH ₃)(μ-H) (36) showing the calculated position of the hydride..... | 28 |
| Figure 2.5 Solid state structure of Os ₃ (CO) ₉ (μ ₃ -η ² -C ₇ H ₃ NO(2-CH ₃)(μ-H) (38) showing the calculated position of the hydride..... | 32 |
| Figure 2.6 Solid state structure of Os ₃ (CO) ₉ (μ ₃ -η ² -C ₇ H ₄ NS)(μ-H) (39) showing the calculated position of the hydride..... | 33 |
| Figure 2.7 Solid state structure of Os ₃ (CO) ₉ (μ ₃ -η ² -C ₈ H ₅ N ₂)(μ-H) (43) showing the calculated position of the hydride..... | 34 |

| | | |
|--------------------|--|-----|
| Figure 2.8 | Solid-state structure of $\text{Os}_3(\text{CO})_{10}(\mu\text{-}\eta^2\text{-C}_6\text{H}_4\text{N}_3)(\mu\text{-H})$ (54) showing the calculated position of the hydride..... | 45 |
| Figure 2.9 | Solid-state structure of $\text{Os}_3(\text{CO})_{10}(\mu_3\text{-}\eta^2\text{-C}_7\text{H}_5\text{N}_2\text{S})(\mu\text{-H})$ (56) showing the calculated position of the hydride. | 49 |
| Figure 2.10 | Solid state structure of $\text{Os}_3(\text{CO})_9(\mu_3\text{-}\eta^2\text{-C}_8\text{H}_4(3\text{-CH}_3)\text{N}_2)(\mu\text{-H})$ (66) showing the calculated position of the hydride | 57 |
| Figure 3.1 | Solid state structure of $\text{Os}_3(\text{CO})_9(\mu_3\text{-}\eta^2\text{-L-H})(\mu\text{-H})(n\text{-C}_4\text{H}_9\text{N})$ (L=phenanthridine, 78)..... | 93 |
| Figure 3.2 | Reaction profile diagram for ligand coordination and cleavage, illustrating the proposed differences in the relative stability of the $\mu\text{-}$ and $\mu_3\text{-}$ -bonding modes..... | 94 |
| Figure 4.1 | Electron deficient benzoheterocycles, $\text{Os}_3(\text{CO})_9(\mu_3\text{-}\eta^2\text{-}$ benzoheterocycle- H)($\mu\text{-H}$) (29, 32-33, 37-40, 43, 66, 71)..... | 112 |
| Figure 4.2 | VT ^1H NMR of the aliphatic (left) and hydride (right) regions of 98 at 400 MHz in CDCl_3 | 136 |
| Figure 4.3 | Solid state structure of $\text{Os}_3(\text{CO})_9(\mu_3\text{-}\eta^2\text{-C}_7\text{H}_5\text{NS})(\mu\text{-H}_2)$ (98)..... | 138 |
| Figure 4.4 | VT ^1H NMR of the aliphatic (left) and hydride (right) regions of 102 at 400 MHz in CDCl_3 | 140 |
| Figure 4.5 | Solid state structure of $\text{Os}_3(\text{CO})_9(\mu_3\text{-}\eta^3\text{-C}_6\text{H}_3\text{O})(1\text{-NHC}_2\text{H}_5)$ (5- OH)($\mu\text{-H}$) (106)..... | 146 |
| Figure 5.1 | Solid state structure of $\text{Os}_3(\text{CO})_9(\mu_3\text{-}\eta^3\text{-C}_7\text{H}_5(2\text{-CH}_3)$ | |

| | |
|---|-----|
| (4-C(CH ₃) ₂ CN)N ₂ (μ-H)(111)..... | 167 |
| Figure 5.2 Solid state structure of Os ₃ (CO) ₉ (μ ₃ -η ³ -C ₇ H ₅ (4-C(CH ₃) ₂ CN)NS) (μ-H) (119)..... | 176 |
| Figure 5.3 Structures of nucleophilic addition products with other carbanions..... | 182 |

List of Tables

| | |
|--|----|
| Table 1.1 The synthesized mono-substituted electron deficient quinoline triosmium clusters..... | 11 |
| Table 1.2 Isolated Nucleophilic addition product yields from the reaction of electron deficient quinoline triosmium cluster, Os ₃ (CO) ₉ (μ ₃ - η ³ -C ₉ H ₆ N(μ-H) with carbanions. | 15 |
| Table 2.1 Selected Distances(Å) for Compounds 29, 32-33, 38, 39 and 43 | 37 |
| Table 2.2 Selected Bond Distances (Å) and Angles (°) for 54 | 44 |
| Table 2.3 Selected Bond Distances (Å) and Angles (°) for 56 | 48 |
| Table 2.4 Selected Bond Distances (Å) and Angles (°) for 66 | 56 |
| Table 3.1 Proton Coupled ¹³ C NMR Data for the Phosphine Adducts of the Electron Deficient Benzoheterocycle Complexes..... | 86 |
| Table 3.2 ¹ H NMR of Acetonitrile Adducts of Electron Deficient Benzoheterocycle Clusters..... | 87 |
| Table 3.3 Proton Coupled ¹³ C NMR of the Acetonitrile Adducts of the Electron Deficient Benzoheterocycle Complexes..... | 88 |

| | | |
|-------------------|--|-----|
| Table 3.4 | Selected Distances (Å) and Bond Angles (deg.) for $\text{Os}_3(\text{CO})_9(\mu_3\text{-}\eta^2\text{-L-H})(\mu\text{-H})(n\text{-C}_4\text{H}_9\text{N})$ (L=phenanthridine, 78)..... | 92 |
| Table 3.5. | ^1H NMR, Isomer Ratios, Hydride T_1 and Formation Constants for n-Butyl Amine Adducts of Electron Deficient Benzoheterocycle Clusters..... | 97 |
| Table 3.6 | ^{13}C NMR Data for Amine Adducts of the Electron Deficient Benzoheterocycle Complexes | 98 |
| Table 3. 7 | Hydride Chemical Shifts for Initial Protonation Products of the Electron Deficient Benzoheterocycle Complexes | 104 |
| Table 3.8 | Proton Coupled ^{13}C NMR of the Protonated Electron Deficient Benzoheterocycle Complexes..... | 105 |
| Table 4.1 | Selected Bond Distances (Å) and Angles (°) for 98 | 137 |
| Table 4.2 | Selected Bond Distances (Å) and Angles (°) for 106 | 145 |
| Table 5.1 | Selected Bond Distances (Å) and Angles (°) for 111 | 166 |
| Table 5.2 | Selected Bond Distances (Å) and Angles (°) for 119 | 175 |
| Table 5.3 | Isolated nucleophilic addition product yields from the reaction of Benzoheterocycle complexes, $\text{Os}_3(\text{CO})_9(\mu_3\text{-}\eta^2\text{-L-H})$ ($\mu\text{-H}$) with isobutyronitrile carbanion | 180 |

List of Compounds

| | Page |
|--|------|
| 1* $\eta^6\text{-(C}_8\text{H}_6\text{N)(1-R)-M(CO)}_3$ | 4 |
| 2* $\eta^6\text{-(C}_8\text{H}_5\text{N)(1-R)(2-CO}_2\text{Me)-M(CO)}_3$ | 4 |
| 3* $\eta^6\text{-(C}_8\text{H}_4\text{N)(1-R)(2-TMS)(7-E)-M(CO)}_3$ | 4 |
| 4* $\text{Os}_3(\text{CO})_9(\mu\text{-}\eta^2\text{-C=N(CH}_2)_3\text{Br)}$ | 6 |
| 5* $\text{Os}_3(\text{CO})_{10}(\mu\text{-}\eta^2\text{-C=N(CH}_2)_3(\mu\text{-}\eta^1\text{-C}_6\text{H}_5))$ | 6 |
| 6* $\text{Os}_3(\text{CO})_8(\mu\text{-}\eta^2\text{-C=N(CH}_2)_3(\mu\text{-}\eta^1\text{:}\eta^6\text{-C}_6\text{H}_5))$ | 6 |
| 7a* $\text{Os}_3(\text{CO})_{10}(\mu\text{-}\eta^2\text{-C}_9\text{H}_6\text{N})(\mu\text{-H)}$ | 7 |
| 7b* $\text{Ru}_3(\text{CO})_{10}(\mu\text{-}\eta^2\text{-C}_9\text{H}_6\text{N})(\mu\text{-H)}$ | 7 |
| 7c* $\text{Os}_3(\text{CO})_8(\mu\text{-}\eta^2\text{-C}_9\text{H}_6\text{N})_2(\mu\text{-H})_2$ | 7 |
| 7d* $\text{Ru}_3(\text{CO})_8(\mu\text{-}\eta^2\text{-C}_9\text{H}_6\text{N})_2(\mu\text{-H})_2$ | 7 |
| 8a* $\text{Os}_3(\text{CO})_{10}(\mu\text{-}\eta^2\text{-C}_9\text{H}_8\text{N})(\mu\text{-H)}$ | 7 |
| 8b* $\text{Ru}_3(\text{CO})_{10}(\mu\text{-}\eta^2\text{-C}_9\text{H}_8\text{N})(\mu\text{-H)}$ | 7 |
| 8c* $\text{Os}_3(\text{CO})_{10}(\mu\text{-}\eta^2\text{-C}_9\text{H}_6\text{N})(\mu\text{-H)}$ | 7 |
| 8d* $\text{Ru}_3(\text{CO})_{10}(\mu\text{-}\eta^2\text{-C}_9\text{H}_6\text{N})(\mu\text{-H)}$ | 7 |
| 9 $\text{Os}_3(\text{CO})_{10}(\text{CH}_3\text{CN})_2$ | 8 |
| 10* $\text{Os}_3(\text{CO})_{10}(\mu\text{-}\eta^2\text{-C}_8\text{H}_8\text{NH})(\mu\text{-H)}$ | 8 |
| 11* $\text{Os}_3(\text{CO})_9(\mu\text{-}\eta^2\text{-C}_8\text{H}_7\text{N})(\mu\text{-H})_2$ | 8 |
| 12* $\text{Os}_3(\text{CO})_9(\mu\text{-}\eta^2\text{-C}_8\text{H}_7\text{N})(\mu\text{-H})_2$ | 8 |

| | | |
|---------------|--|----|
| 13* | $\text{Os}_3(\text{CO})_9(\mu_3\text{-}\eta^2\text{-C}_8\text{H}_4\text{NH})(\mu\text{-H})_2$ | 8 |
| 14* | $\text{Os}_3(\text{CO})_9(\mu_3\text{-}\eta^2\text{-C}_9\text{H}_9\text{N})(\mu\text{-H})_2$ | 9 |
| 15* | $\text{Os}_3(\text{CO})_9(\mu_3\text{-}\eta^2\text{-C}_9\text{H}_9\text{N})(\mu\text{-H})_2$ | 9 |
| 16* | $\text{Os}_3(\text{CO})_{10}(\mu\text{-}\eta^1\text{-C}_9\text{H}_{10}\text{N}(\text{CH}_3)\text{CN})(\mu\text{-H})$ | 9 |
| 17* | $\text{Os}_3(\text{CO})_{10}(\mu\text{-}\eta^1\text{-C}_9\text{H}_6\text{N})(\mu\text{-H})$ | 9 |
| 18* | $\text{Os}_3(\text{CO})_{10}(\mu\text{-}\eta^2\text{-C}_9\text{H}_8\text{N})(\mu\text{-H})$ | 9 |
| 19* | $\text{Os}_3(\text{CO})_{10}(\mu\text{-}\eta^2\text{-C}_9\text{H}_8\text{N})(\mu\text{-H})$ | 10 |
| 20* | $\text{Os}_3(\text{CO})_9(\mu_3\text{-}\eta^2\text{-C}_9\text{H}_8\text{N})(\mu\text{-H})$ | 10 |
| 21a-r* | $\text{Os}_3(\text{CO})_{10}(\mu\text{-}\eta^2\text{-C}_9\text{H}(\text{R})\text{N})(\mu\text{-H})$ | 11 |
| 22* | $\text{Os}_3(\text{CO})_{10}(\mu\text{-}\eta^2\text{-C}_9\text{H}_6\text{N})(\mu\text{-H})$ | 11 |
| 23a-r* | $\text{Os}_3(\text{CO})_9(\mu_3\text{-}\eta^2\text{-C}_9\text{H}_5(\text{R})\text{N})(\mu\text{-H})$ | 11 |
| 24a-l* | $\text{Os}_3(\text{CO})_9(\mu_3\text{-}\eta^3\text{-C}_9\text{H}_7(5\text{-R}')\text{N})(\mu\text{-H})$ | 13 |
| 25* | $\text{Os}_3(\text{CO})_{10}(\mu\text{-}\eta^2\text{-C}_9\text{H}_6\text{N})(\mu\text{-H})\text{L}$ | 14 |
| 26a-p* | $\text{Os}_3(\text{CO})_9(\mu_3\text{-}\eta^3\text{-C}_9\text{H}_7(3\text{-or } 4\text{- or } 5\text{-R}')\text{N})(\mu\text{-H})$ | 16 |
| 27 | $\text{Os}_3(\text{CO})_{10}(\mu\text{-}\eta^2\text{-C}_{13}\text{H}_8\text{N})(\mu\text{-H})$ | 21 |
| 28 | $\text{Os}_3(\text{CO})_{10}(\mu\text{-}\eta^2\text{-C}_{13}\text{H}_8\text{N})(\mu\text{-H})$ | 21 |
| 29 | $\text{Os}_3(\text{CO})_9(\mu_3\text{-}\eta^2\text{-C}_{13}\text{H}_8\text{N})(\mu\text{-H})$ | 21 |
| 30 | $\text{Os}_3(\text{CO})_{10}(\mu\text{-}\eta^2\text{-C}_7\text{H}_5\text{N}_2)(\mu\text{-H})$ | 22 |
| 31 | $\text{Os}_3(\text{CO})_{10}(\mu\text{-}\eta^2\text{-C}_6\text{H}_4\text{N}_3)(\mu\text{-H})$ | 22 |
| 32 | $\text{Os}_3(\text{CO})_9(\mu_3\text{-}\eta^2\text{-C}_7\text{H}_4(2\text{-CH}_3)\text{N}_2)(\mu\text{-H})$ | 22 |
| 33 | $\text{Os}_3(\text{CO})_9(\mu_3\text{-}\eta^2\text{-C}_6\text{H}_3(2\text{-CH}_3)\text{N}_3)(\mu\text{-H})$ | 23 |

| | | |
|-----------|--|----|
| 34 | $\text{Os}_3(\text{CO})_{10}(\mu\text{-}\eta^2\text{-C}_7\text{H}_4(2\text{-CH}_2)\text{N}_2)(\mu\text{-H})$ | 24 |
| 35 | $\text{Os}_3(\text{CO})_{10}(\mu\text{-}\eta^2\text{-C}_7\text{H}_4(2\text{-CH})\text{N}_2)(\mu\text{-H})_2$ | 24 |
| 36 | $\text{Os}_3(\text{CO})_{10}(\mu\text{-}\eta^2\text{-C}_6\text{H}_3(3\text{-CH}_3)\text{N}_3)(\mu\text{-H})$ | 24 |
| 37 | $\text{Os}_3(\text{CO})_9(\mu_3\text{-}\eta^2\text{-C}_7\text{H}_4\text{NO})(\mu\text{-H})$ | 29 |
| 38 | $\text{Os}_3(\text{CO})_9(\mu_3\text{-}\eta^2\text{-C}_7\text{H}_3(2\text{-CH}_3)\text{NO})(\mu\text{-H})$ | 29 |
| 39 | $\text{Os}_3(\text{CO})_9(\mu_3\text{-}\eta^2\text{-C}_7\text{H}_4\text{NS})(\mu\text{-H})$ | 29 |
| 40 | $\text{Os}_3(\text{CO})_9(\mu_3\text{-}\eta^2\text{-C}_7\text{H}_3(2\text{-CH}_3)\text{NS})(\mu\text{-H})$ | 29 |
| 41 | $\text{Os}_3(\text{CO})_{10}(\mu\text{-}\eta^2\text{-C}_7\text{H}_4(2\text{-CH}_2)\text{NS})(\mu\text{-H})$ | 30 |
| 42 | $\text{Os}_3(\text{CO})_{10}(\mu\text{-}\eta^2\text{-C}_7\text{H}_4(2\text{-CH})\text{NS})(\mu\text{-H})_2$ | 30 |
| 43 | $\text{Os}_3(\text{CO})_9(\mu_3\text{-}\eta^2\text{-C}_8\text{H}_5\text{N}_2)(\mu\text{-H})$ | 30 |
| 44 | $\text{Os}_3(\text{CO})_{10}(\mu\text{-}\eta^2\text{-C}_8\text{H}_5\text{N}_2)(\mu\text{-H})$ | 31 |
| 45 | $\text{Os}_3(\text{CO})_{10}(\mu\text{-}\eta^2\text{-C}_8\text{H}_5\text{N}_2)(\mu\text{-H})$ | 31 |
| 46 | $\text{Os}_3(\text{CO})_{10}(\mu\text{-}\eta^2\text{-C}_8\text{H}_6\text{N}_2)(\mu\text{-H})$ | 31 |
| 47 | $\text{Os}_3(\text{CO})_{10}(\mu\text{-}\eta^2\text{-C}_8\text{H}_5\text{N}_2)(\mu\text{-H})$ | 31 |
| 48 | $\text{Os}_3(\text{CO})_9(\mu_3\text{-}\eta^2\text{-C}_8\text{H}_5\text{N}_2)(\mu\text{-H})$ | 31 |
| 49 | $\text{Os}_3(\text{CO})_{10}(\mu\text{-}\eta^2\text{-C}_7\text{H}_4\text{NOS})(\mu\text{-H})$ | 39 |
| 50 | $\text{C}_{14}\text{H}_9\text{NOS}$ | 40 |
| 51 | $\text{Os}_3(\text{CO})_{10}(\mu\text{-}\eta^2\text{-C}_7\text{H}_3(2\text{-C}_7\text{H}_7\text{O})\text{NS})(\mu\text{-H})$ | 41 |
| 52 | $\text{Os}_3(\text{CO})_{10}(\mu\text{-}\eta^2\text{-C}_6\text{H}_4\text{N}_3\text{S})(\mu\text{-H})$ | 42 |
| 53 | $\text{Os}_3(\text{CO})_{10}(\mu\text{-}\eta^2\text{-C}_6\text{H}_5\text{N}_4)(\mu\text{-H})$ | 43 |
| 54 | $\text{Os}_3(\text{CO})_{10}(\mu\text{-}\eta^2\text{-C}_6\text{H}_4\text{N}_3)(\mu\text{-H})$ | 43 |

| | | |
|-----------|---|----|
| 55 | $\text{Os}_3(\text{CO})_{10}(\mu\text{-}\eta^2\text{-C}_7\text{H}_5\text{N}_2\text{S})(\mu\text{-H})$ | 47 |
| 56 | $\text{Os}_3(\text{CO})_9(\mu_3\text{-}\eta^2\text{-C}_7\text{H}_5\text{N}_2\text{S})(\mu\text{-H})$ | 47 |
| 57 | $\text{Os}_3(\text{CO})_9(\mu\text{-}\eta^2\text{-C}_7\text{H}_5\text{N}_2\text{S})(\mu\text{-H})$ | 47 |
| 58 | $\text{Os}_3(\text{CO})_9(\mu\text{-}\eta^2\text{-C}_7\text{H}_5\text{N}_2\text{S})(\mu\text{-H})$ | 47 |
| 59 | $\text{Os}_3(\text{CO})_9(\mu\text{-}\eta^2\text{-C}_7\text{H}_5\text{N}_2\text{S}(\text{CH}_3\text{CN}))(\mu\text{-H})$ | 47 |
| 60 | $\text{C}_{15}\text{H}_{12}\text{N}_2\text{O}_2\text{S}$ | 50 |
| 61 | $\text{Os}_3(\text{CO})_{10}(\mu\text{-}\eta^2\text{-C}_{15}\text{H}_{11}\text{N}_2\text{O}_2\text{S})(\mu\text{-H})$ | 51 |
| 62 | $\text{Os}_3(\text{CO})_{10}(\mu\text{-}\eta^2\text{-C}_{15}\text{H}_{11}\text{N}_2\text{O}_2\text{S})(\mu\text{-H})$ | 51 |
| 63 | $\text{C}_{17}\text{H}_{16}\text{N}_2\text{O}_3\text{S}$ | 52 |
| 64 | $\text{Os}_3(\text{CO})_{10}(\mu\text{-}\eta^2\text{-C}_{17}\text{H}_{16}\text{N}_2\text{O}_3\text{S})(\mu\text{-H})$ | 53 |
| 65 | $\text{Os}_3(\text{CO})_9(\mu_3\text{-}\eta^2\text{-C}_{11}\text{H}_{11}\text{N}_2\text{O}_2)(\mu\text{-H})$ | 53 |
| 66 | $\text{Os}_3(\text{CO})_9(\mu_3\text{-}\eta^2\text{-C}_8\text{H}_4(3\text{-CH}_3)\text{N}_2)(\mu\text{-H})$ | 54 |
| 67 | $\text{Os}_3(\text{CO})_{10}(\mu\text{-}\eta^2\text{-C}_8\text{H}_4(3\text{-CH}_3)\text{N}_2)(\mu\text{-H})$ | 54 |
| 68 | $\text{C}_9\text{H}_{10}\text{N}_2$ | 58 |
| 69 | $\text{Os}_3(\text{CO})_{10}(\mu\text{-}\eta^2\text{-C}_7\text{H}_3(2\text{-CH}_3)(3\text{-CH}_3)\text{N}_2)(\mu\text{-H})$ | 59 |
| 70 | $\text{Os}_3(\text{CO})_{10}(\mu\text{-}\eta^2\text{-C}_7\text{H}_4(2\text{-CH}_2)(3\text{-CH}_3)\text{N}_2)(\mu\text{-H})$ | 59 |
| 71 | $\text{Os}_3(\text{CO})_9(\mu_3\text{-}\eta^2\text{-C}_7\text{H}_3(2\text{-CH}_3)(3\text{-CH}_3)\text{N}_2)(\mu\text{-H})$ | 59 |
| 72 | $\text{Os}_3(\text{CO})_9(\mu_3\text{-}\eta^2\text{-C}_{13}\text{H}_8\text{N})(\mu\text{-H})$ | 81 |
| 73 | $\text{Os}_3(\text{CO})_9(\mu_3\text{-}\eta^2\text{-L-H})(\mu\text{-H})$ (L= quinoline)..... | 83 |
| 74 | $\text{Os}_3(\text{CO})_9(\mu\text{-}\eta^2\text{-L-H})(\mu\text{-H})\text{PPh}_3$ (L= 5,6-benzoquinoline)..... | 83 |
| 75 | $\text{Os}_3(\text{CO})_9(\mu\text{-}\eta^2\text{-L-H})(\mu\text{-H})\text{PPh}_3$ (L= quinoxaline)..... | 83 |
| 76 | $\text{Os}_3(\text{CO})_9(\mu\text{-}\eta^2\text{-L-H})(\mu\text{-H})\text{PPh}_3$ (L= 2-methylbenzimidazole)..... | 83 |

| | | |
|------------|---|-----|
| 77 | $\text{Os}_3(\text{CO})_9(\mu\text{-}\eta^2\text{-L-H})(\mu\text{-H})\text{PPh}_3$ (L= benzoxazole)..... | 83 |
| 78 | $\text{Os}_3(\text{CO})_9(\mu_3\text{-}\eta^2\text{-L-H})(\eta\text{-C}_4\text{H}_9\text{N})(\mu\text{-H})$ (L=phenanthridine)..... | 90 |
| 79 | $\text{Os}_3(\text{CO})_9(\mu_3\text{-}\eta^2\text{-L-H})(\eta\text{-C}_4\text{H}_9\text{N})(\mu\text{-H})$ (L=2-methylbenzimidazole).... | 96 |
| 80 | $\text{Os}_3(\text{CO})_9(\mu_3\text{-}\eta^2\text{-C}_{13}\text{H}_9\text{N})(\mu\text{-H})^-$ | 115 |
| 81 | $\text{Os}_3(\text{CO})_9(\mu_3\text{-}\eta^3\text{-C}_{13}\text{H}_{10}\text{N})(\mu\text{-H})$ | 115 |
| 82 | $\text{Os}_3(\text{CO})_9(\mu_3\text{-}\eta^2\text{-C}_8\text{H}_6\text{N}_2)(\mu\text{-H})^-$ | 119 |
| 82' | $\text{Os}_3(\text{CO})_9(\mu_3\text{-}\eta^2\text{-C}_8\text{H}_5\text{DN}_2)(\mu\text{-H})^-$ | 120 |
| 83 | $\text{Os}_3(\text{CO})_9(\mu_3\text{-}\eta^2\text{-C}_8\text{H}_6\text{N}_2)(\mu\text{-H})^-$ | 119 |
| 83' | $\text{Os}_3(\text{CO})_9(\mu_3\text{-}\eta^2\text{-C}_8\text{H}_5\text{DN}_2)(\mu\text{-H})^-$ | 120 |
| 84 | $\text{Os}_3(\text{CO})_9(\mu_3\text{-}\eta^3\text{-C}_8\text{H}_7\text{N}_2)(\mu\text{-H})$ | 119 |
| 84' | $\text{Os}_3(\text{CO})_9(\mu_3\text{-}\eta^3\text{-C}_8\text{H}_5\text{D}_2\text{N}_2)(\mu\text{-H})$ | 120 |
| 85 | $\text{Os}_3(\text{CO})_9(\mu_3\text{-}\eta^2\text{-C}_8\text{H}_7\text{N}_2)(\mu\text{-H})^+$ | 119 |
| 85' | $\text{Os}_3(\text{CO})_9(\mu_3\text{-}\eta^2\text{-C}_8\text{H}_5\text{D}_2\text{N}_2)(\mu\text{-H})^+$ | 120 |
| 86 | $\text{Os}_3(\text{CO})_9(\mu_3\text{-}\eta^2\text{-C}_8\text{H}_6\text{N}_2)(\mu\text{-H})_2$ | 119 |
| 87 | $\text{Os}_3(\text{CO})_9(\mu_3\text{-}\eta^2\text{-C}_8\text{H}_8\text{N}_2\text{O})(\mu\text{-H})_2$ | 119 |
| 87' | $\text{Os}_3(\text{CO})_9(\mu_3\text{-}\eta^2\text{-C}_8\text{H}_7\text{DN}_2\text{O})(\mu\text{-H})_2$ | 120 |
| 88 | $\text{Os}_3(\text{CO})_9(\mu_3\text{-}\eta^2\text{-C}_8\text{H}_5(3\text{-CH}_3)\text{N}_2)(\mu\text{-H})^-$ | 125 |
| 89 | $\text{Os}_3(\text{CO})_9(\mu_3\text{-}\eta^2\text{-C}_8\text{H}_5(3\text{-CH}_3)\text{N}_2)(\mu\text{-H})^-$ | 125 |
| 90 | $\text{Os}_3(\text{CO})_9(\mu_3\text{-}\eta^2\text{-C}_8\text{H}_6(3\text{-CH}_3)\text{N}_2)(\mu\text{-H})$ | 125 |
| 91 | $\text{Os}_3(\text{CO})_9(\mu_3\text{-}\eta^2\text{-C}_6\text{H}_3(2\text{-CH}_3)\text{N}_3)(\mu\text{-H})$ | 126 |
| 92 | $\text{Os}_3(\text{CO})_9(\mu_3\text{-}\eta^2\text{-C}_7\text{H}_5(2\text{-CH}_3)\text{N}_2)(\mu\text{-H})^-$ | 128 |

| | | |
|-------------|--|-----|
| 92' | $\text{Os}_3(\text{CO})_9(\mu_3\text{-}\eta^2\text{-C}_7\text{H}_4\text{D}(2\text{-CH}_3)\text{N}_2)(\mu\text{-H})^-$ | 128 |
| 93 | $\text{Os}_3(\text{CO})_9(\mu_3\text{-}\eta^2\text{-C}_7\text{H}_4(2\text{-CH}_3)(3\text{-CH}_3)\text{N}_2)(\mu\text{-H})^-$ | 130 |
| 93' | $\text{Os}_3(\text{CO})_9(\mu_3\text{-}\eta^2\text{-C}_7\text{H}_3\text{D}(2\text{-CH}_3)(3\text{-CH}_3)\text{N}_2)(\mu\text{-H})^-$ | 130 |
| 94 | $\text{Os}_3(\text{CO})_9(\mu_3\text{-}\eta^3\text{-C}_7\text{H}_5(2\text{-CH}_3)(3\text{-CH}_3)\text{N}_2)(\mu\text{-H})$ | 130 |
| 94' | $\text{Os}_3(\text{CO})_9(\mu_3\text{-}\eta^3\text{-C}_7\text{H}_3\text{D}_2(2\text{-CH}_3)(3\text{-CH}_3)\text{N}_2)(\mu\text{-H})$ | 130 |
| 95 | $\text{Os}_3(\text{CO})_9(\mu_3\text{-}\eta^3\text{-C}_7\text{H}_5(2\text{-CH}_3)\text{NS})(\mu\text{-H})$ | 131 |
| 96 | $\text{Os}_3(\text{CO})_9(\mu_3\text{-}\eta^2\text{-C}_7\text{H}_5\text{NS})(\mu\text{-H})^-$ | 133 |
| 97 | $\text{Os}_3(\text{CO})_9(\mu_3\text{-}\eta^2\text{-C}_7\text{H}_6\text{NS})(\mu\text{-H})$ | 133 |
| 98 | $\text{Os}_3(\text{CO})_9(\mu_3\text{-}\eta^2\text{-C}_7\text{H}_5\text{NS})(\mu\text{-H})_2$ | 133 |
| 99 | $\text{Os}_3(\text{CO})_9(\mu_3\text{-}\eta^2\text{-C}_7\text{H}_5\text{NS})(\mu\text{-H})_2$ | 133 |
| 100* | $\text{Os}_3(\text{CO})_9(\mu_3\text{-}\eta^2\text{-C}_9\text{H}_9\text{N})(\mu\text{-H})_2$ | 135 |
| 101* | $\text{Os}_3(\text{CO})_9(\mu_3\text{-}\eta^2\text{-C}_9\text{H}_9\text{N})(\mu\text{-H})_2$ | 135 |
| 102 | $\text{Os}_3(\text{CO})_9(\mu_3\text{-}\eta^2\text{-C}_7\text{H}_5\text{NO})(\mu\text{-H})_2$ | 139 |
| 103 | $\text{Os}_3(\text{CO})_9(\mu_3\text{-}\eta^2\text{-C}_7\text{H}_5\text{NO})(\mu\text{-H})_2$ | 139 |
| 104 | $\text{Os}_3(\text{CO})_9(\mu_3\text{-}\eta^2\text{-C}_7\text{H}_4(2\text{-CH}_3)\text{NO})(\mu\text{-H})^-$ | 141 |
| 104' | $\text{Os}_3(\text{CO})_9(\mu_3\text{-}\eta^2\text{-C}_7\text{H}_3\text{D}(2\text{-CH}_3)\text{NO})(\mu\text{-H})^-$ | 141 |
| 105 | $\text{Os}_3(\text{CO})_9(\mu_3\text{-}\eta^2\text{-C}_8\text{H}_8\text{NO})(\mu\text{-H})$ | 141 |
| 105' | $\text{Os}_3(\text{CO})_9(\mu_3\text{-}\eta^2\text{-C}_8\text{H}_6\text{D}_2\text{NO})(\mu\text{-H})$ | 141 |
| 106 | $\text{Os}_3(\text{CO})_9(\mu_3\text{-}\eta^3\text{-C}_6\text{H}_3\text{O})(1\text{-NHC}_2\text{H}_5)(5\text{-OH})(\mu\text{-H})$ | 143 |
| 107 | $\text{Os}_3(\text{CO})_9(\mu_3\text{-}\eta^2\text{-C}_6\text{H}_3\text{O})(1\text{-NC}_2\text{H}_5)(\mu\text{-H})^{2-}$ | 144 |
| 108 | $\text{Os}_3(\text{CO})_9(\mu_3\text{-}\eta^3\text{-C}_6\text{H}_4\text{O})(1\text{-NHC}_2\text{H}_5)(\mu\text{-H})$ | 144 |

| | | |
|------------|--|-----|
| 109 | $\text{Os}_3(\text{CO})_9(\mu_3\text{-}\eta^3\text{-C}_{13}\text{H}_9(5\text{-C}(\text{CH}_3)_2\text{CN})\text{N})(\mu\text{-H})$ | 161 |
| 110 | $\text{Os}_3(\text{CO})_9(\mu_3\text{-}\eta^2\text{-C}_7\text{H}_3(2\text{-CH}_3)(4\text{-C}(\text{CH}_3)_2\text{CN})\text{N}_2)(\mu\text{-H})$ | 162 |
| 111 | $\text{Os}_3(\text{CO})_9(\mu_3\text{-}\eta^3\text{-C}_7\text{H}_5(2\text{-CH}_3)(4\text{-C}(\text{CH}_3)_2\text{CN})\text{N}_2)(\mu\text{-H})$ | 162 |
| 112 | $\text{Os}_3(\text{CO})_9(\mu_3\text{-}\eta^2\text{-C}_7\text{H}_2(2\text{-CH}_3)(3\text{-CH}_3)(4\text{-C}(\text{CH}_3)_2\text{CN})\text{N}_2)(\mu\text{-H})$ | 168 |
| 113 | $\text{Os}_3(\text{CO})_9(\mu_3\text{-}\eta^3\text{-C}_7\text{H}_4(2\text{-CH}_3)(3\text{-CH}_3)(4\text{-C}(\text{CH}_3)_2\text{CN})\text{N}_2)(\mu\text{-H})$ | 168 |
| 114 | $\text{Os}_3(\text{CO})_9(\mu_3\text{-}\eta^3\text{-C}_8\text{H}_5(3\text{-CH}_3)(4\text{-C}(\text{CH}_3)_2\text{CN})\text{N}_2)(\mu\text{-H})$ | 171 |
| 115 | $\text{Os}_3(\text{CO})_9(\mu_3\text{-}\eta^2\text{-C}_8\text{H}_3(3\text{-CH}_3)(4\text{-C}(\text{CH}_3)_2\text{CN})\text{N}_2)(\mu\text{-H})$ | 171 |
| 116 | $\text{Os}_3(\text{CO})_9(\mu_3\text{-}\eta^3\text{-C}_7\text{H}_4(2\text{-CH}_3)(4\text{-C}(\text{CH}_3)_2\text{CN})\text{NS})(\mu\text{-H})$ | 172 |
| 117 | $\text{Os}_3(\text{CO})_9(\mu_3\text{-}\eta^3\text{-C}_7\text{H}_5(4\text{-C}(\text{CH}_3)_2\text{CN})\text{NS})(\mu\text{-H})$ | 173 |
| 118 | $\text{Os}_3(\text{CO})_9(\mu_3\text{-}\eta^2\text{-C}_8\text{H}_4(5\text{-C}(\text{CH}_3)_2\text{CN})\text{N}_2)(\mu\text{-H})$ | 177 |
| 119 | $\text{Os}_3(\text{CO})_9(\mu_3\text{-}\eta^3\text{-C}_8\text{H}_6(5\text{-C}(\text{CH}_3)_2\text{CN})\text{N}_2)(\mu\text{-H})$ | 177 |
| 120 | $\text{Os}_3(\text{CO})_9(\mu_3\text{-}\eta^2\text{-C}_{13}\text{H}_7(5\text{-C}(\text{CH}_3)_2\text{CN})\text{N})(\mu\text{-H})$ | 179 |
| 121 | $\text{Os}_3(\text{CO})_9(\mu_3\text{-}\eta^2\text{-C}_7\text{H}_2(4\text{-C}(\text{CH}_3)_2\text{CN})\text{NS})(\mu\text{-H})$ | 179 |

* Denotes compounds synthesized by others, reported previously.

Introduction

The promise of using polymetallic complexes as catalysts and reagents for transformation of organic molecules lies in the concept of multisite activation. Two or more metal atoms can simultaneously activate different parts of an organic molecule towards sequential reagents. Alternatively, one metal atom in a cluster can protect or block one portion of an organic molecule while the remaining atoms in the cluster activate another part of the molecule. In this dissertation we will discuss a potentially useful and apparently very general example of the latter in the chemistry of benzoheterocycles with triosmium clusters. In this case, one osmium atom coordinates the pyridinyl nitrogen in quinoline, for example, while the other two atoms bond to carbon atom, C(8) of carbocyclic ring with a three centered-two electron bond.¹⁻³ The ultimate impact of this coordination mode is to block the normal site of nucleophilic attack while activating the carbocyclic ring, normally the site of electrophilic attack, towards regioselective nucleophilic attack by carbanions.

In this thesis we have extended the original work developed for quinoline to a wide range of heterocycles. These heterocycles constitute a class of compounds that have extremely important biomedical applications in the design of new drugs, as agonists and antagonists for neurotransmitter receptors and as anticancer agents.⁴⁻⁶ Because of their biological and pharmacological activities these compounds continue to be a focal point of studies and stimulate us to extend the reactivity observed for quinoline to this class of

heterocycles. The development of these synthetic methods will provide a broad range of novel heterocycles by direct and simple derivatization of the readily available parent benzoheterocycles. Such synthesized compounds could provide the basis for systematic screening of the biological activities of this class of molecules.

The incorporation of biologically important heterocycles into a trimetallic complex also holds out the possibility of utilizing these complexes as biological probes. There are some compelling reasons for extending these avenues of research to the complexes being considered here. First, these heterocycles exhibit specific binding to the serotonin and glutamate neurotransmitter receptor sites.^{7,8} Second, the complexes of these heterocycles coordinate primary amines and sulfhydryl groups at the metal core at room temperature opening up the possibility of bifunctional interactions with bio-macromolecules.⁹ Third, these molecules are highly colored making their incorporation into peptides as chromophores or photo affinity labels a promising area of investigation. Finally, the synthetic methods developed for these complexes will make their incorporation into bio-molecules and their water solubilization quite accessible. Based on these particular features, these electron deficient complexes offer some interesting and even unique possibilities for applications in the biomedical sciences.

Chapter 1

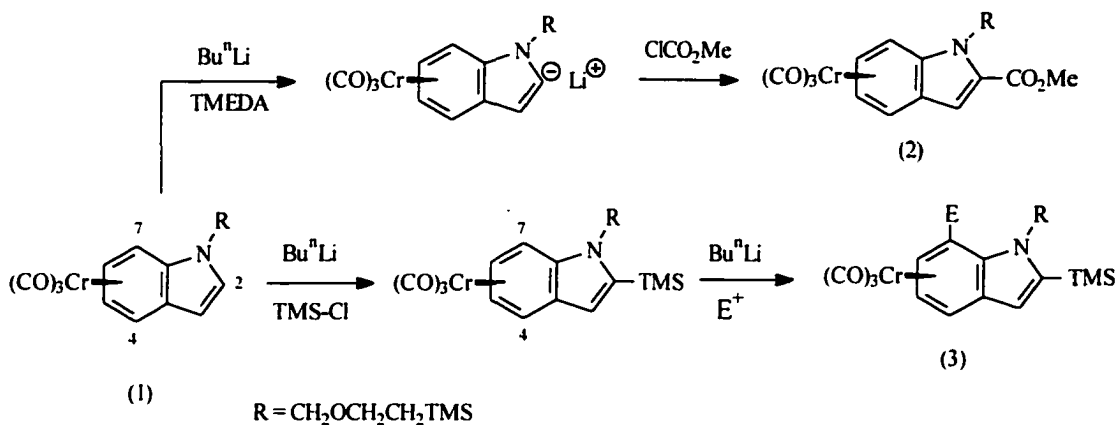
General Background for Transition Metal Activated Aromatic Heterocycles

Transition metals are of increasing importance in chemistry as a means of activating organic molecules towards specific reagents. Transition metals have outer d- orbitals that are only partially filled, acting as donors or acceptors of electron density and enabling them to influence the electron distributions in the coordinated organic molecules. A related and equally important area of chemistry is the study of transition metals being coordinately attached to a ligand for use in asymmetric synthesis.^{10, 11}

The organic chemistry of benzene is dominated by electrophilic aromatic substitution reactions, but as a coordinated ligand benzene undergoes nucleophilic addition / substitution. This sharp contrast in chemical behavior is a good example of the powerful influence coordination to a metal can have on the chemistry of an organic molecule.

Another example of the influence of coordination of a ligand to a metal is shown in complex (1) of N-methyl indole with $\text{Cr}(\text{CO})_3$ which is efficiently deprotonated at C-2 by Bu^nLi in the presence of tetramethyl ethylene diamine (TMEDA). Quenching with ClCO_2Me produces the 2-carboxylate ester (2) in 78% yield.¹² This selectivity is the same as for the uncomplexed indole, but the reaction is faster for the complexed version. Blocking C-2 of compound (1) by in situ silylation allows alternative deprotonation, and providing a chelating unit at the indole nitrogen directs the deprotonation to C-7 with high selectivity (Scheme 1.1).¹¹

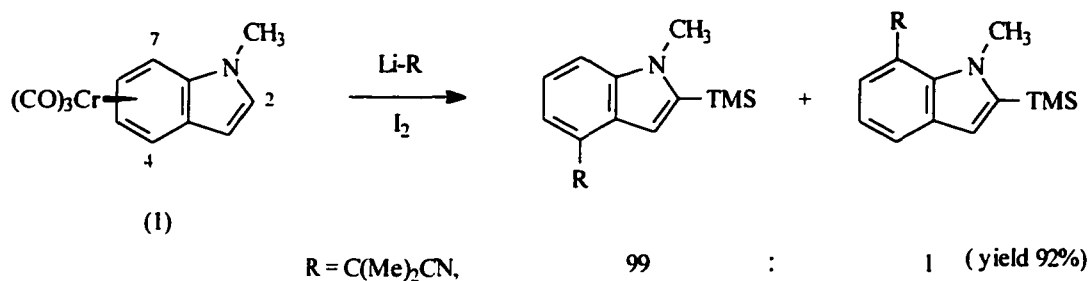
Scheme 1.1



The chemistry of indole is particularly interesting, because the introduction of a transition metal such as $\text{Cr}(\text{CO})_3$ unit selectively activates the six-membered ring, while in free indole the five membered ring dominates the nucleophilic addition reactivity.^{13,14} The selectivity in addition to the $\text{Cr}(\text{CO})_3$ complexes of indole derivatives shows a preference for addition at C-4 and C-7 with steric effects due to substituents at C-3 and N-1 (Equation 1.1). To better learn how these systems work, it is important to understand how the coordination mode of the ligand influences its reactivity.^{10-11,15}

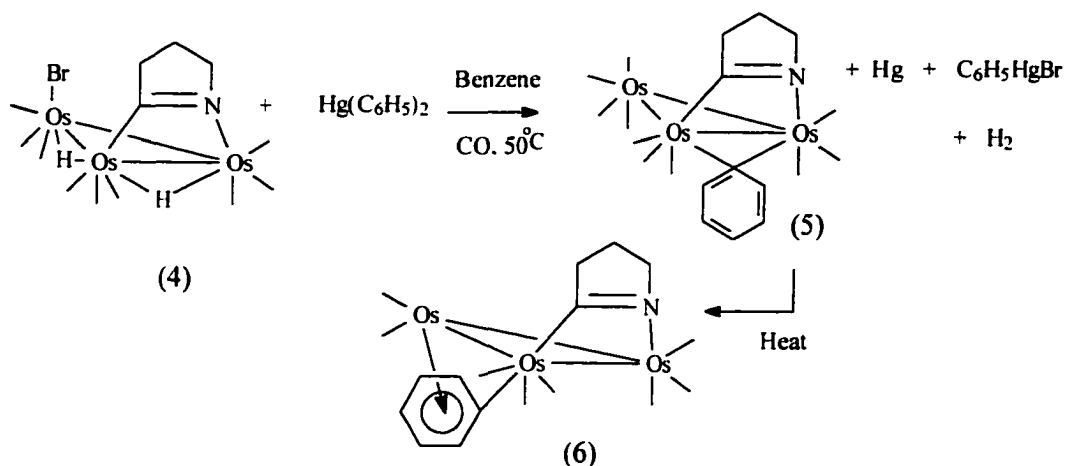
Interest in exploring the scope and selectivity of nucleophilic attack on aromatic systems to yield asymmetric stereoselective products has become increasingly important with the development of pharmaceuticals and agrochemicals which require better methods for producing homochiral materials. This has in turn led the synthetic chemist to explore and invent new methods using transition metals suitable for homochiral synthesis.

Equation 1.1



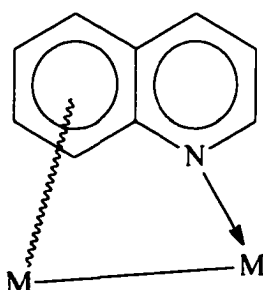
The use of polymetallic complexes containing organic ligands in unusual bonding modes has shed considerable light on how a given organic ligand can interact with a polymetallic site on a metal surface.¹⁶ The use of polymetallic complexes leads to the possibility of multi-site coordination to the ligand. In some cases one metal can coordinate or protect one site, the others can activate the complex by forming an electron deficient bond. An early example showing this bonding mode involves the reaction of a trimetallic cluster containing a terminal halide $\text{Os}_3(\text{CO})_9(\mu\text{-}\eta^2\text{-C=N}(\text{CH}_2)_3\text{Br})$ (**4**) with diphenylmercury under a CO atmosphere, which yielded $\text{Os}_3(\text{CO})_{10}(\mu\text{-}\eta^2\text{-C=N}(\text{CH}_2)_3(\mu\text{-}\eta^1\text{-C}_6\text{H}_5))$ (**5**) (Equation 1.2). Thermolysis of **5** at 100°C leads to rapid decarbonylation and formation of one major product $\text{Os}_3(\text{CO})_8(\mu\text{-}\eta^2\text{-C=N}(\text{CH}_2)_3(\mu\text{-}\eta^1:\eta^6\text{-C}_6\text{H}_5))$ (**6**), making a unique example of a new μ -bonding mode for phenyl ligand. Several other examples of trimetallic clusters containing a $\mu_1\text{-}\eta^1$ -benzene interactions where the benzene ring is part of a more complex ligand system have been reported.¹⁶

Equation 1.2



This multi-metal coordination was extended to include indoline, tetrahydroquinoline (THQ) and quinoline ligands. In this case, the use of polymetallic binding holds out the possibility of multi-site interactions which can alter the molecules reactivity (Scheme 1.2).

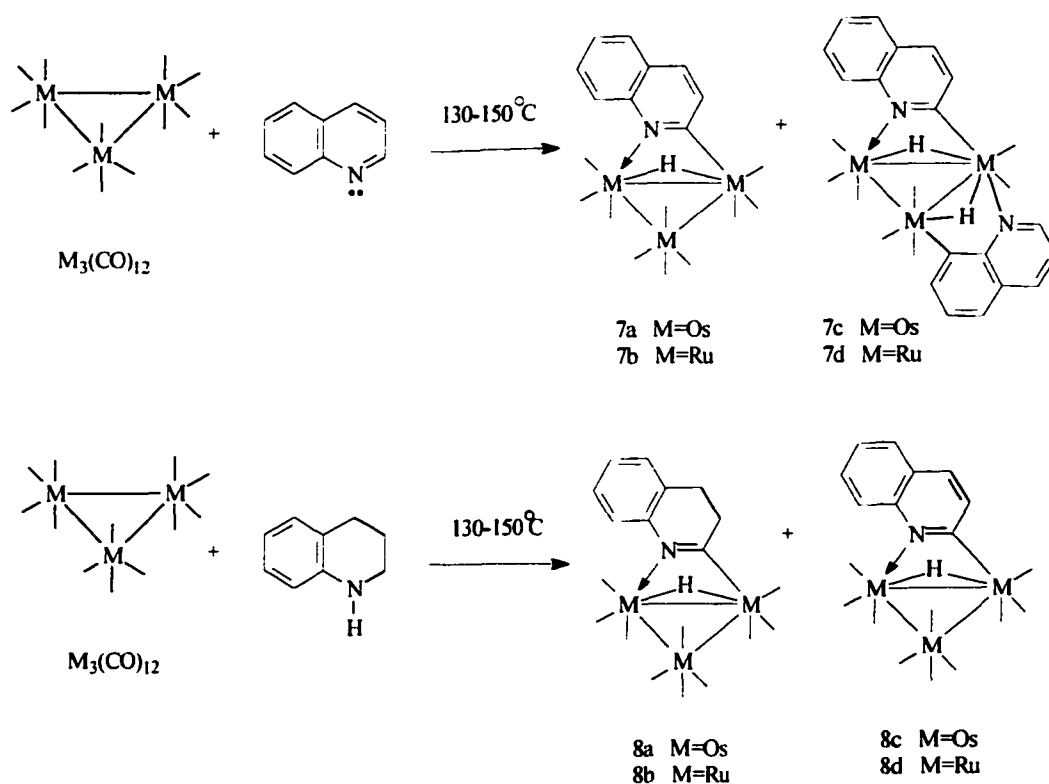
Scheme 1.2



The reaction of quinoline and tetrahydroquinoline (THQ) with $\text{M}_3(\text{CO})_{12}$ ($\text{M}=\text{Ru}, \text{Os}$) at elevated temperatures ($130\text{-}150^\circ\text{C}$) has been previously examined. Quinoline yields both mono- and bis-quinoline adducts $\text{M}_3(\text{CO})_{10}(\mu\text{-}\eta^2\text{-C}_9\text{H}_6\text{N})(\mu\text{-H})$ (**7a** and **7b**) and $\text{M}_3(\text{CO})_8(\mu\text{-}$

η^2 -(C₉H₆N)₂(μ -H)₂ (**7c** and **7d**) but for tetrahydroquinoline monoamine adducts M₃(CO)₁₀(μ - η^2 -C₉H₈N)(μ -H) (**8a** and **8b**) and M₃(CO)₁₀(μ - η^2 -C₉H₆N)(μ -H) (**8c** and **8d**) predominate. For both cases the C(2) C-H bond has oxidatively added to the cluster, coordinating exclusively at the heterocyclic ring via coordination of C(2) and the nitrogen lone pair (Scheme 1.3).^{17,18} The mechanism by which this reaction is thought to occur involves a dissociation of a single CO from the metals at elevated temperature, to open a single coordination site, followed by coordination of the nitrogen lone pair, and rearrangement to an

Scheme 1.3

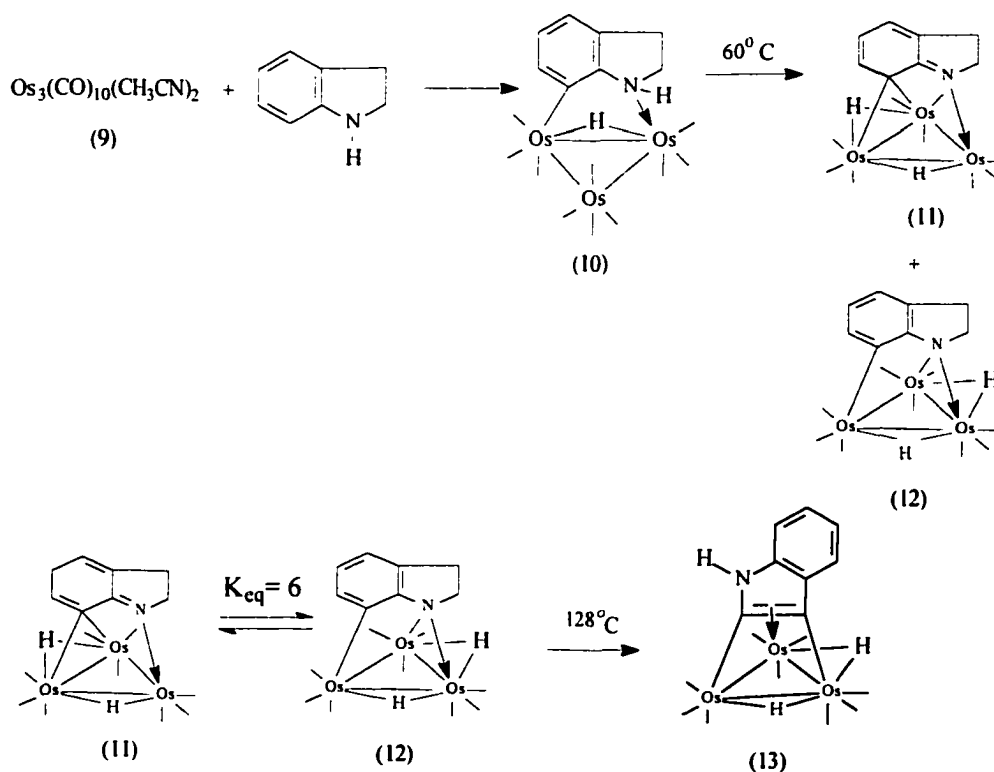


η^2 -C=N complex, dissociation of a second CO and finally C(2)-H bond cleavage.^{17,18} These

complexes are formed in very low yields and were found to be unreactive towards nucleophiles.¹⁷

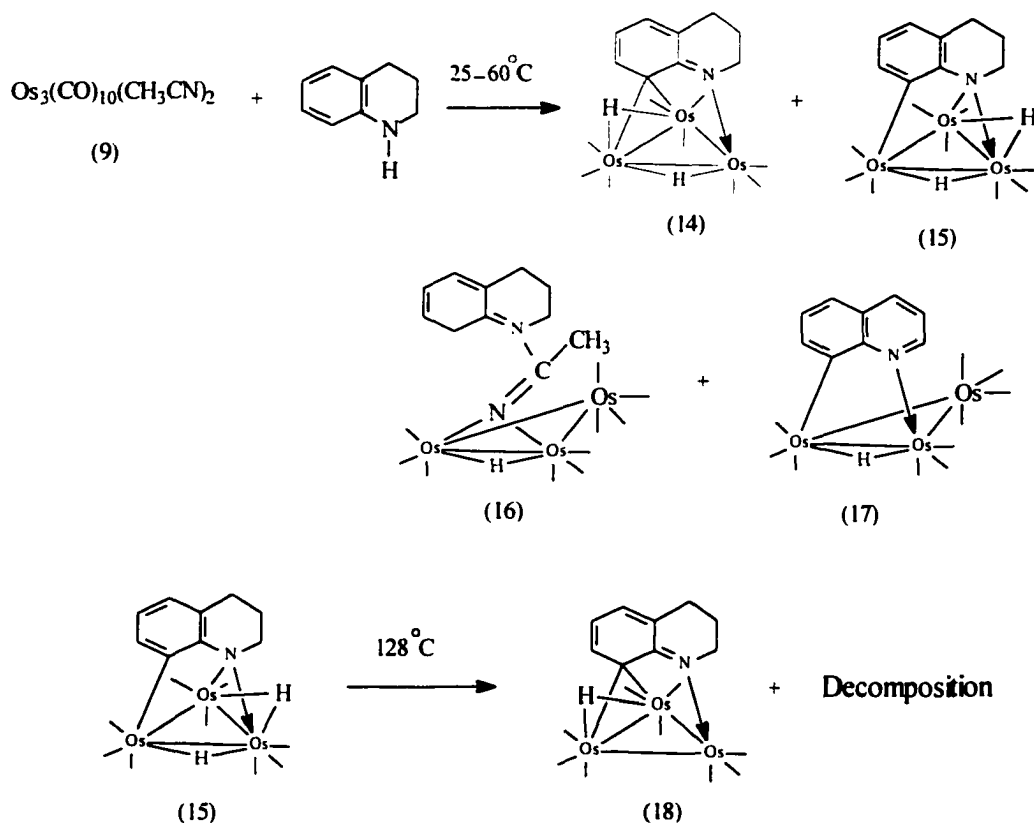
In contrast, the reaction of indoline with the lightly stabilized triosmium cluster $\text{Os}_3(\text{CO})_{10}(\text{CH}_3\text{CN})_2$ (**9**) resulted in coordination of the nitrogen lone pair and the C(7) position of the carbocyclic ring, compound (**10**), which decarbonylates thermally at 60°C to give a mixture of tautomeric complexes $\text{Os}_3(\text{CO})_9(\mu\text{-H})_2(\mu_3\text{-}\eta^2\text{-C}_8\text{H}_7\text{N})(\mu\text{-H})_2$ (**11** and **12**) whose structures differ by having a μ -alkylidene-imino bonding mode (**10**) vs a μ -amido-aryl bonding mode (**11**).¹⁹ Further thermolysis of **11** or **12** yields the dehydrogenated cluster $\text{Os}_3(\text{CO})_9(\mu\text{-H})_2(\mu_3\text{-}\eta^2\text{-C}_8\text{H}_4\text{NH})$ (**13**) (Scheme 1.4).¹⁹

Scheme 1.4



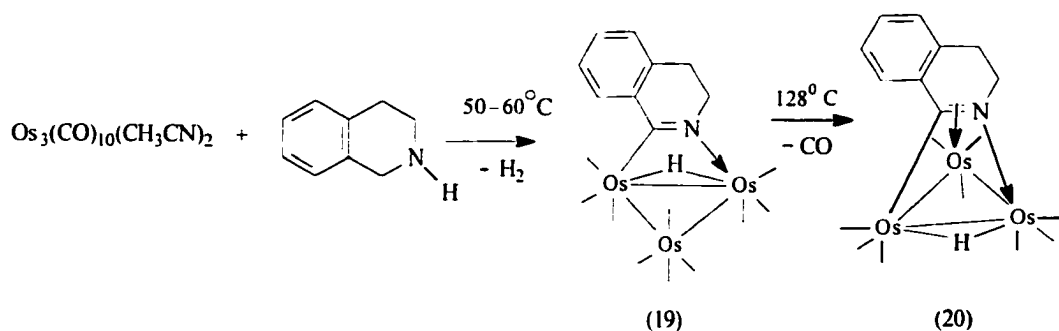
In the case of tetrahydroquinoline (THQ) reacting with (9) no direct analog of (10) is observed but a pair of tautomers $\text{Os}_3(\text{CO})_9(\mu\text{-H})_2(\mu_3\text{-}\eta^2\text{-C}_9\text{H}_9\text{N})$ (14 and 15) directly analogous to 11 and 12 are observed. In addition, a product $\text{Os}_3(\text{CO})_{10}(\mu\text{-H})(\mu\text{-}\eta^1\text{-C}_9\text{H}_{10}\text{N}(\text{CH}_3)\text{CN})$ (16) is obtained, which is the result of an apparent nucleophilic attack of THQ on the coordinated acetonitrile.¹⁹ Thermolysis of 15 yields the dehydrogenated product $\text{Os}_3(\text{CO})_{10}(\mu\text{-H})(\mu\text{-}\eta^2\text{-C}_9\text{H}_8\text{N})$ (18) which maintains the $\eta^2\text{-C(8)-N}$ bonding to the metal core (Scheme 1.5)¹⁹ and has an electron deficient bonding mode between the carbocycle and one edge of the metal triangle.

Scheme 1.5



The reaction of tetrahydroisoquinoline (ITHQ) with (9) in benzene at 50°C yields a single product, $\text{Os}_3(\text{CO})_{10}(\mu\text{-H})(\mu\text{-}\eta^2\text{-C}_9\text{H}_8\text{N})$ (19), in 69% yield. Decarbonylation of 19 is readily accomplished either thermally or photochemically to yield $\text{Os}_3(\text{CO})_9(\mu\text{-H})(\mu_3\text{-}\eta^2\text{-C}_9\text{H}_8\text{N})$ (20) (Equation 1.3).¹⁹

Equation 1.3



Recently the reactions of quinoline (and substituted quinolines) with the lightly stabilized cluster $\text{Os}_3(\text{CO})_{10}(\text{CH}_3\text{CN})_2$ (9) have been studied which at ambient temperatures result in the formation of the major product $\text{Os}_3(\text{CO})_{10}(\mu\text{-}\eta^2\text{-C}_9\text{H}_6\text{N})(\mu\text{-H})$ (21a-r) where the nitrogen lone pair is coordinated and the C(8) carbon hydrogen bond have been oxidatively added to the cluster. Minor amounts of the previously reported isomeric compound $\text{Os}_3(\text{CO})_{10}(\mu\text{-}\eta^2\text{-C}_9\text{H}_6\text{N})(\mu\text{-H})$ (22) were also formed.²⁰ Decarbonylation of 21a-r thermally or photochemically gives the novel electron deficient (46e⁻ system) deep green complexes $\text{Os}_3(\text{CO})_9(\mu_3\text{-}\eta^2\text{-C}_9\text{H}_6\text{N})(\mu\text{-H})$ (23a-r).³ The quinoline ring is bound to the cluster by coordination of the nitrogen lone pair and a three center and two electron bond with C(8) (Scheme 1.6). Table 1.1 shows the synthesized mono-substituted electron deficient quinoline triosmium clusters along with the yields.

Scheme 1.6

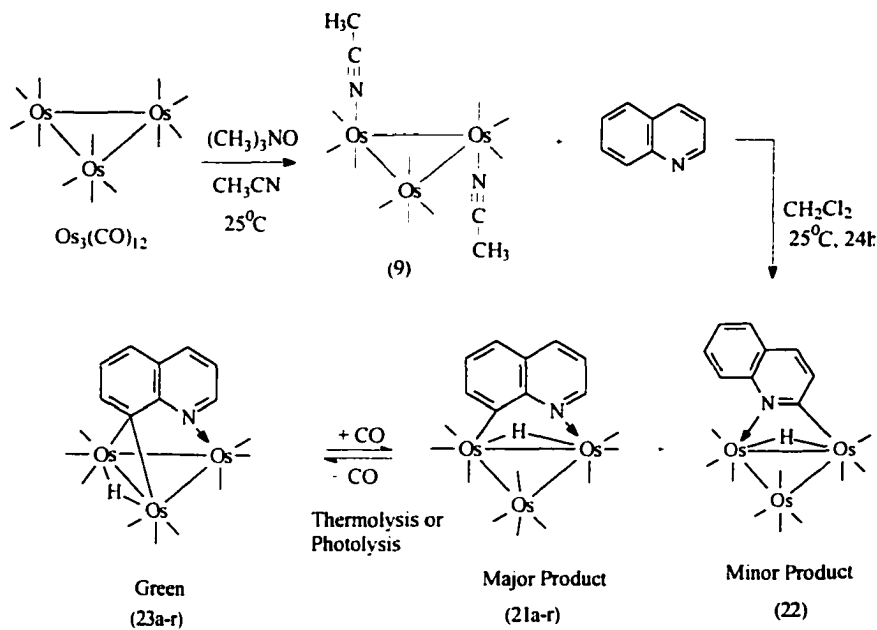


Table 1.1 The synthesized mono-substituted electron deficient quinoline triosmium clusters

| Compound | Yield (%) | Substituent | Compound | Yield (%) | Substituent |
|----------|-----------|--------------------|----------|-----------|-----------------------------------|
| 23a | 68 | H | 23b | 59 | 3-CO ₂ CH ₃ |
| 23c | 50-60 | 3-NH ₂ | 23d | 72 | 4-CH ₃ |
| 23e | 76 | 4-Cl | 23f | 69 | 4-OCH ₃ |
| 23g | 72 | 4-NH ₂ | 23h | 40 | 4-CO ₂ CH ₃ |
| 23i | 70 | 5-F | 23j | 70 | 5-Cl |
| 23k | 83 | 5-Br | 23l | 82 | 5-NH ₂ |
| 23m | 84 | 6-CH ₃ | 23n | 74 | 6-Cl |
| 23o | 56 | 6-OCH ₃ | 23p | 61 | 6-CO ₂ CH ₃ |
| 23q | 50-60 | 6-NH ₂ | 23r | 43 | 6-OH |

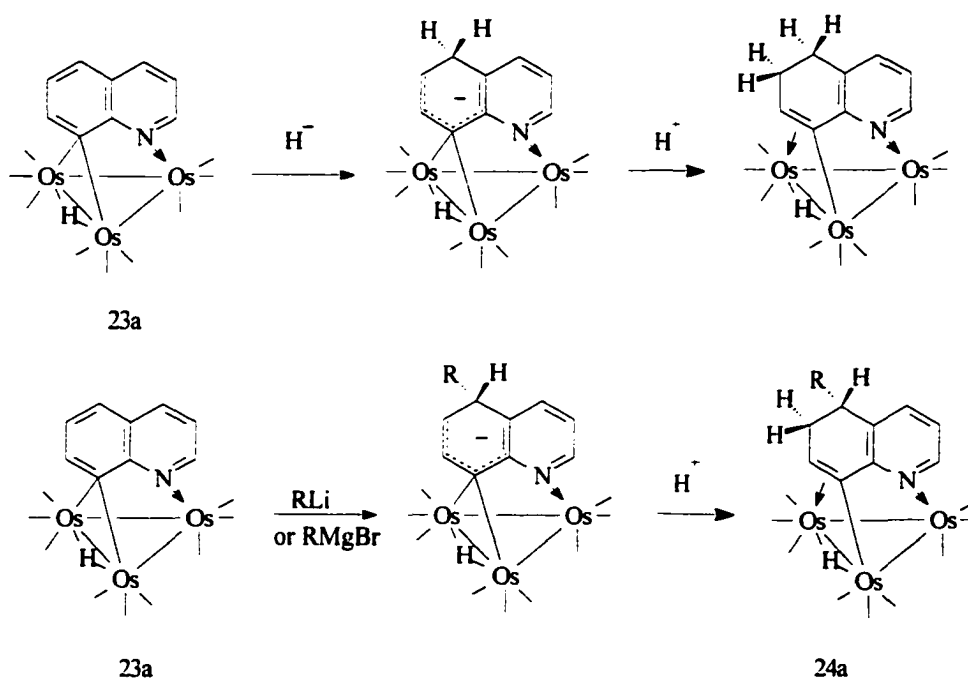
These electron deficient quinoline complexes are shown to undergo phosphine, CO, and H₂ addition to the metal which proceeds reversibly (for CO) under moderate conditions, analogous to other 46e⁻ trimetallic complexes.²¹

The transition metal activated nucleophilic addition and substitution reactions of π -bound arenes have proven to be an extremely useful addition to the organic chemists' arsenal for functionalizing arenes, cyclizations, and asymmetric synthesis.²²⁻²⁴ This technique has been applied to bicyclic arenes, heterocycles²⁵ and indoles.^{25,26} via nucleophilic addition to the coordinated ring. Quinoline prefers η^1 -N coordination over η^6 -coordination to the carbocyclic ring, in sharp contrast to indoles, due to their greater basicity (from having the lone electron pair on the nitrogen atom exocyclic to the ring).²⁷ There are thus few π - η^6 -arene complexes of quinoline, and nucleophilic addition and substitution has been only studied for the η^1 -N transition metal complexes.²⁸

Recently, the reactivity of the family of electron deficient μ_3 - η^2 complexes of quinoline (**23a-r**) which undergo regioselective nucleophilic addition of hydride and a wide range of carbanions at the 5-position (Scheme 1.7) to form a σ - μ vinyl complex of the type **24a** has also been reported.^{1,3,21}

The nucleophilic attack observed at the 5-position of the carbocyclic ring is unprecedented. In quinolines (or η^1 -N coordinated) the normal site of electrophilic attack is the 5- and 8-positions, while nucleophilic attack is usually at the 2- or the 4- position if the former is blocked.^{28,29} Nucleophilic attack on " σ , π vinyl" complexes of triosmium cluster has previously also been reported.²⁸

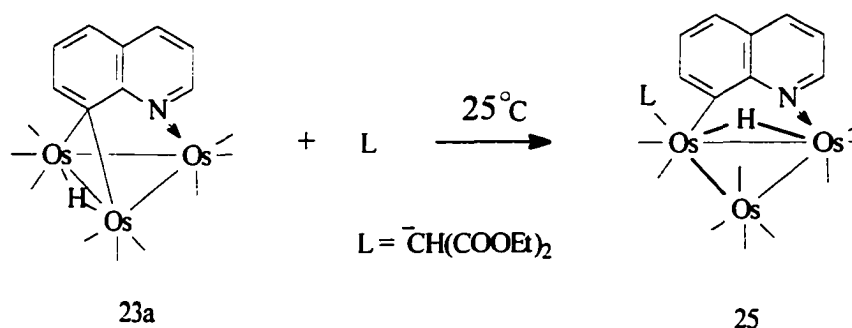
Scheme 1.7



When compounds **23a-l** are reacted with a two-to-three fold excess of the carbanions listed in table 1.2 at -78°C , the nucleophilic addition products $[\text{Os}_3(\text{CO})_9(\mu_3-\eta^3\text{-C}_9\text{H}_7(5\text{-R}')\text{N}(\mu\text{-H}))]$ (**24a-l**) are isolated in moderate to good yields after quenching with acid (Table 1.2). The only carbanion tried that did not result in nucleophilic addition on the ring was sodium diethylmalonate which apparently complexes with **23a** at the metal core to give **25** as evidenced by the reversible color change from green to yellow when this reagent is added to **23a** at -78°C and then warmed to room temperature (Equation 1.4). This behavior, and the associated color change, is similar to that observed for the reaction of **23a** with neutral two electron donors.^{9,21} Methoxide also failed to react with **23a**. It can be seen from the yields listed in Table 1.2 that the harder, more nucleophilic carbanions give somewhat lower yields than the softer nucleophiles. This is probably due to competing attack at the coordinated

carbonyl groups, leading to decomposition. Overall, **23a** reacts with a broader range of nucleophiles relative to the neutral monometallic π -arene complexes.³⁰ This is undoubtedly due to localization of the electron deficiency at the 5- position resulting from the electron deficient bonding to the cluster.^{1,3,21} Thus lithium t-butyl acetate reacts quite well with **23a** while in the case of $(\pi\text{-}\eta^6\text{ arene})\text{Cr}(\text{CO})_3$ yields were quite low except in the presence of very polar solvents such as HMPA or by using the corresponding potassium salt. Methyl lithium

Equation 1.4



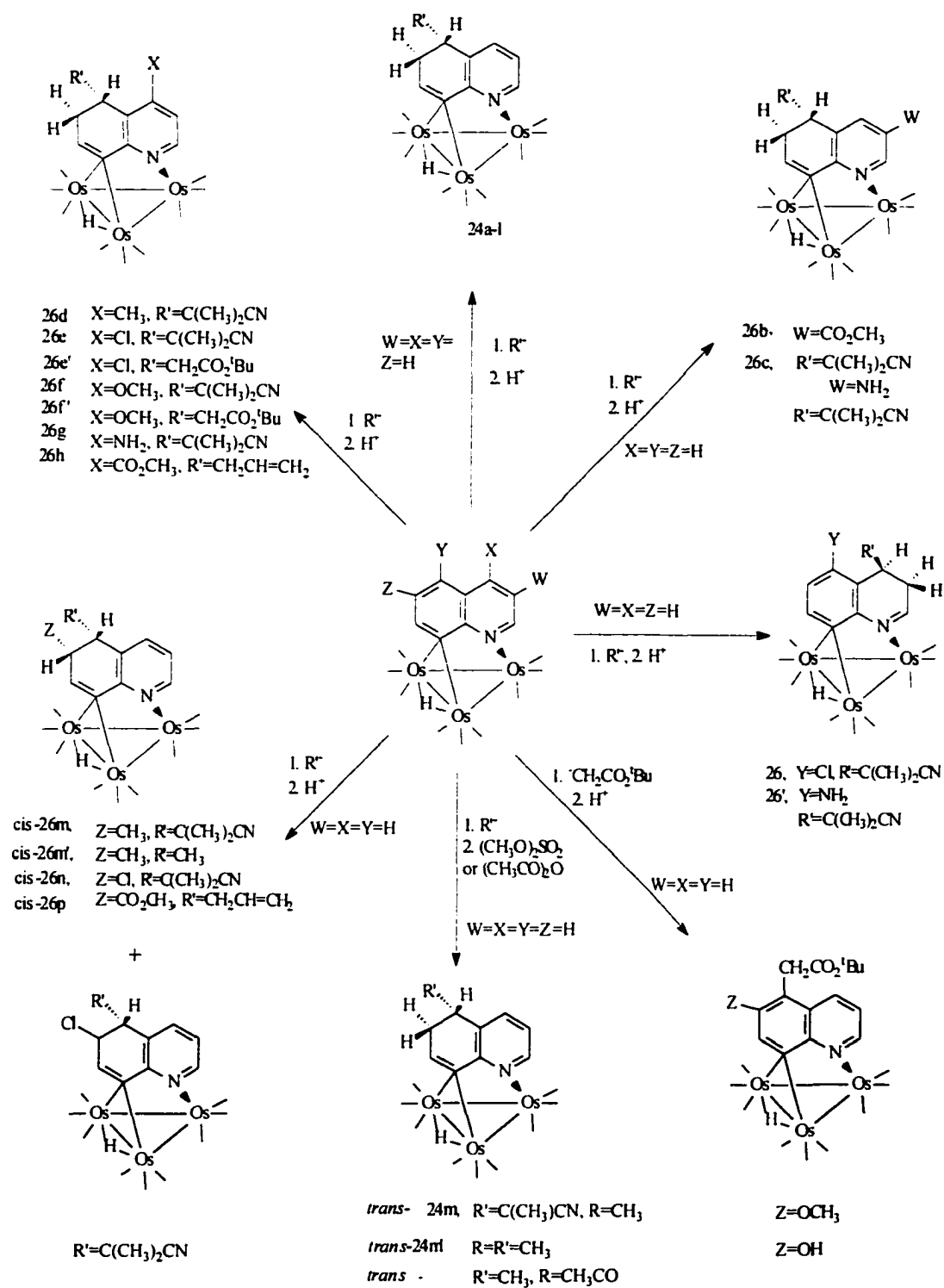
and n-butyl lithium deprotonate $(\pi\text{-}\eta^6\text{-arene})\text{Cr}(\text{CO})_3$ while **23a** yields the usual nucleophilic addition products.³⁰ Indeed deprotonation with lithium diisopropylamide gave no evidence for this mode of reaction with **23a**.³

Reactions of carbanions with electron deficient quinoline trismium clusters, $[\text{Os}_3(\text{CO})_9(\mu_3\text{-}\eta^2\text{-C}_9\text{H}_5(\text{R})\text{N})(\mu\text{-H})]$ (R can be wide range of substituents in the 3-, 4-, 5- and 6-positions of the quinoline ring) are illustrated in scheme (1.8).³ These complexes react with a wide range of carbanions to give the nucleophilic addition products $\text{Os}_3(\text{CO})_9(\mu_3\text{-}\eta^3\text{-C}_9\text{H}_7(5\text{-R}')\text{N})(\mu\text{-H})$ (**24a-l**).

Table 1.2: Isolated nucleophilic addition product yields from the reaction of electron deficient quinoline trismium cluster, $\text{Os}_3(\text{CO})_9(\mu_3-\eta^3\text{-C}_9\text{H}_6\text{N}(\mu\text{-H}))$ with carbanions.

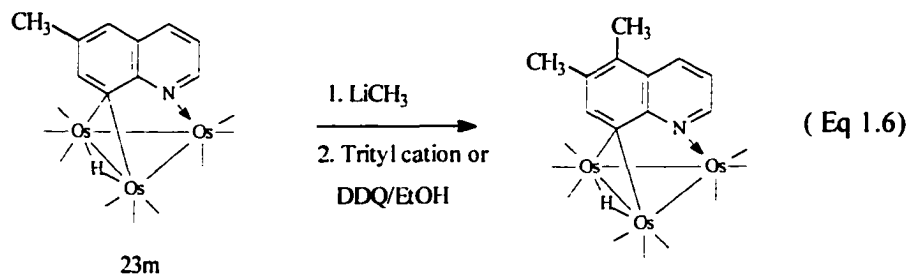
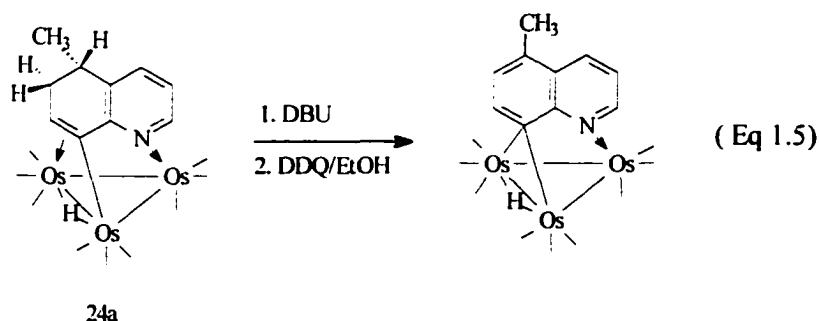
| Compound | Yield(%) | Carbanion | Compound | Yield(%) | Carbanion |
|----------|----------|--|----------|----------|--|
| 24a | 65 | LiMe | 24b | 45 | Li ⁿ Bu |
| 24c | 52 | Li ^t Bu | 24d | 48 | LiBz |
| 24e | 66 | LiPh | 24f | 51 | LiCH=CH ₂ |
| 24g | 48 | LiC ₂ (CH ₂) ₃ CH ₃ | 24h | 72 | LiCH ₂ CN |
| 24i | 69 | LiC(CH ₃) ₂ CN | 24j | 72 | Li-CHS(CH ₂) ₂ S- |
| 24k | 86 | LiCH ₂ CO ₂ ^t Bu | 24l | 53 | CH ₂ =CHCH ₂ MgBr |
| 24a | 43 | MeMgBr | | | |

Substitution at the 3- or 4- position is well tolerated giving the expected nucleophilic addition products $\text{Os}_3(\text{CO})_9(\mu_3-\eta^3\text{-C}_9\text{H}_6(3\text{- or }4\text{-R})(5\text{-R}')\text{N})(\mu\text{-H})$ (**26b-h**). The 6-substituted derivatives give >95% of the cis-diastereomer, $\text{Os}_3(\text{CO})_9(\mu_3-\eta^3\text{-C}_9\text{H}_6(5\text{-R}')(6\text{-R})\text{N})(\mu\text{-H})$ (**26m-p**). The stereochemistry is preserved even in the case of less bulky carbanions (R'=CH₃). The trans-diastereomer of the addition products obtained from the 6-substituted derivatives can be synthesized by the reaction of the unsubstituted complex with R'Li followed by quenching with (CH₃O)₂SO₂. Acetic anhydride can also be used as the quenching electrophile for the intermediate anions generated from the R'Li (trans- $\text{Os}_3(\text{CO})_9(\mu_3-\eta^3\text{-C}_9\text{H}_6(6\text{-CH}_3\text{CO})(5\text{-CH}_3)\text{N})(\mu\text{-H})$). Nucleophilic addition occurs across the 3, 4-bond in the cases where the 5-position is occupied by a substituent.



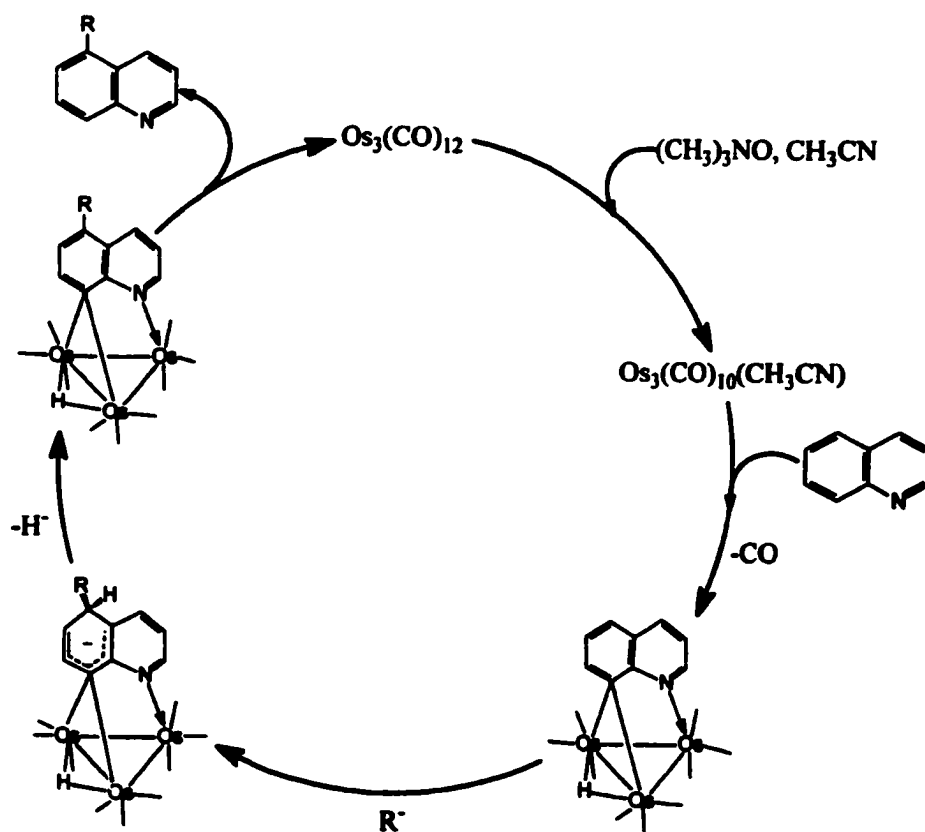
Scheme 1.8

The nucleophilic addition products of the type **24** or **26** can be rearomatized by the reactions with a deprotonating agent diazabicyclononane (DBU) followed by dichlorodicyanoquinone (DDQ)/ EtOH (Equation 1.5) or by the reaction of the intermediate anion formed by an attack of a nucleophile with trityl cation or DDQ followed by an ethanol quench of the resulting hydroquinone anion and excess carbanion (Equation 1.6).



The resulting rearomatized complexes can be cleanly cleaved from the cluster by heating at 70°C in acetonitrile under a CO atmosphere yielding the functionalized quinoline and $\text{Os}_3(\text{CO})_{12}$ as the only two products. Successful cleavage by this method constitutes a stoichiometric cycle for selectively alkylating quinolines at the 5-position (Scheme 1.9). Unfortunately, this method does not extend to the nucleophilic addition products of structural types **24** or **26**. Although cleavage is observed at elevated pressures of carbon monoxide, the reaction is not clean resulting in a mixture of products.

Scheme 1.9



Major Objectives

- 1) To extend the synthesis of electron deficient complexes of triosmium clusters that have been found for quinoline and their substituted derivatives to other benzoheterocycles that contain a pyridinyl nitrogen atom β to the electron deficient bond of a fused benzene ring.
- 2) To understand the influence of the functional groups in forming the electron deficient bonding mode to benzoheterocycles.
- 3) To understand the degree of electronic communication between the benzoheterocyclic ring and the metal core in order to define the stereodynamics of their coordination sites.
- 4) To understand the reactivities of the electron deficient benzoheterocycles with a small nucleophile (H^-) and a relatively larger carbon based nucleophile.

Chapter 2

The Synthesis of Electron Deficient Benzoheterocycles, $\text{Os}_3(\text{CO})_9(\mu_3\text{-}\eta^2\text{-benzoheterocycle-H})(\mu\text{-H})$

2.1 The Reactions of Benzoheterocycles with $\text{Os}_3(\text{CO})_9(\text{CH}_3\text{CN})_2$

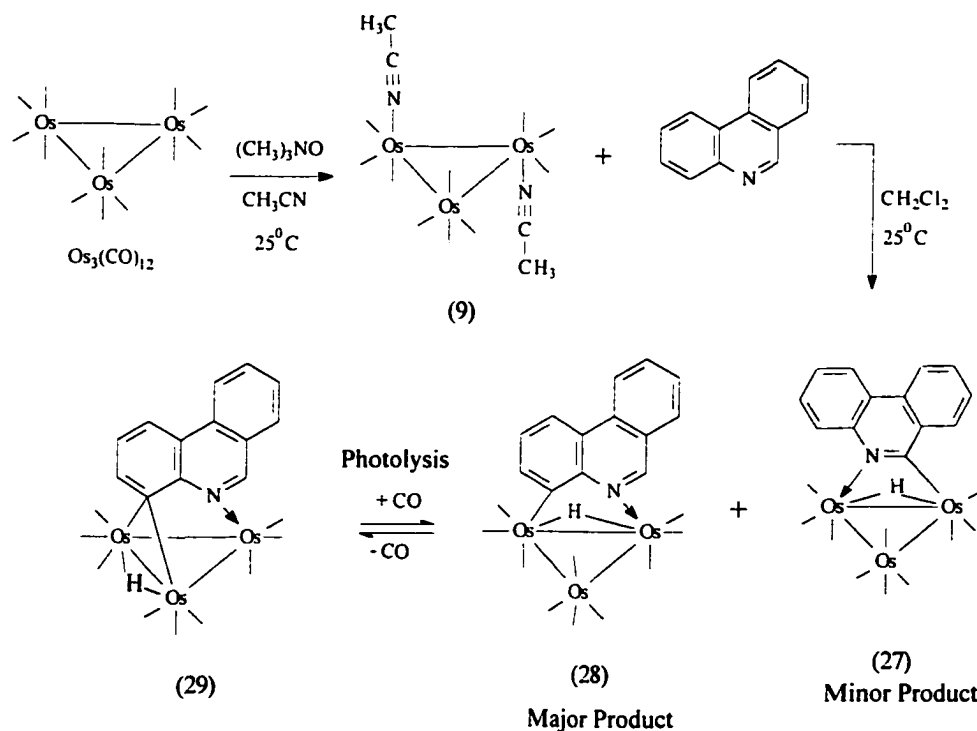
The $\mu_3\text{-}\eta^2$ electron deficient bonding mode which activates the carbocyclic ring of quinoline towards nucleophilic attack at the 5-position is available to an entire class of benzoheterocycles with a pyridinyl nitrogen β to the electron deficient bond of a fused benzene ring. Thus phenanthridine, benzimidazole, benzothiazole, benzoxazole, benzotriazole, quinoxaline all have the same structural features pointing to the possible extension of the synthetic method developed for quinoline to this entire class of heterocycles. The obvious importance of this class of molecules prompted us to explore the generalization of scheme 1.6 (discussed in chapter 1) to these heterocycles.⁴⁻⁸

2.2. Results and Discussion

We have indeed found that the synthesis of electron deficient triosmium complexes can be extended to a wide variety of benzoheterocycles in moderate to good yields. The most obvious extension is to the tricyclic analogs of quinoline. Thus phenanthridine reacts with $\text{Os}_3(\text{CO})_{10}(\text{CH}_3\text{CN})_2$ (**9**) at ambient temperature to give the desired decacarbonyl precursor

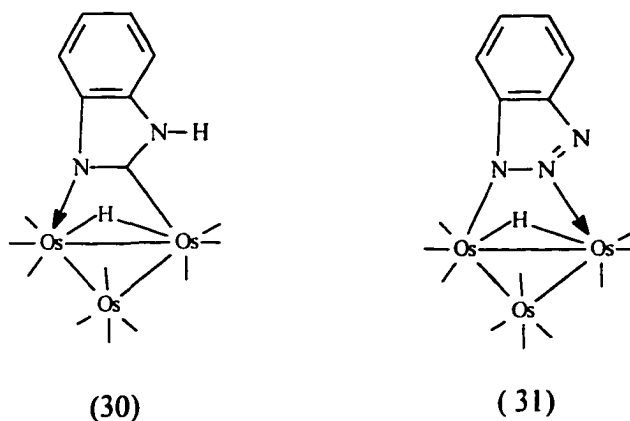
which on photolysis converts to the structural analog of quinoline complex, $\text{Os}_3(\text{CO})_9(\mu_3\text{-}\eta^2\text{-C}_{13}\text{H}_8\text{N})(\mu\text{-H})$ (**29**) in a 60% yield (Scheme 2.1).

Scheme 2.1



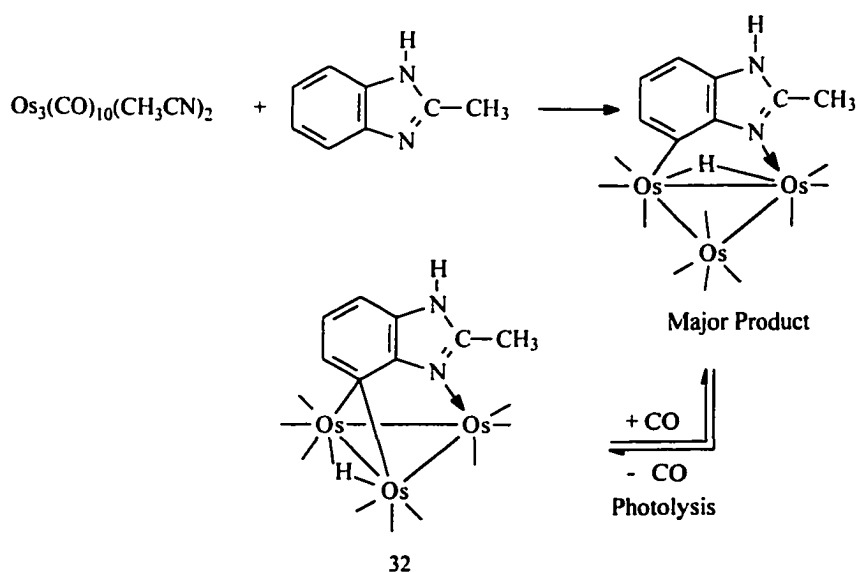
The phenanthridine ring in **29** binds to the cluster by coordination of the nitrogen lone pair and a three center-two electron bond with carbon C(8) giving the novel 46-electron green complex (**29**). The corresponding tricyclic compound 5,6-benzoquinoline reacts in an analogous manner and has been previously reported.³¹ A solid state structure of **29** [$\text{Os}_3(\text{CO})_9(\mu_3\text{-}\eta^2\text{-C}_{13}\text{H}_8\text{N})(\mu\text{-H})$] is shown in Figure 2.1 with the selected bond lengths in Table 2.1. The bond lengths given in table indicate that the aromatic nature of the carbocyclic ring remains unperturbed.

The family of five membered heterocycles containing two heteroatoms and a fused benzene ring is another obvious series to explore. Indeed, the reactions of benzimidazole and benzotriazole with $\text{Os}_3(\text{CO})_{10}(\text{CH}_3\text{CN})_2$ have been reported but the major product is the result of CH or NH activation at the 2-position as shown in structures (30) and (31).^{32, 33}



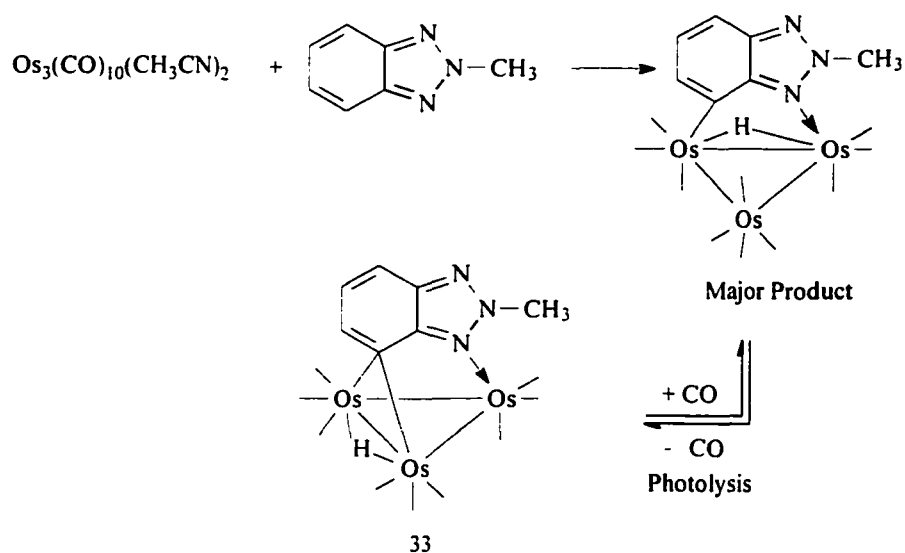
However, if 2-methyl benzimidazole or 2-methyl benzotriazole are used the major product is the decacarbonyl precursor which is the result of CH activation at C(7) which cleanly

Scheme 2.2

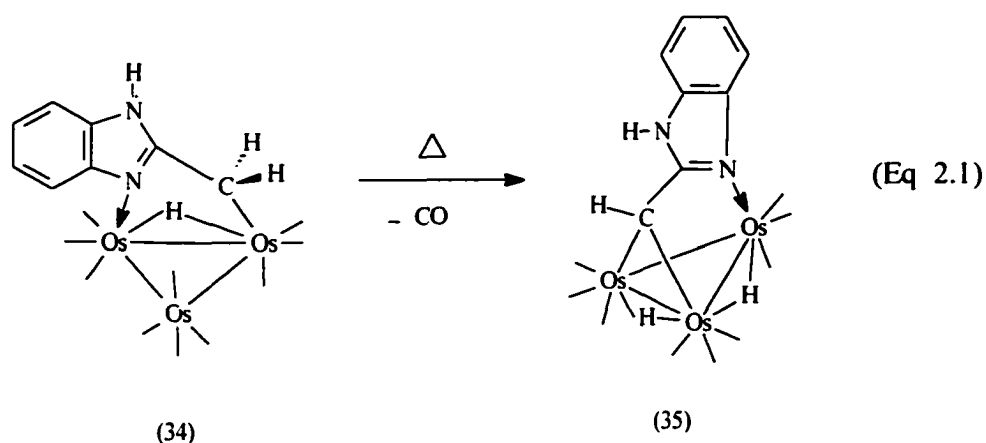


decarbonylate on photolysis to the structural analogs of quinoline[Os₃(CO)₉(μ₃-η²-(2-CH₃)C₇H₄N₂)](μ-H)] (**32**) (Scheme 2.2) and [Os₃(CO)₉(μ₃-η²-(2-CH₃)C₆H₃N)](μ-H)] (**33**) (Scheme 2.3) in yields of 63 and 40% respectively. For quinoline complexes were obtained in the range of 40-80% yields. Solid state structures of **32** and **33** are shown in figures 2.2 and 2.3. In case of 2-methyl benzimidazole, CH activation of methyl side chain at C-2 gives

Scheme 2.3

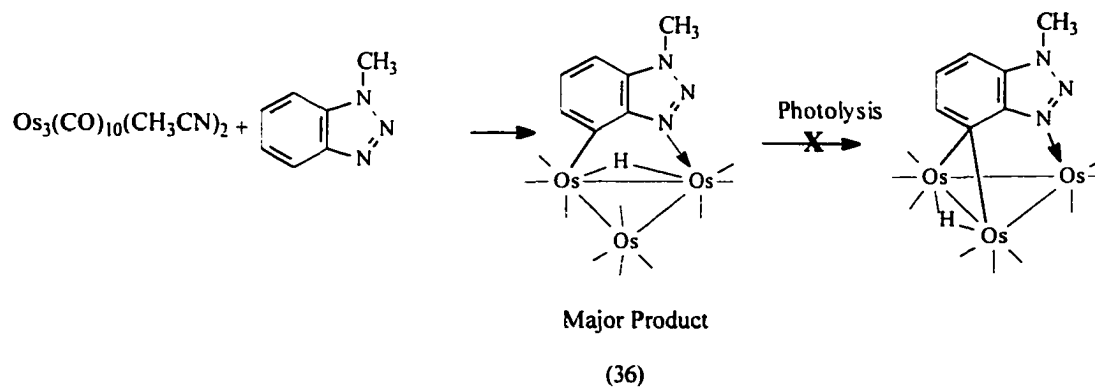


the minor compound (**34**). In the ¹H NMR two doublets at 2.63 ppm and 2.07 ppm are assigned to the two non-equivalent CH₂ hydrogens of the side chain of the product, and the hydride shift comes at -14.21 ppm. Compound (**34**) upon reflux in hexane gives a dihydride complex (**35**) (Equation 2.1). Doublet peaks disappear and a singlet peak appears at 2.16 ppm in the ¹H NMR of **35** and two hydride shifts appear at -14.55 and -14.95 ppm respectively. For 2-methyl benzotriazole only the decacarbonyl precursor is obtained. There is no CH activation of methyl side chain like that of 2-methyl benzimidazole.



Isomeric heterocycle, 1-methyl benzotriazole seems to have produced the desired decacarbonyl precursor (**36**) (as evident from ^1H NMR data and solid state structure, figure 2.4) but photolysis did not result in a $\mu_3\text{-}\eta^2$ complex (Equation 2.2). A solid state structure of **36** is shown in figure 2.4

Equation 2.2



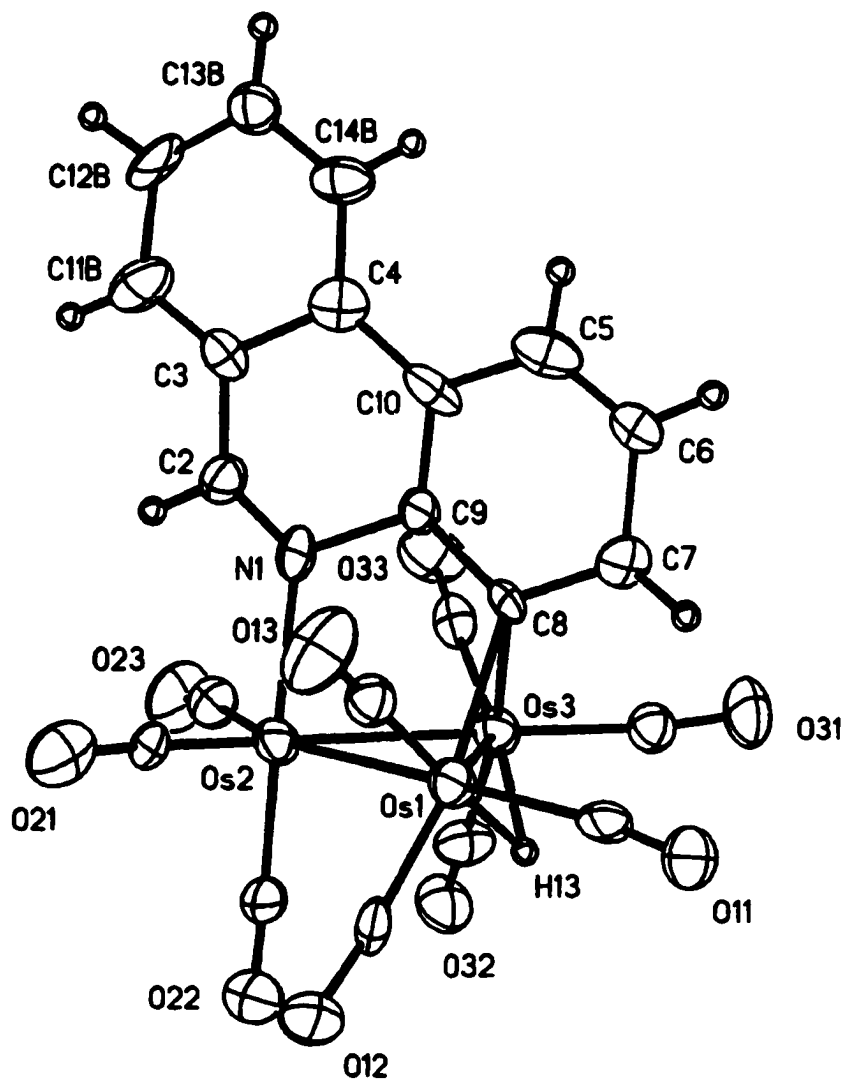


Figure 2.1. Solid state structure of $\text{Os}_3(\text{CO})_9(\mu_3\text{-}\eta^2\text{-C}_{13}\text{H}_8\text{N})(\mu\text{-H})$ (**29**) showing the calculated position of the hydride

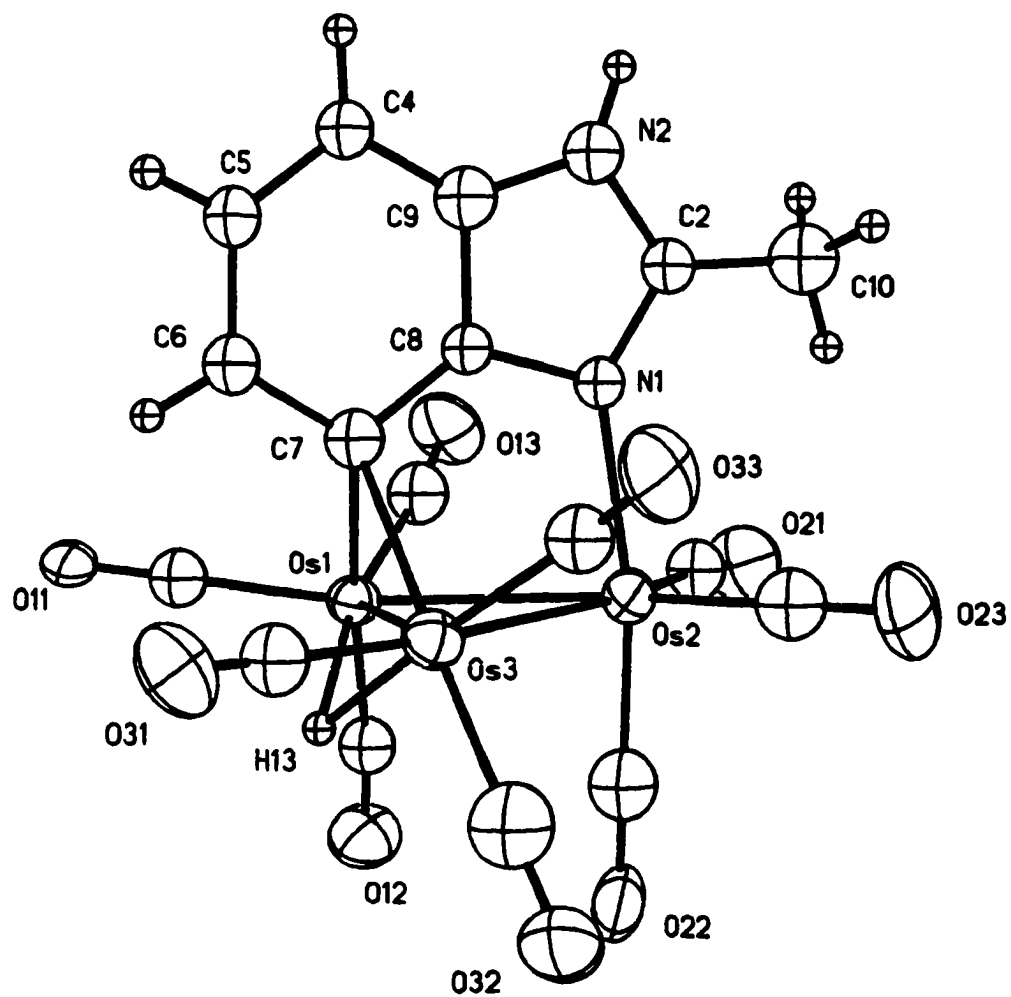


Figure 2.2. Solid state structure of $\text{Os}_3(\text{CO})_9(\mu_3\text{-}\eta^2\text{-C}_7\text{H}_4\text{N}_2(2\text{-CH}_3))(\mu\text{-H})$ (32) showing the calculated position of the hydride.

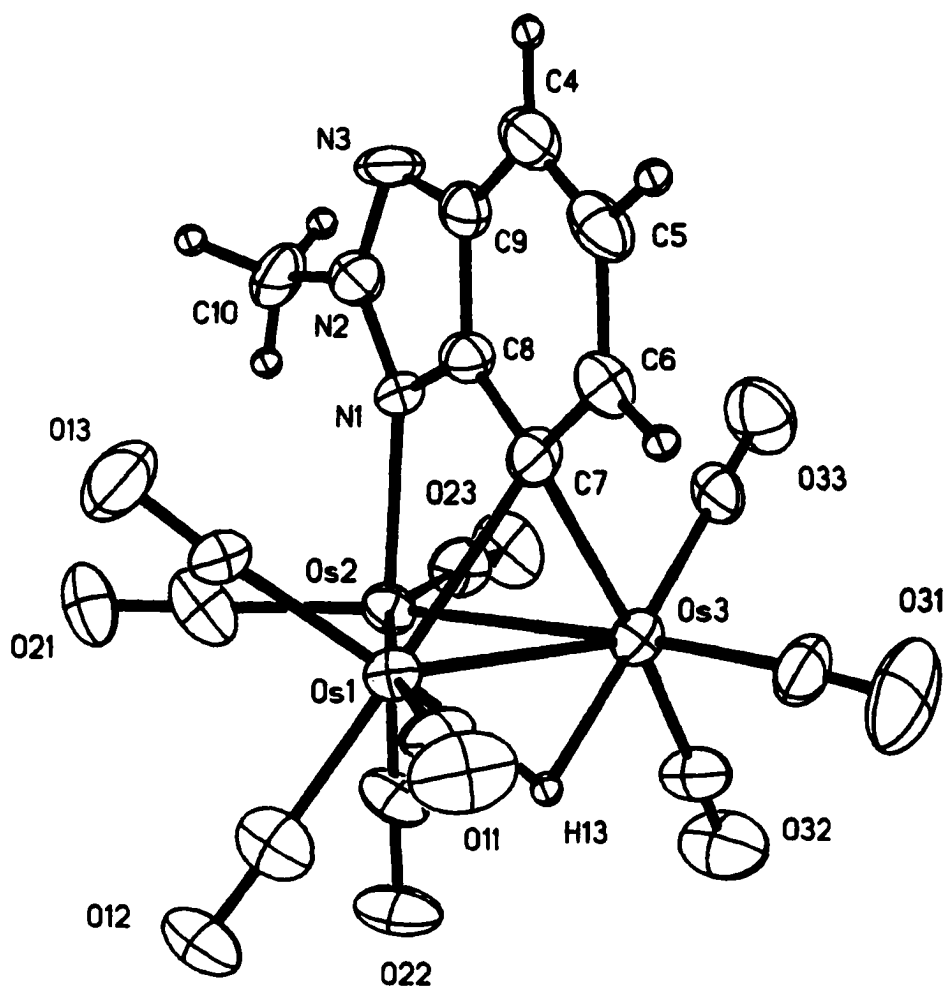


Figure 2.3. Solid state structure of $\text{Os}_3(\text{CO})_9(\mu_3\text{-}\eta^2\text{-C}_6\text{H}_3\text{N}_3(2\text{-CH}_3))(\mu\text{-H})$ (**33**) showing the calculated position of the hydride.

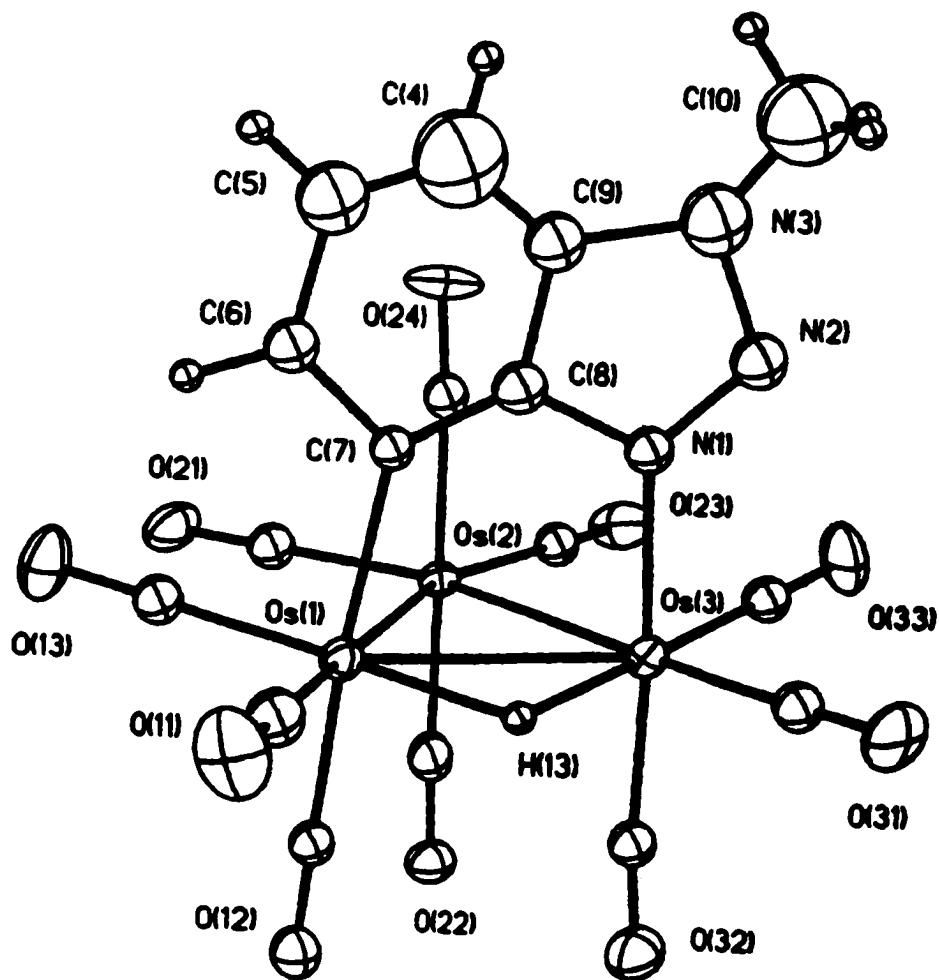
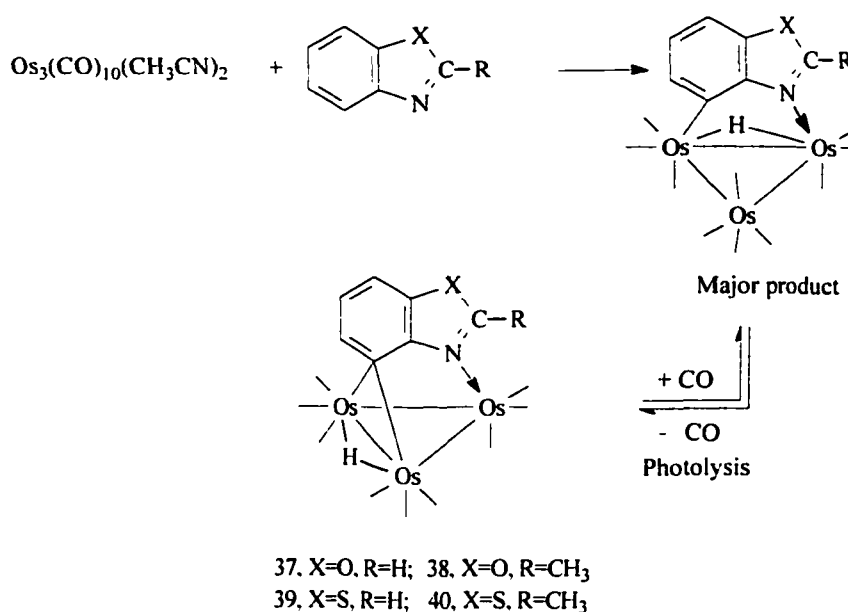


Figure 2.4. Solid state structure of $\text{Os}_3(\text{CO})_{10}(\mu\text{-}\eta^2\text{-C}_6\text{H}_3\text{N}_3(3\text{-CH}_3)(\mu\text{-H})$ (**36**) showing the calculated position of the hydride.

The related heterocycles benzoxazole, 2-methyl benzoxazole, benzothiazole and 2-methyl benzothiazole all give the CH activation at the C(7) and the corresponding analogs of quinoline after photolysis, $[\text{Os}_3(\text{CO})_9(\mu_3\text{-}\eta^2\text{-(2-R)C}_7\text{H}_3\text{NX})(\mu\text{-H})]$ (X=O, R=H, **37**; X=O, R=CH₃, **38**; X=S, R=H, **39**; X=S, R=CH₃, **40**) (Scheme 2.4) in reasonable yields of 37, 50, 59, 55% respectively. Solid state structures of **38** and **39** are shown in figures 2.5 and 2.6.

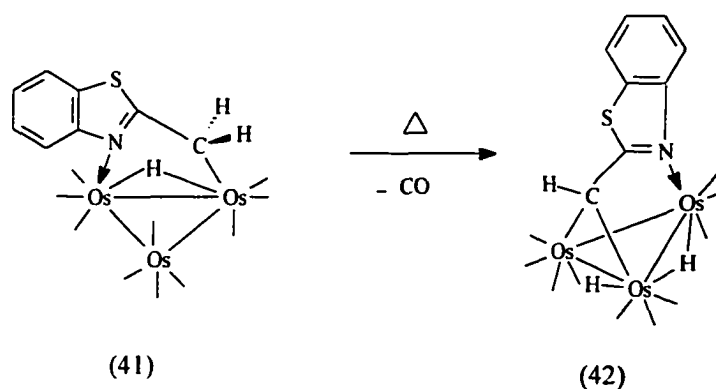
Scheme 2.4



For benzothiazole in addition of decacarbonyl precursor of green product a minor product due to the CH activation at the C-2 occurs like that of quinoline.²¹ While 2-methyl benzoxazole gives only one decacarbonyl precursor and no other product due to CH activation of the methyl side chain, 2-methyl benzothiazole gives a CH activation product of the methyl side chain similar to that of 2-methyl benzimidazole as a minor compound (**41**).

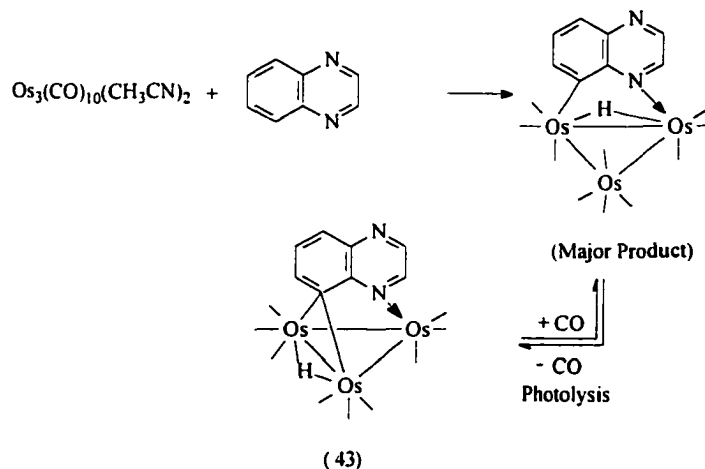
In the ^1H NMR of **41** two doublets appear at 3.20 ppm and 2.60 ppm for two protons of the methylene side chain and the hydride shift comes at -13.57 ppm. Compound (**41**) upon reflux gives a dihydride complex (**42**) (Equation 2.4) where the ^1H NMR spectrum shows only one CH hydrogen of side chain at 2.15 ppm and two hydride shifts at -14.37 and -14.62 ppm respectively.

Equation 2.4



Quinoxaline reacts with $\text{Os}_3(\text{CO})_{10}(\text{CH}_3\text{CN})_2$ to give the analog of quinoline, $[\text{Os}_3(\text{CO})_9(\mu_3\text{-}\eta^2\text{-C}_8\text{H}_5\text{N}_2)(\mu\text{-H})]$ (**43**) after photolysis in good yield, 68% (Scheme 2.5).

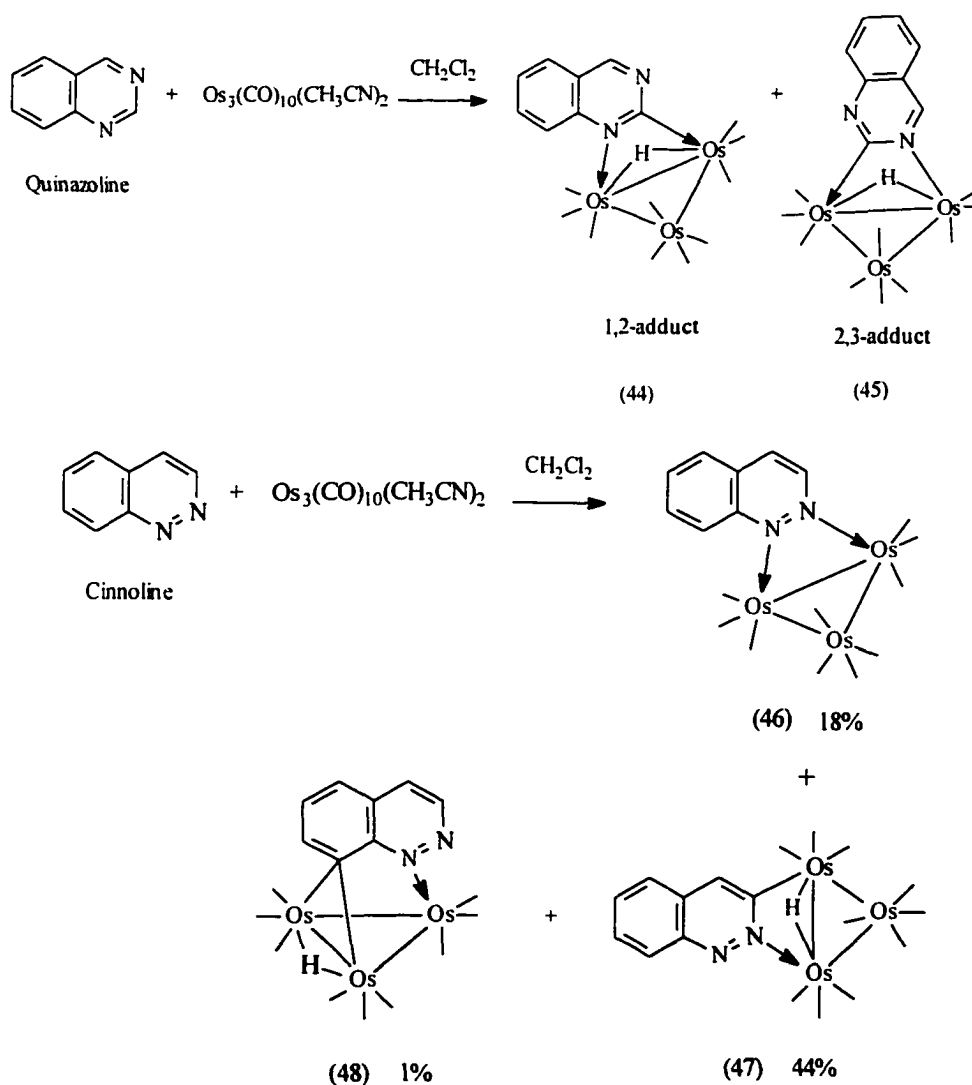
Scheme 2.5



In order to avoid formation of a co-product which appears to be a 2:1 cluster to ligand complex it was necessary to use a larger excess of ligand. The solid state structure of **43** is shown in figure 2.7.

The isomeric heterocycles quinazoline and chinoline do not yield structural analogs of quinoline giving CH activation at C(2) complexes (**44**, **45**) in 1 : 1 ratio and an η^2 -N, N bound complex (**46**) along with a CH (C-2) activation product (**47**) and a very small amount of green complex (**48**) respectively (Scheme 2.6).

Scheme 2.6



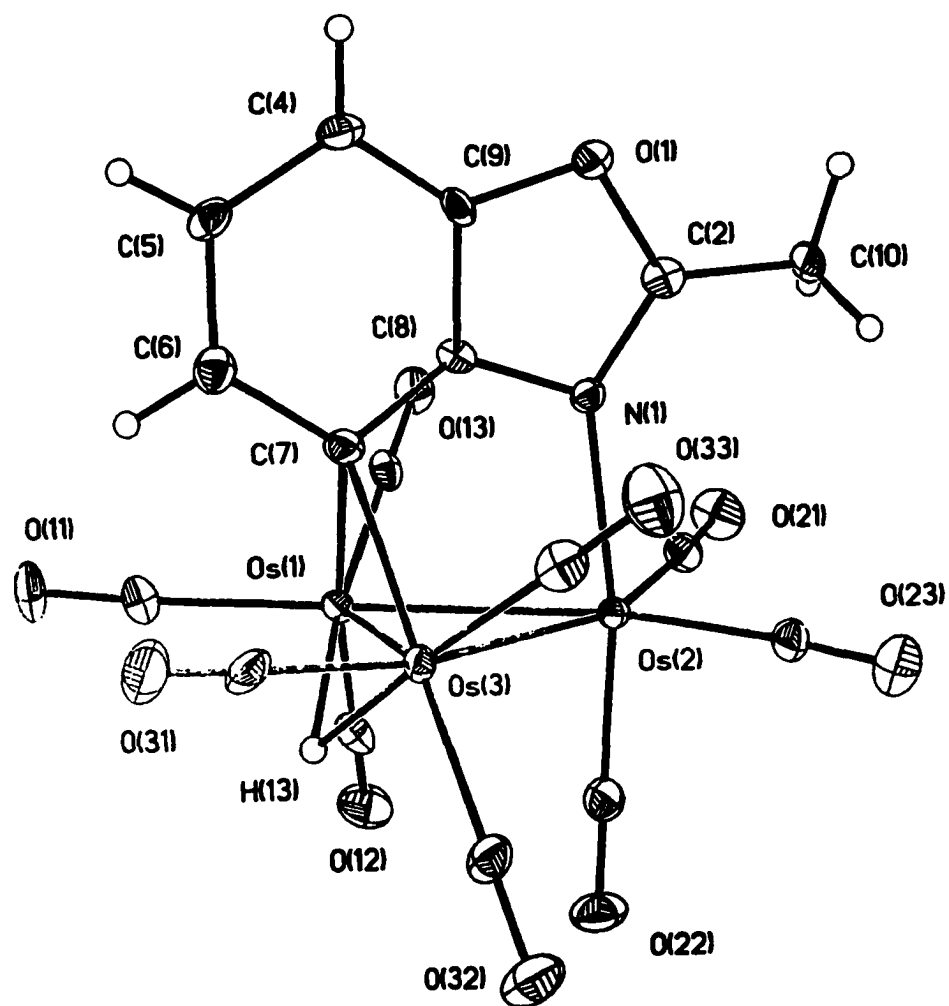


Figure 2.5. Solid state structure of $\text{Os}_3(\text{CO})_9(\mu_3\text{-}\eta^2\text{-C}_7\text{H}_3\text{NO}(2\text{-CH}_3))(\mu\text{-H})$ (**38**) showing the calculated position of the hydride.

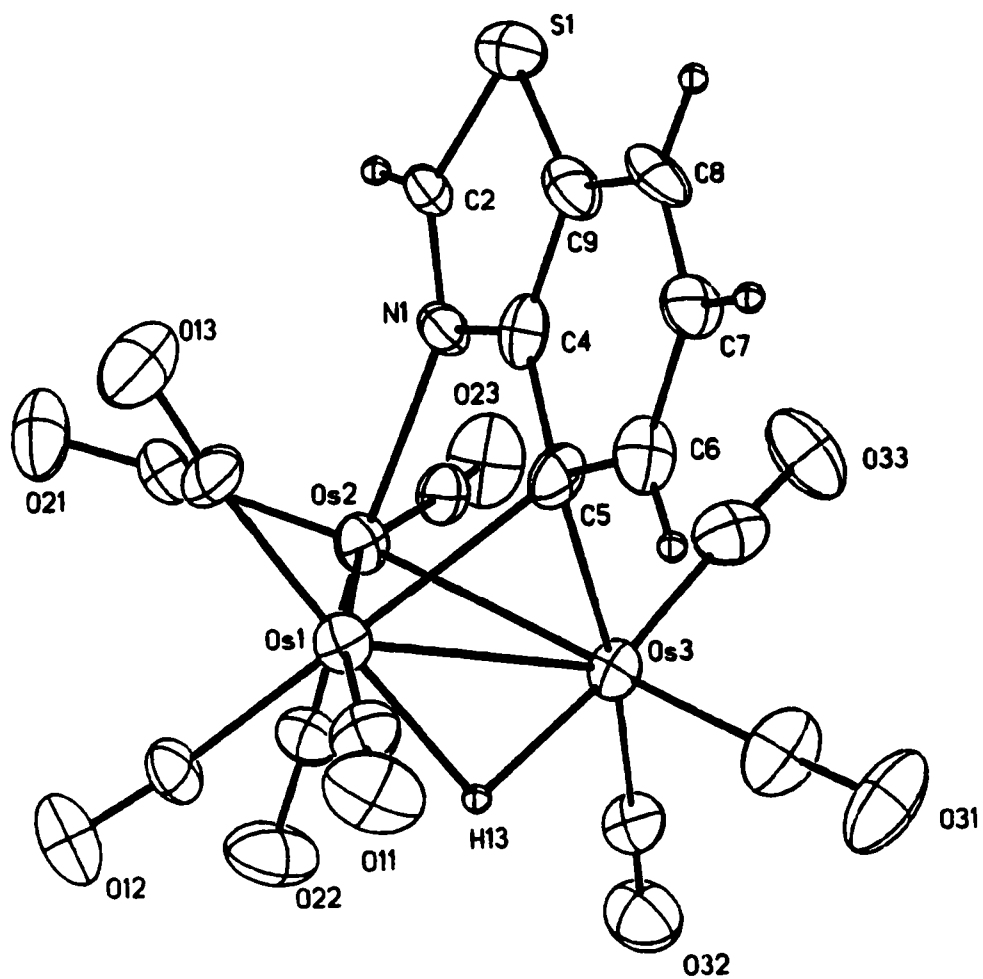


Figure 2.6. Solid state structure of $\text{Os}_3(\text{CO})_9(\mu_3\text{-}\eta^2\text{-C}_7\text{H}_4\text{NS})(\mu\text{-H})$ (**39**) showing the calculated position of the hydride.

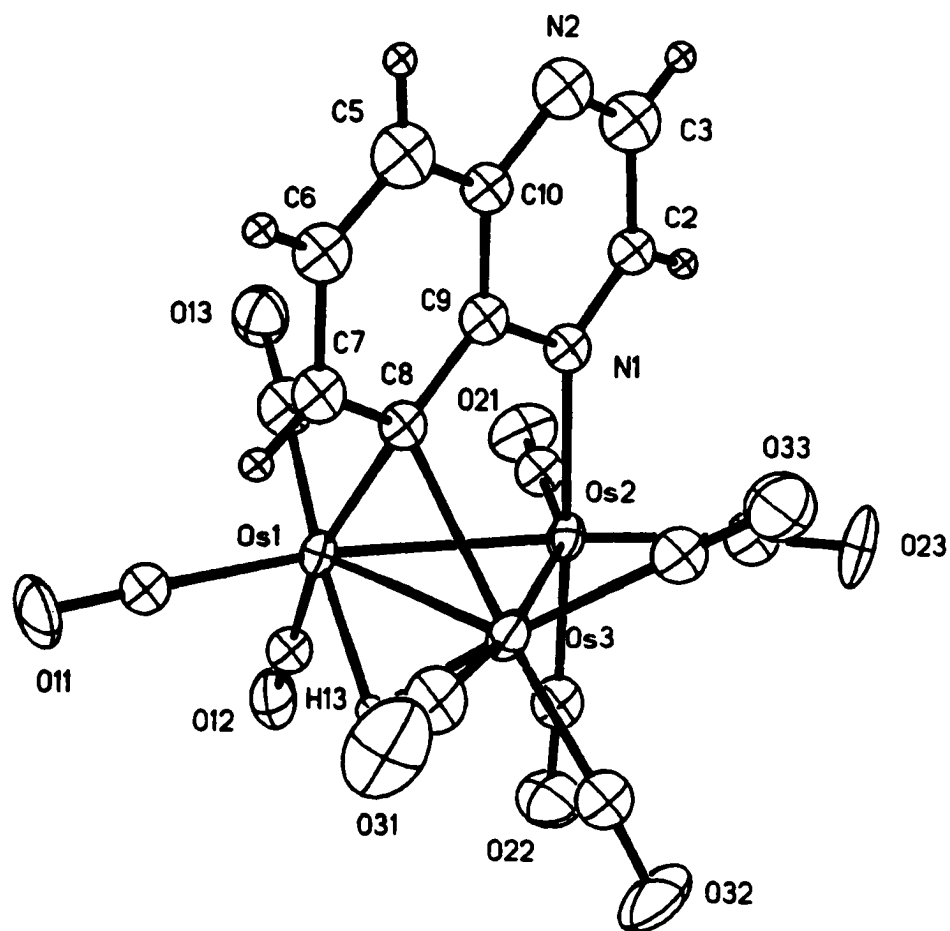
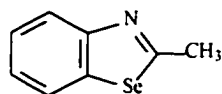
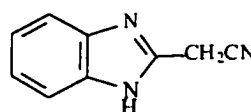


Figure 2.7. Solid state structure of $\text{Os}_3(\text{CO})_9(\mu_3\text{-}\eta^2\text{-C}_8\text{H}_5\text{N}_2)(\mu\text{-H})$ (**43**) showing the calculated position of the hydride.

We also attempted to react 2-methyl benzselazole and 2-benzimidazolyl acetonitrile with $\text{Os}_3(\text{CO})_{10}(\text{CH}_3\text{CN})_2$. Neither produced decacarbonyl precursor of the electron deficient green complexes nor CH activation product of side chain. The apparent reason for 2-Methyl benzselazole is that selenium may open the aromatic ring system and results in decomposed ligand. For 2-benzimidazolyl acetonitrile the nitrile nitrogen may compete with the pyridinyl nitrogen of the ring.



2-Methylbenzselazole



2-Benzimidazolyl acetonitrile

Comparison of the Solid State Structures of 29, 32-33, 38, 39 and 43

The synthesis of this series of electron deficient triosmium clusters, **29**, **32**, **33**, **38**, **39** and **43** provides the opportunity to evaluate the effect of varying the nature of the heterocycle on the metal ligand bonding framework as well as the impact of the cluster on the intraligand bond lengths. The solid state structures of complexes **29**, **32**, **33**, **38**, **39** and **43** are shown in figures 2.1-2.7, and a comparison of relevant bond lengths are given in Table 2.1. The most remarkable aspect of this series of structures is the almost identical nature of the ligand - metal cluster interactions. Thus all of the 3-center 2-electron bond with the Os(1)-Os(3) edge

show highly symmetrical Os-C bonds with an average length of 2.26(2) - 2.31(2) Å (Table 2.1) . All the complexes show a C(5)-C(6) or C(4)-C(5) bond shorter than the average C-C bond of the metal bound carbocyclic ring (Table 2.1). These data suggest that there is an electron deficiency at the carbocyclic ring. The N(1)-C(2) bonds are all in the range of a localized N-C bond, while **29** shows an anomalously short N-C bond. These data are more difficult to understand in light of the atomic and structural differences in the compositions of the heterocyclic rings. Given the essentially perpendicular orientation of the ring relative to the cluster in all of these complexes and the average bond lengths of the carbocyclic rings it is certain that these heterocycles are only involved in σ - interactions with the metal core.

Table 2.1. Selected Distances(Å) for Compounds 29, 32-33, 38, 39 and 43^a

| Compound | C-Os(1) | C-Os(3) | N(1)-Os(2) | C-C Av. Carbocycle(s)^b | N(1)-C(2) | C(5,4)-C(6,5)^c | Av. Os-CO |
|-----------------|----------------|----------------|-------------------|--|------------------|----------------------------------|------------------|
| 29 | 2.29(2) | 2.25(3) | 2.17(2) | 1.41(4) (1.35(4)) | 1.19(3) | 1.32(5) | 1.89(3) |
| 32 | 2.27(2) | 2.26(3) | 2.15(2) | 1.39(3) | 1.31(3) | 1.36(3) | 1.88(1) |
| 33 | 2.31(2) | 2.29(2) | 2.14(1) | 1.39(3) | 1.29(3) | 1.35(3) | 1.90((2) |
| 38 | 2.26(7) | 2.29(6) | 2.15(5) | 1.39(9) | 1.30(8) | 1.39(9) | 1.90(7) |
| 39 | 2.27(1) | 2.25(1) | 2.14(1) | 1.38(2) | 1.30(1) | 1.35(1) | 1.88(2) |
| 43 | 2.30(2) | 2.32(2) | 2.10(1) | 1.37(3) | 1.26(3) | 1.31(3) | 1.89(2) |

a) Numbers following each entry in parentheses are the average standard deviations

b) The average bond lengths of the carbocyclic ring not bound to the metal are given in parentheses

c) Refers to either the C(5)-C(6) or C(4)-C(5) bond lengths in 29 and 43 and 33 and 38 respectively.

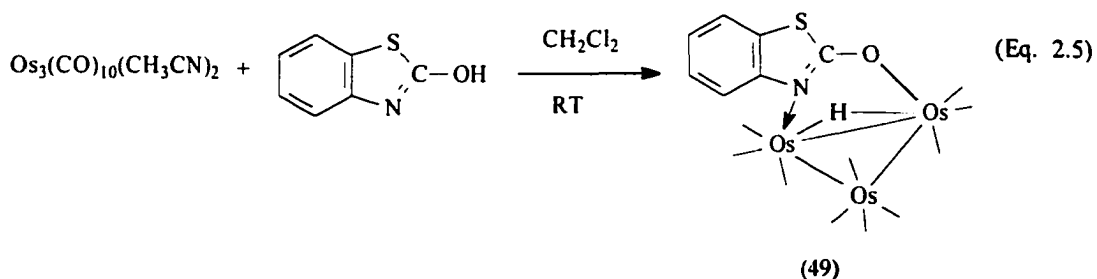
2.3. The Reactions of Functionalized Benzoheterocycles with $\text{Os}_3(\text{CO})_{10}(\text{CH}_3\text{CN})_2$.

We have discussed in section 2.2 the synthesis of a variety of electron deficient triosmium complexes of benzoheterocycles containing a pyridine like nitrogen β -to a CH bond of a fused benzene ring in moderate to good yields (40-68%). The synthesis for these complexes was carried out by reacting benzoheterocycles with $\text{Os}_3(\text{CO})_{10}(\text{CH}_3\text{CN})_2$ at ambient temperature to give the desired decacarbonyl precursor which on photolysis is converted to $\text{Os}_3(\text{CO})_9(\mu_3\text{-}\eta^2\text{-benzoheterocycle-H})(\mu\text{-H})$ (Scheme 2.1). The heterocycles chosen constitute a class of compounds which have extremely important biomedical applications in the design of new drugs as agonists and antagonists for neurotransmitter receptors and as anticancer agents.⁴⁻⁸

Considering the biological importance of these benzoheterocycles with different functional groups we have attempted to extend the synthesis of electron deficient benzoheterocyclic complexes of the parent heterocyclic compounds to a variety of substituted benzoheterocycles. We have discussed here the results of these studies that point out the limitations and possibilities for this synthetic method. We previously found that in the case of substituted quinolines substitution of any functional group in 2- or 7-position completely shuts down the formation of the $\mu_3\text{-}\eta^2\text{-benzoheterocycle}$ complex. On the other hand, substitution of amines or phenols in the 3-, 4-, 5- or 6- positions did not interfere with formation of the expected complexes while substitution of carboxylic acids did.³

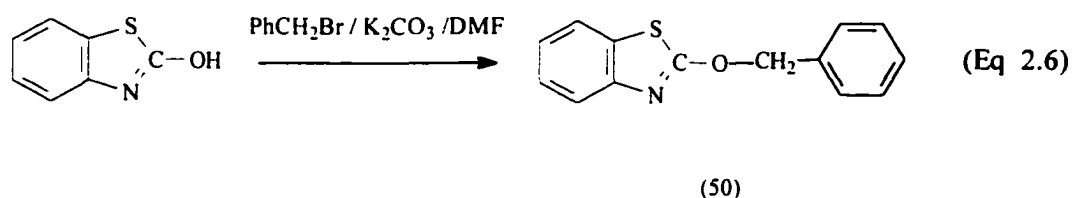
2.4 Results and Discussion

Reaction of 2-hydroxybenzothiazole with the lightly stabilized cluster, $\text{Os}_3(\text{CO})_{10}(\text{CH}_3\text{CN})_2$ at ambient temperature resulted in the formation of $\text{Os}_3(\text{CO})_{10}(\mu\text{-}\eta^2\text{-C}_7\text{H}_4\text{NOS})(\mu\text{-H})$ (**49**) (yield 76%) (Equation 2.5) where the nitrogen atom of the heterocycle is attached to one of the osmium atoms and the oxygen atom of the hydroxyl group has oxidatively added to another osmium atom and thus prevented the formation of the usual $\mu_3\text{-}\eta^2$ -complex where the C(7)-H bond oxidatively adds to metal cluster (Scheme 2.1). Compound (**49**) was characterized by ^1H and ^{13}C -NMR, infrared and elemental analysis. The ^{13}C -NMR spectrum shows the expected ten resonances at 186, 182, 181.5, 176.4, 174.7, 174.6, 174.4, 174.1(2) and 173.9 ppm respectively.



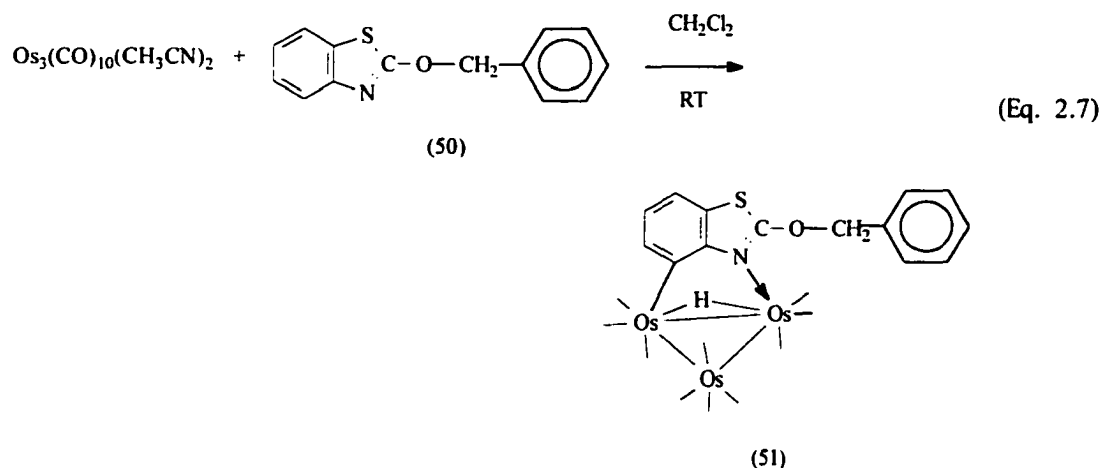
Since the hydroxylic group interfered with making the desired $\mu_3\text{-}\eta^2$ -complex, we attempted to make the green complex by protecting the alcohol group in the form of benzyl ether which could be cleaved later by H_2/Pd . A solution of 2-hydroxybenzothiazole and benzyl bromide in dimethylformamide (DMF) in presence of

K_2CO_3 at $60^\circ C$ yielded 2-benzothiazolyl benzyl ether (**50**) in 89% (Equation 2.6). The product was characterized by IR and 1H -NMR data. In the infrared spectrum of the product the absorption at 3404 cm^{-1} of hydroxyl group of reactant disappeared.



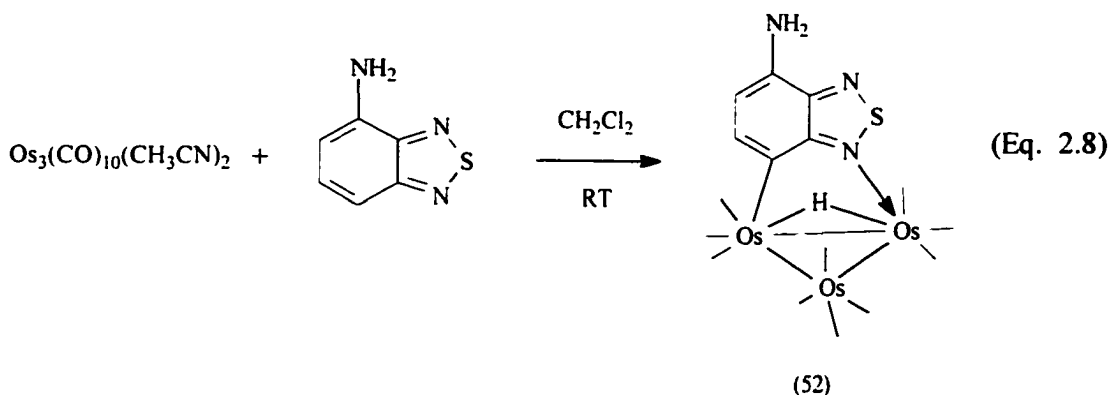
Reaction of 2-benzothiazolyl benzyl ether with $Os_3(CO)_{10}(CH_3CN)_2$ at ambient temperature afforded compound (**51**) with a yield of 32% (Equation 2.7). The compound was separated by thin layer chromatography using silica gel and the solvent used for elution was CH_2Cl_2 and C_6H_{14} (hexane) in the ratio 1 : 3. The 1H -NMR shows the presence of ten protons. Resonances at 7.42(dd), 7.10(dt) and 6.94(dd) ppm correspond to the protons of fused benzene ring. Two dimensional 1H - COSY shows proton at 6.94 ppm correlates with proton at 7.10 ppm which in turn correlates with proton at 7.42 ppm. Five phenyl protons' resonances come at 7.32-7.28 ppm as a multiplet and two benzyl protons come at 5.14 ppm. The Infrared spectrum shows a pattern consistent with a decacarbonyl cluster. Ten ^{13}CO NMR resonances appear at 182.25, 182.19, 180.61, 179.2, 176.63, 176.48, 172.96, 170.4(2) and 169.93 ppm. Based on this evidence we can assign a structure consistent with the desired C(7)-N coordination mode. However, attempts to convert this species to the $\mu_3-\eta^2$ -electron deficient cluster by photolysis failed. This may

be due to the steric hindrance induced on the parallel to perpendicular rearrangement required by the conversion to the electron deficient species.



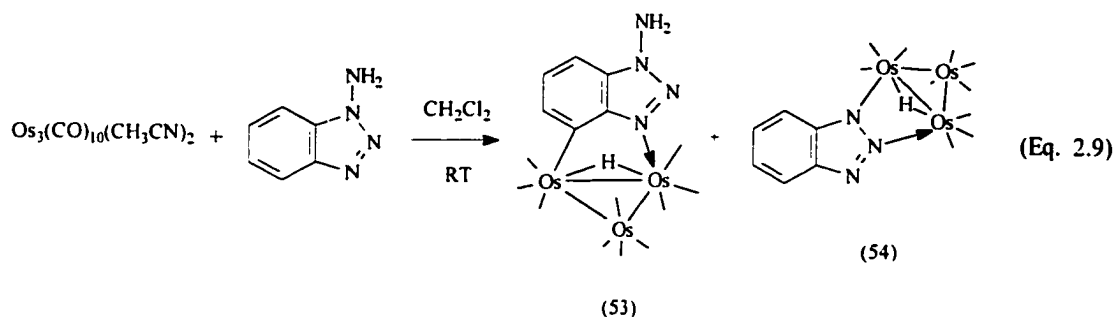
Reaction of 4-amino-2,1,3-benzothiadiazole with $\text{Os}_3(\text{CO})_{10}(\text{CH}_3\text{CN})_2$ at room temperature provided only a small amount of the $\mu-\eta^2$ - complex, $\text{Os}_3(\text{CO})_{10}(\mu-\eta^2-\text{C}_6\text{H}_4\text{N}_2\text{S})(\mu-\text{H})$ (**52**) (Equation 2.8). The color was deep blue and the yield was 5%. No other products were obtained in significant yield except $\text{Os}_3(\text{CO})_{10}(\mu-\text{H})(\mu-\text{Cl})$ and decomposed ligand. Compound (**52**) was identified by ^1H and ^{13}C -NMR, infrared and elemental analysis. In the ^1H -NMR the two aromatic protons come at 7.86 and 6.48 ppm as doublets and the NH_2 protons at 4.31 ppm as a singlet. The hydride peak appears at -13.71 ppm. The ^{13}C -NMR shows the presence of ten carbonyl resonances at 183.2, 177.0, 175.5, 175.2, 174.8, 174.3, 173.2, 172.6, 169.9 and 168.1 ppm respectively. Infrared spectrum also gives a pattern of typical decacarbonyl complex at 2062 s, 2051 s, 2018 s, br, 2004 s, br 1996 w, br cm^{-1} . Owing to the small amount of product obtained it was not useful to attempt conversion to the electron deficient cluster. This particular ligand

appears to be unstable with respect to non-specific decomposition in the presence of the lightly stabilized triosmium cluster.



Reaction of 3-amino benzotriazole with bis-nitrile, $\text{Os}_3(\text{CO})_{10}(\text{CH}_3\text{CN})_2$ at room temperature yielded two compounds, $\text{Os}_3(\text{CO})_{10}(\mu\text{-}\eta^2\text{-C}_6\text{H}_5\text{N}_4)(\mu\text{-H})$ (**53**) and $\text{Os}_3(\text{CO})_{10}(\mu\text{-}\eta^2\text{-C}_6\text{H}_4\text{N}_3)(\mu\text{-H})$ (**54**) in yields of 46% and 39% respectively (Equation 2.9). These complexes were characterized by IR, NMR and elemental analysis. IR spectra of both compounds show the characteristic $(\text{CO})_{10}$ pattern of the complexes where the absorptions are observed at 2064(s), 2051(s), 2019(m) and 2005(m, br) cm^{-1} for compound (**53**) and 2076(s), 2064(s), 2028(s) and 1990 (w, br) cm^{-1} for compound (**54**). ^{13}C -NMR spectra of both compounds show the presence of ten carbonyl groups in the complexes. In case of compound (**53**) amino group is not bound to the cluster as indicated by an ^1H -MNR resonance at 6.80(s, 2H) ppm. But in case of compound (**54**), there is no NH_2 or NH peak in the both ^1H -MNR and IR spectra. Two-dimensional ^1H -COSY for (**54**) shows all the protons are correlated to each other indicating that all four protons are attached to the fused benzene ring and there is no NH group which would have found in

the complex if amino group oxidatively attached to the cluster. Given this unusual result we decided to undertake a solid state structure of **54**.



The solid-state structure of **54** is shown in figure 2.8, selected distances and bond angles are given in Table 2.2. The structure consists of an isosceles triangle of osmium atoms where two nitrogen atoms are bound to two osmium atoms of the cluster. The hydride was located along the longest edge of the metal triangle $\text{Os}(1)\text{-Os}(3) = 2.91(3)\text{\AA}$. The metal nitrogen bond distances are essentially equal $\text{Os}(1)\text{-N}(2) = 2.11(3)$ and $\text{Os}(3)\text{-N}(1) = 2.12(3)\text{\AA}$. The bond lengths of N-N ($1.33(4)\text{\AA}$) and C-C ($1.37(6)\text{-}1.41(5)\text{\AA}$) indicate the aromaticity of the heterocyclic ring is retained.

Photolysis of **(53)** to the $\mu_3\text{-}\eta^2$ -electron deficient complex resulted in the decomposition of the cluster. This may be due to the presence of second pyridinyl nitrogen atom at the 2-position of heterocyclic ring that may interfere to form $\eta^2\text{-N}$, N-adduct during photolysis¹. This case has also been observed for the reaction of 1-methylbenzotriazole with $\text{Os}_3(\text{CO})_{10}(\text{CH}_3\text{CN})_2$ which gave $\mu\text{-}\eta^2$ -decacarbonyl precursor but photolysis of it to convert to the $\mu_3\text{-}\eta^2$ -electron deficient complex failed.² On the other hand, 2-methylbenzotriazole afforded the desired $\mu_3\text{-}\eta^2$ -electron deficient cluster where second pyridinyl nitrogen atom at the 2-position of ligand was absent.²

Table 2.2 Selected Bond Distances (Å) and Angles (°) for 54^a

| Distances | | | |
|-------------------|-----------|------------------|-----------------------|
| Os(1)-Os(2) | 2.87(3) | C(2)-C(7) | 1.41(5) |
| Os(1)-Os(3) | 2.91(3) | C(7)-N(3) | 1.38(5) |
| Os(2)-Os(3) | 2.88(3) | C(6)-C(7) | 1.39(5) |
| Os(1)-N(2) | 2.11(3) | C(4)-C(5) | 1.38(5) |
| Os(3)-N(1) | 2.12(3) | C(5)-C(6) | 1.41(5) |
| N(2)-N(3) | 1.33(4) | C(2)-C(3) | 1.37(6) |
| N(1)-N(2) | 1.33(4) | Os-CO | 1.90(2) ^b |
| C(6)-N(1) | 1.36(4) | C-O | 1.13(3) ^b |
| Angles | | | |
| Os(2)-Os(1)-Os(3) | 59.701(6) | N(1)-N(2)-Os(1) | 112.7(2) |
| Os(1)-Os(2)-Os(3) | 60.84(7) | N(1)-Os(3)-Os(2) | 88.32(8) |
| Os(2)-Os(3)-Os(1) | 59.45(3) | Os-C-O | 175.1(2) ^b |

a numbers in parentheses are estimated standard deviations.

b Average values.

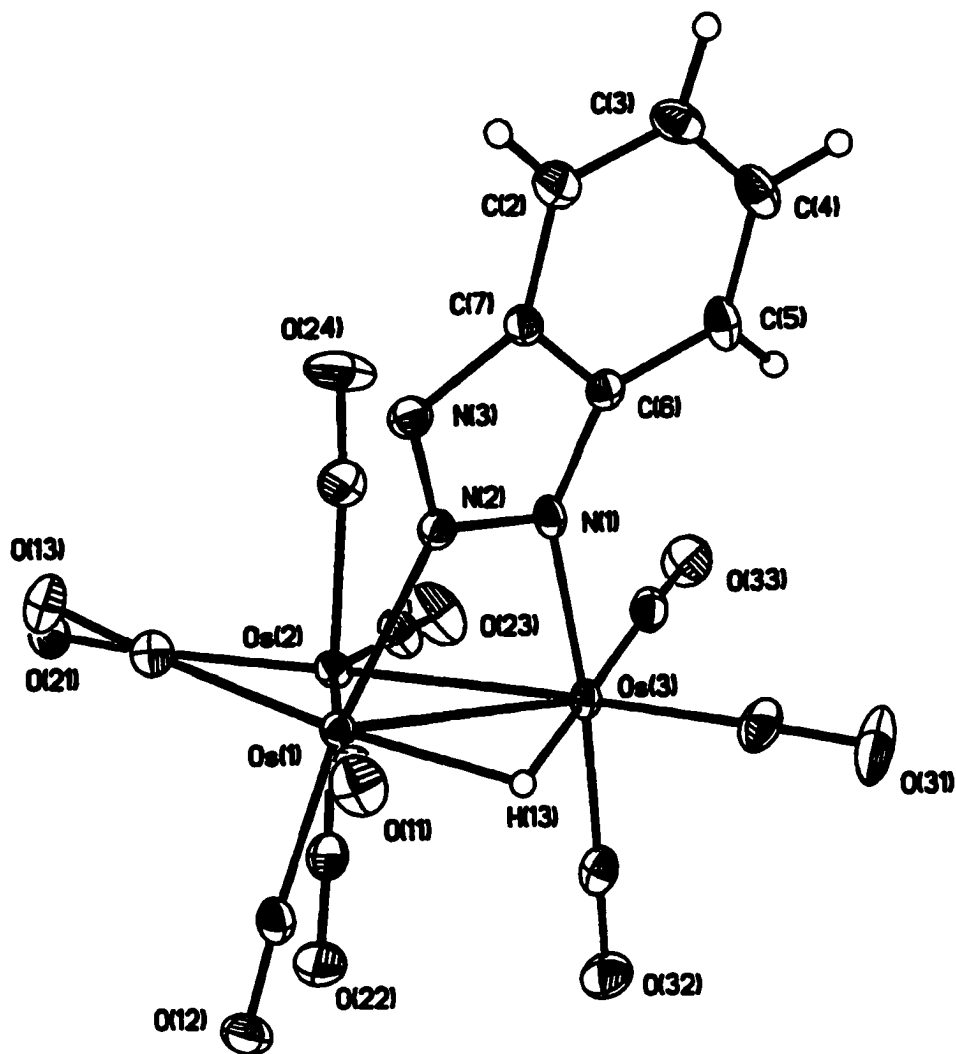
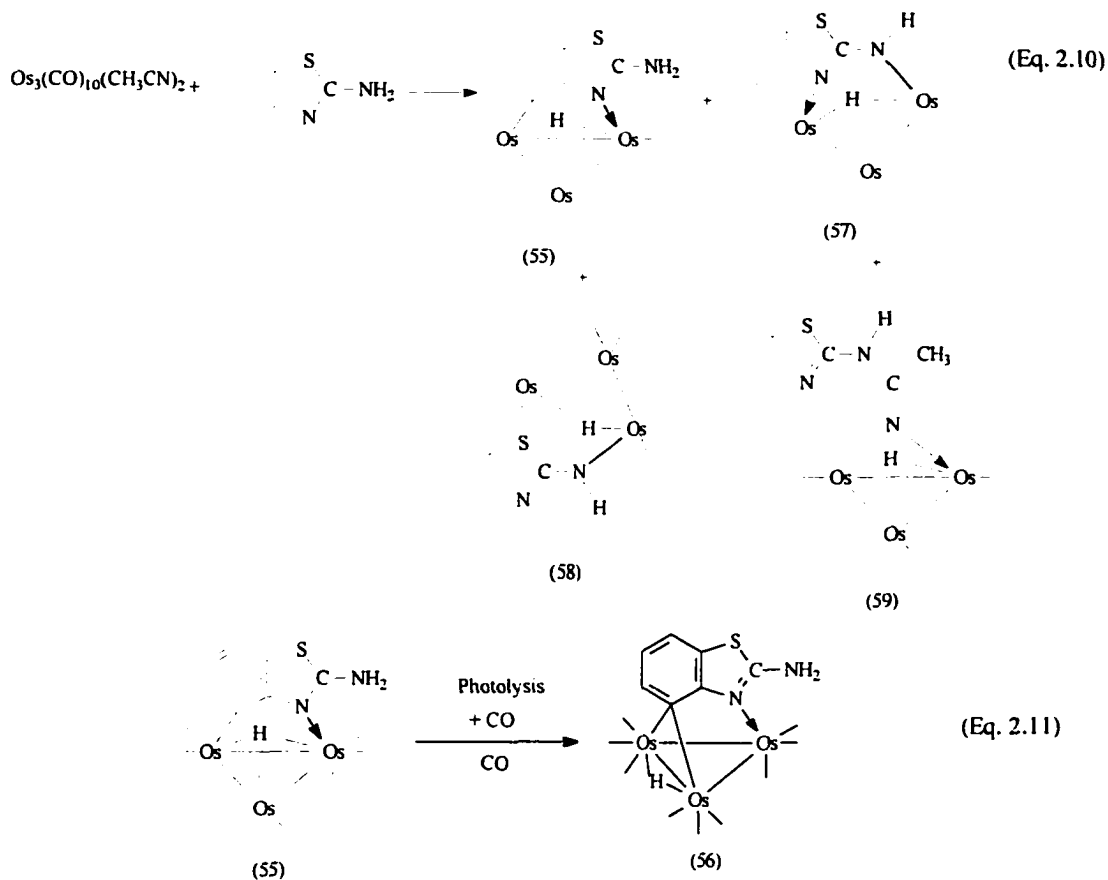


Figure 2.8. Solid-state structure of $\text{Os}_3(\text{CO})_{10}(\mu\text{-}\eta^2\text{-C}_6\text{H}_4\text{N}_3)(\mu\text{-H})$ (54)
 showing the calculated position of the hydride

We reacted 2-amino benzothiazole in an attempt to synthesize an electron deficient $\mu_3\text{-}\eta^2$ -complex, $\text{Os}_3(\text{CO})_{10}(\mu_3\text{-}\eta^2\text{-C}_7\text{H}_5\text{N}_2\text{S})(\mu\text{-H})$ (**56**). It was found that only a small amount of decacarbonyl precursor (**55**) was isolated which on photolysis gave 10% of complex (**56**) (Equation 2.11). In addition two isomeric complexes are formed. One is N, N-bound (**57**) and the other one is S, N-bound (**58**) in the ratio of 2:1 (Equation 2.10). Also about 5% of a complex (**59**) resulting from ligand attachment to an acetonitrile group of $\text{Os}_3(\text{CO})_{10}(\text{CH}_3\text{CN})_2$ was formed (Equation 2.10). This type of structure has been previously observed in the reaction of $\text{Os}_3(\text{CO})_{10}(\text{CH}_3\text{CN})_2$ with tetrahydroquinoline and indoline¹⁹. All these compounds were characterized by ^1H and ^{13}C -NMR and infrared data. The ^1H -NMR of (**56**) shows three resonances at 8.37, 8.15, 6.85 ppm for three aromatic protons and NH_2 peak appears at 5.93 ppm. The ^{13}C -NMR shows the expected 5 resonances at 188.7(2), 184.0(2), 173.6(2), 170.1(1) and 166(2) ppm. The Infrared spectrum also shows the $(\text{CO})_9$ pattern having absorptions at 2074 s, 2048 s, 2017 s, 1987s, br, 1950w, br cm^{-1} . ^1H -NMR of (**57** and **58**) show four aromatic resonances at 7.45, 7.33, 7.20, 7.01 ppm and 7.22, 7.18, 7.01, 6.92 ppm respectively and NH peaks at 4.60 and 6.73 ppm respectively. ^{13}C -NMR of both compounds show the presence of ten carbonyl groups. Resonances are observed at 186.7, 184.8, 183.5, 181.0, 180.3, 177.8, 176.1(2), 174.8, 173.3 and 188.1, 185.7, 183.0, 181.6, 179.4, 177.3(2), 176.0, 173.5, 172.1, 170.9 ppm respectively. It is not possible to say which compound is (**57**) or (**58**) without an X-ray structure. Therefore, we are waiting for a solid state structure of **57** to see if this was indeed the N,N-bound structure. The ^1H -NMR of (**59**) shows four aromatic peaks at 7.16, 7.12, 6.93 and 6.85 ppm. NH and CH_3 protons peaks come at 6.64 and 2.56

ppm as two singlets. The ^{13}C -NMR shows ten resonances at 187.9, 186.1(2), 185.5, 184.6, 182.0, 181.4, 180.8, 177.6 and 174.4 ppm.



A solid-state structure of **56** is shown in figure 2.9, selected distances and bond angles are given in Table 2.3. The 3-center 2-electron bond with the Os(1)-Os(3) edge shows highly symmetrical Os-C bonds with an average length of 2.26(5)Å (Table 2.3). The complex shows a C(4)-C(5) bond shorter than the average C-C bond of the metal bound carbocyclic ring. These data suggest that there is an electron deficiency at the carbocyclic ring. The N(1)-C(2) (1.31(6)Å) bond is in the range of a localized N-C bond.

Table 2.3 Selected Bond Distances (Å) and Angles (°) for 56^a

| Distances | | | |
|-------------------|-----------|-----------------|-----------------------|
| Os(1)-Os(2) | 2.80(3) | C(2)-S(1) | 1.75(5) |
| Os(1)-Os(3) | 2.77(3) | S(1)-C(8) | 1.74(5) |
| Os(2)-Os(3) | 2.80(3) | N(1)-C(7) | 1.39(6) |
| Os(2)-N(1) | 2.15(4) | C(4)-C(5) | 1.39(7) |
| Os(1)-C(6) | 2.16(5) | C(5)-C(6) | 1.41(7) |
| Os(3)-C(6) | 2.28(5) | C(6)-C(7) | 1.41(7) |
| C(2)-N(1) | 1.31(6) | C-O | 1.13(3) ^b |
| C(7)-C(8) | 1.41(6) | | |
| Angles | | | |
| Os(2)-Os(1)-Os(3) | 60.48(8) | C(7)-C(6)-Os(1) | 113.1(3) |
| Os(1)-Os(2)-Os(3) | 59.19(7) | C(7)-N(1)-Os(2) | 117.8(3) |
| Os(1)-Os(3)-Os(2) | 60.32(7) | Os-C-O | 175.1(2) ^b |
| Os(1)-C(6)-Os(3) | 75.06(14) | | |

a Numbers in parentheses are estimated standard deviations.

b Average values.

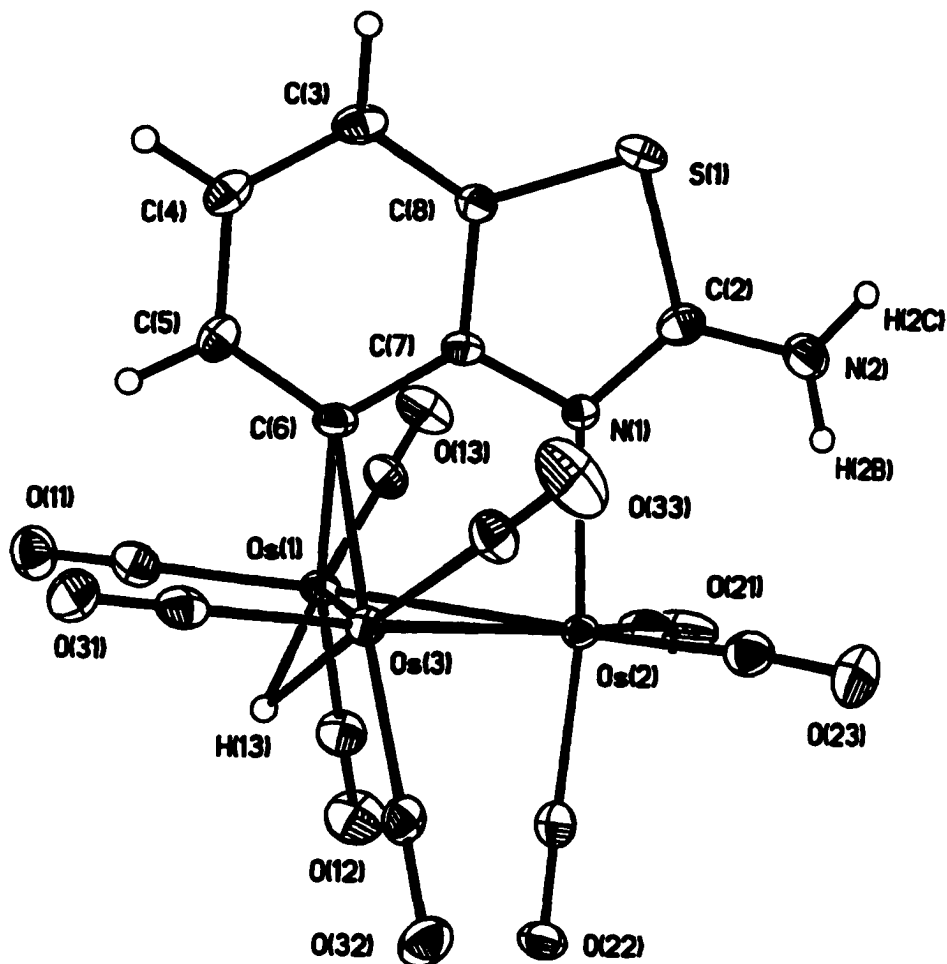
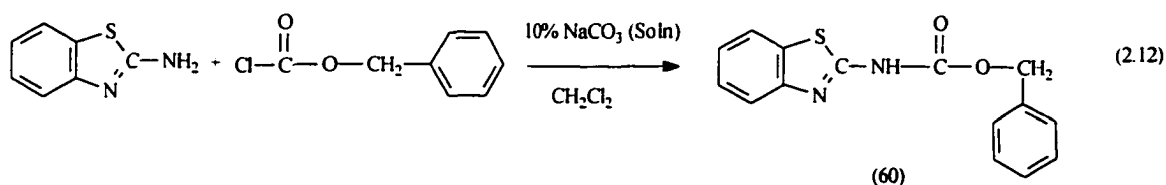


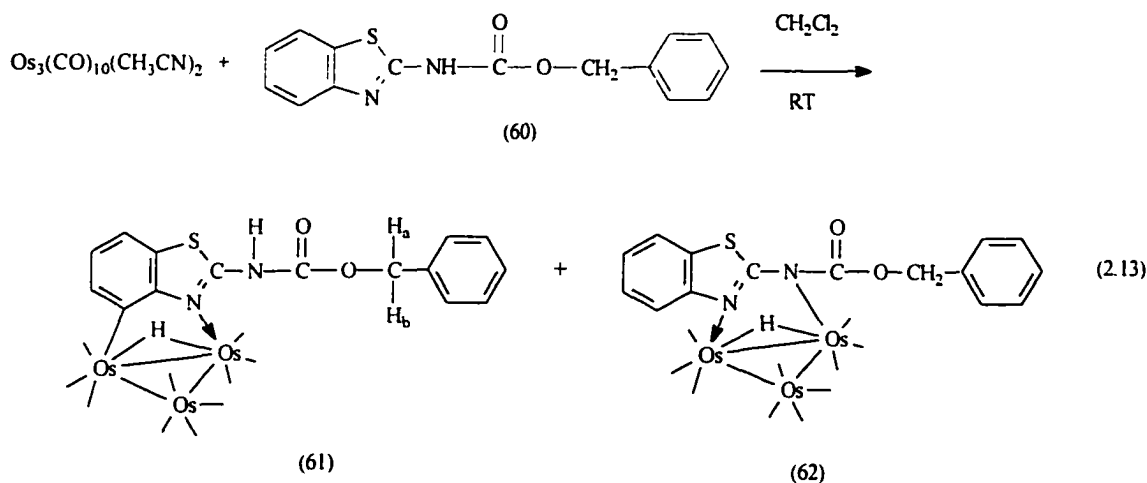
Figure 2.9. Solid-state structure of $\text{Os}_3(\text{CO})_{10}(\mu_3\text{-}\eta^2\text{-C}_7\text{H}_5\text{N}_2\text{S})(\mu\text{-H})$ (**56**) showing the calculated position of the hydride.

In order to avoid the oxidative addition of the amino group to the metal cluster we protected the amino group using carbobenzyloxy chloride (CBz-Cl). The protecting group was reacted with 2-aminobenzothiazole using Shotten-Bauman conditions (aqueous carbonate and methylene chloride) in a two phase-system (Equation 2.12).³⁴ The yield was 79% and the product, 2-carbobenzyloxyamino benzothiazole (**60**) was characterized by IR and ¹H-NMR.data. The protecting group can ultimately be cleaved using H₂/Pd/C in MeOH.³⁴



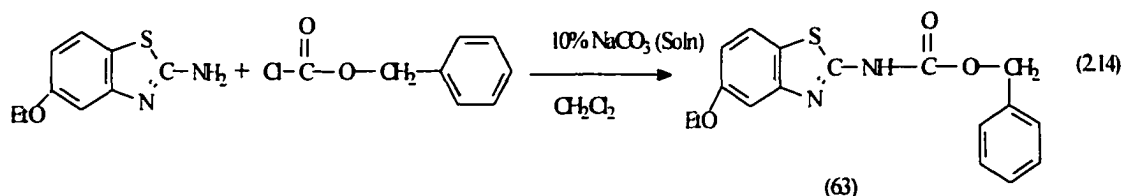
Reaction of benzyloxy carbamate of 2-aminobenzothiazole (**60**) with bis-nitrile, Os₃(CO)₁₀(CH₃CN)₂ at room temperature gave the desired decacarbonyl μ-η²-complex, Os₃(CO)₁₀(μ-η²-C₁₅H₁₁N₂O₂S)(μ-H) (**61**) (Equation 2.13). The yield was 15% and the color was yellow. Another compound, Os₃(CO)₁₀(μ-η²-C₁₅H₁₁N₂O₂S)(μ-H) (**62**) was also formed where the N atom of the carbamate has been oxidatively attached to one of the osmium atoms of the cluster. This cluster was obtained in 20% yield. Both products were isolated by thin layer chromatography using CH₂Cl₂ and C₆H₁₂ (hexane) in the ratio 2:3 as eluant. Photolysis of complex (**61**) did not convert it to a μ₃-μ²-complex. These compounds were characterized by ¹H and ¹³C-NMR, infrared and elemental analysis. ¹³C-NMR for both complexes (**61** and **62**) show the presence of ten carbonyl groups in both

clusters. The $^1\text{H-NMR}$ for (**61**) shows three aromatic protons of the fused benzene ring, one NH proton and two benzylic protons in addition to five phenyl protons of the complex. The $^1\text{H-NMR}$ also shows the presence of an AB pattern of the benzylic protons indicating that the complex is asymmetric and it is $\mu\text{-}\eta^2\text{-(CO)}_{10}$ complex. Electron deficient $\mu_3\text{-}\eta^2$ complex is symmetric whereas $\mu\text{-}\eta^2\text{-(CO)}_{10}$ complex is asymmetric. The $^1\text{H-NMR}$ for (**62**) shows four aromatic protons of the fused benzene ring and two benzylic protons in addition to five phenyl protons but no NH proton indicating that the nitrogen atom of the carbamate has been oxidatively attached to one of the osmium atom and the pyridinyl nitrogen has been coordinated to the other metal of the cluster. These results reveal that conversion of the 2-amino group to an amido NH does not completely prevent the oxidative addition of this, the NH bond to the cluster. Compound **61** did not convert efficiently to the desired electron deficient cluster on photolysis.

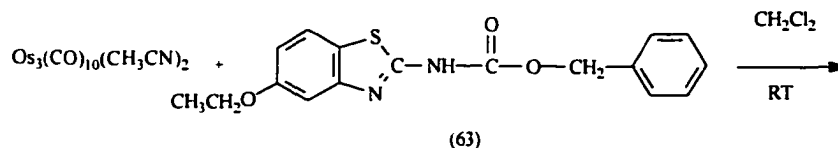


The 6-ethoxy-2-aminobenzothiazole ligand affords the opportunity to test whether substitution in the 6-position (analogous to the 7-position in quinoline) will block the C(7)-N coordination mode. Considering the results obtained for the 2-amino

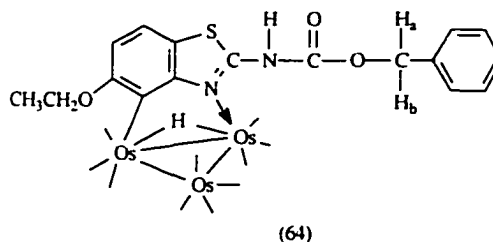
benzothiazole we protected the amino group of 6-ethoxy-2-aminobenzothiazole by CBz-Cl to make the carbamate, $C_{17}H_{16}N_2O_3S$ (**63**) in the same way as it was done for 2-aminobenzothiazole (Equation 2.14). The compound was purified by column chromatography using silica gel as stationary phase and methylene chloride and hexane (1:3) as eluant. The yield was 74%. The compound was characterized by IR and 1H -NMR data.



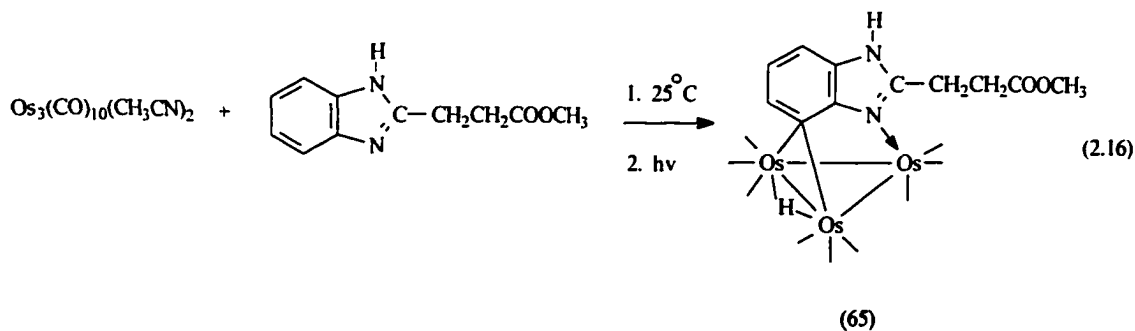
6-Ethoxy-2-benzothiazole benzyloxy carbamate, $C_{17}H_{16}N_2O_3S$ (**63**) was reacted with $Os_3(CO)_{10}(CH_3CN)_2$ at ambient temperature and afforded the μ - η^2 -complex, $Os_3(CO)_{10}(\mu$ - η^2 - $C_{17}H_{15}N_2O_3S)(\mu$ -H) (**64**) (Equation 2.15). The compound was separated by thin layer chromatography using CH_2Cl_2 and C_6H_{12} (hexane) in the ratio 2:3 as eluant. The yield for (**64**) was 21%. Photolysis of compound (**64**) led only to the decomposition. Compound (**64**) was characterized by IR, 1H -, ^{13}C -NMR spectroscopy and elementary analysis. The ^{13}C -NMR shows the presence of ten carbonyl groups in the complex (**26**). The confirmation of this μ - η^2 - $(CO)_{10}$ complex comes from asymmetric AB pattern of benzylic protons observed in the 1H -NMR.



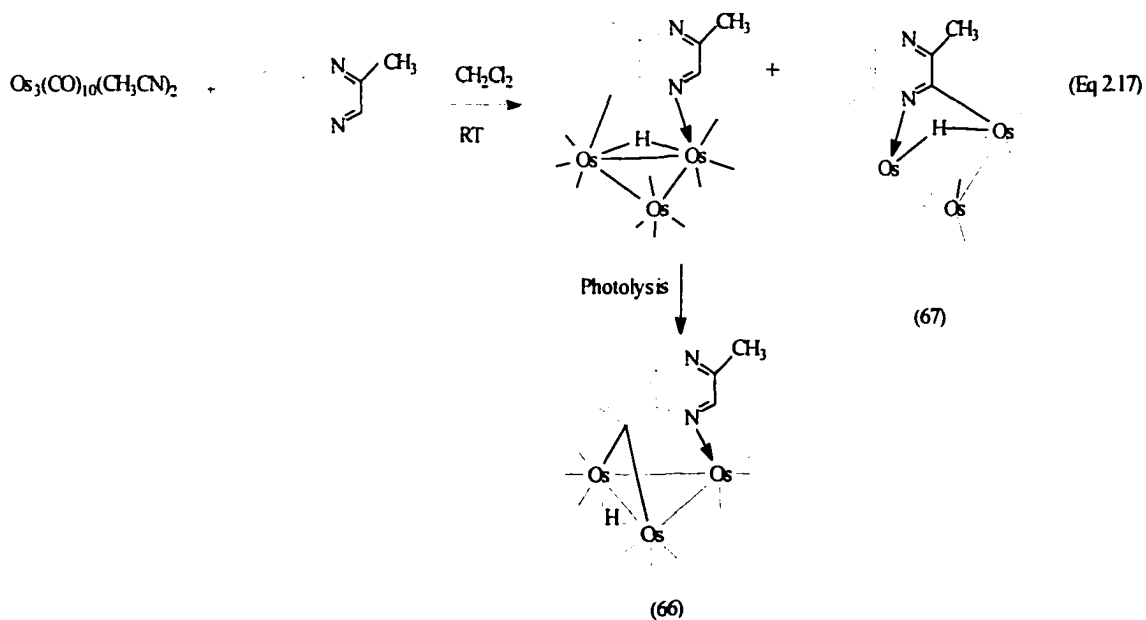
(2.15)



Based on our prior results with quinoline carboxylic acids we converted the commercially available 3-(1H-benzimidazol-2-yl)-propionic acid into corresponding methyl ester by reflux in methanol with added sulfuric acid.^{3,35} 2-Methylpropionate benzimidazole gave the expected major decacarbonyl precursor which on photolysis gave the electron deficient μ_3 - μ^2 -complex, $\text{Os}_3(\text{CO})_9(\mu_3\text{-}\eta^2\text{-C}_{11}\text{H}_{11}\text{N}_2\text{O}_2)(\mu\text{-H})$ (**65**) (Equation 2.16) in 61% overall yield. There was no CH activation of the methylene side chain. Complex (**65**) was characterized by IR, ^1H -, ^{13}C -NMR spectroscopy and elementary analysis. Evidence for μ_3 - μ^2 -complex (**65**) comes from ^{13}C -NMR data of this complex where only five resonances appear at 191.5(2), 182.3(2), 175.(2), 171.0(1) and 167.1(2) ppm.



Since 2-Methylquinoline did not provide an electron deficient $\mu_3\text{-}\eta^2$ -complex³, we wanted to see if 2-methylquinoxaline behaves like that of 2-methylquinoline or affords the desired electron deficient complex when reacted with $\text{Os}_3(\text{CO})_{10}(\text{CH}_3\text{CN})_2$. In fact, reaction with $\text{Os}_3(\text{CO})_{10}(\text{CH}_3\text{CN})_2$, 2-methylquinoxaline provided an electron deficient complex, $\text{Os}_3(\text{CO})_9(\mu_3\text{-}\eta^2\text{-C}_8\text{H}_4(3\text{-CH}_3)\text{N}_2(\mu\text{-H}))$ (**66**) followed by photolysis of its decacarbonyl precursor where the nitrogen atom furthest from the methyl group coordinated with the cluster along with the CH-7 oxidative addition to one of the metal atoms of the cluster (Equation 2.17). The yield of the complex was 51%. A small amount of complex **67** resulting from the CH-3 activation with the cluster was also obtained in a 4% yield. After chromatographic separation both compounds were characterized by IR,



^1H NMR and elemental analysis. In the ^1H NMR of **67** four aromatic resonances are observed as two doublets and two triplets at 7.78, 7.58, 7.75 and 7.88 ppm respectively. The methyl and hydride resonances come as two singlets at 2.89 and -14.11 ppm respectively. In the ^1H NMR of **66** three aromatic resonances are observed as two doublets of doublets and a doublet of triplets at 8.67, 8.59 and 7.41 ppm respectively. CH(2), methyl and hydride resonances appear as singlets at 9.02, 2.72 and -12.21 ppm respectively.

A solid state structure of **66**, $\text{Os}_3(\text{CO})_9(\mu_3\text{-}\eta^2\text{-C}_8\text{H}_4(3\text{-CH}_3)\text{N}_2(\mu\text{-H}))$ is shown in figure 2.10 with the selected bond lengths and angles in table 2.4. The bond lengths given in table 2.10 indicate the aromatic nature of the carbocyclic ring remains unperturbed making complex **66** an electron deficient species containing a μ_3 -methyl substituted quinoxaline ligand.

Table 2.4 Selected Bond Distances (Å) and Angles (°) for 66^a

| Distances | | | |
|-------------|---------|-----------|----------------------|
| Os(1)-Os(2) | 2.76(3) | C(3)-N(2) | 1.32(7) |
| Os(1)-Os(3) | 2.75(3) | C(9)-N(2) | 1.36(7) |
| Os(2)-Os(3) | 2.78(3) | N(1)-C(8) | 1.38(6) |
| Os(2)-N(1) | 2.15(4) | C(5)-C(6) | 1.40(7) |
| Os(1)-C(7) | 2.25(5) | C(6)-C(7) | 1.41(7) |
| Os(3)-C(7) | 2.30(5) | C(7)-C(8) | 1.44(7) |
| C(2)-N(1) | 1.30(7) | C-O | 1.14(7) ^b |
| C(8)-C(9) | 1.43(7) | | |

| Angles | | | |
|-------------------|-----------|-----------------|-----------------------|
| Os(2)-Os(1)-Os(3) | 60.09(7) | C(8)-C(7)-Os(1) | 112.7(3) |
| Os(1)-Os(2)-Os(3) | 59.30(7) | C(8)-N(1)-Os(2) | 118.7(3) |
| Os(1)-Os(3)-Os(2) | 60.60(7) | Os-C-O | 177.2(5) ^b |
| Os(1)-C(6)-Os(3) | 74.19(15) | | |

a Numbers in parentheses are estimated standard deviations.

b Average values.

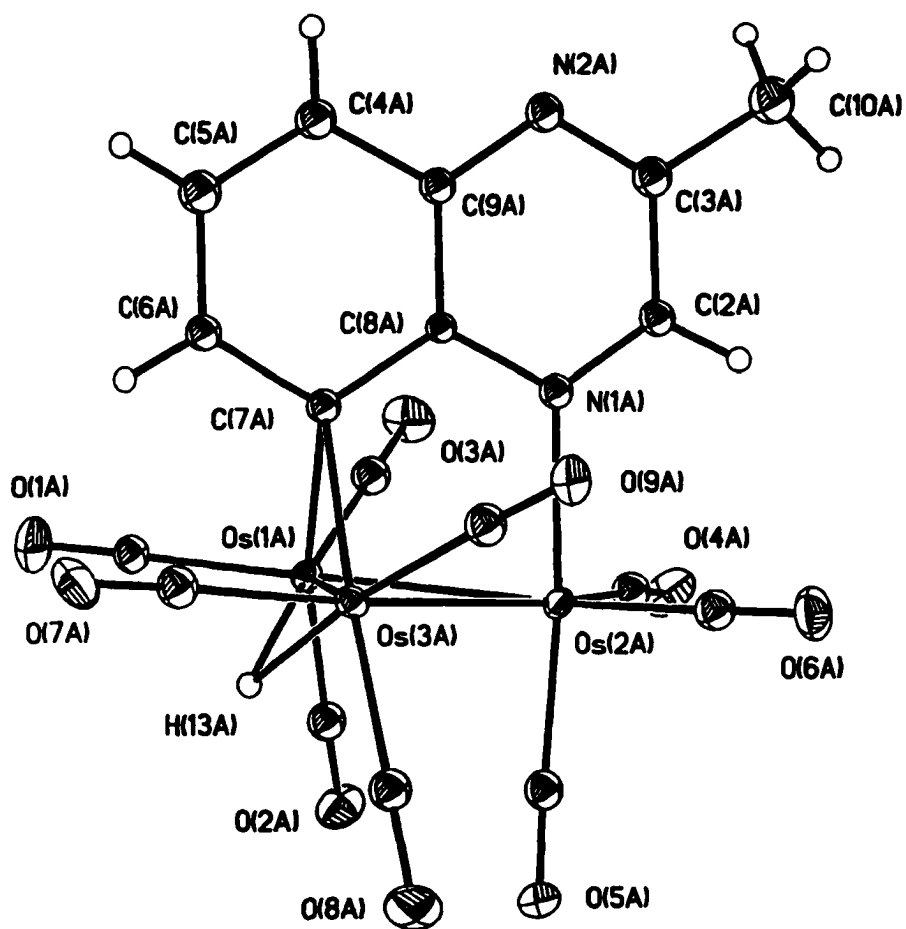
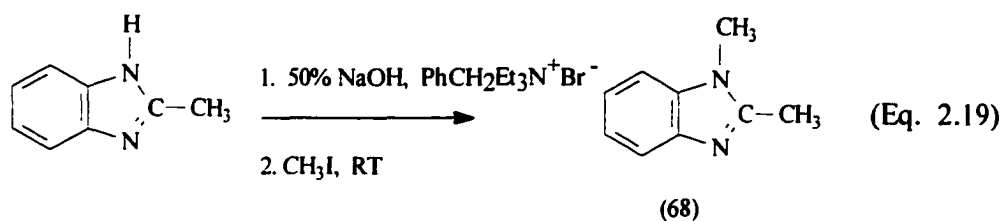
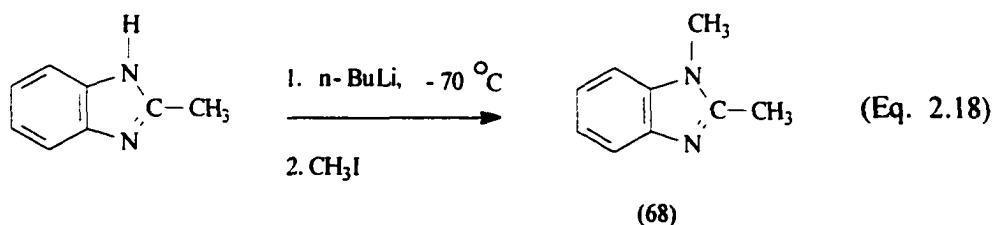


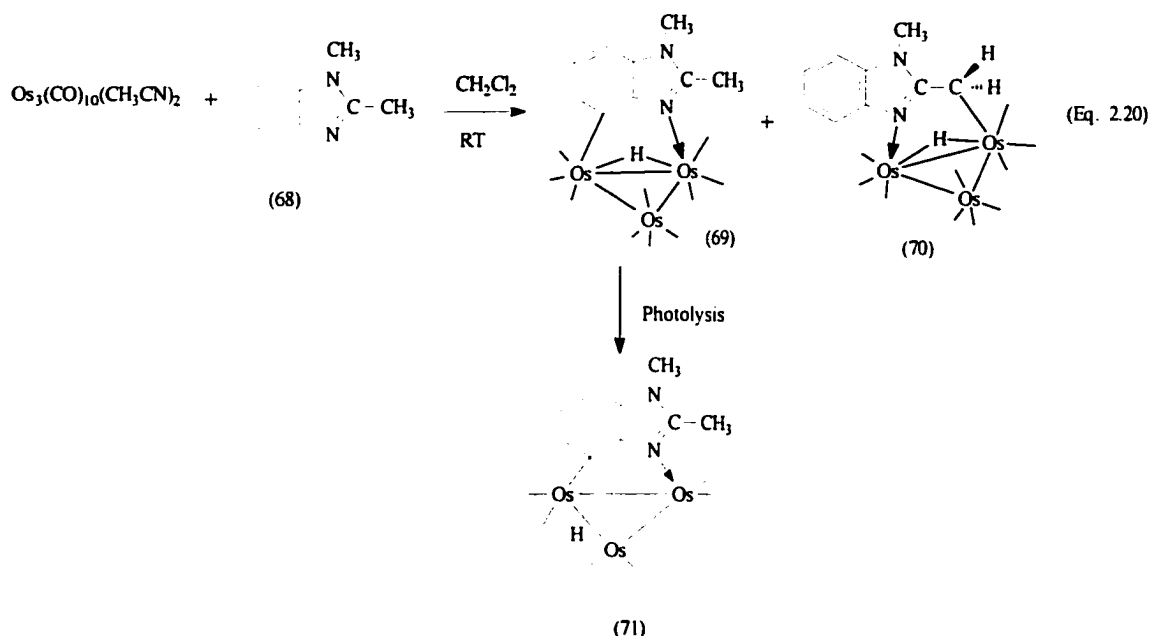
Figure 2.10 Solid state structure of $\text{Os}_3(\text{CO})_9(\mu_3\text{-}\eta^2\text{-C}_8\text{H}_4(3\text{-CH}_3)\text{N}_2(\mu\text{-H}))$ (66)
 showing the calculated position of the hydride

We also made the electron deficient $\mu_3\text{-}\eta^2\text{-2,3}$ -dimethylbenzimidazole complex (71) from 1,2-dimethylbenzimidazole (68). 1,2-Dimethylbenzimidazole (68) was prepared from 2-methylbenzimidazole by two different methods. In one 2-methylbenzimidazole was treated with a deprotonating agent, *n*-BuLi at $-70\text{ }^\circ\text{C}$ followed by dropwise addition of CH_3I (Equation 2.18).



After purification compound (68) was obtained in a 65% yield. The other method involved the treatment of 2-methylbenzimidazole with CH_3I in the presence of aq 50% NaOH and $\text{PhCH}_2\text{Et}_3\text{N}^+\text{Br}^-$ at room temperature (Equation 2.19).³⁶ After purification this method afforded 83% of 1,2-dimethyl benzimidazole (68). Compound (68) was characterized by IR, ^1H NMR, TOF-MS and elemental analysis. The IR shows the band at 3434cm^{-1} for $-\text{NH}$ of the starting material has been disappeared in the product. The ^1H NMR shows two singlets at 3.63ppm and 2.53ppm attributable to N-CH_3 and C-CH_3 protons. A doublet of doublets at 7.65 ppm can most likely be assigned to the C-7 or C-4 protons. The other three aromatic protons appear as an overlapping multiplet at 7.19 ppm.

Reaction of 1,2-dimethylbenzimidazole (**68**) with $\text{Os}_3(\text{CO})_{10}(\text{CH}_3\text{CN})_2$ at room temperature gave the compound, $\text{Os}_3(\text{CO})_{10}(\mu\text{-}\eta^2\text{-C}_7\text{H}_3(2\text{-CH}_3)(3\text{-CH}_3)\text{N}_2(\mu\text{-H}))$ (**69**) as major component due to the CH activation at the CH(7) (Equation 2.20). A minor amount of compound (**70**) resulting from the CH activation of methyl side chain at C-2 was also obtained in a 6% yield. This type of compound formation was also observed in the case of 2-methylbenzimidazole activation by trimetallic osmium carbonyl². Decarbonylation of (**69**) by photolysis at room temperature afforded the $\mu_3\text{-}\eta^2$ -electron deficient complex, $\text{Os}_3(\text{CO})_9(\mu_3\text{-}\eta^2\text{-C}_7\text{H}_3(2\text{-CH}_3)(3\text{-CH}_3)\text{N}_2(\mu\text{-H}))$ (**71**) in a 48% yield (Equation 2.20).



Both compounds (**70**) and (**71**) were purified by chromatographic separation on silica gel plate using hexane and methylene chloride as elutant in 3:2 ratio and characterized by IR, ¹H NMR and elemental analysis. In ¹H NMR of (**70**) hydride chemical shift comes as a

doublet at -14.16 ppm ($J = 0.8$ Hz) and two methylene protons as two doublets at 1.83 ($J = 18.8$ Hz) and at 2.58 ppm ($J = 18.8$ Hz). A singlet of relative intensity 3 at δ 3.67 ppm is due to the $-\text{CH}_3$ protons. All the aromatic protons at C-4, C-7, C-5, C-6 appear as two doublets and two triplets at 7.21, δ 7.61, δ 7.30 and δ 7.38 ppm respectively.

The ^1H NMR of (71) shows two singlets of relative intensity 3 each at 3.81 and 2.70 ppm due to the N-CH₃ and C-CH₃ protons respectively. Two doublets of doublets at 8.17 and 8.19 ppm are for C-4 and C-6 aromatic protons and a doublet of triplets at 7.04 ppm is for C-7 proton. Hydride resonance comes at -11.77 ppm.

2.5 Conclusions:

After studying the reactions of functionalized benzoheterocycles with trimetallic osmium cluster we have come to the following conclusions:

- 1) Many heterocycles containing a pyridinyl nitrogen β -to a CH bond of a fused benzene ring is able to form an electron deficient μ_3 - η^2 -complex in moderate to good yields.
- 2) Compounds containing two adjacent pyridinyl nitrogen or one pyridinyl nitrogen and one indole type nitrogen atoms adjacent to each other prevent formation of electron deficient complexes by forming η^2 -1,2- N, N and η^2 -2,3-N,C adducts.^{1,2}
- 3) Substitution at the 2-position by OH, NH₂, COOH also prevents formation of the desired μ_3 - η^2 -complex due to the oxidative addition of O-H and N-H bonds of these functional groups.

4) Substitution at the 6-position is at least somewhat tolerated for the benzoheterocycle in contrast to the 7-position of quinoline.

5) Protection of the OH and NH₂ functional groups at the 2 position by a suitable protecting group also provides decacarbonyl precursors of the electron deficient $\mu_3\text{-}\eta^2$ -complex but these decacarbonyl complexes do not turn into electron deficient complexes. Rather these decompose on attempted photolysis, probably due to the interference of the protecting groups except in the case of compound (65) where the protecting group is small and is separated by three carbon atoms from the binding site of the ligand to the cluster. The take home message from these results is that although substitution at the 2- and 6- position is tolerated from the steric point of view, the oxidative addition of X-H bonds (X= O,N) effectively competes with C-H activation at C(-7). Furthermore, although protection of the X-H does redirect the reaction towards the desired compound, the presence of bulky substitution at the 2-position blocks conversion to the electron deficient cluster.

2.6 Experimental Section for Synthesis of the Benzoheterocycle Complexes

Materials and General Considerations

All reactions were carried out under an atmosphere of nitrogen but were worked up in air. Methylene chloride and acetonitrile were distilled from calcium hydride and tetrahydrofuran was distilled from benzophenone ketyl. Acetone-d₆, methylene chloride-

d_2 , and methanol- d_4 were purchased from Aldrich Chemical Co. in single ampules and used as received. Chloroform- d_1 was dried over molecular sieves before use.

Infrared spectra were recorded on a Perkin-Elmer 1600 FT-IR spectrometer and 1H and ^{13}C NMR were recorded on a Varian Unity Plus 400 MHz. Elemental analyses were done by Schwarzkopf Microanalytical Labs, Woodside, New York. Chemical shifts are reported downfield relative to tetramethylsilane.

Osmium carbonyl was purchased from Strem Chemical, used as received and converted to $Os_3(CO)_{10}(CH_3CN)_2$ by published procedures.³⁷ All the benzoheterocycles used were purchased from Aldrich Chemical. Benzothiazole, 2-methylbenzothiazole, 2-methyl- benzoxazole were distilled from calcium hydride before use. 2-Methylbenzotriazole was prepared from benzotriazole (purchased from Aldrich Chemical) by methylation with dimethylsulfate and distilled from calcium hydride before use. Dimethylsulfate was also distilled over phosphorus pentoxide before use. Methyl ester of 2-benzimidazolepropionic acid was prepared from the corresponding acid via an esterification reaction by refluxing for 2hr in a 10% (H_2SO_4 -MeOH) solution.³⁵

Preparation of Electron Deficient Benzoheterocycles, $Os_3(CO)_9(\mu_3-\eta^2$ -benzohetero cycle)(μ -H) (29, 32-33, 37-40, 43, 56, 65-66 and 71).

The following procedure was used for synthesizing all of the above the electron deficient benzoheterocycle triosmium complexes. [$Os_3(CO)_{10}(CH_3CN)_2$ (0.250-0.500g, 0.27-0.54 mmol)] was dissolved in 150-300 mL CH_2Cl_2 and a two fold molar excess of

the appropriate heterocyclic ligand was added (except in the case of quinoxaline where better yields were obtained using a 5 x molar excess). The reaction mixture was stirred for 12-20h and then filtered through a short silica gel column to remove excess ligand. The pure decacarbonyl precursors (the slowest moving yellow-orange band) were isolated by preparative TLC before photolysis. The dark green solutions obtained after photolysis were then filtered through a short column of silica gel, concentrated to 10-25mL by rotary evaporation and cooled to 0°C to yield 100-300 mg of dark green crystals. The mother liquor was rotary evaporated and the crude product was dissolved in a minimum amount of CH₂Cl₂ and fractionated on 0.1x20x40 cm silica gel TLC plates using CH₂Cl₂/hexane (20-50% CH₂Cl₂) as the eluent. Two bands were eluted. The faster moving yellow band contained minor amounts of the decacarbonyl benzoheterocycle triosmium complex and slower moving dark green band contained additional product which was crystallized from methylene chloride and hexane. The combined total yields (based on Os₃(CO)₁₂) of the products are given below with the analytical and spectroscopic data.

Synthesis of 2-benzothiazolyl benzyl ether (50).

A solution of 2-hydroxybenzothiazole (1.00g, 6.67 mmoles) and benzyl bromide (1.18mL, 10mmole) in dimethylformamide(DMF)(11.7 mL) was treated with K₂CO₃ (1.83g, 13 mmole), and the resulting mixture was heated at 60°C overnight.³⁸ After cooling and filtration, the mixture was evaporated to dryness. The residue was dissolved in ethyl acetate (16 mL), and the organic solution was washed with 1M aq. HCl (3×8 mL)

and brine (2×8 mL), then was dried over anhydrous magnesium sulfate, filtered and evaporated. The residue was recrystallized from hexane to yield 1.45g, 89% of product, 2-benzothiazolyl benzyl ether (**50**).

Synthesis of 2-Benzyloxycarbamate benzothiazole (60) and 6-Ethoxy-2-benzyloxy carbamate benzothiazole (63).

A solution of 2-aminobenzothiazole (2.0g, 13.4 mmoles) or 6-ethoxy-2-aminobenzothiazole (2.2g, 13.4 mmoles) and carbobenzyloxy chloride (Cbz-Cl) (2.5g, 13.9 mmoles) in CH₂Cl₂ (20 mL) was treated with 10% aqueous Na₂CO₃ solution (20ml) at room temperature for 3 h. The organic layer was separated and dried over anhydrous Na₂SO₄ and the product, depending on which reactant was used, carbobenzyloxyate of 2-aminobenzothiazole (**60**) or 6-ethoxy-2-aminobenzothiazole (**63**), was purified by column chromatography on silica gel using CH₂Cl₂ and hexane in the ratio 1:3. The yield was 2.97g, 79% for compound **60** and 2.75g, 74% for **63**.

Synthesis of 1,2-Dimethylbenzimidazole (68)

Method 1: 2-Methylbenzimidazole (1.0g, 7.6 mmoles) was dissolved in 50 mL dry THF in a 100 mL round bottom flask and the temperature of the solution was brought down to -70°C. A slight excess of the equivalent amount of n-BuLi in hexanes (0.05 mL, 7.7 mmoles) was added slowly while the mixture was stirred continuously. After complete addition of n-BuLi, CH₃I (0.50 mL, 7.7 mmoles) was added dropwise and

stirred for 5 min at -78°C . The temperature of the reaction mixture was raised to room temperature slowly and stirred for 10 more min. When the reaction went to completion (checked by TLC), the mixture was washed three times with 15 mL portion of aq. saturated NH_4Cl solution. The organic layer was separated and dried over anhydrous Na_2SO_4 . The solution was rotary evaporated, the crude was washed twice with hexane to give the pure 1,2-dimethylbenzimidazole (**68**) in 65% (708mg) yield.

Method 2: 2-Methylbenzimidazole (1.0g, 7.6 mmol) was dissolved in 25 mL CH_2Cl_2 in a 100 mL round bottom flask and treated at room temperature with 25 mL 50% aq. NaOH solution. 50 mg (5% by weight) of $\text{PhCH}_2\text{Et}_3\text{N}^+\text{Br}^-$ was added to the mixture with continuous stirring. When all the reagents fully dissolved, CH_3I was added dropwise and the mixture was stirred overnight at room temperature. The reaction was monitored by TLC. After completion of reaction, the mixture was diluted with 25 mL of water, the organic layer was separated and worked up as described in method 1. The yield of the compound (**68**) was 83% (896 mg).

Preparation of other Benzoheterocycle Complexes (36, 44-49, 51-59, 61-62, 64,).

The following procedure was used for synthesizing all of the above benzoheterocycle triosmium complexes. $[\text{Os}_3(\text{CO})_{10}(\text{CH}_3\text{CN})_2]$ (0.250-0.500g, 0.27-0.54 mmol) was dissolved in 150-300 mL CH_2Cl_2 and a two fold molar excess of the appropriate heterocyclic ligand was added. The reaction mixture was stirred for 12-20h and then filtered through a short silica gel column to remove excess ligand. The solutions were then concentrated by rotary evaporation and the pure complexes (yellow-orange band) were isolated by preparative TLC using CH_2Cl_2 and hexane as solvents in the ratio 1:3,

except for compounds **51**, **52**, **54** and **64** where the eluted solvents were in 2:3 ratio. The yellow complexes were taken up in a minimal volume of dry CH_2Cl_2 , two volumes of dry hexane were added and then cooled to 0°C to yield crystals. Photolysis using Rayonet Photochemical Reactor was carried out in CH_2Cl_2 solution to see if these complexes provide the desired electron deficient complexes. The dark green solutions (if obtained) after photolysis were then filtered through a short column, concentrated to 10-25 mL and cooled to 0°C to yield green crystals. The combined total yields (based on $\text{Os}_3(\text{CO})_{12}$) of the products are given below with the analytical and spectroscopic data.

Crystal Structure Analysis

Suitable crystals of **29**, **32-33**, **38-39**, **43**, **54**, **56** and **66** were coated with paratone oil, suspended in a small fiber loop and placed in a cooled nitrogen gas stream at 100 K on a Bruker D8 SMART APEX CCD sealed tube diffractometer with graphite monochrome MoK_α (0.7103 Å) radiation.

Data were measured using series of combination of phi and omega scans with 10 second frame exposures and 0.3° frame widths. Data collection, indexing, and initial cell refinements were all carried out using smart software.³⁹ Frame integration and final cell refinement were done using SAINT software.⁴⁰ The final cell parameters were determined from least-squares refinement on 6088 reflection. The SADABS⁴¹ program was used to carry out absorption corrections

The structure was solved using Direct method and difference Fourier techniques (SHELXTL, V5.10).⁴² Hydrogen atoms were placed in their expected chemical positions

using the HFIX command and were included in a final cycles of least squares with isotopic U_{ij} 's related to the atoms's ridden upon. C-H distances were fixed at 0.93 Å (aromatic and amide), 0.98 Å (methine), 0.97 Å (methylene), or 0.96 Å (methyl). All non-hydrogen atoms were refined anisotropically. Scattering factors and anomalous dispersion corrections are taken from the *International Tables for the X-ray Crystallography*.⁴³ Structure solution, refinement, graphics and generation of publication materials were performed by SHELXTL, V5.10 software.

Analytical and Spectroscopic Data for Compounds 29 through 71.

Compound 29: Yield for **29**: 60%. Anal Calcd. for $C_{22}H_9NO_9Os_3$: C, 26.37; H, 0.90; N, 1.40%. Found: C, 26.33; H, 0.48; N, 1.19%. IR (ν CO) in CH_2Cl_2 : 2064 s, 2055 s, 2025 s, 2013 s, br, 1994 br, 1979 w, br cm^{-1} . 1H NMR of **29** at 400 MHz in $CDCl_3$: δ 9.79 (s, H(2)), 9.24 (d, H(7)), 8.68 (d, H(5)), 8.49 (d, H(9)), 7.97 (dd, 2H(10 & 12), 7.76 (dd, H(11)), 7.31 (dd, H(6), -12.11(s, hydride).

Compound 32: Yield for **32**: 63 %. Anal Calcd. for $C_{17}H_8N_2O_9Os_3$: C, 21.38; H, 0.84; N, 2.94%. Found: C, 21.45; H, 0.67; N, 2.86%. IR (ν CO) in CH_2Cl_2 : 2073 m, 2043 s, 2014 s, 1984 br, 1942 w, br cm^{-1} . 1H NMR of **32** at 400 MHz in $CDCl_3$: δ 8.72 (s, br, NH), 8.16 (dd, 2H(4 & 6)), 6.98 (dd, H(5)), 2.74 (s, CH_3), -11.78 (s, hydride).

Compound **33**: Yield for **33**: 40%. Anal Calcd. for $C_{16}H_7N_3O_9Os_3$: C, 20.10; H, 0.73; N, 4.40%. Found: C, 20.15; H, 0.42; N, 4.29%. IR (ν CO) in CH_2Cl_2 : 2080 m, 2052 s, 2021 s, 1993 s, br, 1956, w, br, 1941 w, br cm^{-1} . 1H NMR of **33** at 400 MHz in $CDCl_3$: δ 8.58 (d, H(6)), 8.46 (d, H(4)), 7.24 (dd, H(5)), 4.46 (s, CH_3), -11.91 (s, hydride).

Compound **34**: Yield for **34**: 4%. IR (ν CO) in CH_2Cl_2 : 2100 m, 2072 s, 2056 w, 2043 s, 1015 m, br, 1996 w, br cm^{-1} . 1H NMR of **34** at 400 MHz in $CDCl_3$: δ 8.90 (s, NH), 7.58(d, H(7)), 7.38 (dd, H(4)), 7.27 (dd, 2H(5 & 6)), 2.63 (d, (CH)), 2.07(d, (CH)), -14.21(s, hydride).

Compound **35**: Yield for **35**: 90% (conversion from compound **34** to **35**). IR (ν CO) in CH_2Cl_2 : 2101 s, 2072 s, 2043 s, 1013 s, br, 1995 s, br 1956 m, br cm^{-1} . 1H NMR of **35** at 400 MHz in $CDCl_3$: δ 8.63 (s, NH), 7.16(d, H(7)), 7.06(dd, 2H(5 and 6)), 7.00 (d, 4(H)), 2.16 (s, CH), -14.55 (s, hydride), -14.95 (s, hydride).

Compound **36**: Yield for **36**: 27%. Anal Calcd.for $C_{17}H_7N_3O_{10}Os_3$: C, 20.10; H, 0.73; N, 4.40%. Found: C, 20.96 (out of range); H, 0.82; N, 4.13%. IR (ν CO) in CH_2Cl_2 : 2063 s, 2050 s, 2017 s, 2005 s, br, 1990 w, br cm^{-1} . 1H NMR of **36** at 400 MHz in $CDCl$: δ 7.78 (dd, H(6)), 7.20 (dd, H(5)), 6.96 (dd, (H)), 4.19 (s, NCH_3), -14.03(s, hydride).

Compound **37**: Yield for **37**: 37 %. Anal Calcd.for $C_{16}H_5NO_{10}Os_3$: C, 20.40; H, 0.53; N, 1.48%. Found: C, 20.19; H, 0.60; N, 1.55%. IR (ν CO) in CH_2Cl_2 : 2079 s, 2051 s, 2022 s,

1989 s, br, 1965 w, br cm^{-1} . ^1H NMR of **37** at 400 MHz in CD_3COCD_3 : δ 9.93 (s, H (2)), 8.86 (d, H(6)), 8.55 (d, H(4)), 7.45 (t, H(5)), -11.96 (s, hydride).

Compound **38**: Yield for **38**: 50 %. Anal Calcd.for $\text{C}_{17}\text{H}_7\text{NO}_{10}\text{Os}_3$: C, 21.36; H, 0.73; N, 1.47%. Found: C, 21.47; H, 0.54; N, 1.43%. IR (ν CO) in CH_2Cl_2 : 2078 s, 2049 s, 2021 s, 1990 s, br, 1952 w, 1942 w, br cm^{-1} . ^1H NMR of **38** at 400 MHz in CDCl_3 : δ 8.28 (dd, 2H (4 & 6)), 7.09 (dd, H(5)), 2.91 (s, CH_3), -11.91 (s, hydride).

Compound **39**: Yield for **39**: 59%. Anal Calcd.for $\text{C}_{16}\text{H}_5\text{NO}_9\text{Os}_3$: C, 20.06; H, 0.52; N, 1.46%. Found: C, 20.15; H, 0.38; N, 1.36%. IR (ν CO) in CH_2Cl_2 : 2072 s, 2050 s, 2022 s, 1992 s, br, 1954 w, 1941 w, br cm^{-1} . ^1H NMR of **39** at 400 MHz in CDCl_3 : δ 9.04 (s, H(2)), 8.74 (dd, H(6)), 8.58 (dd, H(4)), 7.18 (dd, H(5)), -11.84 (s, hydride).

Compound **40**: Yield for **40**: 55%. Anal Calcd.for $\text{C}_{17}\text{H}_7\text{NO}_9\text{Os}_3$: C, 21.01; H, 0.72; N, 1.44%. Found: C, 21.22; H, 0.61; N, 1.34%. IR (ν CO) in CH_2Cl_2 : 2076 m, 2049 s, 2019 s, 1989 s, br, 1952 w, br cm^{-1} . ^1H NMR of **40** at 400 MHz in CDCl_3 : δ 8.59 (dd, H(6)), 8.44 (dd, H(4)), 7.09 (dd, H(5)), 3.03 (s, CH_3), -12.03 (s, hydride).

Compound **41**: Yield for **41**: 2.5%. IR (ν CO) in CH_2Cl_2 : 2072 m, 2059 s, 2049 s, 2019 s, br, 1990 w, br cm^{-1} . ^1H NMR of **41** at 400 MHz in CDCl_3 : δ 8.08 (d, H(7)), 7.62(d, H(4)), 7.41 (dd, 2H(5 & 6)), 3.20 (d, (CH)), 2.60(d, (CH)), -13.57 (s, hydride).

Compound **42**: Yield for **42**: 88%(conversion from compound **41** to **42**). IR (ν CO) in CH_2Cl_2 : 2076 s, 2068 s, 2049 w, 2027 s, br, 2015 s, 2001 w, br, 1990 s, br cm^{-1} . ^1H NMR

of **42** at 400 MHz in CDCl₃: δ 7.95 (d, H(7)), 7.80(d, H(4)), 7.69 (dd, H(6)), 7.51 (dd, H(5)), 2.15 (s, (CH)), -14.37 (s,hydride), -14.62 (s, hydride).

Compound **43**: Yield for **43**: 68%. Anal Calcd.for C₁₇H₆N₂O₉Os₃: C, 21.43; H, 0.63; N, 2.94%. Found: C, 21.46; H, 0.48; N, 2.83%. IR (ν CO) in CH₂Cl₂: 2077 s, 2051 s, 2020 s, 1991 s, br, 1952 w, 1941 w, br cm⁻¹. ¹H NMR of **43** at 400 MHz in CDCl₃: δ 9.15 (d, H(2)), 8.72 (dd, H(7)), 8.67 (dd, H(5)), 8.54 (d, H(3)), 7.46 (dd, H(6), -12.16(s, hydride).

Compound **44**: Yield for **44**: 35%. IR (ν CO) in CH₂Cl₂: 2065 s, 2051 s, 2020 s, 2008 s, br, 1995 w, br cm⁻¹. ¹H NMR of **44** at 400 MHz in CDCl₃: δ 8.40 (s, H(4)), 8.00 (d, H(8)), 7.86 (dd, 2H (6 &7)), 7.75 (d, H(5)), -14.65 (s, hydride).

Compound **45**: Yield for **45**: 35%. IR (ν CO) in CH₂Cl₂: 2064 s, 2053 s, 2022 s, 2010 s, br, 1992 m, br cm⁻¹. ¹H NMR of **45** at 400 MHz in CDCl₃: δ 8.87 (s, H(4)), 7.80 (d, H(8)), 7.73 (dd, H (7)), 7.65 (dd, H(6)), 7.44 (d, H(5)), -14.82 (s, hydride).

Compound **46**: Yield for **46**: 18%. IR (ν CO) in CH₂Cl₂: 2061 s, 2055 s, 2023 s, br 1990 w, br, cm⁻¹. ¹H NMR of **46** at 400 MHz in CDCl₃: δ 9.18 (d, H(3)), 8.64 (d, H(4 or 8)), 8.30 (d, H (8 or 4)), 8.23 (dd, H(7)), 8.01 (dd, H(6)), 7.85 (d, H(5)).

Compound **47**: Yield for **47**: 44%. IR (ν CO) in CH₂Cl₂: 2066 s, 2053 s, 2019 s, br 1993 w, br, cm⁻¹. ¹H NMR of **47** at 400 MHz in CDCl₃: δ 8.04(d, H(8)), 7.75 (s, H(4)), 7.65 (dd, H (7)), 7.58 (dd, H(6)), 7.51 (d, H(5)), -14.82 (s, hydride).

Compound 48: Yield for **48:** 1%. IR (ν CO) in CH_2Cl_2 : 2082 s, 2028 s, 2015 s, 1980 s, br, 1956 w, br cm^{-1} . ^1H NMR of **48** at 400 MHz in CDCl_3 : δ 9.50 (d, H(3)), 8.25 (dd, H(7)), 8.13 (d, H(4)), 7.98 (dd, H(6)), 7.50 (d, H(5)), -11.08 (s, hydride).

Compound 49: Yield 76%. Anal Calcd. for $\text{C}_{17}\text{H}_5\text{NO}_{11}\text{SO}_3$: C, 20.37; H, 0.50; N, 1.40; S, 3.20%. Found: C, 20.50; H, 0.60, N, 1.44, S, 3.25%. IR (ν CO) in CH_2Cl_2 : 2069 s, 2060 s, br 2018 s, br, 1985 w, br cm^{-1} . ^1H -NMR of **49** at 400 MHz in CDCl_3 : δ 7.58 (d, H(7)), 7.42(ddd, H(6)), 7.34(dd, H(4)), 7.16(t, H(5)) and -10.78(s, hydride).

Compound 50: Yield 89%. Anal Calcd. for $\text{C}_{14}\text{H}_{11}\text{NOS}$: C, 69.71; H, 4.56; N, 5.81%. Found: C, 69.65; H, 4.18; N, 5.65%. IR (ν) in CH_2Cl_2 : 3020(w), 2980(w), 1669(s), 1589(m), 1471(s), 1375(m) and 1322(m) cm^{-1} .
 ^1H -NMR of **50** at 400 MHz in CDCl_3 : δ 7.42(dd, H(7)), 7.39(dd, H(4)), 7.32-7.26(m, 5H(phenyl)), 7.20(d of t, H(5)), 7.12(d of t, H(6)) and 5.15(s, 2H(- CH_2 -)).

Compound 51: Yield 32%. Anal Calcd. for $\text{C}_{24}\text{H}_{11}\text{NO}_{11}\text{SO}_3$: C, 26.40; H, 1.01; N, 1.28%. Found: C, 26.49; H, 1.18; N, 1.14%.

IR (ν CO) in CH_2Cl_2 : 2066 s, 2058 s, 2016 s, br, 1994 br, 1980 w, br cm^{-1} .

^1H -NMR of **51** at 400 MHz in CDCl_3 : δ 7.42(dd, H(7)), 7.32-7.28(m, 5H(phenyl)), 7.10(t, H(5)), 6.94(dd, H(4)), 5.14(s, 2(H)) and -12.63(s, hydride).

Compound 52: Yield 5%. Anal Calcd. for $\text{C}_{15}\text{H}_5\text{N}_3\text{O}_9\text{SO}_3$: C, 18.50; H, 0.51; N, 4.31%

Found: C, 18.17; H, 0.58; N, 4.42%.

IR (ν CO) in CH_2Cl_2 : 2062 s, 2051 s, 2018 s, br, 2004 s, br, 1991 s, br, 1966w, br cm^{-1} .

^1H -NMR of **52** at 400 MHz in CDCl_3 : δ 7.86 (d, H(6)), 6.48(d, H(5)), 4.31(s, 2H(-NH₂-)) and -13.71(s, hydride).

Compound **53**: Yield 46%. Anal Calcd. for $\text{C}_{16}\text{H}_7\text{N}_4\text{O}_{10}\text{Os}_3$: C, 19.49; H, 0.71; N, 5.69%

Found: C, 19.27; H, 0.89; N, 5.38%.

IR (ν CO) in CH_2Cl_2 : 2064 s, 2051 s, 2019 s, br, 2005 s, br 1992 w, br cm^{-1} .

^1H -NMR of **53** at 400 MHz in CDCl_3 : δ 7.77 (dd, H(6)), 7.22 (dd, H(4)), 7.08(d, H(5)), 6.80 (s, 2H(NH₂)) and -14.00 (s, hydride).

Compound **54**: Yield 39%. Anal Calcd. for $\text{C}_{16}\text{H}_5\text{N}_4\text{O}_{10}\text{Os}_3$: C, 19.49; H, 0.51; N, 5.69%

Found: C, 19.66; H, 0.51; N, 5.44%

IR (ν CO) in CH_2Cl_2 : 2062 s, 2050 s, 2022 s, br, 2005 s, br 1990 w, br cm^{-1} .

^1H -NMR of **54** at 400 MHz in CDCl_3 : δ 7.83 (dd, H(7)), 7.41(dd H(4)), 7.28-7.25 (m, 2H(5 & 6)) and -13.28 (s, hydride).

Compound **56**: Yield for **56**: 10%. Anal Calcd. for $\text{C}_{16}\text{H}_6\text{N}_2\text{O}_9\text{SO}_3$: C, 19.75; H, 0.62; N, 2.88%. Found: C, 19.96; H, 0.39; N, 2.76%.

IR (ν CO) in CH_2Cl_2 : 2074 s, 2048 s, 2017 s, 1987 s, br, 1950 w, br cm^{-1} .

^1H NMR of **56** at 400 MHz in CDCl_3 : δ 8.37 (d, H(6)), 8.15 (d, H(4)), 6.85 (dd, H(5)), 5.93 (s, 2H(-NH₂)) -12.05 (s, hydride).

Compound **57**: Yield for **57**: 45%. Anal Calcd. for $C_{17}H_6N_2O_{10}SO_3$: C, 20.40; H, 0.60; N, 2.80%. Found: C, 20.65; H, 0.56; N, 2.90%.

IR (ν CO) in CH_2Cl_2 : 2064 s, 2056 s, 2018 s, br 1995 w, br, cm^{-1} .

1H NMR of **57** at 400 MHz in $CDCl_3$: δ 7.45 (d, H(7)), 7.33 (dd, H(6)), 7.20 (d, H (4)), 7.01 (dd, H(5)), 4.60 (s, N-H) -12.34 (s, hydride).

Compound **58**: Yield for **58**: 22%. Anal Calcd. for $C_{17}H_6N_2O_{10}SO_3$: C, 20.40; H, 0.60; N, 2.80%. Found: C, 20.91; H, 0.52; N, 2.67%.

IR (ν CO) in CH_2Cl_2 : 2062 s, 2053 s, 2014 s, 1992 m, br, cm^{-1} .

1H NMR of **58** at 400 MHz in $CDCl_3$: δ 7.22 (d, H(7)), 7.18 (ddd, H(6)), 7.01(ddd, H (5)), 6.92 (d, H(4)), 6.73 (s, -NH), -14.92 (s, hydride).

Compound **59**: Yield for **59**: 5%. Anal Calcd. for $C_{19}H_9N_3O_{10}SO_3$: C, 21.90; H, 0.90; N, 4.03%. Found: C, 21.74; H, 1.39; N, 3.61%.

IR (ν CO) in CH_2Cl_2 : 2084 w, 2045 s, 2024 s, 1998 w, br, 1978 s, br, cm^{-1} . 1H NMR of **59** at 400 MHz in $CDCl_3$: δ 7.16 (d, H(7)), 7.12 (dd, H(6)), 6.93 (dd, H (5)), 6.85 (d, H(4)), 6.64 (s, -NH), 2.56 (s, - CH_3), -14.08 (s, hydride).

Compound **60**: Yield 79%. Anal Calcd. for $C_{15}H_{12}N_2O_2S$: C, 63.38; H, 4.22; N, 9.86%. Found: C, 63.66; H, 4.43; N, 9.78%.

IR (ν) in CH_2Cl_2 : 3410 m, 3011w, 2981 m, 1664 s, 1612 s, 1500 m, 1361 m and 1331 m cm^{-1} . 1H -NMR of **60** at 400 MHz in $CDCl_3$: δ 7.77(d, H(7)), 7.71(d, H(4)), 7.47-7.41(m, 5H(phenyl)), 7.25(t, H(6)), 7.12(t, H(5)), 5.56(s, NH) and 5.30(s, 2H(- CH_2 -)).

Compound 61: Yield 15%. Anal Calcd. for $C_{24}H_{12}N_2O_{11}SO_3$: C, 26.04; H, 1.08; N, 2.53%. Found: C, 25.57; H, 0.93; N, 2.40%.

IR (ν CO) in CH_2Cl_2 : 2076 s, 2059 s, 2026 s, 2015 s, br 1993 br, 1985 w, $br\ cm^{-1}$.

1H -NMR of **61** at 400 MHz in $CDCl_3$: δ 8.00 (d, H(6)), 7.56 (d, H(4)), 7.52-7.50(m, 2H(o-phenyl)), 7.42-7.39(m, 3H(m & p-phenyl)), 7.28 (d of t, H(5)), 6.52 (s, H(NH)), 5.45(d, H(H_a or H_b)), 5.18 (d, H(H_a or H_b)) and -11.22 (s, hydride).

Compound 62: Yield 20%. Anal Calcd. for $C_{25}H_{12}N_2O_{11}SO_3$: C, 26.46; H, 1.06; N, 2.47%. Found: C, 26.34; H, 1.25; N, 2.26%.

IR (ν CO) in CH_2Cl_2 : 2060 s, 2027 s, 2000 s, $br\ cm^{-1}$.

1H -NMR of **62** at 400 MHz in $CDCl_3$: δ 7.82(d, H(7)), 7.67(d, H(4)), 7.64(t, H(6)), 7.47-7.41(m, 5H(phenyl)), 7.36(t, H(5)), 5.27(s, 2H(- CH_2 -)) and -10.64(s, hydride).

Compound 63: Yield 74%. Anal Calcd. for $C_{17}H_{16}N_2O_3S$: C, 62.20; H, 4.90; N, 8.54%.

Found: C, 61.89; H, 4.57; N, 8.28%. IR (ν) in CH_2Cl_2 : 3404 m, 3005w, 2978 s, 1665 s, 1615 s, 1409 m, 1358 m and 1338 m cm^{-1} .

1H -NMR of **63** at 400 MHz in $CDCl_3$: δ 7.54(d, H(7)), 7.43-7.39(m, 5H(phenyl)), 7.21(d, H(5)), 7.20(d, H(4)), 6.62(d, H(NH)), 5.33(s, 2H(- CH_2 -)), 4.03(q, 2H(CH_3CH_2O -)) and 1.43(t, 3H(CH_3CH_2O -)).

Compound 64: Yield 21%. Anal Calcd. for $C_{26}H_{16}N_2O_{12}SO_3$: C, 27.20; H, 1.40; N, 2.44%. Found: C, 27.16; H, 1.61; N, 2.27%.

IR (ν CO) in CH₂Cl₂: 2067 s, 2057 s, 2025 s, 2014 s, br, 1993 br, 1986 w, br cm⁻¹.

¹H-NMR of **64** at 400 MHz in CDCl₃: δ 7.90(d, H(5)), 7.53-7.40(m, 5H(phenyl)), 7.09(d, H(4)), 7.04(d, H(NH)), 5.44(d, H(H_a or H_b)), 5.17(d, H(H_a or H_b)), 4.06(q, 2H(CH₃CH₂O-)), 1.43(t, 3H(CH₃CH₂O-)) and -11.23(s, hydride).

Compound **65**: Yield 61%. Anal Calcd. for C₂₀H₁₂N₂O₁₁SO₃ : C, 23.39; H, 1.17; N, 2.73%. Found: C, 23.51; H, 1.28; N, 2.78%.

IR (ν CO) in CH₂Cl₂: 2073 s, 2042 s, 2015 s, 1984 s, br, 1945 w, br, cm⁻¹.

¹H-NMR of **65** at 400 MHz in CDCl₃: δ 10.25(s, NH), 8.19(dd, H(6)), 8.16(dd, H(4)), 6.98(dd, H(5)), 3.70(s, OCH₃), 3.30(m, CH₂), 2.86(m, CH₂) and -11.76(s, hydride).

Compound **66**: Yield 51%. Anal Calcd. for C₁₈H₈N₂O₉Os₃ : C, 22.36; H, 0.83; N, 2.90%. Found: C, 22.36; H, 0.58; N, 2.51%.

IR (ν CO) in CH₂Cl₂: 2075 m, 2044 s, 2015 s, 1984 s, br, 1944 w, br, cm⁻¹.

¹H-NMR of **66** at 400 MHz in CDCl₃: δ 8.67(dd, H(7)), 7.41(d of t, H(6)), 8.59(dd, H(5)), 2.72(s, CH₃), 9.02(s, H(2)) and -12.21(s, hydride).

Compound **67**: Yield 4%. IR (ν CO) in CH₂Cl₂: 2064 m, 2055 s, 2017 s, 2001 s, br, 1988 w, br, cm⁻¹. ¹H-NMR of **67** at 400 MHz in CDCl₃: δ 8.75(d, H(8)), 7.78(t, H(6)), 7.78(d, H(5)), 7.75 (t, H(7)), 2.89(s, CH₃), 9.02(s, H(2)) and -14.11(s, hydride).

Compound **68**: Yield 83%. Anal Calcd. for C₉H₁₀N₂ : C, 73.97; H, 6.85; N, 19.18%. Found: C, 73.78; H, 6.74; N, 19.11%

TOF MS (m/s) Calcd. for **68** (M+H) 147.00, found 147.00

$^1\text{H-NMR}$ of **68** at 400 MHz in CDCl_3 : δ 7.19(m, 3H(5,6,4 or 7)), 7.65(dd, H(7 or 4)), 3.63(s, N- CH_3), 2.53 (s, N- CH_3).

Compound **70**: Yield 6%. IR (ν CO) in CH_2Cl_2 : 2076 m, 2067 s, 1960 m, 2043 s, 2012 m, br, 1994w, br, cm^{-1} .

$^1\text{H-NMR}$ of **70** at 400 MHz in CDCl_3 : δ 7.61(d, H(7)), 7.38(d, H(4)), 7.30(t, H(6)), 7.21(t, H(5)), 3.67(s, N- CH_3), 2.58 (d, $J=18.8\text{Hz}$ (CH)), 1.83(d, $J=18.8\text{Hz}$, (CH)), and -14.16 (s, hydride).

Compound **71**: Yield 48%. Anal Calcd. for $\text{C}_{18}\text{H}_{10}\text{N}_2\text{O}_9\text{Os}_3$: C, 22.31; H, 1.03; N, 2.89%. Found: C, 22.47 H, 0.80; N, 2.55%.

IR (ν CO) in CH_2Cl_2 : 2076 m, 2048 s, 2012 s, 1987 s, br, 1943 w, br, cm^{-1} .

$^1\text{H-NMR}$ of **71** at 400 MHz in CDCl_3 : δ 8.19(dd, H(7)), 7.04(d of t, H(6)), 8.17(d, H(5)), 3.81(s, N- CH_3), 2.70(s, C- CH_3).and -11.77 (s, hydride).

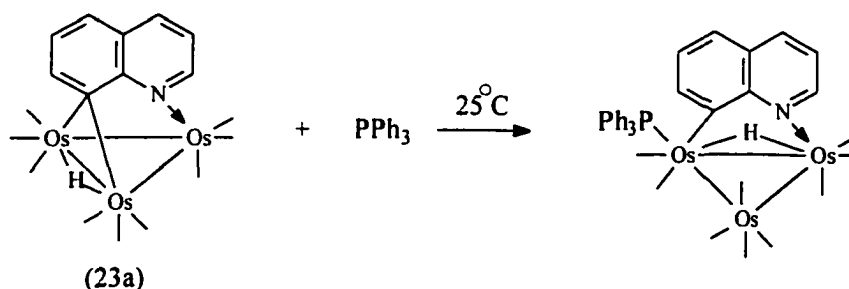
Chapter 3

Reactions of Electron Deficient Benzoheterocyclic Clusters, $\text{Os}_3(\text{CO})_9(\mu_3\eta^2\text{-heterocycle-H})(\mu\text{-H})$ with Heteroatom Nucleophiles and Protic Acids

3.1 Introduction

It has been shown that the reactions of electron deficient clusters of quinoline, $\text{Os}_3(\text{CO})_9(\mu_3\eta^2\text{-C}_9\text{H}_6\text{N})(\mu\text{-H})$ (**23a**) with soft nucleophiles such as phosphines results in ligand addition at the metal core along with rearrangement (Equation 3.1).^{1, 21}

Equation 3.1



On the other hand, reaction with hydride²¹ or carbanions³ results in nucleophilic attack at the 5-position of the quinoline ring. Subsequent protonation leads to a nucleophilic addition product, and hydride abstraction from the intermediate anions effects overall

nucleophilic substitution.³ In light of this diverse reactivity, a study of the reactivity of **23a** with amines and carboxylic acids which are intermediate in nucleophilicity relative to phosphines and carbanions was done in order to define the stereodynamics of their coordination sites.

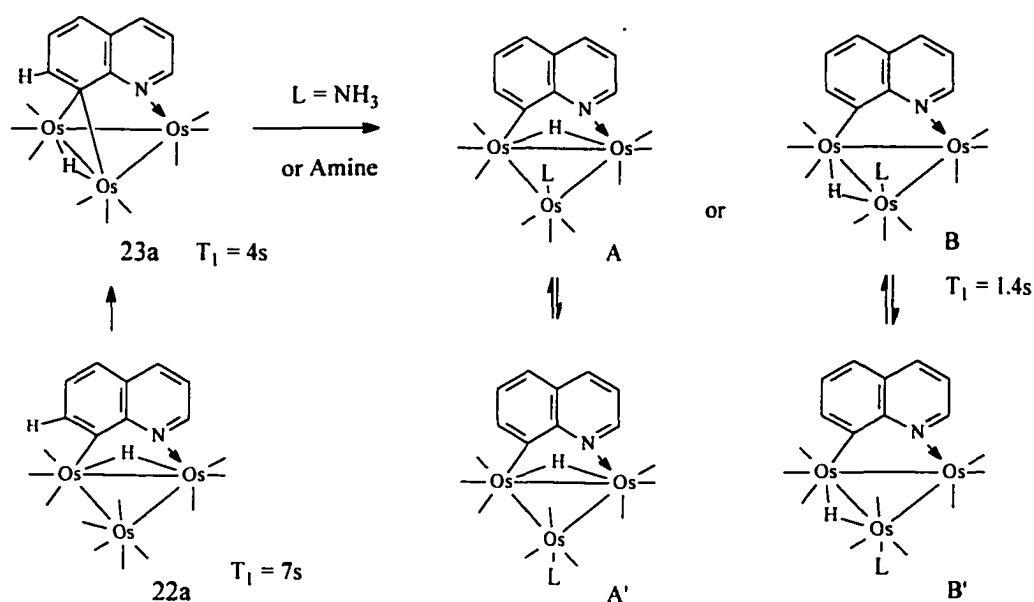
The addition of a large excess (10 fold) of ammonia and various aliphatic amines to **23a** results in an instant color change from green to orange, and yields two new isomers. Initial formation of one isomer is followed by the gradual appearance of a second one. Two alternative structures for the set of isomers formed from the interaction of amines with **23a** were proposed. One set has the hydride and the quinoline ring sharing a common edge while the amine occupies either axial site on the third unbridged osmium atom (Structures A, A', Scheme 3.1). This structure is directly analogous to that observed in the related imido complexes.⁴⁴

On the other hand, coordination of the amine at the electron deficient Os edge of **23a** could lead to a structure where the quinoline ring and the hydride are on different edges with amine occupying an axial position on the osmium atom bridged by the hydride but not by the quinoline ring (Structures B, B', Scheme 3.1). This type of structure has been observed in the case of one imido complex⁴⁵ and proposed as a short-lived intermediate from the selective incorporation of carbon monoxide into **23a**.¹ In the case of phosphines reacting with **23** such an intermediate is probably the initial product as well but goes on to rearrange as shown above (Equation 3.1).^{1, 21}

In order to try to distinguish between structures A and B the change in longitudinal relaxation time (T_1) of hydrides in metal clusters induced by proximal ligand protons was

used to quantitatively assess the distance between these two types of hydrogens. In A, when $L = \text{NH}_3$, the ammonia protons are much further away from the hydride than in B and should have no influence on T_1 . For $\text{Os}_3(\text{CO})_{10}(\mu\text{-}\eta^2\text{-C}_9\text{H}_6\text{N})(\mu\text{-H})$ (**22a**) the T_1 of the hydride is 7.0 s while for **23a** it is 4.0s (Scheme 3.1). The shorter relaxation time in **23a** can be attributed to the proximity of the hydrogen of C(7) to the μ -hydride. If the amine

Scheme 3.1



adducts of **23a** have a structure identical to their μ_3 -imidoyl analogs then the T_1 of the μ -hydride would be expected to have a relaxation time similar to **22a**. In fact, the T_1 of the ammonia adduct of **23a** is 1.4 s which is consistent with a structure where the ammonia protons are proximal to the hydride; i.e., the structure resulting from addition of the ligand to the carbon bridged edge of the cluster without further rearrangement (Structure

B, Scheme 3.1). This suggested structure is further supported by the ^1H NMR data obtained for the *s*-butyl adduct of **23a**.⁹ Here, four hydride resonances are observed. This is undoubtedly due to the presence of diastereomers induced by the presence of the chiral center on the *s*-butyl amine. In the structure proposed based on the T_1 measurements (Structure B, Scheme 3.1), the environment on the osmium atom bound to the amine is quite asymmetric owing to the presence of the bridging hydride on one of the two edges of the triangle associate with the amine coordinated osmium atom. In the case of the structure proposed as A, the localized environment on the amine bound nitrogen is more symmetric and indeed only two hydride resonances are observed for the *s*-butyl complex.⁹ Finally, the structure proposed is most consistent with a reversible amine coordination based on the principle of least motion since only the motion of the C(8) carbon pivoting on the coordinated nitrogen is required to reform **23a** from its corresponding amine adduct. This motion is related to the reversible coordination of the C=N bond observed in the μ_3 - to μ - to μ_3 - imidoyl interconversions.⁴⁴

The recent studies of the reactions of **23a** with protic acids⁹ showed that it undergoes simple protonation at the metal core with both HBF_4 and $\text{CF}_3\text{CO}_2\text{H}$. The latter is known to form adducts with related heterocycle triosmium clusters.⁴⁴ It was also found that both the ability to coordinate amines (Lewis acid properties) and the basicity of the metal core were influenced by the nature of the substituent at the 5-position of the quinoline ring. Electron donating groups at this position enhanced the basicity of the metal core and decreased its ability to bind amines.²

Previous studies of the electrochemistry of the electron deficient triosmium clusters, $\text{Os}_3(\text{CO})_9(\mu_3\text{-}\eta^2\text{-L-H})(\mu\text{-H})$ (L= quinoline, **23a**; phenanthridine, **29**; 2-methylbenzimidazole, **32**; 2-methylbenzotriazole, **33**; benzoxazole, **37**; 2-methylbenzoxazole, **38**; benzothiazole, **39**, 2-methylbenzothiazole, **40**; quinoxaline, **43** and 5,6-benzoquinoline, **72**) showed that they all have very different electrochemical properties even though solid state structures reveal that the metal-ligand bond lengths are remarkably similar throughout the series(Os-N=2.10-2.17(2) Å Os-C= 2.25-2.32(2) Å) (Table 2.1, Chapter 2). Thus, compound **23a** exhibits two well separated and chemically irreversible $1e^-$ reduction potentials while the first reduction potentials for **29** and **72** result in the formation of stable radical anions. Compounds **32-33**, **37-40**, on the other hand exhibit two irreversible overlapping $1e^-$ reduction potentials. The first reduction potentials correlate reasonably well with the metal-metal bond n to σ^* transition in the 600-700 nm region, suggesting that they are metal based, but the wide variation in the overall electrochemical behavior of **23a**, **29**, **32-33**, **37-40**, **43**, and **72** suggests that ligand orbitals are important in determining the chemical behavior of these systems despite their structural similarities. In light of the results of the reactions of **23a** with amines and protic acids and the electrochemical behavior of **23a**, **29**, **32-33**, **37-40**, **43**, and **72** discussed above, we thought it would be useful to survey the reactions of these complexes with amines and with protic acids in order to determine if the observed differences in electrochemical behavior carry over to their acid–base properties. We report the results of these studies along with the related reactions of these complexes with acetonitrile and triphenylphosphine in an attempt to define the stereodynamics of its coordination sites

and how these differ from those observed in quinoline complex. One of our research goals in developing the chemistry of these electron deficient complexes was to understand the degree of electronic communication between the benzoheterocyclic ring and the metal core. The equilibrium constants for the reactions of these clusters with amines will give an indication of influence of structural changes in the heterocycles on the electrophilicity of the complexes.

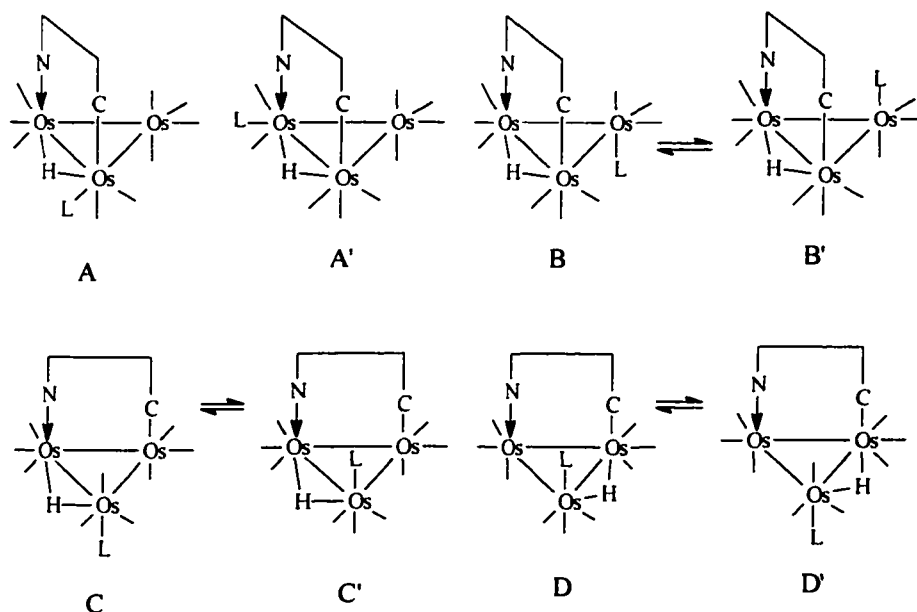
3.2 Results and Discussion

3.2.1 Reactions with Triphenylphosphine, Acetonitrile and n-Butylamine

The complexes **23a**, **29**, **32-33**, **37-40**, **43**, and **72** can be divided into three structural types: 1) those related to quinoline, **23a**, **29**, **72**; 2) quinoxaline, **43**; 3) the 6,5-fused ring systems with two or three heteroatoms, **32-33** and **37-40**. All three of these structural types react with triphenyl phosphine to give the adducts $\text{Os}_3(\text{CO})_9(\mu_3\text{-}\eta^2\text{-L-H})(\mu\text{-H})\text{PPh}_3$ (L= quinoline, **73**; 5,6-benzoquinoline, **74**; quinoxaline, **75**; 2-methyl benzimidazole, **76**; benzoxazole,**77**). The structures of **73** and **74** have been previously reported to have the phosphine ligand in a radial position *cis*- to the hydride and residing on the carbon bound osmium atom, based on a solid state structure of **73** and the almost identical ^{13}C NMR of **73** and **74** (Structure A, Scheme 3.2; Table 3.1).^{1,21,31} A key feature of the ^{13}C NMR of **73** and **74** is the observation of three broadened resonances

attributable to the tripodal motion of three of the four carbonyl groups of the $\text{Os}(\text{CO})_4$ moiety (resonances **g**, **h**, **i**; Table 3.1). At low temperatures ($-40\text{ }^\circ\text{C}$) the expected *trans*- $^{13}\text{C} - ^{13}\text{C}$ coupling of 30-35 Hz is observed between the resonances assigned to carbonyls **g** and **i** confirming the presence of the $\text{Os}(\text{CO})_4$ group. The ^{13}C NMR spectra of compounds **75-77** also exhibit these features and indeed have ^{13}C NMR spectra that are very similar to **73** and **74** (Table 3.1). On this basis we assign structure **A** to all of these phosphine adducts (Scheme 3.2). In the case of benzoxazole, a second minor isomer is observed as evidenced by the observation of a second doublet in the hydride region at

Scheme 3.2



-16.14 ppm ($J^{31}\text{P}-^1\text{H}=14.2\text{ Hz}$) along with companion peaks to the major isomer in the ^1H and ^{13}C NMR. Although overlap of resonances and the inseparability of the two isomers precluded the characterization of this minor product we suggest that it has the phosphine

substituent on the nitrogen bound osmium atom (structure **A'** Scheme 3.2) as has been previously reported for related nitrogen heterocycle triosmium complexes.⁴⁵

It has been reported previously that **23a** and its substituted derivatives undergo ligand cleavage in acetonitrile at 70-80 °C in the presence of 1 atm of CO to yield $\text{Os}_3(\text{CO})_{12}$ and the free quinoline.^{2,3} It seems reasonable to suggest that the first step in this process is the formation of an acetonitrile adduct. However, compounds **23a**, **29** and **72** show no evidence for adduct formation when dissolved in acetonitrile, maintaining their green color and exhibiting only minor shift changes in their ^1H NMR. In sharp contrast compounds **32** and **37** undergo an immediate color change, from dark green to light green and from dark green to yellow respectively, on dissolution in acetonitrile and show significant changes in their ^1H and ^{13}C NMR relative to CDCl_3 (Tables 3.2 and 3.3). In the case of **32** the light green solution shows evidence for the presence of residual starting material in its ^1H NMR as well as the presence of two new hydride resonances at -12.15 and -12.40 ppm and associated new aromatic and NH resonances. The hydride resonances of the two new species present integrate in a ratio of 11.6:1 relative to the hydride resonance attributable to **32**. Using the starting moles of **32** in the solution, the volume of acetonitrile and the hydride integration ratios we can estimate the equilibrium constant for the reaction of **32** with acetonitrile to be 0.68 M^{-1} . The main feature of the proton coupled ^{13}C NMR in the carbonyl region is the observation of two closely spaced doublets ($\Delta\delta=1.4$) with relatively large coupling to the bridging hydride (Table 3.3). This feature is also observed in the decacarbonyl of **37** where $\Delta\delta = 0.80$ (Table 3.3). This small value for the $\Delta\delta$ of the carbonyls *trans*- to the hydride is indicative of a structure

where the benzoheterocycle bridges the same edge as the hydride and the acetonitrile is coordinated to the unbridged osmium (Structure **B**, Scheme 3.2). This same feature was also observed for the acetonitrile adduct of the imido complex $\text{Os}_3(\text{CO})_9(\mu_3\text{-}\eta^2\text{-(CH}_2)_3\text{C=N-})(\mu\text{-H})$ where a crystal structure was obtained ($\Delta\delta=0.05$).⁴⁴ The assignments given in Table 3.3 for the carbonyl groups of the acetonitrile adducts of **32**, **37** and **43** were made on the basis of established trends in chemical shift and coupling constant data for these types of cluster.^{9,44} These assignments are by no means unambiguous but the general features as discussed above allow us to distinguish between the structural isomers possible (*vide infra*). We cannot, of course, differentiate between structures **B** and **B'** (Scheme 3.2) based on the current data; **B** is chosen here based on analogy with previously reported acetonitrile adducts.⁴⁴ Further evidence that the structures of the decacarbonyl and acetonitrile adduct of **32** are the same comes from the fact that they both have the similar T_1 values for the hydride in acetonitrile (7.2 and 8.0 s respectively). Compound **43** undergoes a color change from dark green to red (the same color as the decacarbonyl), and the ^1H and ^{13}C NMR data support formation of an acetonitrile adduct with structure **B** or **B'** (Tables 3.2 and 3.3). In addition to one major adduct isomer and residual starting material solution of **43** in acetonitrile shows the presence of three minor isomers. One of the minor isomers shows a set of sharp resonances partially overlapping with the major isomer and a hydride resonance at -11.04 ppm and can tentatively be assigned to **B'**.⁴⁴ The two other isomers show broad hydride resonances at -13.61 and -13.85 ppm in a relative intensity of 10:1 with companion broad resonances in the aromatic region. The broadness of these lines and the chemical shifts of the hydrides

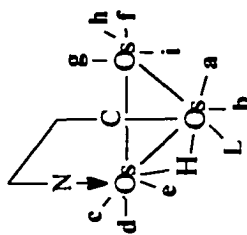


Table 3.1 Proton Coupled ^{13}C NMR Data for the Phosphine Adducts of the Electron Deficient Benzoheterocycle Complexes^a

| Ring | No. | a | b | c | d | e | f | g | h | i |
|-------------------------------------|-----|-----------------------------------|----------------------|-----------------------|-------------------------|--------------------|-----------|-----------|-----------|-----------|
| Quinoline ^b | 73 | 182.53(dd) JCH=7.5 JPC=4.5 | 185.73(d) JPC=6.1 | 177.95(d) JCH=13.7 | 177.68(d) JCH=3.1 | 177.87(d) JCH<1 | 176.54(s) | 184.52(s) | 178.03(s) | 184.22(s) |
| 5,6 Benzo ^c quinoline | 74 | 182.53(dd) JCH=9.0 JPC=4.6 | 185.64(d) JPC=6.2 | 178.10(d) JCH=13.0 | 177.93(d) JCH=4.5 | 177.06(s) | 176.50(s) | 184.50(s) | 178.02(s) | 184.43(s) |
| Quinoxaline | 75 | 182.77(dd) JCH=8.0 JPC=4.6 | 187.04(d) JPC=6.1 | 177.82(d) JCH=14.0 | 178.14 ^d (d) | 178.19(s) | 177.15(s) | 185.72(s) | 178.72(s) | 185.82(s) |
| 2-Me- Benzimidazole | 76 | 184.04(dd) JCH=11.0 JPC=5.0 | 188.24(d) JPC=6.0 | 177.90(d) JCH=13.0 | 176.76(d) JCH=3.0 | 179.25(d) JCH=1 | 178.59(s) | 186.41(s) | 178.59(s) | 185.17(s) |
| Benzoxazole | 77 | 184.18 ^d JPC=6.0 | 186.53(d) JPC=6.0 | 174.10(d) JCH=13.7 | 173.15(d) JCH=3.0 | 177.52(s) | 175.60(s) | 184.27(s) | 176.60(s) | 182.14(s) |

^{a)} Chemical shifts are in ppm downfield positive downfield relative to TMS, coupling constants in Hz

^{b)} From reference 1. ^{c)} From reference 6. ^{d)} JCH not observed due to overlap of resonances.

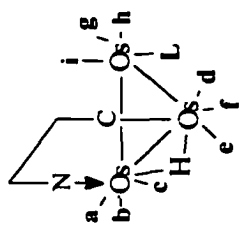
Table 3.2 ¹H NMR of Acetonitrile Adducts of Electron Deficient Benzoheterocycle Clusters^a

| Ring | No | Solvent | H(2) | H(3) | H(4) | H(5) | H(6) | H(7) | 2-Me | NH | Hydride |
|-----------------------|-----------------|--------------------|---------|---------|----------|----------|----------|----------|---------|------------|-----------|
| Quinoxaline | 43 ^b | CDCl ₃ | 9.15(d) | 8.54(d) | | 8.67(dd) | 7.46(dd) | 8.72(dd) | | | -12.16(s) |
| Quinoxaline | 43 | CD ₃ CN | 9.49(d) | 8.49(d) | | 8.61(dd) | 7.36(dd) | 8.53(dd) | | | -11.24(s) |
| 2-Me Benzimidazole | 32 ^b | CDCl ₃ | | | 6.98(dd) | 8.16(m) | 8.16(m) | | 2.75(s) | 9.02(s,br) | -11.78(s) |
| 2-Me Benzimidazole | 32 | CD ₃ CN | | | 7.54(d) | 6.80(m) | 6.80(m) | | 2.65(s) | 7.66(br) | -12.13 |
| Benzoxazole | 37 | CDCl ₃ | 8.29(s) | | 8.46(d) | 7.26(dd) | 8.50(d) | | | | -11.84 |
| Benzoxazole | 37 | CD ₃ CN | 8.69(s) | | 7.03(m) | 6.95(m) | 7.64(d) | | | | -12.52 |

a) Chemical shifts are in ppm downfield positive relative to TMS

b) From reference 5

Table 3.3 Proton Coupled ^{13}C NMR of the Acetonitrile Adducts of the Electron Deficient Benzoheterocycle Complexes^a



B

| Ring | No | L | a | b | c | d | e | f | g | h | i |
|--------------------------|----|--------------------|------------------------|----------------------|-----------|----------------------|----------------------|-----------|-----------|-----------|---------------------------------|
| Quinoxaline ^c | 43 | CD ₃ CN | 181.82(d) JCH=12.1 | 182.34(d) JCH=4.0 | 179.69(s) | 180.91(d) JCH=9.1 | 183.01(d) JCH=2.5 | 182.60(s) | 182.61(s) | 183.94(s) | 185.57(s) |
| 2-Me-Benzimidazole | 32 | CD ₃ CN | 182.00(d) JCH=11.06 | 182.19(d) JCH=3.7 | 180.64(s) | 180.64(d) JCH=8.3 | 181.15(d) JCH=3.7 | 183.84(s) | 183.13(s) | 183.02(s) | 185.04(s) |
| Benzoxazole | 37 | CD ₃ CN | 177.71(d) JCH=12.0 | 178.03(d) JCH=2.7 | 179.72(s) | 179.11(d) JCH=8.5 | 179.72(d) JCH=2.0 | 181.90(s) | 181.83(s) | 182.94(s) | 183.58(s) |
| Benzoxazole | 37 | CO | 173.19(d) JCH=12.3 | 172.96(d) JCH=3.8 | 176.17(s) | 173.97(d) JCH=8.5 | 175.16(d) JCH=3.0 | 177.95(s) | 174.59(s) | 175.639s) | 182.88 (183.13) ^b |

a) Chemical Shifts are downfield positive relative to TMS in ppm and coupling constants are given in Hz

b) Two axial carbonyls are observed with the expected $^{13}\text{C} - ^{13}\text{C}$ satellites

c) Major isomer only.

suggest the population of isomers such as **C/C'** or **D/D'** (Scheme 3.2, *vide infra*). This was not the case for **32** or **37**.

It is important to note here that although **32-33**, **37-40** and **43** form adducts with acetonitrile while **23a**, **29** and **72** do not, the rings are not cleaved from the cluster at any significant rate when heated in this solvent at 70 –80 °C under 1 atm of CO as are **23a**, **29** and **72**. This seems contradictory unless one considers the possibility that cleavage of the ligand is controlled thermodynamically by the relative stability of the μ_3 and μ bonding modes for **23a**, **29** and **72** versus **32-33**, **37-40** and **43** (Figure 3.2). The reasons why the μ -bonding mode should be more stable thermodynamically for **32-33**, **37-40** and **43** than the μ_3 - bonding mode compared with **23a**, **29** and **72** are not apparent and must await a theoretical treatment of the bonding in these systems. It is clear that all the μ_3 - complexes are kinetically stable and that adduct formation must precede ligand cleavage because cleavage of **23a**, **29** and **72** does not proceed in solvents other than acetonitrile.

Compounds **23a**, **29**, **32-33**, **37-40**, **43**, and **72** all react with n-butyl amine to form yellow adducts, but here again there are significant differences between the different structural types. Previous studies with **23a** suggested the isomeric structures **B** and **B'** for the amine adducts with **B** (Scheme 3.1) being the major isomer based on solution NMR data, T_1 measurements and by analogy with related structurally characterized ammonia adducts.⁴⁴ Compounds **29**, **43** and **72** appear to form the same two isomers but in the case of **29** and **72** the adducts precipitated from chloroform necessitating measurement of the isomer ratios and equilibrium constants in acetone (Table 3.5). As for **23a** we observe the

formation of a single isomer and then the gradual appearance of a second isomer. We previously showed that this process involves formation of an isomer with the amine ligand on the same face of the cluster as the heterocycle, followed by an intermolecular equilibration to a mixture of isomers with the amine ligand on either face of the metal triangle.

In the case of **29** we were able to isolate crystals of the amine adduct, $\text{Os}_3(\text{CO})_9(\mu_3\text{-}\eta^2\text{-L-H})(\mu\text{-H})(\text{n-C}_4\text{H}_9\text{N})$ (L=phenanthridine, **78**), suitable for a solid state structural investigation. The solid-state structure of **78** is shown in Figure 3.1 and selected distances and bond angles are given in Table 3.4. The solid-state structure of **78** reveals that the hydride and the benzoheterocycle bridge different edges of the cluster, with the amine ligand and the phenanthridine ring on the same face of the cluster. The hydride bridges the osmium atom coordinated to the amine and the osmium atom bound to C(8) (quinoline numbering system) of the phenanthridine ring. The overall structure is represented by structure **D** (Scheme 3.2). In light of the very similar spectroscopic properties of **23a**, **29**, and **72** we can assign the solution structures of all three amine adducts to an equilibrium mixture of **D** and **D'** (Scheme 3.2 or **B** and **B'** in scheme 3.1). The hydride was located along the longest edge of the metal triangle ($\text{Os}(1)\text{-Os}(2) = 3.0405(6) \text{ \AA}$) using the program Hydex.⁴⁶ The phenanthridine ligand bridges the second longest edge of the metal triangle ($\text{Os}(2)\text{-Os}(3) = 2.8873(6) \text{ \AA}$) while the unbridged edge has the shortest metal-metal bond distance ($\text{Os}(1)\text{-Os}(3) = 2.7810(5) \text{ \AA}$). The metal nitrogen bond distances are essentially equal ($\text{Os}(2)\text{-N}(1\text{S}) = 2.209(7)$ and $\text{Os}(3)\text{-N}(1\text{B}) = 2.195(70) \text{ \AA}$) and are approximately the same as the metal carbon bond distance with the

phenanthridine ligand ($\text{Os}(1)\text{-C}(12\text{B}) = 2.190(9) \text{ \AA}$). These distances are somewhat longer than related distances in $\text{Os}_3(\text{CO})_9(\mu_3\text{-}\eta^2\text{-L-H})(\mu\text{-H})(\text{L}')$ ($\text{L} = \text{quinoline}$, $\text{L}' = \text{n-butyl amine}$) complexes.^{1,2} The n-butylamine ligand and the phenanthridine ligand are perpendicular to the plane of the metal triangle as can be seen from the Os-Os-N(1B), Os-Os-N(1S) and Os-Os-C(12B) angles (Table 3.4). The n-butylamine ligand is disordered, axially with a conformational population of 0.59:0.41 (Figure 3.1).

The formation constants for **23a**, **29** and **72** evaluated after isomer equilibration are quite similar as are the **D/D'** isomer ratios and the hydride chemical shifts (Table 3.5). This might be expected for these very similar heterocycles. The ¹³C NMR patterns for the amine adducts of **23a** and **29** are very similar and the T_1 's of the hydrides are almost identical and are significantly shorter than for **23a** and **29** (4.0 and 5.2 s for **23a** and **29** respectively; Tables 3.5 and 3.6). The short T_1 values for these adducts are attributable to enhanced dipolar relaxation indicative of the close proximity of the hydride to the amine ligand. In the ¹³C NMR of the carbonyl region of ¹³CO enriched samples of the amine adducts of **23a** and **29** no ¹³C-¹³C coupling satellites are observed. Based on this evidence it is reasonable to propose the n-butyl amine adducts of **23a**, **29** and **72** exist in solution as the same set of isomers, **D** and **D'**.

Table 3.4 Selected Distances (Å) and Bond Angles (deg.) for**Os₃(CO)₉(μ₃-η²-L-H)(μ-H)(n-C₄H₉N) (L=phenanthridine, 78)****Distances**

| | | | |
|--------------------|-----------|---------------|----------|
| Os(1)-Os(2) | 3.0405(6) | N(1S)-C(1S) | 1.50(1) |
| Os(1)-Os(3) | 2.7810(5) | N(1B)-C(1B) | 1.297(9) |
| Os(2)-Os(3) | 2.8873(6) | N(1B)-C(13B) | 1.46(1) |
| Os(1)-C(12B) | 2.190(9) | C(1B)-C(2B) | 1.41(1) |
| Os(2)-N(1S) | 2.209(7) | C(11B)-C(12B) | 1.40(1) |
| Os(3)-N(1B) | 2.195(7) | C(12B)-C(13B) | 1.43(1) |
| Os-CO ^b | 1.89(1) | | |

Angles

| | | | |
|---------------------|----------|----------------------|----------|
| Os(1)-Os(2)-Os(3) | 55.88(1) | C(1S)-N(1S)-Os(2) | 117.1(8) |
| Os(1)-Os(3)-Os(2) | 64.85(1) | C(1B)-N(1B)-Os(3) | 118.2(8) |
| Os(2)-Os(1)-Os(3) | 59.27(1) | C(13B)-N(1B)-Os(3) | 123.0(5) |
| Os(1)-Os(2)-N(1S) | 89.7(2) | C(13B)-C(12B)-Os(1) | 125.4(7) |
| Os(3)-Os(2)-N(1S) | 89.1(2) | C(11B)-C(12B)-Os(1) | 119.9(7) |
| Os(1)-Os(3)-N(1B) | 86.8(1) | C(1B)-N(1B)-C(13B) | 118.2(8) |
| Os(2)-Os(3)-N(1B) | 92.7(1) | C(11B)-C(12B)-C(13B) | 114.4(9) |
| Os(2)-Os(1)-C(12B) | 91.3(2) | | |
| Os(3)-Os(1)-C(12B) | 85.6(2) | | |
| Os-C-O ^b | 176.4(9) | | |

a) Numbers in parentheses are average standard deviations.

b) Average values

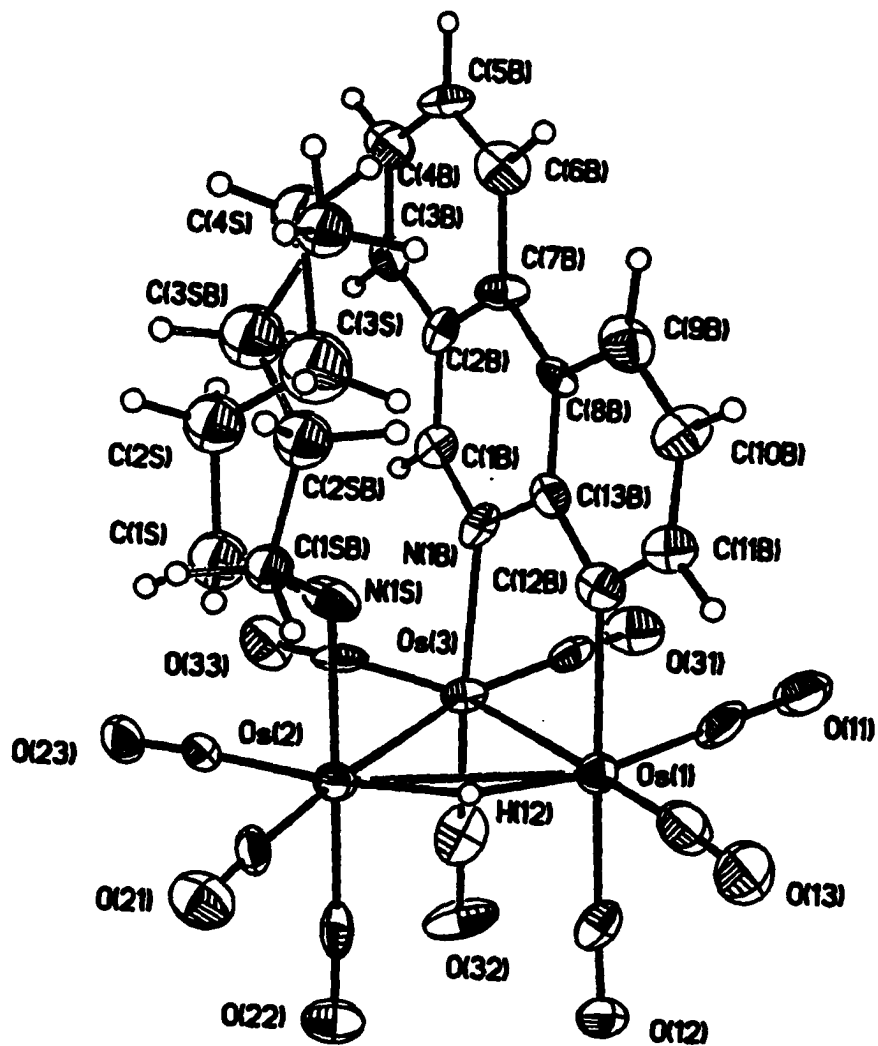


Figure 3.1 Solid state structure of $\text{Os}_3(\text{CO})_9(\mu_3\text{-}\eta^2\text{-L-H})(\mu\text{-H})(n\text{-C}_4\text{H}_9\text{N})$
(L=phenanthridine, 78)

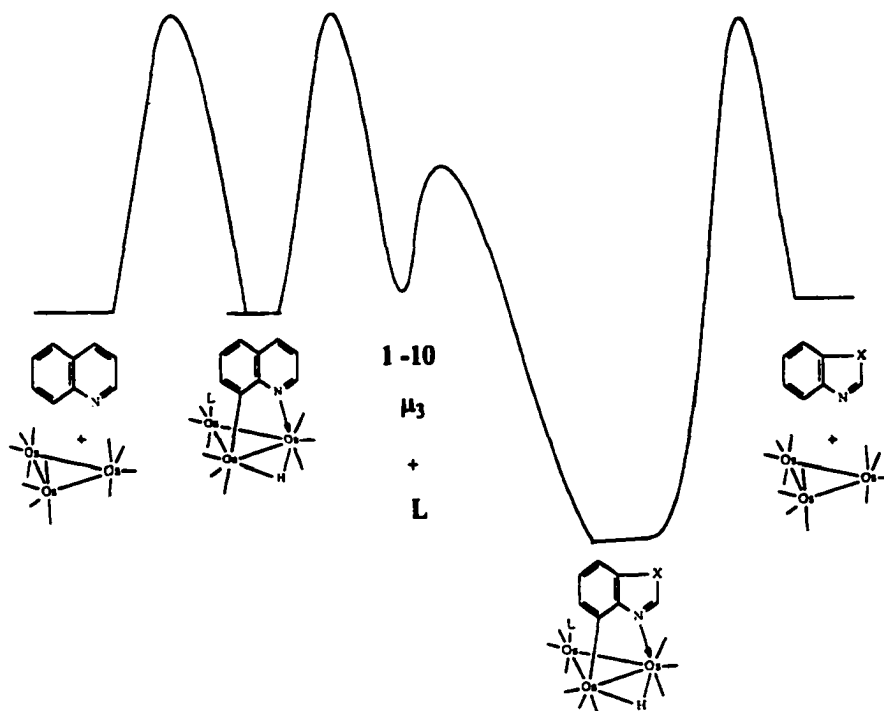


Figure 3.2 Reaction profile diagram for ligand coordination and cleavage, illustrating the proposed differences in the relative stability of the μ - and μ_3 -bonding modes.

Compounds **32-33**, **37-40** and **43** all show an increase in their formation constants with n-butylamine relative to **23a**, **29** and **72** while the **D/D'** ratio remains about the same as in **23a**, **29** and **72** with the exception of **43**. This increase in the formation constant is consistent with the fact **32-33**, **37-40** and **43** form acetonitrile adducts while **23a**, **29** and **72** do not. In addition, the appearance of a third new hydride resonance is observed at slightly lower fields (-11 to 12 ppm) for **32-33**, **37-40** (Table 3.5). In the case of **32** this is the only adduct hydride resonance observed and therefore allowed us to examine the structure of this isomer in detail. The ^{13}C NMR of this adduct has a distinctly different pattern than that observed for **D** in **23a**, **29** and **72** with the carbonyl resonances *trans*- to the hydride being much more well separated ($\Delta\delta = 4.6$) suggesting that the two hydride bridged osmium atoms are in a different environment than in **D** (Scheme 3.2). The T_1 of the n-butyl amine adduct of **32** is 5.2 s which is considerably shorter than the T_1 of the decacarbonyl of **32** (11.5 s) that has structure **B**. The T_1 's of **23a**, **29** and **72** and their amine adducts are, on the other hand, considerably shorter and so we decided to evaluate the T_1 values for the NH_3 and ND_3 adducts of **32** in order to get a more definitive idea of the proximity of the amine hydrogens to the hydride. The values obtained of 6.9 and 15.2 s for the NH_3 and ND_3 adducts respectively, clearly indicate that the amine ligand resides on an osmium atom bound to the bridging hydride. Taken together with the ^{13}C NMR data we suggest structure **C** or **C'** for the amine adduct of **32**. That the T_1 values of **32**, the decacarbonyl of **32** and its amine adduct are all longer than the corresponding values for **23a** probably reflects the replacement of the hydrogen at C(2) with a methyl group. In the case of **37** a fourth hydride resonance is observed at -11.26 ppm very close to the

resonance we have assigned to **C** or **C'** in a relative intensity of 1:1.2. It would appear that both **C** and **C'** populated in this case and this isomer was included in the calculation of the formation constant for the amine adduct of **37** (Table 3.5). That isomers **C** and/or **C'** are preferred for **32** and populated for **32-33**, **37-40** may be attributed to contributions that make the pyridinyl nitrogen more basic and therefore favor the isomer where the acidic hydride bridges the edge of the metal triangle to which both basic nitrogens are bound (Scheme 3.3). In the case of the amine adduct of **32** we were able to isolate analytically pure samples of the n-butylamine adduct $\text{Os}_3(\text{CO})_9(\mu_3\text{-}\eta^2\text{-L-H})(\mu\text{-H})(n\text{-C}_4\text{H}_9\text{N})$ (L=2-me-benzimidazole **79**). These crystals were not suitable for solid state structural analysis but do corroborate the formulation of the adducts with the proposed structure **C**.

Scheme 3.3

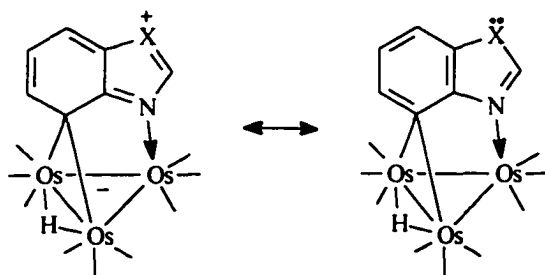


Table 3.5. ¹H NMR, Isomer Ratios, Hydride T₁ and Formation Constants for n-Butyl Amine Adducts of Electron Deficient Benzoheterocycle Clusters^a

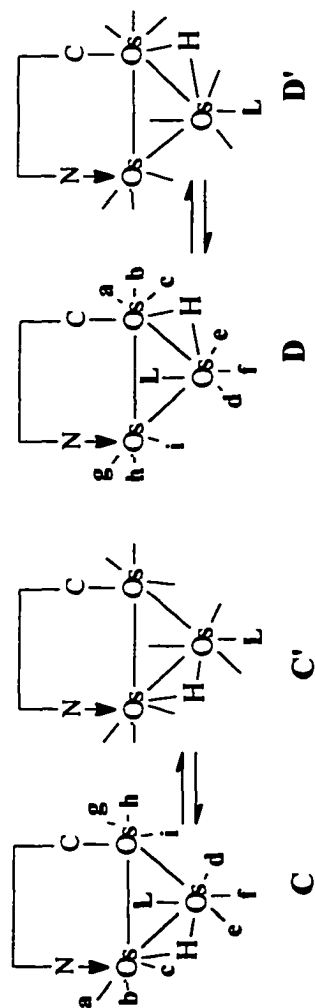
| Ring | No | Solvent | δ(D) | δ(D') | δ(C) | K(D/D') | C/D+D' | Hydride T ₁ | K _{form} (M ⁻¹) ^c |
|--------------------|-----|------------------------------------|--------|--------|--------|---------|--------|-------------------------------|---|
| Quinoline | 23a | CDCl ₃ | -13.39 | -12.76 | | 2.8 | | 1.4 | 44.4 |
| Phenanthridine | 29 | (CD ₃) ₂ CO | -13.23 | -12.56 | | 2.2 | | 1.5 | 18.3 |
| 5,6-Benzoquinoline | 72 | (CD ₃) ₂ CO | -13.33 | -12.73 | | | | | |
| Quinoxaline | 43 | CDCl ₃ | -13.55 | -13.05 | | 0.66 | | | 303 |
| 2-Me-Benzimidazole | 32 | CD ₂ Cl ₂ | | | -11.78 | | | 5.2 6.9(15.2) ^b | 124 |
| 2-Me-Benzotriazole | 33 | CDCl ₃ | -13.67 | -13.15 | -11.67 | 1.56 | 0.69 | | 232 |
| 2-Me-Benzothiazole | 40 | CDCl ₃ | -13.46 | -12.86 | -11.07 | 2.59 | 1.61 | | 47 |
| Benzothiazole | 39 | CD ₂ Cl ₂ | -13.52 | -12.98 | -11.46 | 2.54 | 0.23 | | 274 |
| 2-Me-Benzoxazole | 38 | CDCl ₃ | -13.60 | -13.06 | -11.86 | 2.0 | 2.0 | | 310 |
| Benzoxazole | 37 | CD ₂ Cl ₂ | -13.63 | -13.15 | -12.09 | 1.09 | 0.51 | | 1097 |

a) Chemical shifts in ppm downfield positive from TMS

b) T₁ for NH₃ complex (ND₃ complex).

c) Calculated using the relative intensity of the hydride resonances of all observed isomers, the moles of starting complex and the amount of amine added

Table 3.6 ^{13}C NMR Data for Amine Adducts of the Electron deficient Benzoheterocycle Complexes^a



| Ring Structure | No | a | b | c | d | e | f | g | h | i |
|--|------------|-----------------------|----------------------|-----------|-----------------------|----------------------|-----------|-----------|-----------|-----------|
| Quinoline- ^b Structure D | 23a | 178.8(d) JCH=14.0 | 180.4(s) | 186.5(s) | 177.3(d) JCH=9.0 | 179.8(s) | 187.3(s) | 176.7(s) | 176.2(s) | 185.5(s) |
| Phenanthridine ^c Structure D | 29 | 179.26(d) JCH=12.3 | 181.37(d) JCH=3.8 | 188.54(s) | 178.93(d) JCH=9.2 | 178.44(d) JCH=1.0 | 185.26(s) | 181.36(s) | 180.51(s) | 184.48(s) |
| Benzimidazole Structure - C | 32 | 179.2(d) JCH=9.2 | 180.67(d) JCH=3.1 | 182.53(s) | 183.77(d) JCH=10.8 | 181.66(d) JCH=3.8 | 186.65(s) | 177.26(s) | 179.96(s) | 186.12(s) |

a) Chemical shifts in ppm downfield positive relative to TMS

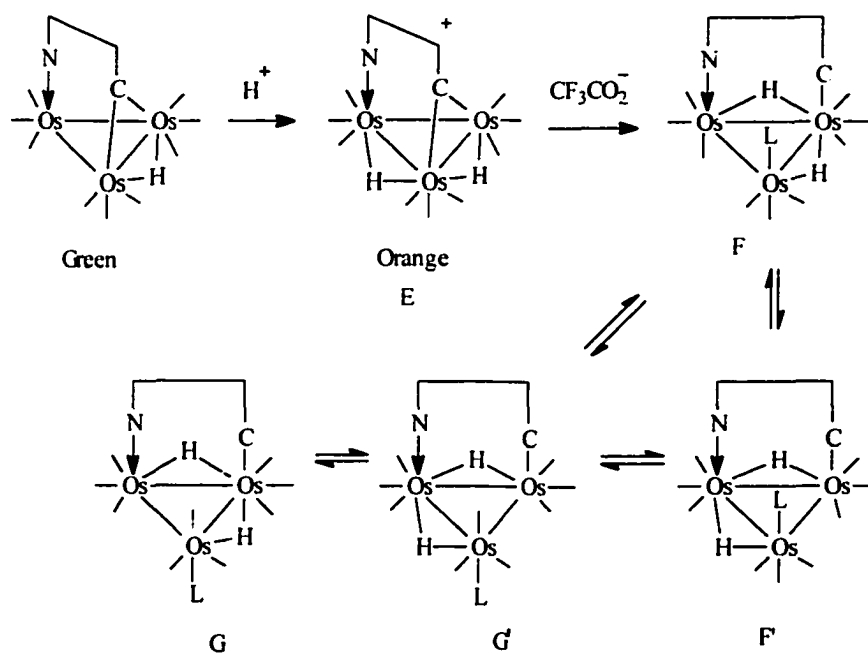
b) From reference 3, L=NH₃

c) L=n-BuNH₂

3.2.2 Reactions with HBF_4 and $\text{CF}_3\text{CO}_2\text{H}$

Compounds **23a**, **29**, **72** undergo simple protonation with HBF_4 and $\text{CF}_3\text{CO}_2\text{H}$ as evidenced from their ^1H and ^{13}C NMR (Tables 3.7 and 3.8). The solutions go from dark green to orange on addition of both acids and the resulting ^1H and ^{13}C NMR spectra are virtually identical and can be assigned to structure **E** (Scheme 3.4).⁹ Compounds **32-33**,

Scheme 3.4



37-40 and **43** also protonate with HBF_4 but with $\text{CF}_3\text{CO}_2\text{H}$ yellow solutions are formed and the ^1H , ^{13}C and ^{19}F spectra give strong evidence for the formation of trifluoroacetate

adducts (Scheme 3.4), consistent with the greater tendency of these compounds to form adducts with Lewis bases as described above.⁴⁷ The changes in the spectra of **32-33**, **37-40** and **43** vary from compound to compound and will be discussed individually below. In the case of **32-33**, **37-40** and **43** we observed no evidence of protonation of the heteroatoms and this is particularly surprising in the case of **43** but consistent with the decreased basicity of the uncoordinated lone pair and the enhanced basicity of the metal core in this complex.

Addition of a two-fold excess of CF₃COOH to a CD₂Cl₂ solution of **43** results in an instantaneous color change from green to orange-yellow. The hydride region of the ¹H NMR consists of two broad resonances at -12.24 and -14.08 ppm along with a small amount of starting material at -12.33 ppm. As the temperature is lowered to -50 °C these resonances sharpen and are resolved into two sets of hydrides at -12.10 and -13.78 ppm and -12.38 and -14.88 ppm, in a relative intensity of 1:2. This behavior can be understood in terms of the averaging of two isomeric adducts **F** and **F'** by hydride exchange. This is supported by the observation of two ¹⁹F NMR resonances at 1.81 and 0.66 ppm relative to free CF₃COOH at -50 °C, in the same relative intensity as the two sets of hydride resonances, which average with each other but not with the free acid as the temperature is increased. This behavior is very similar to that observed for the related imidoyl adduct, Os₃(CO)₉(μ₃-η²-(CH₂)₃C=N-)(μ-H)₂(CF₃COO) that has a solid state structure analogous to **F**.⁴⁷

Compound **32** undergoes only simple protonation with CF₃COOH as evidenced by the observation of two sharp hydride resonances of equal intensity at -12.63 and -13.38

ppm. These shifts are almost identical to those observed on reaction of **32** with HBF_4 and the ^{19}F NMR spectrum shows only free trifluoroacetate ion.

The behavior of **33** with CF_3COOH is distinctly different than that of **43**. Addition of one equivalent of this acid results in the appearance of two broad hydride resonances at -13.51 and -13.92 ppm of equal relative intensity with about 50% of the starting material remaining as a sharp resonance at -11.92 ppm. On standing overnight the relative intensity of the starting material diminishes and the two broad resonances sharpen and shift to -13.04 and -13.92 ppm. The ^{19}F NMR initially shows a somewhat broadened free trifluoroacetate peak and a broad peak at 1.68 ppm that sharpens and shifts to 1.95 ppm. Addition of a five-fold excess of acid to the solution leads only to the disappearance of the starting material and a slight further shift of the hydride signals. The ^{19}F NMR shows free trifluoroacetate and a sharp signal at 1.95 ppm in the presence of excess acid. These data are best understood in terms of formation of an adduct with structure **F** or **F'** where formation of the adduct is slow on the NMR time scale, followed by isomerization to **G** or **G'** by an intermolecular (dissociative) process in the intermediate exchange regime (Scheme 3.4). Apparently only one of the two possible isomers **G** or **G'** is populated and the hydrides are fluxional at ambient temperature.

Compound **40** like **32** undergoes simple protonation with CF_3COOH as evidenced by the appearance of two sharp hydride resonances at -12.52 and -13.45 ppm, again almost identical to the hydrides observed with HBF_4 . As for **32** the ^{19}F NMR shows only free trifluoroacetate/trifluoroacetic acid. Based on our observations so far it appears that adduct formation is associated with the introduction of hydride fluxionality while simple protonation results in rigid dihydride species. This behavior is reminiscent of the addition

of phosphine to the rigid trihydride $\text{Os}_3(\text{CO})_8(\mu_3\text{-}\eta^2\text{-(CH}_2\text{)}_3\text{C=N-})(\mu\text{-H})_3$ where conversion of a μ_3 -capping ligand to a μ -edge bridging mode results in inducing a high degree of fluxionality to the hydride ligands.⁴⁸

The behavior of **39** in the presence of one equivalent of CF_3COOH is a composite of **43** and **33**. At ambient temperature a series of broad resonances is observed but on lowering the temperature to $-60\text{ }^\circ\text{C}$ three pairs of hydride resonances can be seen at -13.29 and 13.68 ppm, -12.79 and -14.71 ppm and -12.85 and -13.70 ppm. A sharp peak is observed at -11.78 ppm attributable to unreacted **39**. At $-90\text{ }^\circ\text{C}$ these resonances shift somewhat and overlap but become sharper. On standing the pair of resonances at -12.85 and -13.70 ppm increases in intensity and finally becomes the dominant species present in solution. This behavior is paralleled in the ^{19}F NMR where three resonances at 2.15, 2.31 and 2.34 ppm are initially observed at $-90\text{ }^\circ\text{C}$ in addition to free trifluoroacetate at 0.0 ppm. On standing overnight the resonance at 2.15 ppm increases while the other two resonances disappear and the trifluoroacetate peak diminishes in intensity. These data can be understood in terms of initial formation of **F** and **F'** which undergo interconversion by hydride edge hopping on the NMR time scale followed by gradual conversion to either **G** or **G'** (Scheme 3.4).

The reaction of **38** with CF_3COOH takes a similar course but with some slight differences. As for **39** addition of one equivalent of CF_3COOH leads to the formation of a dihydride species with broad resonances at -13.58 and -13.99 ppm that gradually convert to a second broadened set of hydride signals on standing overnight at -13.60 and -13.88 ppm. In contrast to **39** however, this latter set of hydrides is resolved into two sets of hydrides at -13.35 and -13.83 ppm and -13.72 and -13.90 ppm in a ratio of 3:4 on

lowering the temperature to $-90\text{ }^{\circ}\text{C}$. This behavior is paralleled in the ^{19}F NMR where an initial peak at 1.75 ppm gradually converts to a peak at 2.25 ppm on standing at room temperature. Additionally, we were able to observe two sharp doublets in the hydride region of the ^1H NMR at -12.61 and -13.43 ppm that we assign to the presence of 38H^+ . Thus the formation of **F** and **F'** is followed by conversion to **G** and **G'** where hydride edge hopping is in the fast exchange regime for both sets of isomers but where conversion of **F** to **G** is slow. That 38H^+ can be detected in this case during the conversion of **F** to **G** provides good circumstantial evidence that this conversion is intermolecular in nature. A similar equilibrium between a protonated species and a trifluoroacetate adduct was reported for $\text{Os}_3(\text{CO})_9(\mu_3\text{-}\eta^2\text{-(CH}_2)_3\text{C=N-})(\mu\text{-H})_2(\text{CF}_3\text{COO})$.⁴⁷ Addition of more CF_3COOH to solutions of the adduct of **38** causes no substantial changes in the NMR spectra but does result in chemical shift changes of the ^1H hydride, the aromatic hydrogen resonances, the ^{13}C carbonyl and the ^{19}F trifluoroacetate resonances. These shifts are probably due to hydrogen bonding interactions with excess acid but do not affect the interpretations presented here.

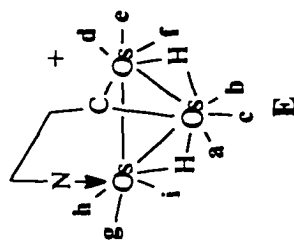
The reaction of **37** with CF_3COOH takes a distinctly different, yet simpler course than that of **38**. In presence of one equivalent of acid a single broad hydride resonance is observed at -14.05 ppm at room temperature. At $-65\text{ }^{\circ}\text{C}$ this broad resonance resolves into one major pair of hydride resonances at -13.94 and -14.09 ppm with very minor companion peaks at -12.18 , -12.28 , -13.15 , -13.62 , -13.67 and -14.95 whose low

Table 3. 7 Hydride Chemical Shifts for Initial Protonation Products of the Electron Deficient Benzoheterocycle Complexes^a

| Ring | No. | δ (hydride) | δ (hydride) | Acid |
|-----------------------|------------|--------------------|--------------------|-----------------------------------|
| Quinoline | 23a | -13.70(d) (1.6) | -11.65(d) | HBF ₄ |
| Quinoline | 23a | -13.66(d) (1.7) | -11.61(d) | CF ₃ CO ₂ H |
| Phenanthridine | 29 | -13.71(d) (1.6) | -11.73(d) | HBF ₄ |
| Phenanthridine | 29 | -13.70(d) (1.7) | -11.73(d) | CF ₃ CO ₂ H |
| 5,6Benzoquinoline | 72 | -14.08(d) (1.6) | -11.74(d) | HBF ₄ |
| 5,6Benzoquinoline | 72 | -14.10(d) (1.6) | -11.73(d) | CF ₃ CO ₂ H |
| Quinoxaline | 43 | -13.71(d) (1.6) | -11.63(d) | HBF ₄ |
| 2-Me Benzimidazole | 32 | -13.36(d) (1.7) | -12.61(d) | HBF ₄ |
| 2-Me Benzotriazole | 33 | -13.22(d) (1.6) | -11.98(d) | HBF ₄ |
| 2-Me Benzothiazole | 40 | -13.50(d) (1.4) | -12.42(d) | HBF ₄ |
| Benzothiazole | 39 | -13.41(d) (1.2) | -12.24(d) | HBF ₄ |
| 2-Me Benzoxazole | 38 | -13.43(d) (1.4) | -12.61(d) | HBF ₄ |
| Benzoxazole | 37 | -13.38(s) | -12.66(s) | HBF ₄ |

a) Chemical shifts in ppm downfield positive from TMS numbers in parenthesis are coupling constants between the hydrides in Hz.

Table 3.8 Proton Coupled ^{13}C NMR of the Protonated Electron Deficient Benzoheterocycle Complexes^a



| Ring | No | a | b | c | d | e | f | g | h | i |
|------------------------|------------|-----------------------------------|-----------------------------------|-----------|----------------------|-----------|-----------|-----------|----------------------|-----------|
| Quinoline ^b | 23a | 159.99(dd) JCH=13.7 JCH=6.1 | 159.84(dd) JCH=13.7 JCH=4.6 | 172.36(s) | 172.45(d) JCH=7.6 | 168.13(s) | 172.92(s) | 166.71(s) | 180.65(d) JCH=9.2 | 178.78(s) |
| Quinoxaline | 43 | 161.51(dd) JCH=13.7 JCH<1 | 160.96(dd) JCH=12.7 JCH<1 | 173.69(s) | 173.22(d) JCH=9.1 | 169.42(s) | 174.81(s) | 168.20(s) | 181.86(d) JCH=9.0 | 181.46(s) |
| 2-Me Benzimidazole | 32 | 159.85(dd) JCH=13.8 JCH=1 | 158.53(dd) JCH=10.8 JCH=1 | 171.74(s) | 171.95(d) JCH=7.7 | 167.82(s) | 173.29(s) | 167.82(s) | 180.14(d) JCH=9.2 | 175.66(s) |
| Benzoxazole | 37 | 160.70(dd) JCH=12.8 JCH<1 | 159.08(dd) JCH=13.7 JCH<1 | 171.66(s) | 172.99(d) JCH=8.4 | 169.28(s) | 173.87(s) | 167.66(s) | 178.62(d) JCH=9.1 | 175.68(s) |

a) Chemical Shifts are downfield positive relative to TMS in ppm and coupling constants are given in Hz. Data from reference 3.

intensities made it impossible to assign them as pairs. Similarly, the observation of one major peak at 1.35 ppm and three minor peaks at 1.61, 1.67 and 2.65 ppm in the ^{19}F NMR at $-65\text{ }^\circ\text{C}$ confirms that the hydride signals are due to adduct formation. Thus in the case of **37** only one isomer of the acid adduct is significantly populated at $-65\text{ }^\circ\text{C}$, most likely **F**, and at room temperature the hydrides and the minor isomers are exchanging on the NMR time scale.

3.3 General Conclusions

These studies have revealed some significant differences in the chemistry of **23a**, **29**, **32-33**, **37-40**, **43** and **72**. First, complexes **32-33**, **37-40** and **43** have a much greater tendency to undergo addition of two electron donors than **23a**, **29** and **72**. This is reflected in the larger formation constants of the amine adducts and in the formation of adducts with the weaker donors acetonitrile and trifluoroacetate. This can be rationalized by the apparent greater thermodynamic stability for the μ versus the μ_3 bonding mode for **32-33**, **37-40** and **43** relative to **23a**, **29** and **72** (Figure 3.2). This most likely arises from the contribution of resonance structures that make the pyridinyl nitrogen a stronger donor in the case of **32-33** and **37-40** (Scheme 3.3). Second, reaction of **23a**, **29**, **32-33**, **37-40**, **43** and **72** with the bulky, soft electron donor triphenylphosphine drives all the products of the resulting adducts to a common structure while the harder and less bulky ligands *n*-butyl amine and trifluoroacetate ligands result in a variety of isomeric adducts with a range of fluxionality and stability. Indeed, although the overall behavior of these electron deficient clusters parallels the related μ_3 -imidoyl triosmium clusters the structures of some of the adducts of **23a**, **29**,

32-33, 37-40, 43 and **72** remain in doubt for lack of solid state structural data that were available for the imidoyls.^{45,47,48} Particularly puzzling, and also intriguing, are the factors governing the remarkable differences in the behavior of **32** and **40** versus **33, 43,** and **37-39** towards trifluoroacetic acid. We are hopeful that theoretical modeling of the bonding geometries of **23a, 29, 32-33, 37-40, 43** and **72** currently underway in Dr Rosenberg's laboratories will further elucidate these differences in reactivity. In any case, the studies reported here will be of direct value for the applications planned for these molecules as site selective markers for bio-macromolecules as there is now a better understanding of their basic coordination chemistry.

3.4 Experimental Section

Materials and General Considerations

Compounds **23a, 29, 32-33, 37-40, 43** and **72** were synthesized by published literature procedures.^{2,3,31} The NMR solvents CDCl_3 , CD_2Cl_2 , CD_3CN and $(\text{CD}_3)_2\text{CO}$ (Norell) were dried over molecular sieves (Type 4A, Mallincrodt). Trifluoroacetic acid (Aldrich) was distilled from phosphorous pentoxide before use. Perfluoroboric acid (Aldrich), n-butylamine (Aldrich) and triphenylphosphine (Strem) were used as received.

Spectra and Analyses

NMR spectra were measured on a Varian Unity Plus 400 MHz Spectrometer and on a Jeol-EX 400 MHz Spectrometer. Infrared spectra were measured on a Perkin Elmer

1600 and a Thermo-Nicolet 633 FT IR Spectrometers. Schwarzkopf Microanalytical Laboratories, Woodside, New York, performed elemental analyses.

Synthesis of the Phosphine Derivatives 75-77

Compounds **32**, **37** or **43** (95 mg, 0.1 mmol) were dissolved in 20 mL CH₂Cl₂ and 26 mg (0.1 mmol) PPh₃ in 5 mL of the same solvent was slowly added to the green solution under an atmosphere of nitrogen. The solution turned from green to yellow-orange immediately. After stirring for 15 min the solution was evaporated, taken up in a minimum volume of CH₂Cl₂ and purified by thin layer chromatography using 20-40% CH₂Cl₂ -hexane as eluent. A single orange band was eluted yielding 110-120 mg (90-95%) of **75-77**.

Analytical and Spectroscopic Data for 75

Anal. Calcd. for C₃₅H₂₁N₂O₉Os₃P: C, 34.59; H, 1.74; N, 2.30. Found: C, 34.14; H, 1.90; N, 2.33. IR (ν CO) in CH₂Cl₂: 2091(m), 2051(s), 2010(s), 1990(s), 1931(w) cm⁻¹. ¹H NMR in CD₂Cl₂ δ: 9.21(d, 1H), 8.45(d, 1H), 7.85(d, 1H), 7.35-7.15(m, 16H), 6.9(dd, 1H), -11.92(d, ²J_{P-H}=15.6 Hz, hydride).

Analytical and Spectroscopic Data for 76

Anal. Calcd. for C₃₅H₂₃N₂O₉Os₃P: C, 34.53; H, 1.90; N, 2.30. Found: C, 35.93; H, 2.40; N, 2.05. IR (ν CO) in CH₂Cl₂: 2084(m), 2040(s), 2000(s), 1985(br), 1933(w) cm⁻¹. ¹H NMR in CDCl₃ δ: 8.83(s,br 1H), 7.35-7.15(m, 15H), 6.93(d, 1H), 6.51(m, 2H), 2.62(s, 3H), -12.65(d, ²J_{P-H}=15.1 Hz, hydride).

Analytical and Spectroscopic Data for 77

Anal. Calcd. for $C_{34}H_{21}NO_{10}Os_3P$: C, 33.77; H, 1.75; N, 1.15. Found: C, 33.37; H, 1.77; N, 1.00. IR (ν CO) in CH_2Cl_2 : 2087(m), 2048(s), 2000(s), 1979(br), 1941(w) cm^{-1} . 1H NMR in CD_2Cl_2 δ : 8.29(s, 1H), 7.15-7.38(m, 15H), 6.99(d, 1H), 6.78(d, 1H), 6.65(dd, 1H), -13.10(d, $^2J_{P-H}=14.4$).

Synthesis of the Amine Adducts 78 and 79

Compound **29** or **32** (50 mg, ~ 0.05 mmol) was dissolved in CH_2Cl_2 (5 mL) and 50 μL (~ 20 fold molar excess) in 5 mL hexane was added slowly to the solution under a nitrogen atmosphere. The dark green solution gradually turned to an amber yellow. After one hour the solution was concentrated to half volume under a stream of nitrogen and stored at -20 $^{\circ}C$ overnight. Yellow orange crystal of the adducts precipitated (20-30 mg, 40-50% yield).

Analytical and Spectroscopic Data for 78

Anal. Calcd. for $C_{26}H_{20}N_2O_9Os_3$: C, 29.05; H, 1.88; N, 2.60. Found: C, 30.66; H, 2.20; N, 3.13. IR (ν CO) in CH_2Cl_2 : 2097(w), 2073(w), 2018(s,br), 1972(m), 1935(s,br) cm^{-1} . 1H NMR in $CDCl_3$ (major isomer only) δ : 9.10 (s, 1H), 8.60(d, 1H), 8.27(d, 1H), 8.10(d, 1H), 7.99(d, 1H), 7.85(dd, 1H), 7.67(dd, 1H), 7.31(d, 1H), 6.78(br, 2H), 4.58 (m, br, 1H), 4.04(m,br), 3.40(m,br, 2H), 2.88 (t,br, 3H), 2.76 (m,br,2H), -13.23 (s,br, hydride).

Analytical and Spectroscopic Data for 79

Anal. Calcd. for $C_{21}H_{18}N_3O_9Os_3$: C, 24.54; H, 1.85; N, 4.09. Found: C, 25.16; H, 2.22; N, 4.18. IR (ν CO) in CH_2Cl_2 : cm^{-1} . 1H NMR in CD_2Cl_2 major isomer only δ : 9.45(s,br, 1H), 7.65(dd, 1H), 6.94(m, 2H), 2.75(s, 3H), 2.12(m, 2H), 1.56(s,br, 2H), 1.38(m, 2H), 0.89(m, 2H), 0.56(t, 3H), 0.25(m, 2H) -11.78 (s, hydride).

Measurement of the Formation Constants for the Amine Adducts

20-30 mg of compounds **23a**, **29**, **32-33**, **37-40**, **43** and **72** were weighed directly into an NMR tube and 0.75 mL of $CDCl_3$, CD_2Cl_2 or $(CD_3)_2CO$ were added by syringe. A 10-20 fold molar excess of n-butyl amine (25-50 μ L) was added slowly by syringe, the tube was shaken vigorously and the 1H NMR were measured immediately, 5 h later and after 24 h. Equilibrium constants were calculated from the relative intensity of the hydride 1H NMR signals and the known concentrations of **23a**, **29**, **32-33**, **37-40**, **43** and **72** and n-butyl amine.

Crystal Structure Analysis of 78

A suitable crystal of **78**, obtained by crystallization from a methylene chloride solution containing an excess of n-butyl amine, was mounted on a glass fiber using superglue. The crystal was placed in a nitrogen gas stream at 110 K on a Bruker D8 SMART APEX CCD sealed tube diffractometer with graphite monochromated MoK_{α} radiation. A sphere of data was measured using a series of combinations of phi and omega scans with 10 s frame exposures and 0.3° frame widths. Data collection indexing and initial cell refinements were all handled using SMART³⁹ software. Frame integration and final

cell refinements were carried out using SAINT⁴⁰ software. The final cell parameters were determined from least squares refinement on a maximum of 9999 reflections. The SADABS⁴¹ was used to carry out absorption corrections.

The structure was solved using direct methods and difference Fourier techniques (SHELXTL, V5.10).⁴² Hydrogen atoms were placed in their expected chemical positions using the HFIX command and were included in the final cycles of least squares with isotropic U_{ij} 's related to the atoms ridden upon. The C-H distances were fixed at 0.93 Å, 0.98 Å (methane), 0.97 Å (methylene), or 0.96 Å (methyl). The position of the hydride was calculated using the program HYDEX.⁴⁶ All non-hydrogen atoms were refined anisotropically except for the n-butylamine ligand atoms. Scattering factors and anomalous dispersion corrections are taken from the *International Tables for X-ray Crystallography*.⁴³ Structure, solution refinement, graphics and generation of publication materials were performed using SHELXTL, V5.10⁴² software.

Chapter 4

Reactivity of Electron Deficient Benzoheterocycles with H/H^+

4.1 Introduction

We have discussed in chapter 2 the synthesis of a class of 46- electron trimetallic clusters having a three-centre two-electron bond with a phenyl group β to a pyridinyl nitrogen contained in a fused five- or six-membered heterocyclic ring (Figure 4.1).² The aromatic nature of the rings of these clusters remains relatively unperturbed, making them a unique example of an electron deficient trimetallic species containing a μ_3 -

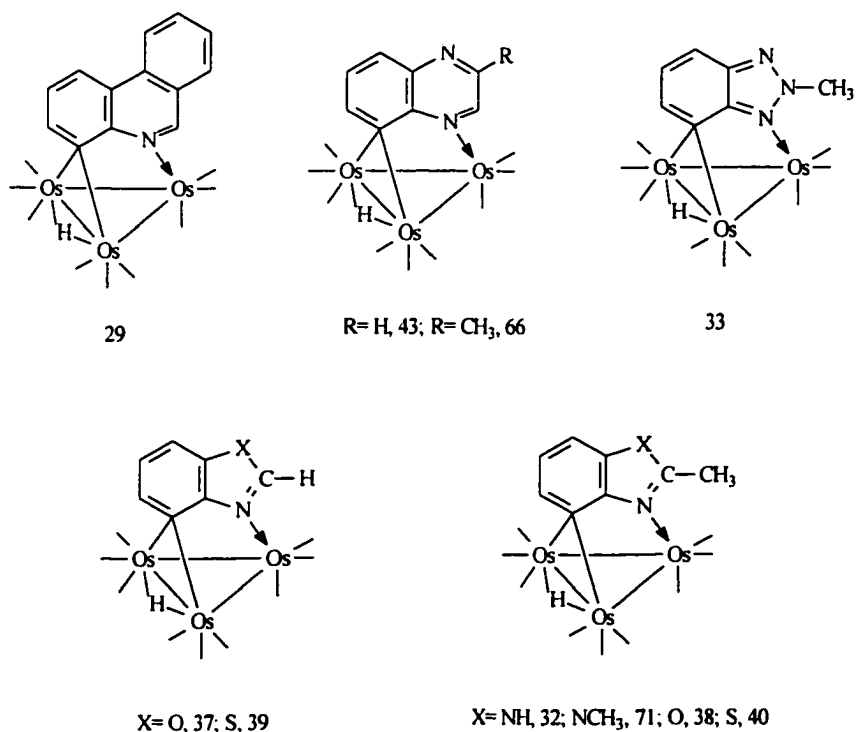


Figure 4.1

heterocyclic aromatic capping ligand. The three-center two electron bond at the carbocyclic carbon can redirect the normal reactivity of these ligands when bound to a metal cluster. $^1\text{H-NMR}$ studies of these complexes showed that the proton on C(5) (in the case of structures having a six-membered heterocyclic ring fuse to a carbocyclic ring) or C(4) (in the case of structures having a five-membered heterocyclic ring fuse to a carbocyclic ring) all show significant downfield shifts (.8 to 1.32 ppm) relative to their electron precise decacarbonyl precursors ($48 e^-$ species). This indicates a drastic change of electron distribution centered around C(5) or C(4) of the carbocyclic ring and points to a possible nucleophilic attack at this site similar to that observed for the electron deficient complexes of quinoline and its derivatives.³ Previously, it was reported that electron deficient complexes of quinoline and its derivatives undergo regioselective nucleophilic addition of hydride and a wide range of carbanions at the 5-position of carbocyclic ring (Equation 4.1).^{3,19} In quinoline the normal site of nucleophilic attack is usually at the 2- or 4- position if the former is blocked.³⁵

The heterocyclic ligands themselves of these complexes represent a class of compounds well known for their biological activities.⁴⁻⁸ Any addition or modification of these ligands by adding an alkyl group or other functional group, or by putting an additional heterocyclic or carbocyclic ring by subsequent cyclization of that functional group can change these heterocyclic molecules into a new class of compounds which might have extremely biological applications in the design of new drugs, as agonists and antagonists for neurotransmitter receptors and as anticancer agents.⁴⁻⁸ Considering these points we prompted to extend the nucleophilic addition chemistry that has been observed

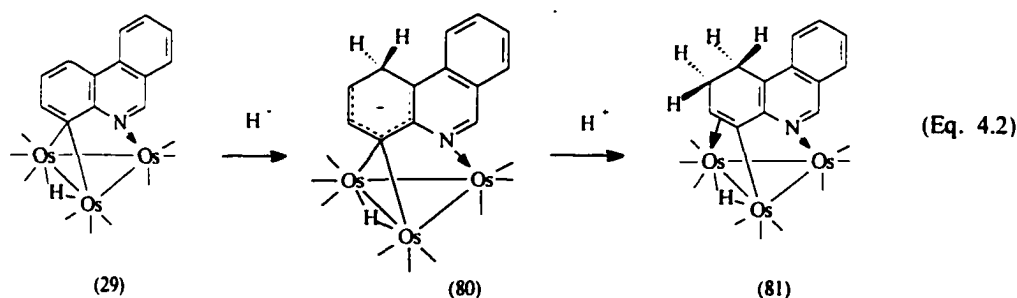
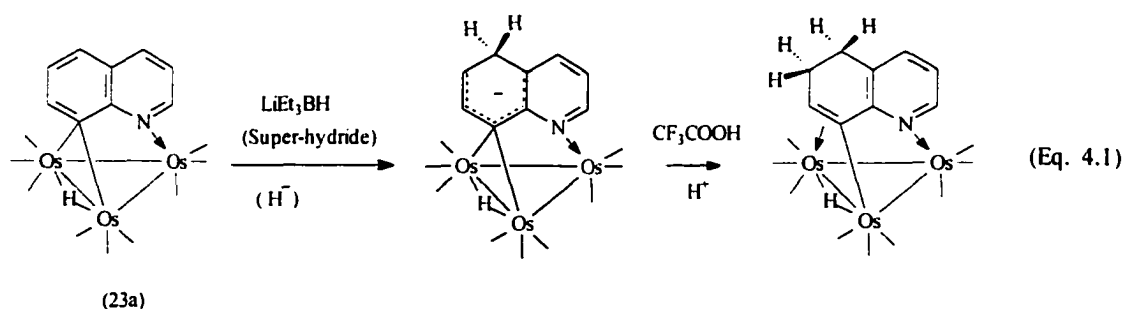
for quinoline to other benzoheterocycles and their substituted derivatives which have been shown to adopt the $\mu_3\text{-}\eta^2$ -electron deficient bonding mode (Figure 4.1) by carrying out reactivity studies of these complexes with H^-/H^+ .

We report here the reactivity of this family of electron deficient $\mu_3\text{-}\eta^2$ -complexes of benzoheterocycles with the small nucleophile, a hydride (H^-) followed by neutralization of the anion with H^+ in order to locate the nucleophilic site for our synthetic explorations. Free phenanthridine and quinoxaline molecules undergo facile nucleophilic addition reactions at the heterocyclic ring.^{35,49} Nucleophilic reactions for free benzothiazole, benzoxazole, benzimidazole, benzotriazole and their 2-substituted methyl derivatives are directed towards the 2-position of heterocyclic ring.^{49,50} No nucleophilic reaction in the carbocyclic ring has been reported so far.^{35,49,50} Reactivity studies of the electron deficient $\mu_3\text{-}\eta^2$ -complexes of these 2-methylbenzoheterocycles show unprecedented nucleophilic attack at the 5- or 4- position (depending on the 6- or 5-membered heterocyclic ring fused to carbocyclic ring) of the carbocyclic ring. A discussion of the addition of the hydride nucleophile to the benzoheterocyclic ligand of these complexes is presented in this chapter. These results represent the foundation of a potentially useful synthetic method not available via complexation by monometallic species. The structural features of the compounds are reported and the mechanistic implications of the reported transformation are discussed.

4.2 Results and Discussion

4.2.1 Reactions of $\text{Os}_3(\text{CO})_9(\mu_3\text{-}\eta^2\text{-C}_{13}\text{H}_8\text{N})(\mu\text{-H})(29)$ with LiEt_3BH and CF_3COOH

When Compound (29) which is the structural analog of quinoline was reacted with 1 equivalent of LiEt_3BH in CH_2Cl_2 , the dark green solution turned brown resulting in regioselective nucleophilic attack of hydride (H^-) at the C(5) of the phenanthridine ring to give the anionic complex, $\text{Os}_3(\text{CO})_9(\mu_3\text{-}\eta^2\text{-C}_{13}\text{H}_9\text{N})(\mu\text{-H})^-$ (80) (Equation 4.2). This anion's general structure is evident from its ^1H NMR and 2D-COSY data and the previous report of quinoline complexes which suggests a $\mu_3\text{-}\eta^2$ -alkylidene structure as evidenced by a resonance electron delocalization to the metal core.²¹ In the ^1H NMR, a



broadened resonance of relative intensity 2 at 3.86 ppm coupled to a doublet of triplets at 4.10 ppm ($J = 9.3$ and 3.2 Hz), which in turn coupled to a doublet of triplets at 5.85 ppm ($J = 9.3$ and 0.8 Hz).

Protonation of **80** with 1 equivalent of CF_3COOH led to further color change of the solution to yellow selectively reducing the double bond between C(5) and C(6) to give a 48-electron σ - π -vinyl complex, $\text{Os}_3(\text{CO})_9(\mu_3\text{-}\eta^3\text{-C}_{13}\text{H}_{10}\text{N})(\mu\text{-H})$ (**81**) similar to quinoline complexes which undergo nucleophilic addition reactions at the C(5)-C(6) position to give σ - π -vinyl complexes (Equation 4.1).^{19,21} In the σ - π -vinyl complexes of quinoline the C(8) of the ring is involved in σ - interaction with one of the osmium atoms, and C(7) and C(8) have π interaction with another osmium atom.²¹ The nucleophilic addition product (**81**) was isolated by chromatographic purification in a 78% yield. Compound (**81**) was characterized by IR, ^1H NMR, 2D-COSY and elemental analysis and based, by analogy, on similar σ - π -vinyl complexes of quinoline obtained from the nucleophilic addition reactions of the electron deficient quinoline complexes.²¹ In the ^1H NMR of **81** the hydride chemical shift comes at -17.07 ppm characteristic of the σ - π -vinyl complexes of quinoline.²¹ The ^1H NMR assignments for all the protons of the compound are unambiguous except for the resonances at 7.76 (m) and 7.51 (m) ppm which could be assigned protons either at C(10) or C(11) of the ring. A two-dimensional COSY experiment allowed complete assignment of all the resonances. 2D-COSY correlates a multiplet at 2.94 (CH₂(5)) ppm to the multiplet at 2.30 (CH₂(6)) ppm which in turn coupled to a multiplet at 4.26 (H(7)) ppm. A doublet of doublets at 7.76 (H(10)) ppm couples to a doublet of doublet at 7.84 (H(9)) ppm and to a doublet of triplets at 7.51

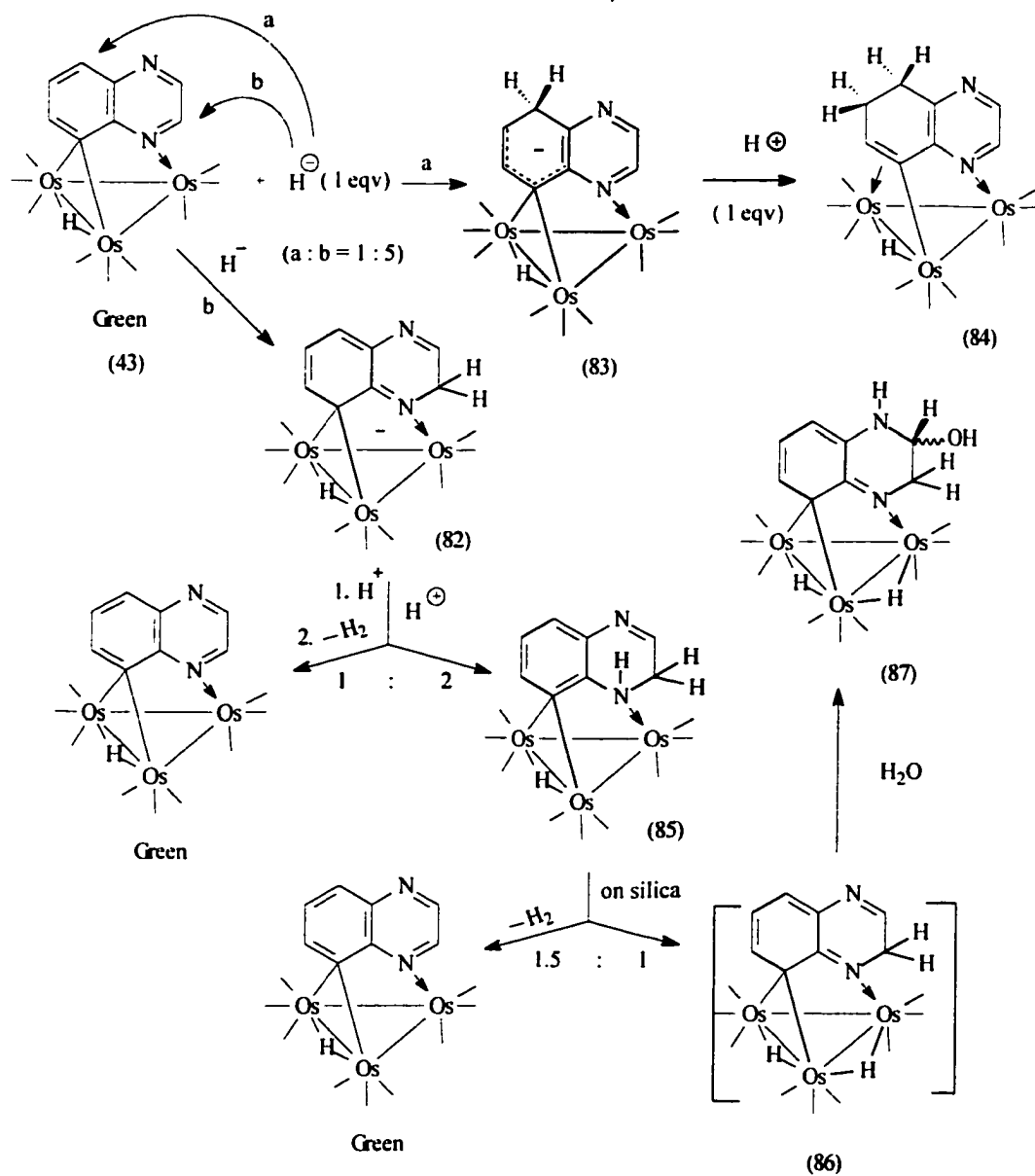
(H(11)) ppm and the latter couples to two doublets of doublets at 7.76(2H(10 and12)) ppm.

4.2.2 Reactions of Quinoxaline and 3-Methylquinoxaline Triosmium Carbonyl Clusters, $\text{Os}_3(\text{CO})_9(\mu_3\text{-}\eta^2\text{-C}_8\text{H}_4(3\text{-R})\text{N}_2(\mu\text{-H}))$ (R = H, 43; R = CH₃, 66) with LiEt_3BX and CF_3COOX (X = H or D)

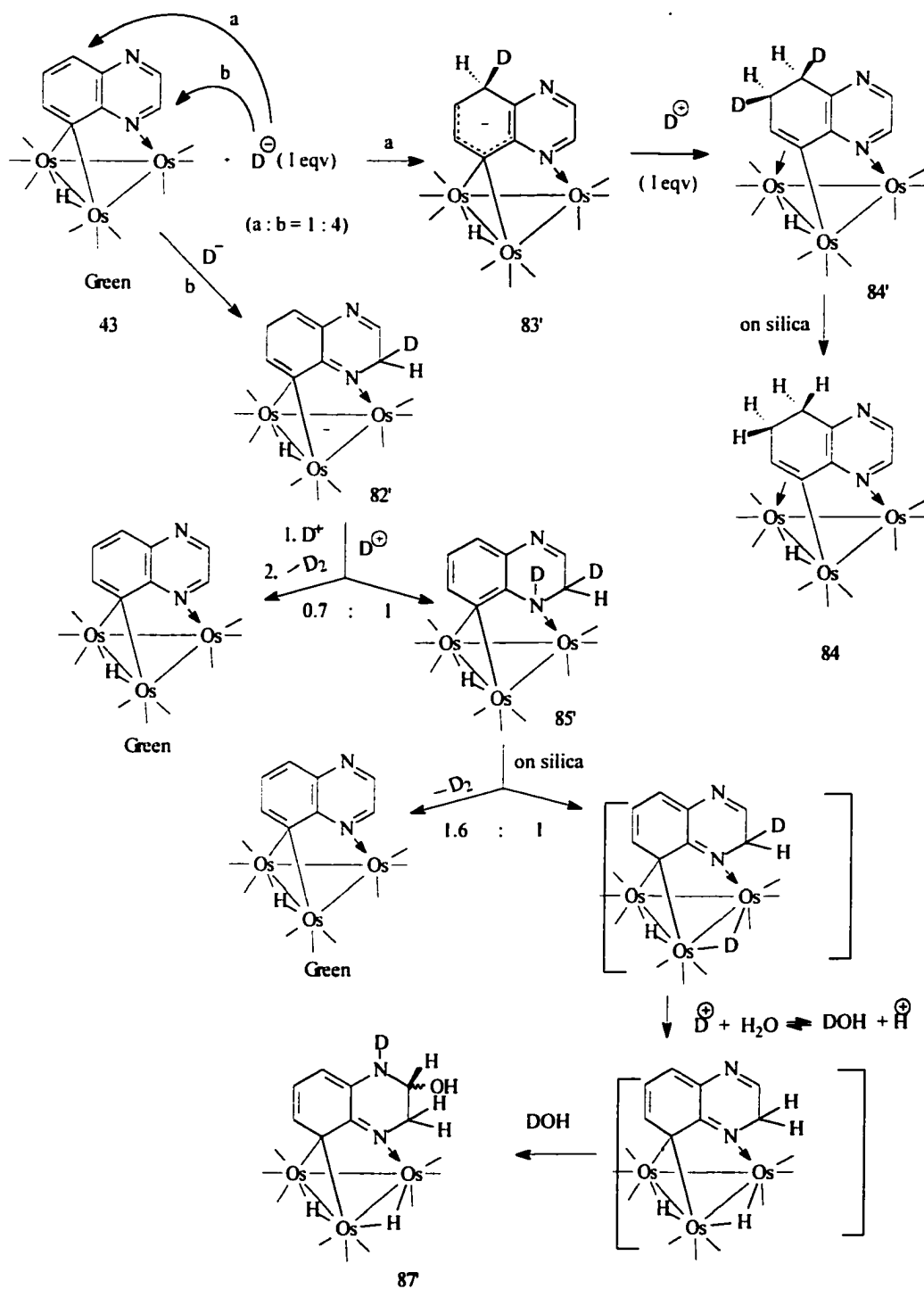
Benzoheterocyclic complex containing two nitrogen heteroatoms in the six-membered ring fused to a benzene ring such as electron deficient $\mu_3\text{-}\eta^2$ -quinoxaline complex (**43**) underwent nucleophilic attack of hydride mainly at the heterocyclic ring upon addition of 1 equivalent of LiEt_3BH in CD_2Cl_2 to afford the anionic complex, $\text{Os}_3(\text{CO})_9(\mu_3\text{-}\eta^2\text{-C}_8\text{H}_6\text{N}_2(\mu\text{-H}))^-$ (**82**) along with a minor amount of the anionic complex, $\text{Os}_3(\text{CO})_9(\mu_3\text{-}\eta^2\text{-C}_8\text{H}_6\text{N}_2(\mu\text{-H}))^-$ (**83**) resulting from the hydride attack at the 5- position of carbocyclic ring(Scheme 4.1). During the course of the reaction the color of the solution changed from green to amber. The ratio of the formation of **82** and **83** is 5:1 as evident from the integration of hydride peaks of two anionic complexes along with the companion peaks in aliphatic and aromatic regions. Although these anions have not been isolated, their general structures are evident from the ^1H NMR data of both deuterated and undeuterated forms. Deuterium-labeling studies of **43** with super-deuteride, LiEt_3BD also afforded two sets of deuterated anionic complexes, **82'** and **83'** in a ratio of 4:1 similar to those of undeuterated forms (Scheme 4.2).

In anionic complex **83**, a broadened resonance of relative intensity 2 at 3.88 ppm is coupled to a doublet of triplets at 4.00 ppm ($J = 9.3$ and 3.2 Hz), which in turn coupled to a doublet of triplets at 6.20 ppm ($J = 9.3$ and 0.9 Hz). This pattern of ^1H NMR data is identical to that has been observed for anionic complex of phenanthridine. The two hydrogen atoms at the C(3) and C(2) of heterocyclic ring appear as two doublets at 6.75 ppm ($J = 3.3$ Hz) and 7.12 ppm ($J = 3.2$ Hz) respectively with relative intensity 1 indicating hydride attack occurred at the carbocyclic ring similar to that of phenanthridine or quinoline complex. Deuterated anionic complex **83'** formed from the D^- attack on the complex **43** shows identical ^1H NMR data but with decreased multiplicity in the carbocyclic region. The relative intensity of the broadened resonance at 3.88 ppm also becomes 1 indicating that deuterium incorporation has occurred at the C(5) of the carbocyclic ring.

When anionic complex, **83** was neutralized by H^+ , the amber color of the solution turned to red giving the expected σ - π vinyl complex, **84** as a minor product (7%) reducing the double bond between C(5) and C(6) of the carbocyclic ring. Compound (**84**) was characterized by IR and ^1H NMR. In ^1H NMR the hydride peaks comes at -16.83 ppm which is characteristic of σ - π vinyl complexes.¹⁹ The four methylene protons at C(5) and C(6) are observed as four separate multiplets at 2.96, 2.76, 2.42, 2.30 ppm respectively. The proton at C(7) also appears as a multiplet at 4.10 ppm. The two doublets at 8.14 ($J = 3.2$ Hz) and 8.34 ppm ($J = 3.2$ Hz) are due to two protons at C(2) and C(3) respectively of the heterocyclic ring.



Scheme 4.1



Scheme 4.2

When anion **83'** was neutralized by D^+ , it gave a deuterated σ - π vinyl complex (**84'**) as evidenced from its 1H NMR data where all the chemical shift peaks are compatible with those of undeuterated compound (**84**). Some changes occur in the peak multiplicities of carbocyclic protons which come as doublets instead of multiplets due to deuterium incorporation. Compound (**84'**) could not be isolated. On purification over silica gel undeuterated form (**84**) was isolated instead. This is apparently due to the deuterium exchange with hydrogen on silica gel.

In the major anionic complex (**82**) resulting from the H^- attack at the 2-position of heterocyclic ring, a broadened resonance of relative intensity 2 at 4.81 ppm is coupled to a doublet of triplets at 6.88 ppm ($J = 8.2$ and 3.2 Hz). The three protons at C-5, C-6 and C-7 appear as three sets of doublet of triplets at 6.58 ppm ($J = 8.1$ and 0.8 Hz), 5.33 ppm ($J = 8.1$ and 0.8 Hz) and 6.90 ppm ($J = 8.1$ and 0.8 Hz) respectively. Mechanistic studies using labeled hydride (D^-) reproduces the identical spectroscopic data in 1H NMR of **82'** but shows a decrease in the peak multiplicities for the C-2 and C-3 protons and a decrease in peak intensity for the C-2 proton where the broadened resonance at 4.78 ppm becomes 1 in intensity and the multiplicity at 6.88 ppm ($J = 3.6$ Hz) reduces to a doublet. This demonstrates that deuterium has been incorporated in the 2-position of heterocyclic ring. The protonation of the anionic complex (**82**) gave rise to compound (**85**) where nitrogen atom that is coordinated with one of the metal atoms becomes protonated reducing the double bond across the N(1)-C(2) bond, and the carbocyclic ring becomes rearomatized. The neutralization of the anionic complex also simultaneously formed green starting material (**43**) by deprotonating complex **82**.

Examination of the crude reaction mixture by $^1\text{H-NMR}$ in CD_2Cl_2 prior to chromatographic purification shows the presence of compounds **85** and **43** in a ratio of 2:1. The $^1\text{H-NMR}$ of **85** shows only one singlet in the hydride region at -13.31ppm . The three aromatic protons for C-5, C-7 and C-6 are observed as two separate doublets and a doublet of doublets at 7.16, 7.38 and 6.55 ppm respectively. The multiplet resonance of relative intensity 2 at 6.47 ppm is attributable to two methylene protons ($-\text{CH}_2$) at C-2 and the multiplet at 7.48 ppm is for the C-3 proton which is coupled strongly to methylene protons. The broad resonance at 5.50 ppm can be assigned to NH proton where the nitrogen atom is bound to a metal atom of the cluster.

When anionic complex, **82'** was treated with D^+ , deuterated compound **85'** was formed. The chemical shift resonances observed in the aromatic and aliphatic regions of the $^1\text{H-NMR}$ of **85'** are consistent with those of undeuterated form **85** except that no resonance is observed at 5.5 ppm which was due to the NH proton of **85** indicating that deuterium has been incorporated at the N atom. Changes are also observed in the peak multiplicities of resonances at 6.46 ppm and 7.49 ppm where they appear as two doublets due to the presence of a deuterium atom at C-2 as compared to the splitting observed in **85**.

Purification of compound **85** on silica gel gave rise to the green starting material **43** (by H_2 elimination) as well as compound **87** via the intermediate structure **86** (where hydrogen has been transferred from the ligand atom to the metal core). The ratio of the formation of **43** to **87** was 1.5:1. Intermediate structure **86** could not be isolated. Water on the silica gel is undoubtedly responsible for the formation of **87**.

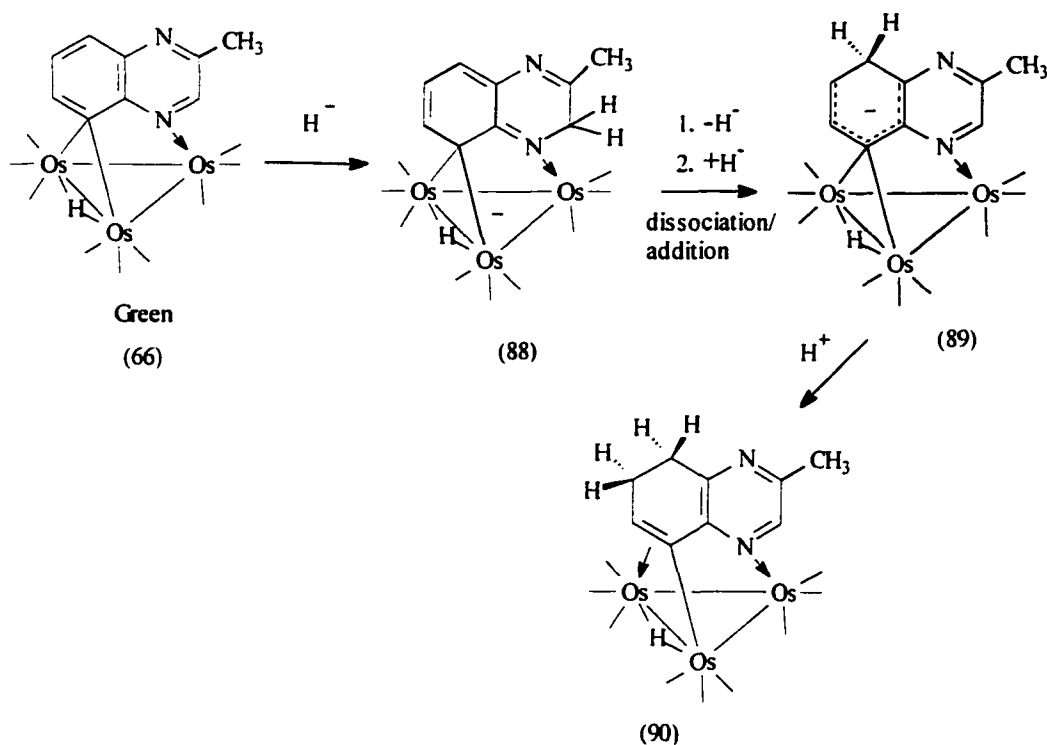
Compound **87** was obtained in a 28% yield, and was characterized by $^1\text{H-NMR}$ and 2D-COSY data. $^1\text{H-NMR}$ shows two doublets in the hydride region at -12.87 ppm ($J=2$ Hz) and at -13.71 ppm ($J=2$ Hz). 2D COSY shows the doublet at 6.22 ppm of the C-5 proton is coupled to the doublet of doublets at 5.41 ppm of the C-6 proton, which in turn coupled to the doublet at 6.30 ppm of the C-7 proton. The two methylene protons at C-2 are asymmetric owing to the introduction of chirality at the neighboring carbon, for which the resonances come as two separate multiplets at 3.52 and 3.66 ppm. 2D-COSY also shows that they are coupled to each other and with the neighboring proton (C-3) at 2.97 ppm. The broad resonance at 2.96 ppm is assigned to the $-\text{OH}$ proton, which also couples to the neighboring proton as observed from 2D-COSY. The uncoupled broad resonance at 3.59 ppm can be attributed to the $-\text{NH}$ proton.

Purification of deuterium incorporated compound **85'** on silica gel also gave green starting material **43** as well as **87'** in a 1.6:1 ratio. The chemical shifts and peak multiplicities in the $^1\text{H-NMR}$ of **87'** are consistent with the undeuterated form of **87'** except that no peak is observed at 3.59 ppm which was due to the NH of compound **87**. This demonstrates the presence of the deuterium atom at N-3 in **87'**. On silica gel deuterium exchanges with the hydrogen of water to form mono-deuterated water (HOD) that adds across the C(3)-N(4) double bond to yield **87'**. To confirm this assignment based on $^1\text{H NMR}$ and COSY data, we are awaiting for a solid state structure of **87**.

Since quinoxaline complex **43** mainly underwent nucleophilic attack at the C-2 position of the heterocyclic ring, we wanted to see if introduction of an alkyl group at the C-2 position of the ring redirects the nucleophilic attack towards the carbocyclic ring. In fact, interaction of 2-methyl quinoxaline with $\text{Os}_3(\text{CO})_{10}(\text{CH}_3\text{CN})_2$ gave only 3-methyl quinoxaline triosmium complex, $\text{Os}_3(\text{CO})_9(\mu_3\text{-}\eta^2\text{-C}_8\text{H}_4(3\text{-CH}_3)\text{N}_2(\mu\text{-H}))$ (**66**) but not 2-methyl quinoxaline complex (discussed in chapter 2). This is apparently due to the steric factor which makes the cluster molecule intolerable when the methyl is situated closer to the metal carbonyl moiety. This type of behavior has been observed previously in the case 2-methyl quinoline where attempted cluster formation with $\text{Os}_3(\text{CO})_{10}(\text{CH}_3\text{CN})_2$ failed.^{2,3}

When 3-methyl quinoxaline complex (**66**) was reacted with H^- , the color of the green solution changed to amber converting it to anionic complex **88** by nucleophilic attack at the heterocyclic ring (Scheme 4.3). The ^1H NMR of **88** prior to neutralization shows spectroscopic data similar to the anionic complex (**82**), which was resulted from the H^- attack at the C-2 position of the heterocyclic ring. The hydride peak appears as a singlet at -12.91 ppm. The three protons at C-5, C-7 and C-6 come as two doublets of doublets and a doublet of triplets at 6.51, 6.80 and 5.33 ppm respectively. The broadened resonance of relative intensity 2 at 4.88 ppm is due to $-\text{CH}_2(2)$. The $-\text{CH}_3$ chemical shift is observed as a singlet at 1.80 ppm. This anionic complex appears to be a kinetic product which undergoes rearrangement on standing to produce thermodynamically more stable anion **89**. The rearrangement may be due to the steric repulsion, the methylene protons experience from the both methyl group and metal carbonyl moiety being in the close

Scheme 4.3



proximity. The structure of **89** is evident from its proton ^1H NMR spectrum. The hydride resonance is observed at -13.85 ppm (the hydride resonance of **83** comes at -13.01 ppm). The chemical shifts and peak multiplicities in the aromatic and aliphatic regions of **89** are similar to those of anionic complex (**83**), which was obtained from the H^- attack at the carbocyclic ring of quinoxaline complex (**43**). The broadened resonance at 3.94 ppm is for $-\text{CH}_2(5)$ and the two doublets of triplets at 4.30 ppm ($J=9.4$ and 3.2 Hz) and at 6.29 ppm ($J=9.4$ and 0.9 Hz) are for the C-6 and C-7 protons respectively. The C-2 and $-\text{CH}_3$ protons are observed as two singlets at 8.29 and 2.48 ppm respectively.

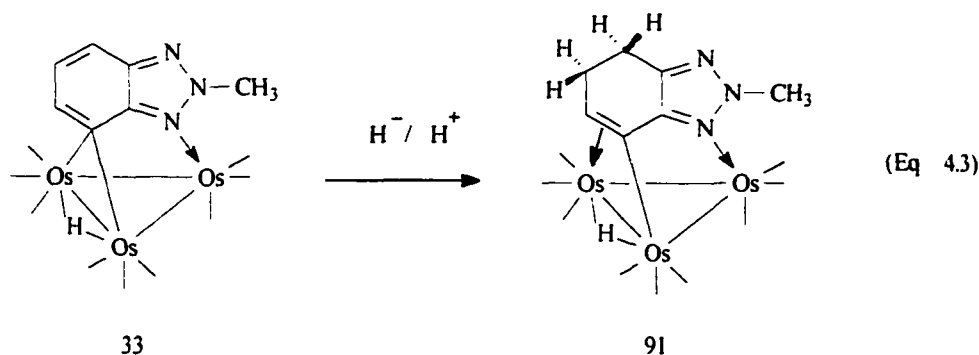
Protonation of the anionic complex **89** resulted in a change in color of the solution from amber to red yielding the σ - π vinyl complex, $\text{Os}_3(\text{CO})_9(\mu_3\text{-}\eta^3\text{-C}_8\text{H}_6(3\text{-CH}_3)\text{N}_2(\mu\text{-H}))$ (**90**). This nucleophilic addition product was isolated by chromatographic separation on silica gel in a 68% yield. Compound **90** was characterized by IR, ^1H NMR and elemental analysis. The three multiplets of relative intensity 2:2:1 at 2.79, 2.38 and 4.18 ppm can be fairly assigned to the four methylene protons at C-5 and C-6, and a vinyl proton at C-7. The two singlets at 8.23 and 2.35 ppm with relative intensity 1:3 are attributable to C-2 and -CH_3 protons. The hydride resonance is observed at -16.81 ppm.

4.2.3 Reactions of 2-Methylbenzotriazole Complex, $\text{Os}_3(\text{CO})_9(\mu_3\text{-}\eta^2\text{-C}_6\text{H}_3\text{N}_3(2\text{-CH}_3)(\mu\text{-H}))$ (**33**) with LiEt_3BH and CF_3COOH

The benzoheterocyclic complex containing three nitrogen atoms in a five-membered ring fused to a carbocyclic ring $\text{Os}_3(\text{CO})_9(\mu_3\text{-}\eta^2\text{-C}_6\text{H}_3\text{N}_3(2\text{-CH}_3)(\mu\text{-H}))$ (**33**) underwent regioselective nucleophilic attack at the C-4 position of carbocyclic ring when treated with H^- followed by H^+ to give a σ - π vinyl complex, $\text{Os}_3(\text{CO})_9(\mu_3\text{-}\eta^3\text{-C}_6\text{H}_5\text{N}_3(2\text{-CH}_3)(\mu\text{-H}))$ (**91**) reducing the double bond across the C(4)-C(5) bond (Equation 4.3). During these reactions the color of the solution changed from green to yellow, and then to orange. This nucleophilic addition product (**91**) was purified by chromatographic separation, and was obtained in a 75% yield.

Compound (**91**) was characterized by IR, ^1H NMR and elemental analysis. In the ^1H NMR two closely related multiplets of relative intensity 2 each at 2.75 and 2.70 ppm

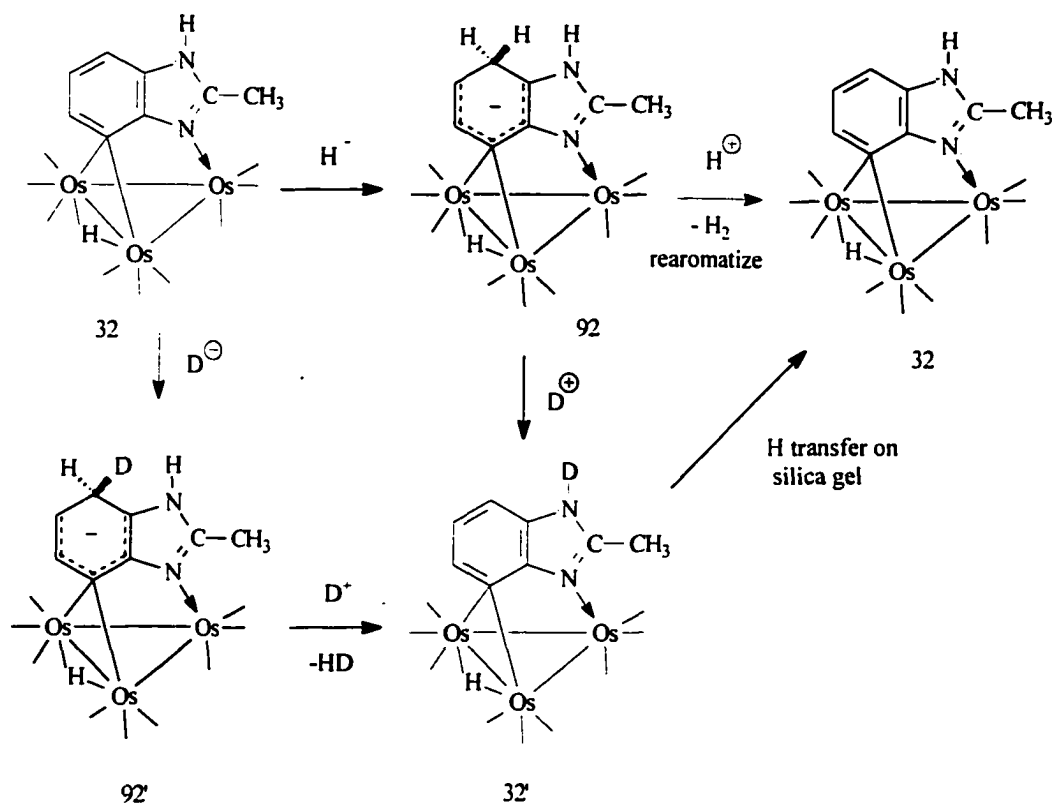
account for $-\text{CH}_2(4)$ and $-\text{CH}_2(5)$ respectively. The vinyl proton at C-6 is observed as another multiplet at 4.88 ppm. The methyl and hydride resonances come as singlets at 4.03 and -16.14 ppm respectively.



4.2.4 Reactions of the 2-Methylbenzimidazole and 2,3-Dimethylbenzimidazole Complexes, $\text{Os}_3(\text{CO})_9(\mu_3-\eta^2-\text{C}_7\text{H}_3(2-\text{CH}_3)\text{N}_2(3-\text{R}))(\mu-\text{H})$ ($\text{R} = \text{H}$, 32; $\text{R} = \text{CH}_3$, 71) with LiEt_3BX and CF_3COOX ($\text{X} = \text{H}$ or D)

When the 2-Methylbenzimidazole complex, $\text{Os}_3(\text{CO})_9(\mu_3-\eta^2-\text{C}_7\text{H}_4(2-\text{CH}_3)\text{N}_2)(\mu-\text{H})$ (32) was reacted with H^- , the green solution of the complex turned bluish in color giving an anionic complex 92 from the H^- attack at the 4-position of the carbocyclic ring (Scheme 4.4). The evidence of the hydride attack at the carbocyclic ring comes from its ^1H NMR studies prior to neutralization. The existence of a broad resonance at 8.23 ppm indicates the presence of $-\text{NH}$ in the anionic complex. A doublet and a triplet at 7.72 ($J=7.2$ Hz) ppm and at δ 6.60 ppm ($J=8.0$ Hz) account for two protons at C-5 and C-6 respectively. The $-\text{CH}_2(4)$ resonance is obscured by the THF. The $-\text{CH}_3$ and hydride

Scheme 4.4



chemical shifts come as singlets at 2.50 ppm and -12.0 ppm respectively. The anionic complex **92** upon protonation rearomatized back to the green starting material (**32**). Acid first protonates the nitrogen atom which initiates the electronic rearrangement to give rise to the green starting material (**32**) upon one mole of hydrogen elimination.

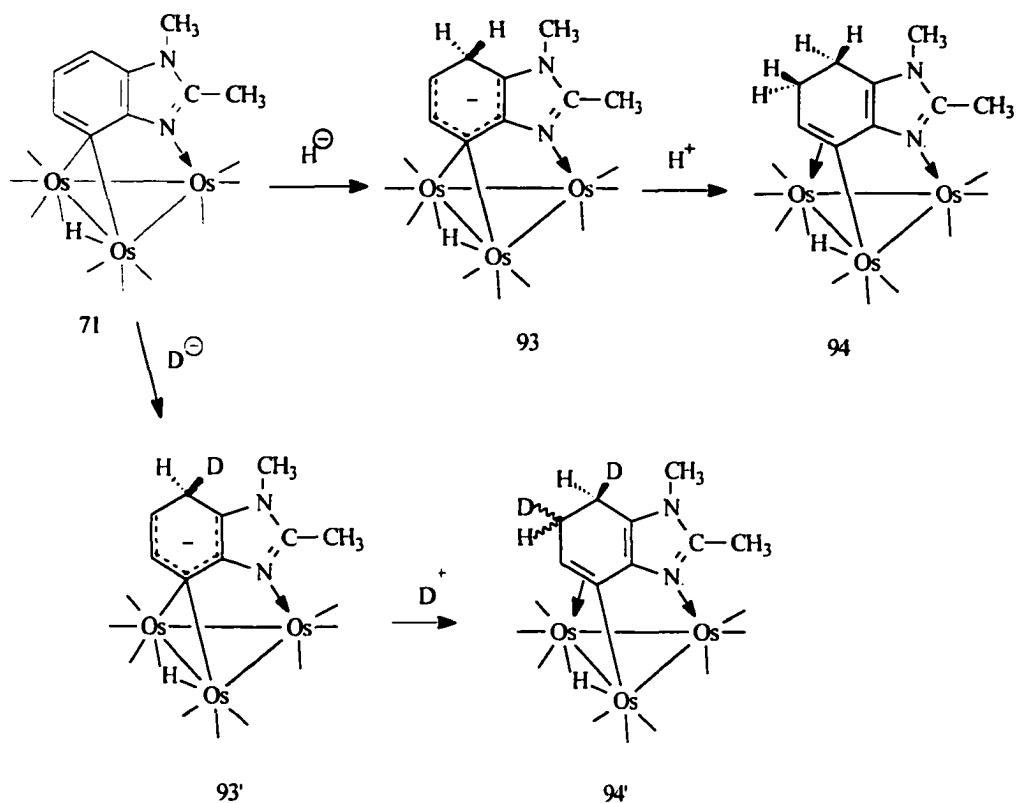
When **92** was treated with CF_3COOD , D^+ deuterated the nitrogen atom, and upon electronic rearrangement and elimination of HD rearomatized it back to the deuterated green starting material (**32'**). The treatment of **92'** (which was resulted from the labeled-hydride (D^-) attack on **32**) with D^+ also produced deuterated starting material **32'** but with H^+ , on the other hand, yielded compound **32** by HD elimination.

The ^1H NMR of **32'** reproduces the identical spectroscopic data of **32**. The only change is found in the -NH region where no peak is observed for **32'** demonstrating that deuterium has been incorporated. Compound **32'** could not be isolated which on purification over silica gel gave rise to **32** by deuterium exchange with hydrogen.

Unlike 2-methylbenzimidazole cluster (**32**) where anionic complex resulting from the H^- addition at the C-4 position rearomatized back to the starting material upon protonation, 2,3-dimethyl benzimidazole complex, $\text{Os}_3(\text{CO})_9(\mu_3\text{-}\eta^2\text{-C}_7\text{H}_3(2\text{-CH}_3)\text{N}_2(3\text{-CH}_3)(\mu\text{-H})$ (**71**) underwent nucleophilic attack at the C(4)-position of the carbocyclic ring to yield, after protonation, the $\sigma\text{-}\pi$ vinyl complex, $\text{Os}_3(\text{CO})_9(\mu_3\text{-}\eta^3\text{-C}_7\text{H}_5(2\text{-CH}_3)\text{N}_2(3\text{-CH}_3)(\mu\text{-H})$ (**94**) via anionic complex **93** upon sequential attack of H^-/H^+ (Scheme 4.5). The presence of a methyl group on the nitrogen atom prevents the formation of a rearomatized nucleophilic addition product owing to the fact that release of a methyl anion required for rearomatization when H^+ attack the nitrogen atom is more difficult than a hydride. The structure of the anionic complex **93** was evident from its ^1H NMR and 2D-COSY data. The broadened resonance at 3.40 ppm due to $\text{-CH}_2(4)$ is coupled to a multiplet at 4.56 ppm of CH(5) which in turn coupled to a doublet of triplets at 6.14 ppm ($J = 9.2, 0.8$ Hz) of CH(6). The N- CH_3 , C- CH_3 and hydride resonances come as three singlets at 3.37 and 2.18 and -14.79 ppm respectively.

The protonation of the anionic complex **93** occurs at the carbocyclic ring to yield the nucleophilic addition product **94**. After chromatographic separation the product was isolated in a 66% yield, and was characterized by IR, ^1H NMR and elemental analysis.

Scheme 4.5



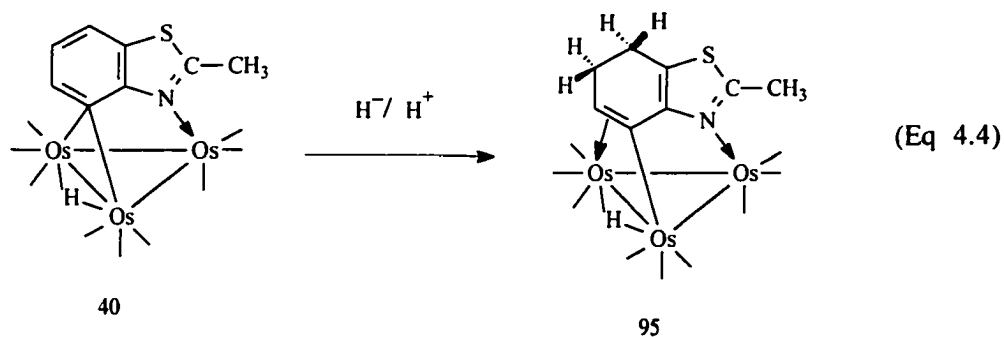
In the ^1H NMR the two multiplets of relative intensity 2 each at 2.51 and 2.48 ppm are for $-\text{CH}_2(4)$ and $-\text{CH}_2(5)$ respectively. The vinyl proton appears as a doublet of doublets at 4.53 ppm. The N- CH_3 , C- CH_3 and hydride resonances are observed as three singlets at δ 3.39 and 2.30 and -16.40 ppm respectively.

The sequential attack of D^-/D^+ on **71** gave the identical chemical reactions to those of H^-/H^+ to afford the deuterated σ - π vinyl complex **94'** through the intermediate anionic complex **93'**. The ^1H NMR of **94'** shows almost identical chemical shifts in the carbocyclic and heterocyclic region to those of compound **94** but decreased in intensities and multiplicities in the carbocyclic region indicating that deuterium has been

incorporated in the carbocyclic ring. A decrease in the multiplicities is observed for all the peaks in the carbocyclic region of **94'** and intensities have reduced to 1 at 2.54 and 2.51 ppm due to CHD(4) and CHD(5). For **93'** decreased multiplicities are found at 4.56 and 3.40 ppm, and intensity has reduced to 1 at 3.40 ppm due to CHD(4) in the ^1H NMR of **93'**.

4.2.5 Reactions of $\text{Os}_3(\text{CO})_9(\mu_3\text{-}\eta^2\text{-C}_7\text{H}_3(2\text{-R})\text{NX})(\mu\text{-H})$ (R= H, X = S, **39; R = CH₃, X= S, **40**; R = H, X = O, **37**; R= CH₃, X= O, **38**;) with LiEt_3BX (X=H or D) and CF_3COOH**

The electron deficient complexes containing two heteroatoms in the heterocyclic ring such as 2-methylbenzothiazole complex, $\text{Os}_3(\text{CO})_9(\mu_3\text{-}\eta^2\text{-C}_7\text{H}_3(2\text{-CH}_3)\text{NS})(\mu\text{-H})$ (**40**) underwent nucleophilic reduction at the carbocyclic ring on treatment with H^-/H^+ to give the 48-electron, $\sigma\text{-}\pi$ vinyl complex, $\text{Os}_3(\text{CO})_9(\mu_3\text{-}\eta^3\text{-C}_7\text{H}_5(2\text{-CH}_3)\text{NS})(\mu\text{-H})$ (**95**) in a 74% yield (Equation 4.4). This compound was isolated by purification over silica gel and



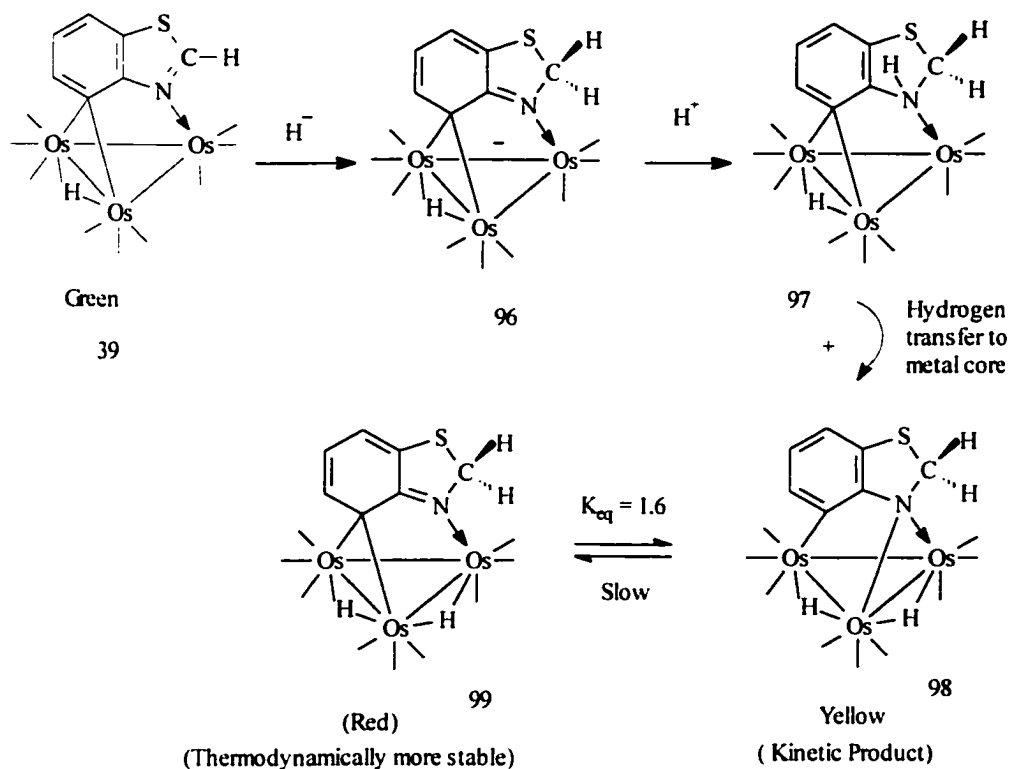
was characterized by IR, ^1H NMR and elemental analysis. In the ^1H NMR two multiplets of relative intensity 2 appear at 2.65 and 2.38 ppm due to $\text{CH}_2(4)$ and $\text{CH}_2(5)$, and the

vinyl proton at C-6 is observed as a doublet of doublets at 4.46 ppm. The $-\text{CH}_3$ and hydride chemical shifts are obtained as two singlets at 2.62 and -16.93 ppm respectively. All these data are consistent with the formation of a σ - π vinyl complex.¹⁹

When benzothiazole complex, $\text{Os}_3(\text{CO})_9(\mu_3\text{-}\eta^2\text{-C}_7\text{H}_4\text{NS})(\mu\text{-H})$ (**39**) was reacted with LiEt_3BH , the hydride attacked at the C-2 position of the heterocyclic ring to give rise of the anionic complex (**96**) (Scheme 4.6). The general structure of **96** is similar to the anionic complex of quinoxaline (**82**) where hydride attacked at the C-2 of heterocyclic ring. In the ^1H NMR of **96**, the three carbocyclic proton chemical shifts appear at a higher field than the aromatic proton resonance indicating aromaticity in the ring has been significantly disrupted. The resonances for C-4, C-6 and C-5 protons are observed as two doublets at 6.31 and 6.84 ppm and a doublet of doublets at 5.25 ppm respectively. The two methylene protons, $-\text{CH}_2(2)$ come as a singlet of relative intensity 2 at 5.06 ppm.

When the anionic complex **96** was treated with H^+ , protonation took place at the nitrogen atom as evidenced by the appearance of a broad resonance at 7.12 ppm in the ^1H NMR to yield complex **97**. Protonation also occurred simultaneously at the metal core to give a dihydride complex, $\text{Os}_3(\text{CO})_9(\mu_3\text{-}\eta^2\text{-C}_7\text{H}_5\text{NS})(\mu\text{-H}_2)$ (**98**). Examination of ^1H NMR at room temperature prior to purification shows the relative intensity of the hydride peaks at -14.06 ppm (of complex **98**) and -14.03 ppm (of complex **97**) in 2:1 ratio and all the companion peaks in the aromatic and aliphatic regions in 1:1 ratio. This indicates complex **98** is a dihydride and both complex **97** and **98** are formed in 1:1 ratio.

Scheme 4.6



For complex **97** ^1H NMR shows three aromatic protons at 7.68 (dd, H(6)), 6.80 (dd, H(4)) and 6.38 (d of t, H(5)) ppm and two methylene protons as a doublet at 6.30 ppm. For complex **98** ^1H NMR shows three aromatic resonances at 7.21 (dd, H(6)), 6.62 (dd, H(4)), 6.56 (dd, H(5)) ppm and the two methylene protons as a broad resonance of relative intensity 2 at 5.2-3.9 ppm.

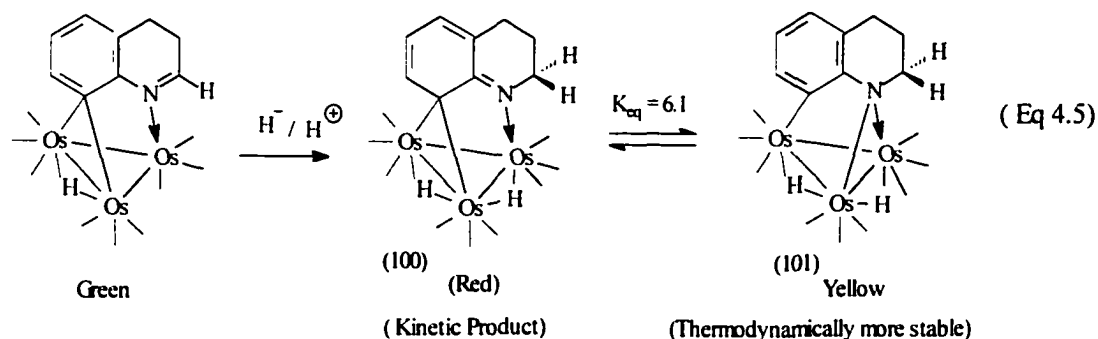
During purification over silica gel compound **97** converted to **98** by proton transfer from the amino N-H to the metal core. This similar type of proton transfer has been observed previously in the case of quinoxaline complex (discussed earlier). The yield of **98** was 79%.

Compound **98** is a deep yellow and shows a fluxional behavior which indicates hydride exchange in the temperature range examined. Thus, at -45°C in CDCl_3 we observe two doublet hydride resonances at -14.06 ($J = 2$ Hz) and -14.10 ($J = 2$ Hz) ppm and two aliphatic resonances at 5.05 (d) ($J = 12$ Hz) and 3.95 (d) ($J = 12$ Hz) ppm, all of equal relative intensity. VT ^1H NMR shows the separation of the two hydride signals as the temperature is decreased (Figure 4.2). At room temperature, a single sharp hydride resonance at -14.06 ppm is observed while the two methylene protons resonances average to a broadened resonance in the range 5.2 - 3.9 ppm. At -45°C , 2D-COSY shows these two protons are correlated to each other. The aromatic resonances remained unchanged through this temperature range at 7.21 , 6.62 and 6.56 ppm. This behavior is consistent with a process in which one of the hydrides moves from edge-to-edge to induce a symmetry plane followed by edge-to-edge migration of either hydride.⁵¹ The kinetic product **98** converts slowly to the thermodynamically more stable product, $\text{Os}_3(\text{CO})_9(\mu_3\text{-}\eta^2\text{-C}_7\text{H}_5\text{NS})(\mu\text{-H}_2)$ (**99**) at room temperature. The approximate half-life is 3 h at 90°C . The conversion of **98** to **99** follows first order kinetics. The rate constant for this conversion is $(6.42 \pm 0.6) \times 10^{-5} \text{ s}^{-1}$.

Compound **99** is deep red and completely rigid on the NMR time scale. The lone pair of electrons on the nitrogen form a double bond with C(8), breaking the aromaticity of the carbocyclic ring and allowing the formation of an electron-precise bridging bond at C(7) with two osmium along one edge of the cluster. This compound was characterized by IR, ^1H NMR, 2D-COSY and elemental analysis. In the ^1H NMR the two hydride resonances are observed at -13.05 ($J = 2$ Hz) and -13.43 ($J = 2$ Hz) ppm and the two

methylene protons are appeared as two doublets at 5.02 ($J = 12$ Hz) and 4.79 ($J = 12$ Hz) ppm. 2D COSY shows the two methylene protons are coupled to each other. In the aromatic region a doublet of doublets at 6.34 ppm is coupled to a doublet of triplets at 5.45 ppm which in turn coupled to a doublet of doublets at 6.88 ppm.

Compounds **98** and **99** appear to be involved in a tautomeric equilibrium ($K_{eq}=1.6$) since heating of **98** (> 25 h) at 90°C results in a constant ratio 1.6:1 of (**99**:**98**). This formation of the yellow kinetic product and the subsequent conversion to the red thermodynamically stable product is completely in contrast to that had been observed previously with the dihydroquinoline complex.^{1,19} The reaction of H^-/H^+ with dihydroquinoline resulted in the formation of two tautomeric products (**100**) and (**101**) ($K_{eq}=6.1$) where the kinetic product (**100**) was red which slowly converted to the thermodynamically more stable yellow product (**101**) (Equation 4.5).



The solid state structure of **98** is shown in Figure 4.3, selected distances and bond angles are given in table 4.1. The structure **98** consists of an isosceles triangle of osmium atoms with the elongated edge bridged by the more in plane hydride ligand and the shortest edge having the single atom amido bridge and a highly tucked hydrogen ligand.

It is clear from the N(1)-C(7) and C(7)-C(6) bond lengths (1.47(3) and 1.37(2)Å respectively) that the carbocyclic ring is aromatic. The C(7)-C(8) bond lengths fall into a much narrower value of 1.39 Å suggesting significant benzenoid character in the ring.

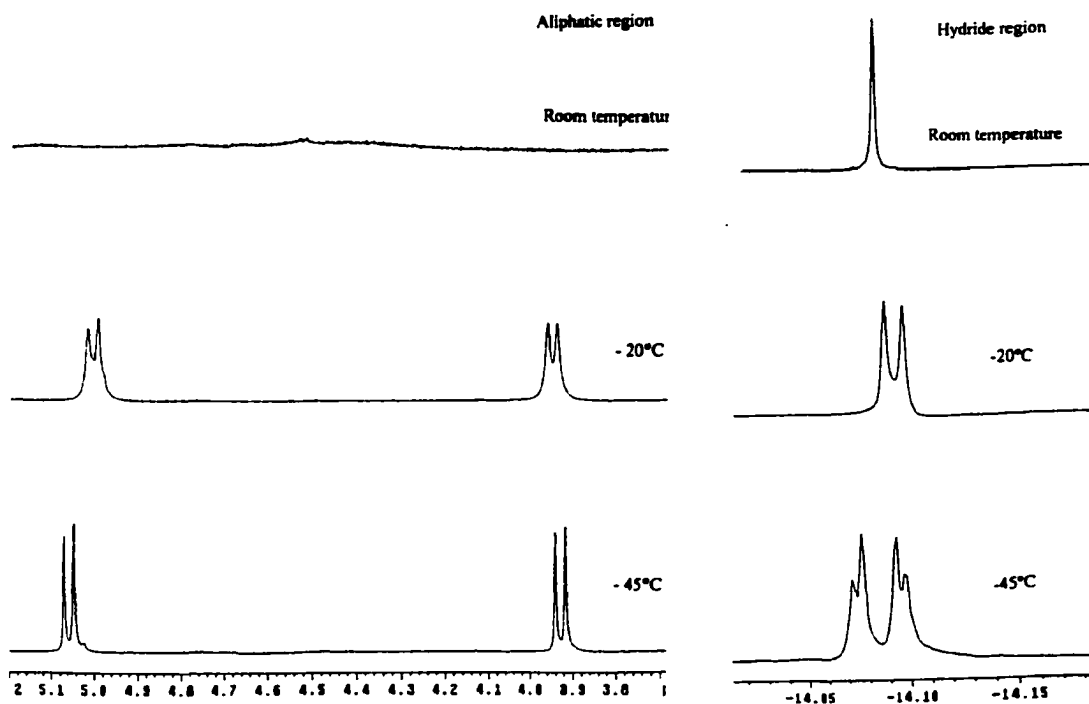


Figure 4.2 VT ^1H NMR of the aliphatic (left) and hydride (right) regions of **98** at 400 MHz in CDCl_3

The C(6)-Os(2) (2.11(2)Å) bond has shortened somewhat compared to the corresponding bonds of the electron deficient benzoheterocyclic complexes (discussed in chapter 2) on becoming terminal while N(1)-Os(1) (2.16(10)Å) bond has become slightly elongated on becoming a bridging amido and exhibits a very slight asymmetry.

Table 4.1 Selected Bond Distances (Å) and Angles (°) for 98^a

| Distances | | | |
|-------------------|-----------------------|------------------|----------------------|
| Os(1)-Os(2) | 2.80(11) | C(7)-C(8) | 1.39(3) |
| Os(1)-Os(3) | 2.79(11) | C(7)-N(3) | 1.38(5) |
| Os(2)-Os(3) | 3.00(11) | C(6)-C(7) | 1.39(5) |
| Os(1)-N(1) | 2.16(16) | C(4)-C(5) | 1.38(5) |
| Os(3)-N(1) | 2.10(3) | C(5)-C(6) | 1.45(3) |
| C(6)-Os(2) | 2.11(2) | C(2)-S(1) | 1.81(6) |
| N(1)-C(2) | 1.51(2) | Os-CO | 1.91(2) ^b |
| C(7)-N(1) | 1.47(3) | C-O | 1.12(3) ^b |
| Angles | | | |
| Os(2)-Os(1)-Os(3) | 65.06(3) | C(6)-C(7)-N(1) | 119.7(18) |
| Os(1)-Os(2)-Os(3) | 57.31(3) | C(5)-C(6)-Os(2) | 128.5(16) |
| Os(2)-Os(3)-Os(1) | 57.63(3) | Os(3)-N(1)-Os(1) | 81.7(5) |
| Os-C-O | 173.1(2) ^b | | |

a numbers in parentheses are estimated standard deviations.

b Average values.

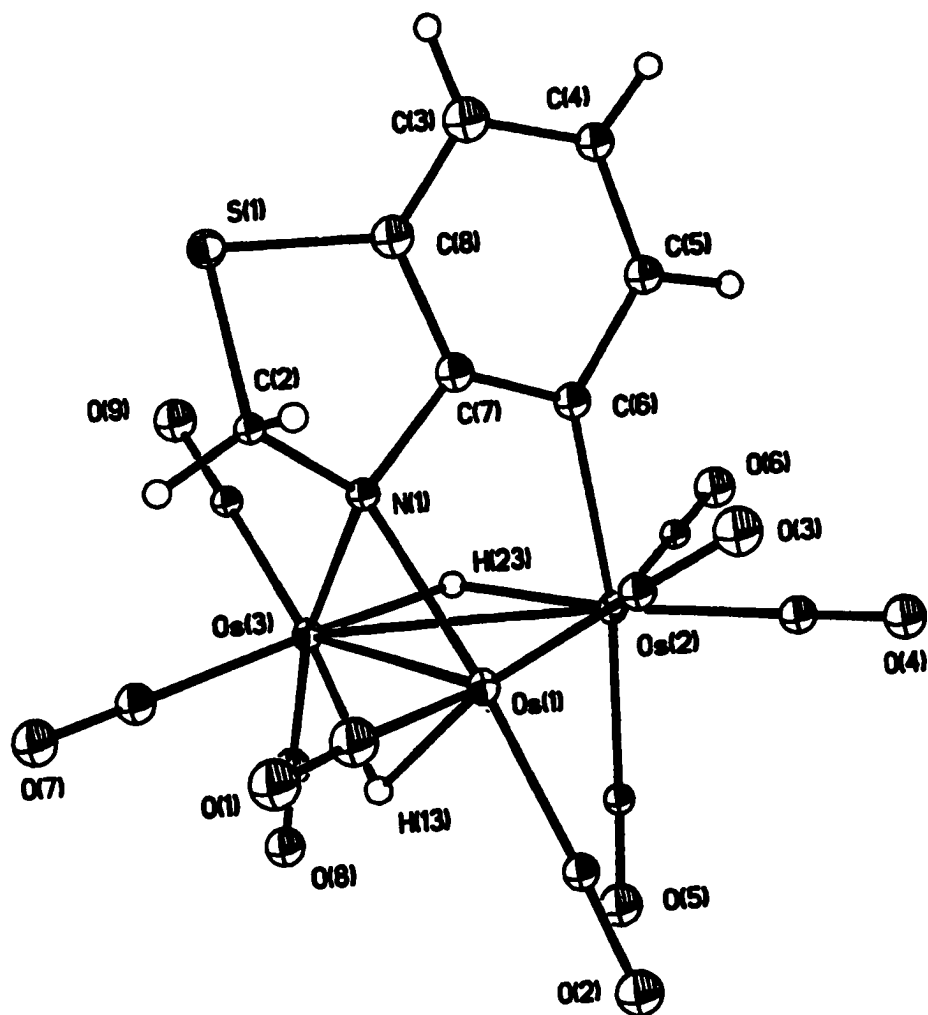
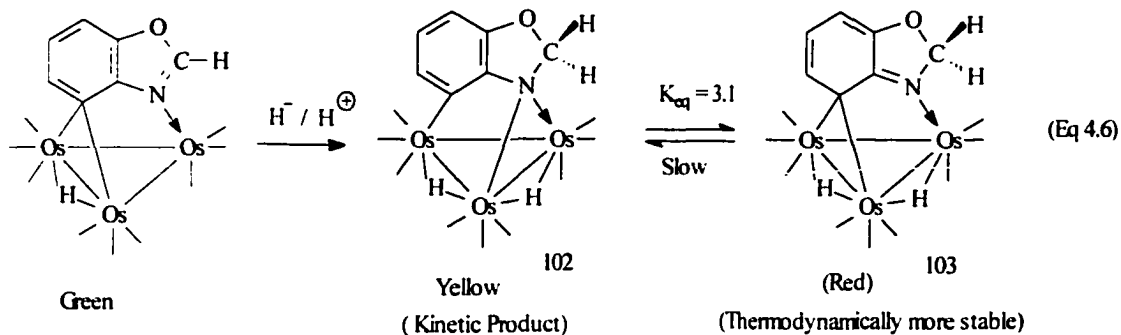


Figure 4.3. Solid state structure of $\text{Os}_3(\text{CO})_9(\mu_3\text{-}\eta^2\text{-C}_7\text{H}_5\text{NS})(\mu\text{-H}_2)$ (**98**)

The sequential reaction of H^-/H^+ on benzoxazole complex, $Os_3(CO)_9(\mu_3-\eta^2-C_7H_4NO)(\mu-H)$ (**37**) gave two isomers $Os_3(CO)_9(\mu_3-\eta^2-C_7H_5NO)(\mu-H_2)$ (**102**) and $Os_3(CO)_9(\mu_3-\eta^2-C_7H_5NO)(\mu-H_2)$ (**103**) (Equation 4.6). Like compound **98** and **99**, compound **102** and **103** are related by a tautomeric equilibrium for which the equilibrium ratio is 3.1:1 of (**67:68**). Interestingly, the rate of equilibration is significantly higher than in the case of **98** converting to **99** having a half-life of 1.5 h at 90°C and $K_{eq}=3.1$. The rate constant for this conversion is $(1.28\pm 0.1)\times 10^{-4} s^{-1}$. Just as for compound **98**, **102** is fluxional on the NMR time scale and is deep yellow, while **103** is structurally rigid on the NMR time scale and is deep red as for compound **99**.



The 1H NMR for **102** at $-45^\circ C$ shows two sharp hydride resonances at -13.84 and -14.07 ppm and two aliphatic resonances at 5.28 ($J=5$ Hz) and 5.04 ($J=5$ Hz) ppm similar to compound **98**. VT 1HNMR of **102** is shown in figure 4.3. The two aliphatic resonances are coupled to each other in the 2D-COSY at $-45^\circ C$. At room temperature, a single sharp hydride resonance at -13.95 ppm is observed while the aliphatic resonances average to a

broadened resonance at 5.17 ppm. The aromatic resonances remained unchanged through this temperature range at 6.96, 6.53 and δ 6.28 ppm.

The ^1H NMR for **103** at room temperature shows two hydrides as two doublets at -13.16 ($J=2$ Hz) and -13.22 ($J=2$ Hz) ppm and two aliphatic resonances at 5.47 ($J=8$ Hz) and 5.30 ($J=8$ Hz) ppm as doublets as well. The aromatic resonances come at 6.25, 6.14 and 5.50 ppm as two separate doublets and a triplet for C-6, C-4 and C-5 protons respectively.

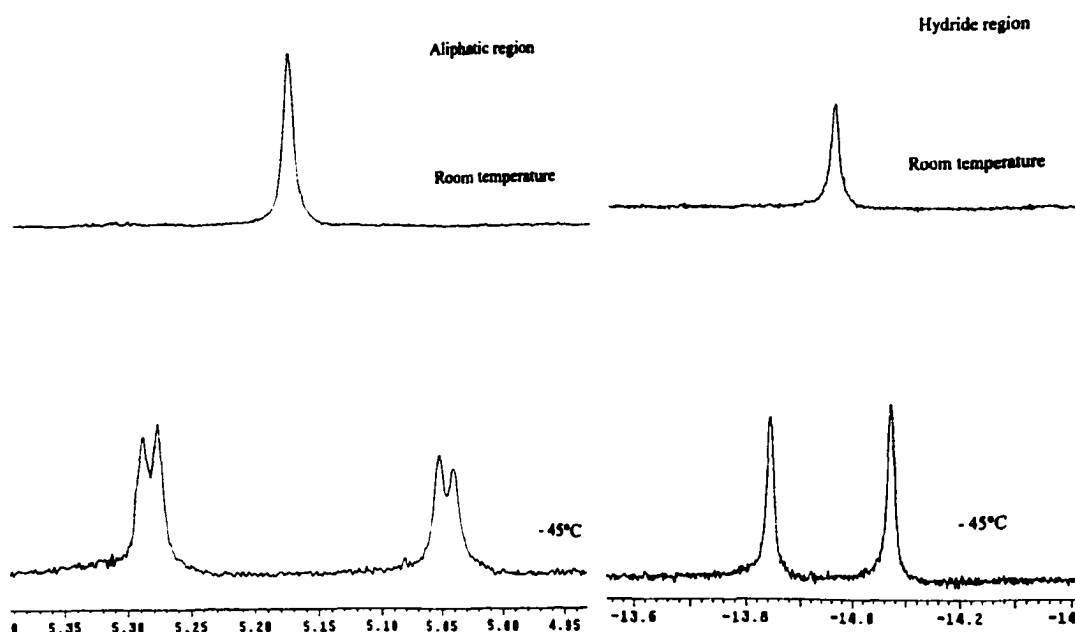
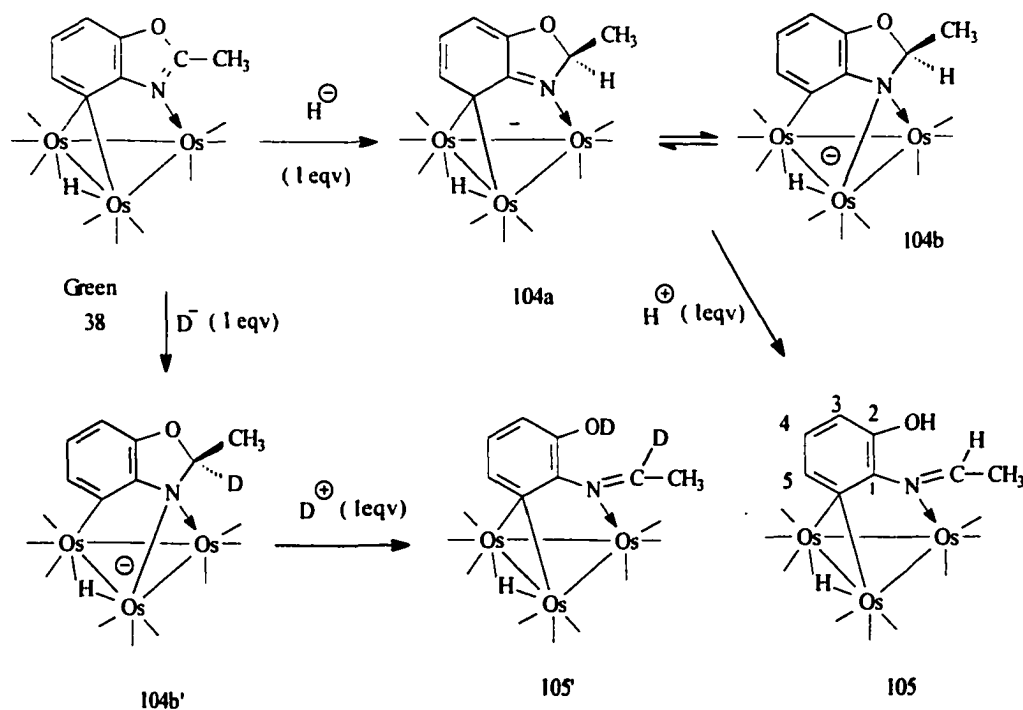


Figure 4.4 VT ^1H NMR of the aliphatic (left) and hydride (right) regions of **102** at 400 MHz in CDCl_3

When 2-Methylbenzoxazole complex, $\text{Os}_3(\text{CO})_9(\mu_3\text{-}\eta^2\text{-C}_7\text{H}_4\text{NO})(2\text{-CH}_3)(\mu\text{-H})$ (**38**) was reacted with one equivalent of LiEt_3BH , hydride attacked on the 2-position of the heterocyclic ring giving rise to a red anionic complex, **104a** (Scheme 4.7) as evident from the ^1H NMR data. In the ^1H NMR, the methyl chemical shift becomes a doublet at 1.29 ($J = 10$ Hz) ppm and the -CH(2) appears as a quartet at 5.30 ppm. The carbocyclic ring shows three proton resonances at 6.13 (d) ppm for C(6)-H, at 6.10(d) ppm for C(4)-H and at 7.37(d) ppm for C(5)-H indicating aromaticity in the ring has been disrupted. Deuterium labeling studies proves this assignment as no splitting of methyl group is observed in the ^1H NMR, when D^- attacks on the C-2 position of the ring to afford anionic complex **104'**. Also the peak at 5.30 ppm for CH(2) of anionic complex (**104**) was missing in the ^1H NMR of **104'** demonstrating deuterium incorporation at C-2 in **104**.

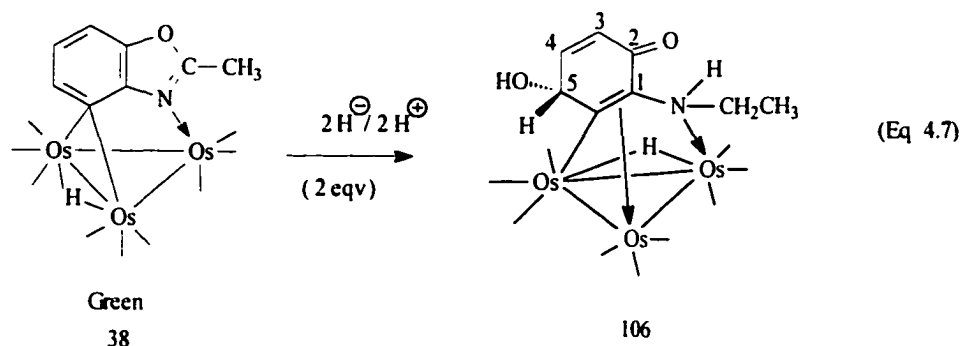
Scheme 4.7



Anionic complex **104a** may exist in tautomeric equilibrium with **104b**. When this complex was neutralized with H^+ , protonation occurred at the oxygen atom resulting in the ring opened compound (**105** (Scheme 4.7)). After chromatographic separation on silica gel, this compound was obtained in a 40% yield. Compound **105** was characterized by 1H NMR and 2D-COSY data. The 1H NMR shows the aromatic nature of the carbocyclic ring where the three aromatic protons of C-5, C-4 and C-3 at 7.37, 6.42 and 6.09 ppm appear as a doublet, a doublet of doublets and a doublet respectively. The phenolic proton is observed as a doublet at 6.76 ppm. The $-CH_3$ and $N=CH$ proton chemical shifts come as a doublet and a quartet at 1.66 and 5.55 ppm respectively and they are coupled to each other in the 2D-COSY. COSY shows the aromatic protons are coupled to each other. The proton at 7.37 ppm for C-5 is coupled to a proton at 6.42 ppm for C-4 proton which in turn is coupled to a C-3 proton at 6.09 ppm. The phenolic proton at 6.75 ppm is weakly coupled to C-3 proton.

Deuteration of anionic complex **104b'** with D^+ formed a deuterated ring opened complex (**105'**). The two peaks which were due to OH at 6.76(d) and $N=CH$ at 5.55 (q, $J=6$ Hz) ppm of complex **105** are no longer observed in the 1H NMR of **105'** and the $-CH_3$ resonance has become a singlet. The resonances of all the other protons of the ring are compatible with those of undeuterated form of **105'** with same intensities and multiplicities. This labeled hydride studies demonstrates that two deuterium atoms have been incorporated in the cluster to yield the deuterated form of **105**, and confirms the structure **105** assigned on the basis of 1H NMR and 2D-COSY data. To further confirm this structure we are awaiting for a solid state structure.

Treatment of electron deficient complex of 2-methylbenzoxazole, **38** with 2 equivalents of hydride and quenching the resulting anion with two equivalents of acid gave a σ - π vinyl complex of a keto alcohol type $\text{Os}_3(\text{CO})_9(\mu_3\text{-}\eta^3\text{-C}_6\text{H}_3\text{O})(1\text{-NHC}_2\text{H}_5)(5\text{-OH})(\mu\text{-H})$ (**106** (Equation 4.7) by breaking the carbon oxygen bond. A possible mechanism for this transformation is shown in scheme 4.8.

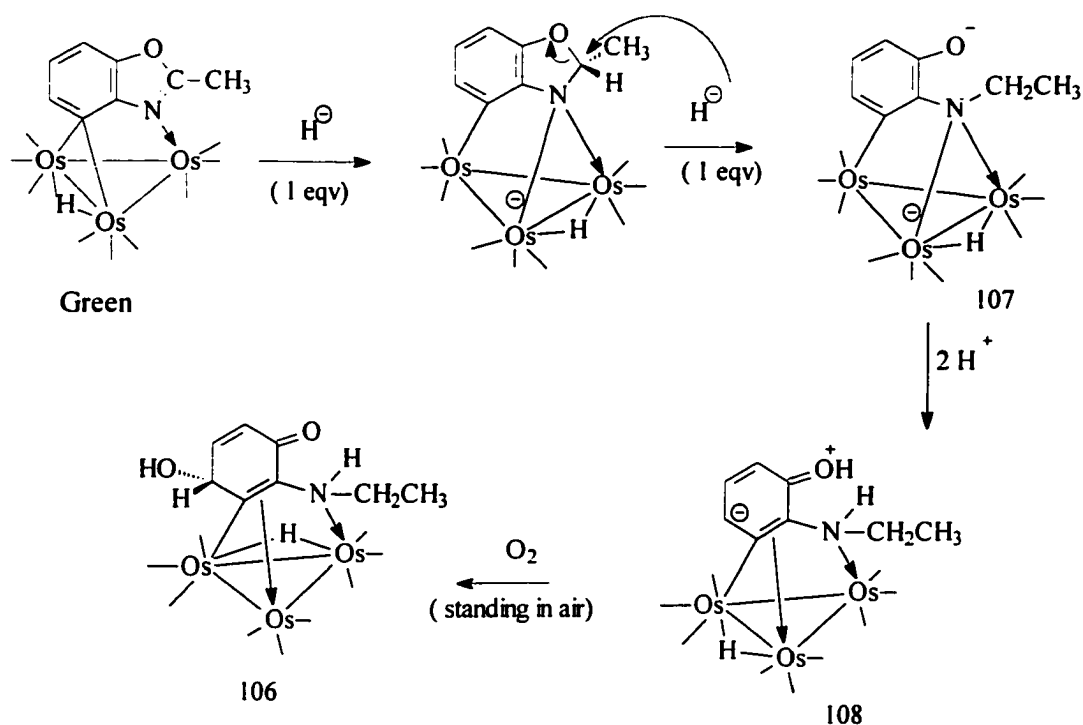


Hydride first attacks at the 2-position of the heterocyclic ring which is followed by second hydride attack at the same atom to open the ring by breaking the carbon oxygen bond and form a dianionic complex (**107**). One negative charge of the dianion is apparently delocalized around the metal core and the other one is localized on the oxygen atom. While neutralization, this complex takes up two protons at the nitrogen and oxygen atoms to form complex (**108**) which during purification on the silica gel is oxidized in the air to give a σ - π vinyl complex **106**.

This compound was characterized by ^1H NMR, COSY, elemental analysis and a solid state structure after chromatographic separation on silica gel. In the ^1H NMR of **106**, NH is observed as a broad peak at 5.12 ppm and -OH is appeared as a doublet at 2.21 ppm which is coupled to a C(5) proton at 5.0 ppm in the 2D COSY. COSY also correlates a

triplet resonance of $-\text{CH}_3$ at 0.84 ppm to two separate multiplets at 2.50 and 2.38 ppm of $-\text{CH}_2-\text{CH}_3$. A doublet resonance of C-3 proton at 6.06 ppm is coupled to a doublet of doublets of C-4 proton at 6.83 ppm which in turn is coupled to a doublet of C-5-proton at 5.0 ppm.

Scheme 4.8



The solid state structure of **106** is shown in figure 4.5. Selected distances and bond angles are given in Table 4.2. The structure **106** consists of an isosceles triangle of osmium atoms with the most elongated metal-metal bond being between Os(2) and Os(3) (2.96Å). The hydride is slightly tucked below the plane of metal triangle. The calculated position for the hydride is confirmed by the position of carbonyl groups CO(21) and CO(31). The most interesting aspects of the structure is that C(5)-C(6) bond

length(1.53(Å)) is in the single bond range and C(3)-C(4) (1.33(Å)) and C(2)-O(1) (1.22(Å)) is in the double bond range. The C(6)-C(1) (1.44(Å)) is somewhat lengthened as a result of σ - π interaction with Os(1) and Os(3). All the C(1)-N(1) (1.48 Å), C(7)-N(1) (1.50(Å)), C(7)-C(8) (1.50(Å)) and C(5)-O(2) (1.44(Å)) bond lengths fall in the single bond range. The assignment of σ interaction between Os(3)-C(6) (2.08(Å)) and π interaction between C(6)-Os(1) 2.21(2.21(5)) and C(1)-Os(1) 2.25(Å) is consistent with previous studies of σ - π interactions on osmium clusters.^{1,19}

Table 4.2 Selected Bond Distances (Å) and Angles (°) for 106^a

| Distances | | | |
|-------------------|-----------|-----------------|-----------------------|
| Os(1)-Os(2) | 2.81(3) | C(7)-C(8) | 1.50(7) |
| Os(1)-Os(3) | 2.80(3) | C(6)-C(7) | 1.39(5) |
| Os(2)-Os(3) | 2.96(3) | C(3)-C(4) | 1.33(8) |
| Os(2)-N(1) | 2.19(4) | C(5)-C(6) | 1.53(6) |
| Os(3)-C(6) | 2.08(4) | C(1)-Os(1) | 2.25(5) |
| C(6)-C(1) | 1.44(7) | C(2)-O(1) | 1.22(6) |
| N(1)-C(1) | 1.48(6) | Os-CO | 1.93(2) ^b |
| C(5)-O(2) | 1.44(6) | C-O | 1.10(3) ^b |
| C(7)-N(1) | 1.50(7) | Os(1)-C(6) | 2.21(5) |
| Angles | | | |
| Os(2)-Os(1)-Os(3) | 63.24(7) | N(1)-C(1)-Os(1) | 107.1(3) |
| Os(1)-Os(2)-Os(3) | 57.97(6) | C(7)-N(1)-Os(2) | 120(3) |
| Os(2)-Os(3)-Os(1) | 58.31(7) | C(1)-C(6)-Os(3) | 122.7(3) |
| Os(3)-C(6)-Os(1) | 81.41(16) | Os-C-O | 173.1(2) ^b |

^a numbers in parentheses are estimated standard deviations.

^b Average values.

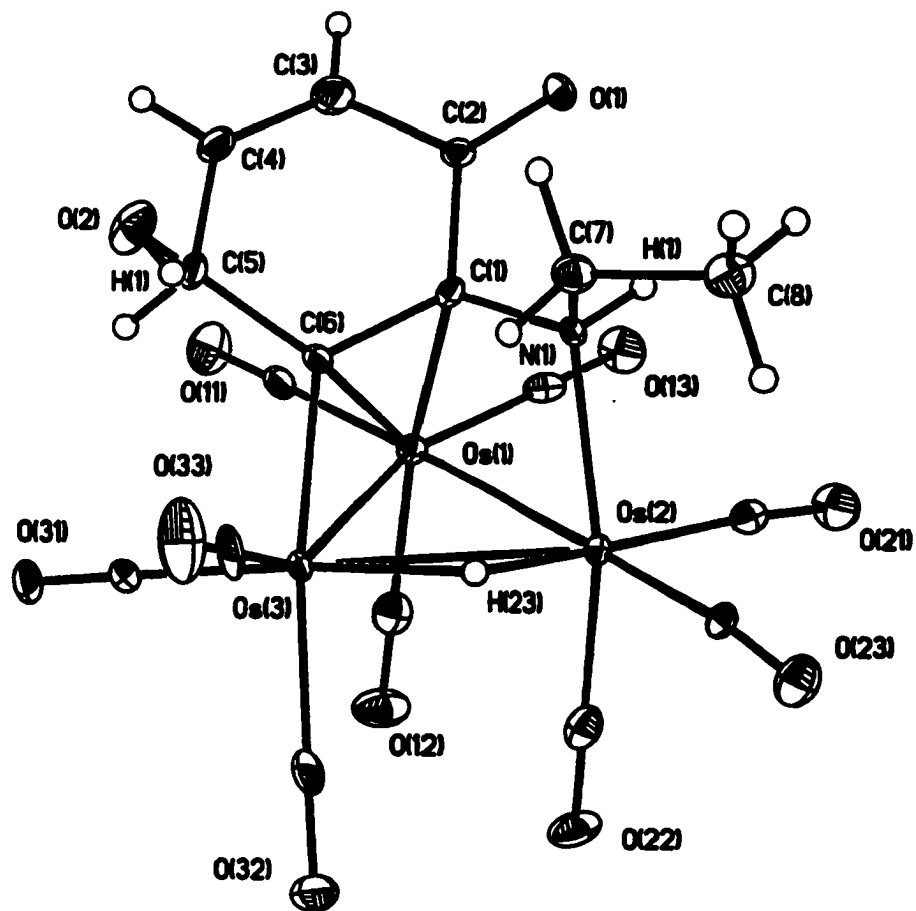


Figure 4.5 Solid state structure of $\text{Os}_3(\text{CO})_9(\mu_3\text{-}\eta^3\text{-C}_6\text{H}_3\text{O})(1\text{-NHC}_2\text{H}_5)(5\text{-OH})(\mu\text{-H})$ (106)

4.3 Conclusions

$\mu_3\text{-}\eta^2$ -Electron deficient complexes of benzoheterocycles with an alkyl group at the C(2) (of benzothiazole, benzimidazole, benzotriazole complexes) or C(3) (of quinoxaline complex) position of the heterocyclic ring except for 2-methylbenzoxazole undergo regioselective nucleophilic addition reactions at the carbocyclic ring to form $\sigma\text{-}\pi$ vinyl complexes. For 2-methylbenzoxazole nucleophilic addition occurs at the 2-position of the heterocyclic ring to give a ring opened $\sigma\text{-}\pi$ vinyl complex. 2-Methylbenzimidazole undergoes hydride attack at the carbocyclic ring, it does not form a $\sigma\text{-}\pi$ vinyl complex. Rather the anionic complex, resulted from hydride attack at the carbocyclic ring, rearomatizes back to the green starting material.

Electron deficient benzoheterocycle complexes without an alkyl group undergo hydride (H^-) attack at the C(2) position of the heterocyclic ring followed by protonation at the metal core to form dihydride complexes.

4.4 Experimental Section

Materials and General Considerations

All reactions were performed under a dry nitrogen or argon atmosphere in a two neck flask fitted with a vacuum line or in a M-Braun (manual MB-150-M) dry box. The flask was flamed dried under vacuum for every reaction. Dichloromethane was distilled

from CaH_2 and trifluoroacetic acid was distilled over phosphorus pentoxide prior use. Trifluoroacetic-d, lithium triethylborohydride, lithium triethylborodeuteride, dichloromethane- d_2 were purchased from Aldrich Chemical Co. and used as received. Electron deficient benzoheterocycles were synthesized according to the procedures outlined in chapter 2. Crystals for solid state structure determination were grown from hexane and methylene chloride at -10°C . Thin-layer chromatography was performed on 20 x 40 cm glass plates using a 2 mm layer of silica gel PF-254 (E & M science). Two or three elutions were necessary to obtain adequate resolution of the bands. NMR solvents were stored over molecular sieves (Mallincrodt 4Å). Reactions involving deuterated compounds were done in a M-Braun manual MB-150-M dry box or in a 5 mm sealed NMR tube. The tube was vacuum dried and filled with argon before use. Infrared spectra were recorded on a Thermo-Nicolet 633 FT IR Spectrometers and NMR spectra were done on a Varian 400 MHz Unity Plus NMR. Schwarzkopf Microanalytical Laboratories, Woodside, New York, performed elemental analyses.

Reactions of $\text{Os}_3(\text{CO})_9(\mu_3\text{-}\eta^2\text{-benzoheterocycle-H})(\mu\text{-H})$ (29, 33 and 40) with LiEt_3BH and CF_3COOH

Dark green crystals of **29** (100 mg, 0.99 mmol) or **33** (100 mg, 0.106 mmol) or **40** (100 mg, 0.104 mmol) were dissolved in 25 mL of CH_2Cl_2 in a 50 mL two-necked round bottom flask and fitted with a gas inlet tube evacuated and filled with argon. A 1.0 M solution of LiEt_3BH (105 μL , 0.105 mmol) in THF was then added dropwise to the cluster solution, and a color change was observed from green to brown for **29**, green to yellow for **33** and **40**. The solution was then neutralized with CF_3COOH (8.1 μL , 0.105

mmol). A color change was again observed from brown to yellow for **29**, yellow to orange for **33** and **40**. The solution was removed from the vacuum line or drybox, and the solvent was removed in *vacuo*. The residue was then purified by TLC on silica gel. Elution with hexane/CH₂Cl₂ (3:1) gave the expected complex **81**, **91** and **95** in 78%, 75% and 79% yields.

Reactions of Os₃(CO)₉(μ₃-η²-Quinoxaline(or 3-Methylquinoxaline)-H)(μ-H) (43** or **66**) with LiEt₃BH and CF₃COOH**

Green crystals of **43** (100 mg, 0.105 mmol) or **66** (100 mg, 0.10mmol) were dissolved in 25 mL of CH₂Cl₂ in a 50 mL two-necked round bottom flask and fitted with a gas inlet tube evacuated and filled with argon. A 1.0 M solution of LiEt₃BH (105 μL, 0.105 mmol) in THF was added dropwise to the cluster solution, and a color change was observed from green to amber. The solution was then neutralized with CF₃COOH (8.1 μL, 0.105 mmol) and the color of the solution changed from amber to red. The solution was rotary evaporated and the residue was taken up in CH₂Cl₂ and purified by TLC on silica gel. Elution with hexane /CH₂Cl₂ (3:2) gave three bands. The top band was identified as the starting material (**43**). The middle band afforded **84** in a 7% yield and the slowest moving band afforded **87** in a 28% yield. For 2-methylquinoxaline complex (**66**) only one yellow orange band was found, giving compound **90** in a 68% yield.

Reactions of Os₃(CO)₉(μ₃-η²-Quinoxaline-H)(μ-H) (43**) with LiEt₃BD and CF₃COOD**

Green crystals of **43** (50 mg, 0.052 mmol) were dissolved in 0.6 mL of CD_2Cl_2 in a sealed 5 mm NMR tube and fitted with a gas inlet tube evacuated and filled with argon. A 1.0 M solution of LiEt_3BD (52 μL , 0.052 mmol) in THF was added dropwise to the cluster solution, and a color change was observed from green to amber. The solution was checked by NMR and was then neutralized with CF_3COOD (4.05 μL , 0.053 mmol). A color change was then observed from amber to red. The solution was again checked by NMR and the solvent was finally removed in *vacuo*. The residue was then purified by TLC on silica gel. Elution with hexane/ CH_2Cl_2 (3:2) gave two resolved bands for electron deficient quinoxaline complex. The faster moving band afforded **84'** in 8% yield and the slower moving band afforded **87'** in a 25% yield.

Reactions of $\text{Os}_3(\text{CO})_9(\mu_3\text{-}\eta^2\text{-2-Methyl (or 2,3-Dimethylbenzimidazole)-H})(\mu\text{-H})$ (32** or **71**) with LiEt_3BH and CF_3COOH**

Green crystals of **32** (100 mg, 0.104 mmol) or **71** (100 mg, 0.101 mmol) were dissolved in 25 mL of CH_2Cl_2 in a 50 mL two-necked round bottom flask and fitted with a gas inlet tube evacuated and filled with argon. A 1.0 M solution of LiEt_3BH (105 μL , 0.105 mmol) in THF was added dropwise to the cluster solution, and a color change was observed from green to bluish for **32** and green to brown for **71**. The solution was then neutralized with CF_3COOH (8.1 μL , 0.105 mmol). A color change was then observed from bluish to green for **32** and brown to yellow for **71**. The solution was removed from the vacuum line, and the solvent was removed in *vacuo*. The residue was then purified by TLC on silica gel. Elution with hexane/ CH_2Cl_2 (3:2) gave green starting material for **32** in a 80% yield and a $\sigma\text{-}\pi$ vinyl complex (**94**) for **71** with a reasonable yield (66%).

Reactions of $\text{Os}_3(\text{CO})_9(\mu_3\text{-}\eta^2\text{-2-Methyl (or 2, 3-Dimethyl)benzimidazole-H})(\mu\text{-H})$ (32** or **71**) with LiEt_3BD and CF_3COOD**

Green crystals of **32** (50 mg, 0.052 mmol) or **71** (50 mg, 0.050 mmol) were dissolved in 0.6 mL of CD_2Cl_2 in a sealed 5 mm NMR tube and fitted with a gas inlet tube evacuated and filled with argon. A 1.0 M solution of LiEt_3BD (53 μL , 0.053 mmol) in THF was added dropwise to the cluster solution, and a color change was observed from green to bluish for **32** and green to brown for **71**. The solution was checked by NMR and was then neutralized with CF_3COOD (4.05 μL , 0.053 mmol). At this stage color of the solution changed from bluish to green for **32** and from brown to yellow for **71**. The reaction mixture was again checked by NMR and the solvent was finally removed in *vacuo*. The residue was then chromatographed by TLC on silica gel. Elution with hexane/ CH_2Cl_2 (3:2) gave green starting material for **32** in a 79% yield and a $\sigma\text{-}\pi$ vinyl complex, (**94'**) with a 61% yield for **71**.

Reactions of $\text{Os}_3(\text{CO})_9(\mu_3\text{-}\eta^2\text{-C}_7\text{H}_3(2\text{-R})\text{NX})(\mu\text{-H})$; (R=H, X=O, **37; R=CH₃, X=O, **38**; R=H, X=S, **39**) with LiEt_3BH and CF_3COOH**

Dark green crystals of **37** (100 mg, 0.101 mmol) or **38** (100 mg, 0.103 mmol) or **39** (100 mg, 0.104 mmol) were dissolved in 25 mL of CH_2Cl_2 in a 50 mL two-necked round bottom flask and fitted with a gas inlet tube evacuated and filled with argon. A 1.0 M solution of LiEt_3BH (105 μL , 0.105 mmol) in THF was then added dropwise to the cluster solution, and a color change was observed from green to orange for all of these clusters. The solution was then neutralized with CF_3COOH (~8.1 μL , 0.105 mmol). A color

change was observed from orange to yellow. The solution was removed from the vacuum line or dry box, and the solvent was removed in *vacuo*. The residue was chromatographed by TLC on silica gel. Elution with hexane/CH₂Cl₂ (3:1) gave the complex **102** for **37**, **105** for **38** and **93** for **39** in 41%, 40% and 79% yields respectively.

For reaction of complex **38** with 2 equivalent of H⁻/H⁺ the same procedure as described above for 1 equivalent was used and the compound **106** was isolated by elution with hexane and CH₂Cl₂ (3:2) on TLC plates. The product was obtained in a moderate yield, 51%.

Reactions of complex **38** with the labeled-hydride and proton were done in a sealed 5mm NMR tube filled with argon by the same procedure as mentioned for complexes **32** and **71**. Complex **105'** was obtained in a 41% yield when treated with 1 equivalent of D⁻/D⁺.

Evaluation of Equilibrium Constant (K_{eq}) for Complexes **98 and **99**, and **102** and **103**.**

Solutions of **98** and **102** (30mg, ~0.03 mmol) in 0.6 mL of C₆D₅CD₃ were inserted in two separate 5 mm sealed NMR tubes and heated at 90°C until an equilibrium was reached. The solutions were checked by NMR every two hours. When the equilibrium was reached, K_{eq} was calculated by the ratio of the integration of the hydride peaks of the two compounds in equilibrium.

Kinetics of Conversions of **98 to **99** and **102** to **103**.**

Solution of **98** or **102** (0.02 mmol) in 0.6 mL of CD₆CD₃ was inserted into a sealed 5 mm NMR tube. The solution was heated to 90°C and a ¹H NMR spectrum was taken

every 1 h for **98**, and every ½ h for **102** for 15 h. The rate constants for the conversions of **98** to **99** and **102** to **103** were evaluated by measuring the relative intensities of each isomer, and plotting these values against time [$\ln(C)$ versus t] using equation $\ln(C) = \ln(C_0) - kt$. The errors reported are $\pm 10\%$ on the basis of the expected error in relative integrated intensities for the NMR technique ($\pm 5\%$).

Analytical and Spectroscopic Data of Complexes **80** through **106**

Compound **81**: Yield for **81**: 78%. Anal Calcd. for $C_{22}H_{11}NO_9Os_3$: C, 26.32; H, 1.10; N, 1.40%. Found: C, 26.40; H, 1.16; N, 1.19%.

IR (ν CO) in CH_2Cl_2 : 2078 m, 2046 s, 2023 s, 1991 m, br, 1969 w, br, cm^{-1} .

1H -NMR of **81** at 400 MHz in $CDCl_3$: δ 9.27(s, H(2)), 7.84(dd, H(9)), 7.76(dd, 2H(10 and 12)), 7.51(d of t, H(11)), 4.26(m, H(7)), 2.94(m, CH_2 (5)), 2.30(m, CH_2 (6)) and – 17.07(s, hydride).

1H NMR of **80**: δ 8.27 (s, H(2)), 7.35(dd, H(9)), 7.28(dd, 2H(10 and 12)), 7.19(d of t H(11)), 5.85(d of t, $J = 9.3$ and 0.8 Hz, H(7)), 4.10 (d of t, $J = 9.3$ and 3.2 Hz, H(6)), 3.86 (s, br, CH_2 (5)) and –14.10 (s, hydride).

1H NMR of **83** in CD_2Cl_2 : δ 7.12 (d, $J=3.2$ Hz, H(2)), 6.75 (d, $J= 3.4$ Hz, H(3)), 6.2 (d of t, $J= 9.3, 0.9$ Hz, H(7)), 4.0 (d of t, $J= 9.3, 3.2$ Hz, H(6)), 3.88(br, 2H(5)) and –13.01 (s, hydride).

^1H NMR of **83'** in CD_2Cl_2 : δ 7.12 (d, $J=3.2$ Hz, H(2)), 6.75 (d, $J= 3.4$ Hz, H(3)), 6.2 (d, H(7)), 4.0 (t, H(6)), 3.88 (br, H(5)) and -13.01 (s, hydride).

Compound **84**: Yield for **84**: 7%. IR (ν CO) in CH_2Cl_2 : 2076 m, 2048 s, 2023 s, 1990 m, br, 1965 s, br cm^{-1} .

^1H NMR of **84** in CDCl_3 : δ 8.34 (d, $J=3.2$ Hz, H(2)), 8.14 (d, $J= 3.4$ Hz, H(3)), 4.10 (m, H(7)), 2.96 (m, CH(5)), 2.76 (m, CH(5)), 2.42 (m, CH(6)), 2.30 (m, CH(6)) and -16.83 (s, hydride).

^1H NMR of **84'** in CD_2Cl_2 : δ 8.37 (d, $J=3.2$ Hz, H(2)), 8.16 (d, $J= 3.4$ Hz, H(3)), 4.12 (d, H(7)), 2.85 (d, H(6)), 2.66 (d, H(5)) and -16.79 (s, hydride).

^1H NMR of **82** in CD_2Cl_2 : δ 6.90 (d of t, $J= 8.1, 0.8$ Hz, H(7)), 6.88 (d of t, $J= 8.2, 3.2$ Hz, H(3)), 6.58 (d of t, $J= 8.1, 0.8$ Hz, H(5)), 5.33 (d of t, $J= 8.1, 0.8$ Hz, H(6)), 4.81 (br, 2H(2)) and -12.81 (s, hydride).

^1H NMR of **82'** in CD_2Cl_2 : δ 6.90 (d, H(7)), 6.88 (d, $J= 3.6$ Hz, H(3)), 6.58 (d, H(5)), 5.33 (t, H(6)), 4.78 (br, H(2)) and -12.81 (s, hydride).

^1H NMR of **85** in CD_2Cl_2 : δ 7.48 (m, H(3)), 7.38 (dd, H(7)), 7.16 (dd, H(5)), 6.55 (d of t, H(6)), 6.47 (m, 2H(2)) 5.50 (br, NH) and -13.31 (s, hydride).

^1H NMR of **85'** in CD_2Cl_2 : δ 7.49 (d, H(3)), 7.38 (d, H(7)), 7.16 (d, H(5)), 6.55 (t, H(6)), 6.46 (d, H(2)) and -13.31 (s, hydride).

Compound **87**: Yield for **87**: 28%. Anal Calcd. for $\text{C}_{17}\text{H}_9\text{N}_2\text{O}_{10}\text{Os}_3$: C, 21.01; H, 0.93; N, 2.88%. Found: C, 21.14; H, 1.00; N, 2.79%.

IR (ν CO) in CH_2Cl_2 : 2073, m; 2053 s, 2027 s, 1998 s, 1984 m and 1951 w, br cm^{-1} .

^1H NMR of **87** in CDCl_3 : δ 6.30 (d, H(7)), 6.22 (d, H(5)), 5.41(dd, H(6)), 3.59 (br, NH(4)), 3.66(m, CH(2)), 3.52 (m, CH(2)), 2.96(br, OH), 2.97 (m, CH(3)), -12.87 (d, $J=2$ Hz, hydride) and -13.71 (d, $J=2$ Hz, hydride).

^1H NMR of **87'** in CDCl_3 : δ 6.30 (d, H(7)), 6.22 (d, H(5)), 5.41(t, H(5)), 3.66(m, CH(2)), 3.52 (m, CH(2)), 2.96(br, OH), 2.97 (m, CH(3)), -12.87 (d, $J=2$ Hz, hydride) and -13.71 (d, $J=2$ Hz, hydride).

^1H NMR of **88** in CD_2Cl_2 : δ 6.80 (dd, H(7)), 6.51 (dd, H(5)), 5.33 (d of t, H(6)), 4.58(br, 2H(2)), 1.80 (s, $-\text{CH}_3$) and -12.91 (s, hydride).

^1H NMR of **89** in CD_2Cl_2 : δ 8.29 (s, H(2)), 6.29 (d of t, $J=9.4$ and 0.9 Hz, H(7)), 4.30 (d of t, $J=9.4$, 3.2 Hz, H(6)), 3.94(br, 2H(5)) 2.48 (s, $-\text{CH}_3$) and -13.84 (s, hydride).

Compound **90**: Yield for **90**: 68%. Anal Calcd. for $\text{C}_{18}\text{H}_{10}\text{N}_2\text{O}_9\text{Os}_3$: C, 22.31; H, 1.03; N, 2.89%. Found: C, 22.63; H, 0.93; N, 2.29%.

IR (ν CO) in CH_2Cl_2 : 2081 m, 2051 s, 2027 s, 1993 m, br, 1970 w, br cm^{-1} .

^1H NMR of **90** in CDCl_3 : δ 8.23 (s, H(2)), 4.18 (m, H(7)), 2.79 (m, 2H(5)), 2.38(m, 2H(6)), 2.38 (s, $-\text{CH}_3$) and -16.81 (s, hydride).

Compound **91**: Yield for **91**: 75%. Anal Calcd. for $\text{C}_{16}\text{H}_9\text{N}_3\text{O}_9\text{Os}_3$: C, 20.06; H, 0.94; N, 4.39%. Found: C, 20.35; H, 0.72; N, 4.22%.

IR (ν CO) in CH_2Cl_2 : 2096 w, 2080 m, 2071 m, 2050 s, 2023 m, 1997 m, br, 1970 w, br, cm^{-1} . ^1H NMR of **91** in CDCl_3 : δ 4.88(m, H(6)), 4.03 (s, $-\text{CH}_3$), 2.75 (m, 2H(4)), 2.70(m, 2H(5)) and -16.14 (s, hydride).

^1H NMR of **92** in CD_2Cl_2 : δ 8.23 (br, NH), 7.72 (d, $J=7.2$ Hz, H(6)), 6.60 (t, $J=8.0$ Hz, H(5)), 2.50(s, CH_3) and -12.0 (s, hydride) ppm. $\text{CH}_2(4)$ resonance was obscure by THF.

^1H NMR of **92'** in CD_2Cl_2 : δ 8.23 (br, NH), 7.72 (d, $J=7.2$ Hz, H(6)), 6.64 (t, $J=8.0$ Hz, H(5)), 2.50(s, CH_3) and -12.0 (s, hydride) ppm. CHD(4) resonance was obscure by THF.

^1H NMR of **32'** in CD_2Cl_2 : δ 8.17 (d, H(6)), 8.14 (d, H(4)), 6.98 (t, H(5)), 2.61(s, CH_3) and -11.81 (s, hydride) ppm.

^1H NMR of **93** in CD_2Cl_2 : δ 6.14 (d of t, $J=9.2, 0.8$ Hz, H(6)), 4.56 (m, H(5)), 3.37 (br, $\text{CH}_2(4)$), 3.37 (s, N- CH_3) 2.18(s, C- CH_3) and -14.79 (s, hydride) ppm.

^1H NMR of **93'** in CD_2Cl_2 : δ 6.14 (dd, H(6)), 4.56 (dd, H(5)), 3.37 (br, CHD(4)), 3.37 (s, N- CH_3) 2.18(s, C- CH_3) and -14.79 (s, hydride) ppm.

Compound **94**: Yield for **94**: 66%. Anal Calcd. for $\text{C}_{18}\text{H}_{12}\text{N}_2\text{O}_9\text{Os}_3$: C, 22.27; H, 1.24; N, 2.89%. Found: C, 22.25; H, 0.99; N, 2.86%.

IR (ν CO) in CH_2Cl_2 : 2075 m, 2046 s, 2025 s, 1996 m, br, 1969 w, br cm^{-1}

^1H NMR of **94** in CDCl_3 : δ 4.53 (dd, H(6)), 2.51 (m, 2H(4)), 2.48 (m, 2H(5)), 3.39 (s, N- CH_3) 2.30(s, C- CH_3) and -16.40 (s, hydride) ppm.

Compound **94'**: Anal Calcd. for $\text{C}_{18}\text{H}_{10}\text{D}_2\text{N}_2\text{O}_9\text{Os}_3$: C, 22.22; H, 1.00; N, 2.88%. Found: C, 22.08; H, 0.97; N, 2.82%.

^1H NMR of **94'** in CD_2Cl_2 : δ 4.63 (d, H(6)), 2.54 (br, H(4)), 2.51 (br, H(5)), 3.39 (s, N- CH_3) 2.30(s, C- CH_3) and -16.40 (s, hydride) ppm.

Compound 95: Yield for **95**: 74%. Anal Calcd. for $C_{17}H_9NSO_9Os_3$: C, 20.97; H, 0.92; N, 1.41%. Found: C, 21.13; H, 0.70; N, 1.10%.

IR (ν CO) in CH_2Cl_2 : 2077 m, 2047 s, 2021 s, 1989 s, br, 1971 w, br cm^{-1} .

1H NMR of **95** in $CDCl_3$: δ 4.46 (dd, H(6)), 2.65 (m, 2H(4)), 2.38 (m, H(5)), 2.62(s, - CH_3) and -16.93 (s, hydride) ppm.

1H NMR of **96** in CD_2Cl_2 : δ 6.84 (d, H(6)), 6.31 (d, H(4)), 5.25 (dd, H(5)), 5.06(br, 2H(2)), and -12.63 (s, hydride) ppm.

1H NMR of **97** in CD_2Cl_2 : δ 7.68 (dd, H(6)), 7.12 (br, NH), 6.80 (dd, H(4)), 6.36 (d of t, H(5)), 6.30 (d, br, 2H(2)), and -14.03 (s, hydride) ppm.

Compound 98: Yield for **98**: 79%. Anal Calcd. for $C_{16}H_7NSO_9Os_3$: C, 20.02; H, 0.73; N, 1.46%. Found: C, 19.99; H, 0.49; N, 1.03%.

IR (ν CO) in CH_2Cl_2 : 2083 s, 2051 s, 2026 w, 2008 w, br, 1994 w, br, cm^{-1}

1H NMR of **98** in $CDCl_3$ (at room temp): δ 7.21 (dd, H(6)), 6.62 (dd, H(4)), 6.56 (d of t, H(5)), 5.2-3.9 (br, 2H(2)), and -14.06 (s, hydride) ppm.

1H NMR of **98** in $CDCl_3$ (at $-45^\circ C$): δ 7.21 (dd, H(6)), 6.62 (dd, H(4)), 6.56 (d of t, H(5)), 5.05(d, $J = 12$ Hz, H(2)), 3.95 (d, $J = 12$ Hz, H(2)), -14.06 (s, $J = 2$ Hz, hydride) and -14.10 (s, $J = 2$ Hz, hydride) ppm.

Compound 99: IR (ν CO) in CH_2Cl_2 : 2082 s, 2050 s, 2023 w, 2005 w, br, 1993 w, br, 1976 w, br cm^{-1}

^1H NMR of **99** in CDCl_3 : δ 6.88 (dd, H(6)), 6.34 (dd, H(4)), 5.45 (d of t, H(5)), 5.02(d, $J=12$ Hz, H(2)), 4.79(d, $J=12$ Hz, H(2)), -13.05 (d $J=2$ Hz, hydride) and -13.43 (d, $J=2$ Hz, hydride) ppm.

Compound **102**: Yield for **102**: 41%. IR (ν CO) in CH_2Cl_2 : 2078, m, 2051 s, 2024 w, br, 1992 w, br, 1967 w, br cm^{-1} . ^1H NMR of **102** in CDCl_3 (at room temp): δ 6.96 (d, H(6)), 6.28 (d, H(4)), 6.53 (t, H(5)), 5.17 (br, 2H(2)), and -13.95 (s, hydride) ppm.

^1H NMR of **102** in CDCl_3 (at -45°C): δ 6.96 (d, H(6)), 6.28 (d, H(4)), 6.53 (t, H(5)), 5.04(d, $J=5$ Hz, H(2)), 5.28 (d, $J=5$ Hz, H(2)), -13.84 (s, hydride) and -14.07 (s, hydride) ppm.

Compound **103**: IR (ν CO) in CH_2Cl_2 : 2076 m, 2051 s, 2022 w, br, 1990 w, br, 1966 w, br, cm^{-1}

^1H NMR of **103** in CDCl_3 : δ 6.25 (d, H(6)), 6.14 (d, H(4)), 5.50 (t, H(5)), 5.47(d, $J=8$ Hz, H(2)), 5.30 (d, $J=5$ Hz, H(2)), -13.16 (d, $J=2$ Hz, hydride) and -13.22 (d, $J=2$ Hz, hydride) ppm.

^1H NMR of **104** in CD_2Cl_2 : δ 6.13 (d, H(6)), 6.0 (t, H(5)), 6.10(d, H(4)), 5.30 (q, H(2)), 1.29 (d, H(- CH_3)) and -12.50 (s, hydride).

^1H NMR of **104'** in CD_2Cl_2 : δ 6.13 (d, H(6)), 6.0 (t, H(5)), 6.10(d, H(4)), 1.29 (s, H(- CH_3)) and -12.50 (s, hydride).

Compound **105**: Yield for **105**: 40%. IR (ν CO) in CH_2Cl_2 : 2089 m, 2049 s, 2031w, br 2015 w, br, 1976 w cm^{-1} . IR (ν OH) in CH_2Cl_2 : 3155 cm^{-1} .

^1H NMR of **105** in CDCl_3 : δ 7.37 (d, J = 8.4 Hz, H(5)), 6.42 (t, J = 7.6 Hz, H(4)), 6.09(d, J = 6.8 Hz, H(3)), 6.76 (d, OH), 5.55 (q, J = 6 Hz, H(N=CH)), 1.66(d, J = 10 Hz, $-\text{CH}_3$) and -14.85 (s, hydride).

^1H NMR of **105'** in CDCl_3 : δ 7.37 (d, J = 8.4 Hz, H(5)), 6.43 (dd, J = 7.6 Hz, H(4)), 6.10(d, J = 6.8 Hz, H(3)), 1.66(s, $-\text{CH}_3$) and -14.86 (s, hydride).

Compound **106**: Yield for **106**: 51%. IR (ν CO) in CH_2Cl_2 : 2094 m, 2067 s, 2037w, br 2014 w, br, 1975 w cm^{-1} . ^1H NMR of **106** in CDCl_3 : δ 6.83 (dd, H(4)), 6.06(d, H(3)), 5.12 (br, NH), 5.00(t, H(5)), 2.50 (m, H(CH-CH $_3$)), 2.38 (m, H(CH-CH $_3$)), 2.21(d, J = 5.2 Hz, OH), 0.84(t, 3H($-\text{CH}_3$)) and -15.67 (s, hydride).

Chapter 5

Reactions of Electron Deficient Benzoheterocycles, $\text{Os}_3(\text{CO})_9(\mu_3\text{-}\eta^2\text{-benzoheterocycle-H})(\mu\text{-H})$ with Carbanions

A major goal of this thesis is to make novel benzoheterocycles with different functionalities by extending the nucleophilic addition chemistry observed for quinoline with carbon based nucleophiles to other heterocycles (and their substituted derivatives) that have been shown to adopt the $\mu_3\text{-}\eta^2$ -electron deficient bonding mode. The investigation of the reactivity of the electron deficient complexes with H^-/H^+ has laid the basic foundation for the studies of these complexes (29, 32-33, 37-40, 43, 66 and 71) with carbon based bulkier carbanions. We have found that with a small nucleophile such as hydride (H^-) the primary site of nucleophilic addition to complexes with an alkyl group at the heterocyclic ring is the 4-position of carbocyclic ring for benzothiazole, benzimidazole and benzotriazole (except benzoxazole where nucleophilic attack occurs at 2-position) or the 5-position for phenanthridine and 2-methylquinoxaline. For benzoheterocycle complexes without an alkyl group the primary site of nucleophilic attack is at the 2-position of the heterocyclic ring.

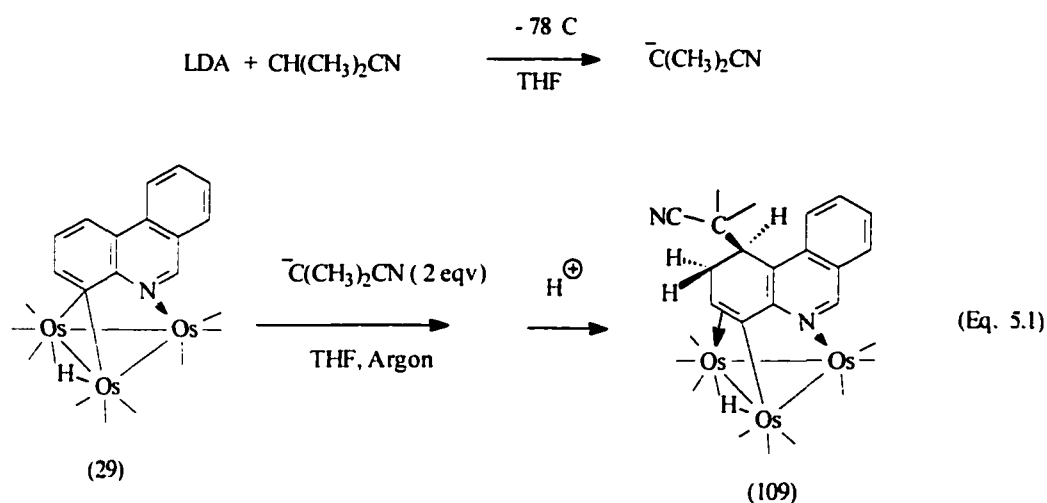
We discussed, in this chapter, the addition of carbon based nucleophiles to these benzoheterocycles (29, 32-33, 39-40, 43, 66 and 71) (Figure 4.1). Reactions of these electron deficient complexes with a bulkier carbanion such as iso-butyronitrile carbanion gives rise to nucleophilic addition products resulting from carbanion attack at

the 4- or 5-position of carbocyclic ring. Attack at the carbocyclic ring even prevails for benzothiazole with a bulkier carbanion owing to steric crowding at the 2-position of the heterocyclic ring. We have excluded 2-methylbenzoxazole and benzoxazole from our survey of electron deficient complexes with bulkier nucleophiles because these two complexes undergo ring opening reactions with harder nucleophile such as hydride (described in chapter 4). We have chosen iso-butyronitrile carbanion as a probe of nucleophilicity centered around 4- or 5- position of carbocyclic ring of these complexes because this carbanion was found to give good yields with the quinoline family.³

5.1 Results and Discussion

5.1.1 Reaction of Phenanthridine Complex, $\text{Os}_3(\text{CO})_9(\mu_3\text{-}\eta^2\text{-C}_{13}\text{H}_8\text{N})(\mu\text{-H})(\mathbf{29})$ with the Isobutyronitrile Carbanion.

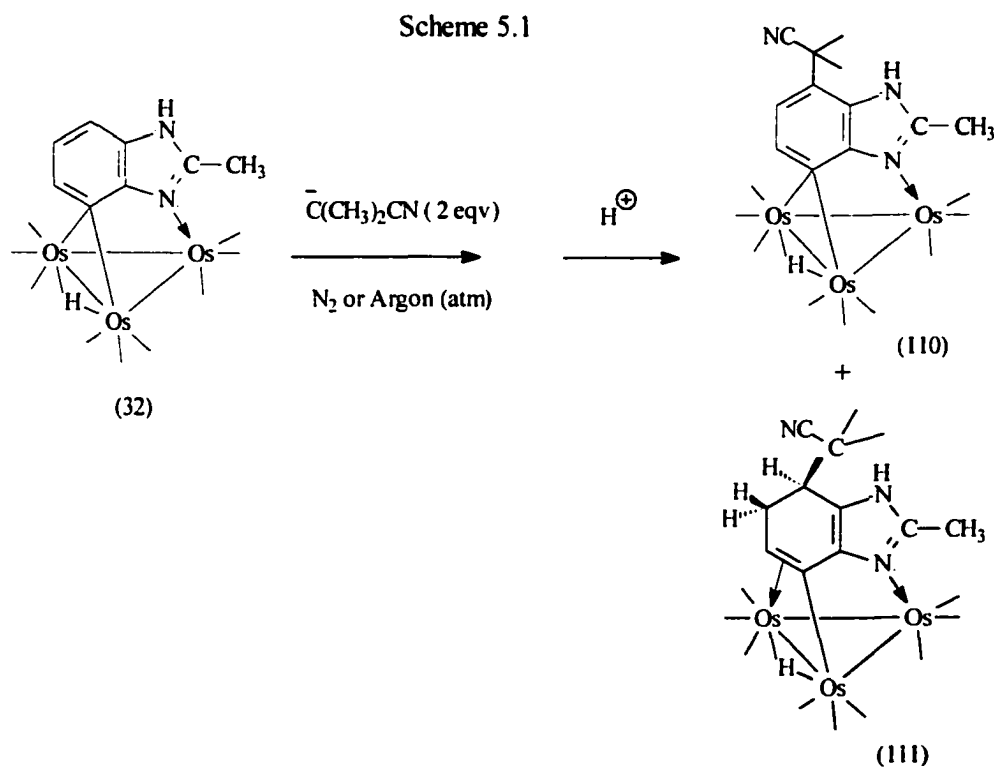
When compound **29** was reacted with a two-to-three fold excess of isobutyronitrile carbanion at -78°C , the dark green THF solution turned orange. After stirring and warming to 0°C the solution was cooled to -78°C and quenched with a slight excess (relative to the total carbanion added) of trifluoroacetic acid to give a light orange solution (Equation 5.1). After chromatographic purification, the nucleophilic addition product $[\text{Os}_3(\text{CO})_9(\mu_3\text{-}\eta^3\text{-C}_{13}\text{H}_9(5\text{-C}(\text{CH}_3)_2\text{CN})\text{N})(\mu\text{-H})](\mathbf{109})$ was isolated in a 79% yield. Compound (**109**) was characterized by IR, ^1H NMR and elemental analysis and by comparison of its spectral properties with similar $\sigma\text{-}\pi$ vinyl complexes of



quinoline obtained from both the H^-/H^+ and the carbon based nucleophilic addition reactions for which solid state structures are reported. In the ^1H NMR the chemical absorption peaks in the aliphatic region of carbocyclic ring shows the formation of a σ - π vinyl complex where the two protons at C-6 appear as two separate multiplets at 2.87 and 2.29 ppm and the other two protons at C-5 and C-7 come as a doublet and a quartet at 3.38 and 4.08 ppm respectively. The presence of the iso-butyronitrile group is vindicated by the appearance of two closely related singlets of relative intensity of 3 each at 1.49 and δ 1.45 ppm. The chemical absorptions obtained for all other protons of the aromatic region are consistent with the proposed structure (Equation 5.1). The hydride chemical shift comes at -17.14 ppm, a typical value for hydrides of σ - π vinyl complexes of benzoheterocycles.

5.1.2 Reaction of 2-methylbenzimidazole complex, $\text{Os}_3(\text{CO})_9(\mu_3\text{-}\eta^2\text{-C}_7\text{H}_4(2\text{-CH}_3)\text{N}_2)(\mu\text{-H})$ (32) with the Isobutyronitrile Carbanion.

The reaction of **32** with $\text{LiC}(\text{CH}_3)_2\text{CN}$ gave both rearomatized and unrearomatized ($\sigma\text{-}\pi$ vinyl) nucleophilic addition products, **110** and **111** (Scheme 5.1). Thus, when a two fold excess of carbanion was added to compound **32** at -78°C , the bright green solution turned orange immediately. After quenching with equivalent



amount (relative to carbanion added) of trifluoroacetic acid the solution changed back to green to give the rearomatized nucleophilic addition product, $\text{Os}_3(\text{CO})_9(\mu_3\text{-}\eta^2\text{-C}_7\text{H}_3(2\text{-$

$\text{CH}_3)(4\text{-C}(\text{CH}_3)_2\text{CN})\text{N}_2)(\mu\text{-H})$ (**110**) as a major compound. Rearomatization was also achieved by stirring the anionic mixture in air.

Rearomatized nucleophilic addition product was also obtained for **32** when it was reacted with H^-/H^+ (described in chapter 4). In this case one molecule of hydrogen was eliminated as H^+ was added to the anionic complex which gave rise to the green starting material **32** (Scheme 4.4). But with bulkier nucleophile elimination of one molecule of H_2 leaves the bulky group on the ligand while nucleophilic addition product is rearomatized to give compound **110**. This rearomatized green nucleophilic addition product (**110**) was purified by chromatographic separation and isolated in 72% yield.

Compound (**110**) was characterized by IR, ^1H NMR and elemental analysis. The ^1H NMR shows two protons in the carbocyclic region which come as two doublets at 8.16 and 6.82 ppm for C-6 and C-5 protons respectively. 2D-COSY experiment shows they are correlated to each other. The NH proton is observed as a broad singlet at 9.68 ppm and the methyl group of the heterocyclic ring is appeared as a sharp singlet at 2.76 ppm. The two methyl groups of isobutyronitrile side chain of carbocyclic ring are also observed as a sharp singlet at 1.81 ppm. The appearance of these two methyl groups as a singlet peak is expected due to the symmetric nature of $\mu_3\text{-}\eta^2$ -complexes. Solid state structures of $\mu_3\text{-}\eta^2$ -complexes (shown in chapter 2) show that they are all structurally symmetric. The hydride resonance is obtained as a singlet at -11.72 ppm which is in accordance with hydride chemical shifts for $\mu_3\text{-}\eta^2$ -complexes of benzoheterocycles.

During the purification of the reaction mixture on silica gel a yellow band in addition to a green band was also obtained. Separation of this band provided a $\sigma\text{-}\pi$ vinyl

nucleophilic addition product, $\text{Os}_3(\text{CO})_9(\mu_3\text{-}\eta^3\text{-C}_7\text{H}_5(2\text{-CH}_3)(4\text{-C}(\text{CH}_3)_2\text{CN})\text{N}_2)(\mu\text{-H})$ (**111**) as a minor compound. This compound was obtained in a 16% yield.

This product (**111**) was characterized by IR, ^1H NMR, elemental analysis and X-ray crystallography. ^1H NMR shows a pattern of chemical absorption peaks for the carbocyclic protons which is consistent with the formation of a $\sigma\text{-}\pi$ vinyl complex. Two separate multiplets are observed at 4.46 and 2.82 ppm for the C-6 vinyl and C-4 protons respectively. The two methylene protons at C-4 come as a multiplet in the region of 2.68-2.58 ppm. A broad singlet at 8.48 ppm and a sharp singlet at 2.39 ppm of relative intensity 1:3 can be assigned to the -NH and methyl side chain of the heterocyclic ring. The introduction of isobutyronitrile group is confirmed by the presence of two sharp singlets of relative intensity 3 each at 1.35 and 1.25 ppm.

A solid state structural investigation was also undertaken for this compound. The solid state structure is shown in Figure 5.1, selected distances and bond angles in Table 5.1. The structure consists of an approximately equilateral triangle of Os atoms with three approximately equal metal-metal bonds (Os(1)-Os(2) (2.88(4)Å), Os(1)-Os(3) (2.83(19)Å), Os(2)-Os(3) (2.85(4)Å)). The hydride was located using the program HYDEX.²⁴ The hydride is tucked below the plane of the metal triangle along the doubly bridged Os(1)-Os(3) edge. The N(1)-C(10) (1.30(3) Å), C(14)-C(15) (1.36(5)Å) and C(11)-C(16) (1.42(4)Å) bond lengths are in the range of double bond (1.32-1.41Å) and the rest other bonds, for example, C(13)-C(14) (1.62(6)Å), C(12)-C(13) (1.56(5)Å) and C(11)-C(12) (1.51(4)Å) can be considered single bonds. The assignment of a σ interaction between Os(1)-C(15) (2.07(4)Å) and a π interaction between Os(3)-

C(15)(2.28(4)Å) and Os(3)-C(14)(2.57(4)Å) is consistent with previous studies of the σ - π interaction on triosmium clusters.⁵²

Table 5.1 Selected Bond Distances (Å) and Angles (°) for 111^a

| Distances | | | |
|-------------------|-----------------------|--------------------|----------------------|
| Os(1)-Os(2) | 2.88(4) | C(14)-C(15) | 1.36(5) |
| Os(1)-Os(3) | 2.83(19) | C(13)-C(14) | 1.62(6) |
| Os(2)-Os(3) | 2.85(4) | C(12)-C(13) | 1.56(5) |
| Os(2)-N(1) | 2.22(2) | C(12)-C(11) | 1.51(4) |
| Os(3)-C(14) | 2.57(4) | C(16)-C(11) | 1.42(4) |
| Os(1)-C(15) | 2.07(4) | C(12)-C(18) | 1.50(5) |
| Os(3)-C(15) | 2.28(4) | C(10)-C(17) | 1.53(4) |
| C(10)-N(1) | 1.30(3) | C-O | 1.16(5) ^b |
| C(10)-N(2) | 1.36(3) | Os-CO ^b | 1.92(4) |
| C(16)-N(1) | 1.32(3) | C(11)-N(2) | 1.36(3) |
| Angles | | | |
| Os(1)-Os(2)-Os(3) | 59.32(4) | Os(1)-Os(2)-N(1) | 83.8(10) |
| Os(1)-Os(3)-Os(2) | 60.83(15) | C(13)-C(14)-C(15) | 128.0(4) |
| Os(2)-Os(1)-Os(3) | 59.85(15) | C(12)-C(13)-C(14) | 108.0(3) |
| Os(1)-C(15)-C(14) | 129.0(3) | C(11)-C(12)-C(18) | 115.0(3) |
| Os(3)-C(15)-C(14) | 86.0(3) | C(13)-C(12)-C(11) | 112.0(3) |
| Os(3)-C(14)-C(15) | 62.0(2) | C(10)-N(1)-C(16) | 112.0(2) |
| Os-C-O | 173.4(4) ^b | | |

^a numbers in parentheses are estimated standard deviations.

^b Average values.

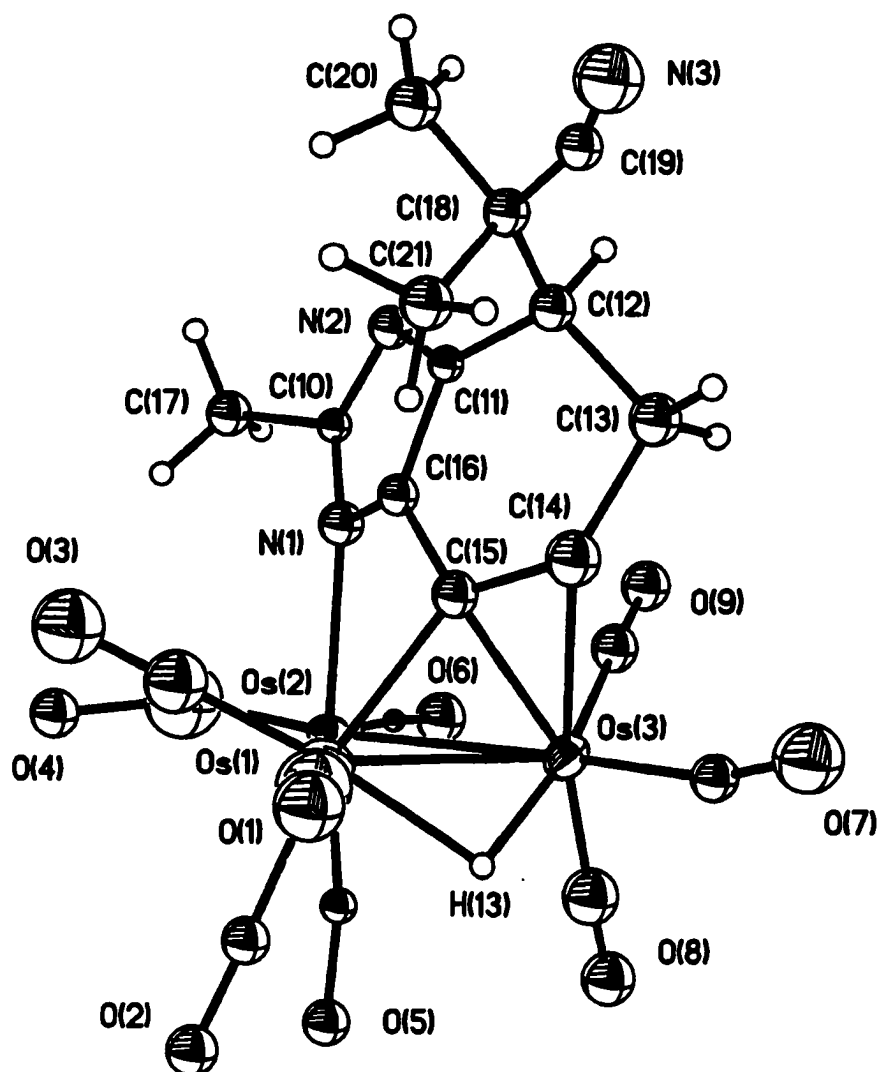
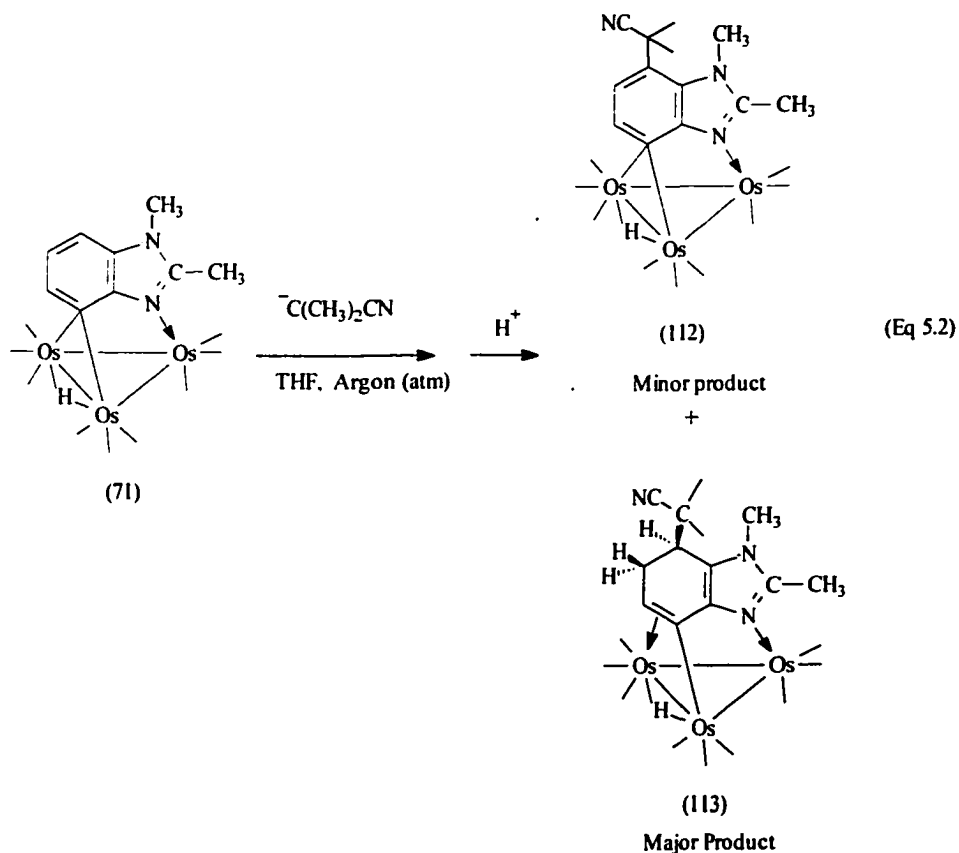


Figure 5.1 Solid state structure of $\text{Os}_3(\text{CO})_9(\mu_3\text{-}\eta^3\text{-C}_7\text{H}_5(2\text{-CH}_3)(4\text{-C}(\text{CH}_3)_2\text{CN})\text{N}_2)$

($\mu\text{-H}$) (111)

5.1.3 Reaction of 2,3-Dimethylbenzimidazole Complex, $\text{Os}_3(\text{CO})_9(\mu_3\text{-}\eta^2\text{-C}_7\text{H}_3(2\text{-CH}_3)(3\text{-CH}_3)\text{N}_2)(\mu\text{-H})$ (71) with the Isobutyronitrile Carbanion

When the amino hydrogen of 2-methylbenzimidazole complex was replaced by a relatively bulkier methyl group, the resulting 2,3-dimethylbenzimidazole complex (71) underwent nucleophilic reduction with H^-/H^+ across the C(4)-C(5) double bond to give a $\sigma\text{-}\pi$ vinyl complex (Scheme 4.5, chapter 4). On reaction with isobutyronitrile, 2,3-dimethylbenzimidazole complex (71) gives a mixture of both rearomatized and unrearomatized nucleophilic addition products (112 and 113) in 1:2 ratio (Equation 5.2). The formation of rearomatized product in this case may be due to the imposition of an



electron donating group on the carbocyclic ring which favors the elimination of the elements of hydrogen to form rearomatized nucleophilic addition product (**112**).

During the course of reaction the addition of a two-fold excess of carbanion to compound (**71**) at -78°C changed the green color of the solution first to amber, then orange. Quenching of the solution with trifluoroacetic acid and subsequent warming to 0°C turned the color to yellow which then changed to green standing in the air at room temperature. Chromatographic separation of the crude reaction mixture provided rearomatized nucleophilic addition product, $\text{Os}_3(\text{CO})_9(\mu_3\text{-}\eta^2\text{-C}_7\text{H}_2(2\text{-CH}_3)(3\text{-CH}_3)(4\text{-C}(\text{CH}_3)_2\text{CN})\text{N}_2)(\mu\text{-H})$ (**112**) in 27% yield along with un-rearomatized product, $\text{Os}_3(\text{CO})_9(\mu_3\text{-}\eta^3\text{-C}_7\text{H}_4(2\text{-CH}_3)(3\text{-CH}_3)(4\text{-C}(\text{CH}_3)_2\text{CN})\text{N}_2)(\mu\text{-H})$ (**113**) in 56% yield. These two compounds were characterized by IR, ^1H NMR and elemental analysis.

In the ^1H NMR of (**112**) the two doublets appeared in the aromatic region at 8.15 and 6.90 ppm can be fairly assigned to C-6 and C-5 protons of the heterocycle. The two methyl groups on nitrogen and carbon atoms in the heterocyclic ring are observed as two sharp singlets at 4.29 and 2.77 ppm respectively. The two methyl groups of isobutyronitrile side chain of carbocyclic ring are also observed as a sharp singlet at 1.89 ppm like that of compound (**110**) due to the symmetric nature of the $\mu_3\text{-}\eta^2$ complex. Hydride chemical shift is obtained at -11.71 ppm as a singlet.

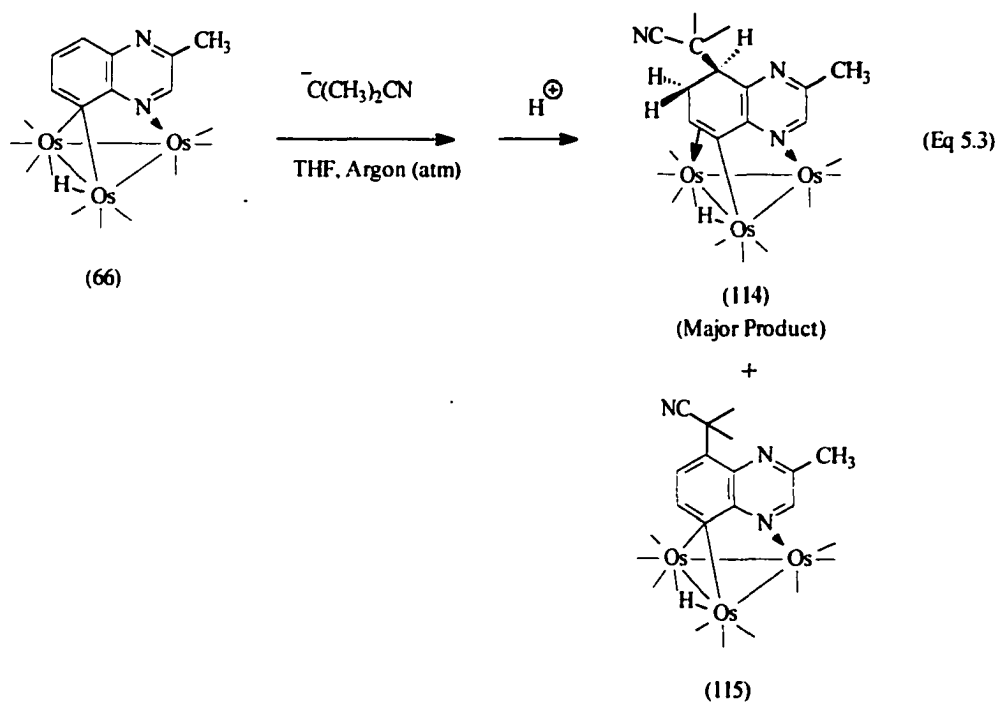
^1H NMR of (**113**) shows a similar pattern of resonances for the carbocyclic protons to those of other $\sigma\text{-}\pi$ vinyl complexes. The vinyl proton at C-6 comes as a doublet of doublets at 4.38 ppm. The C-4 proton and two methylene protons at C-5 also come as three separate doublet of doublets at 2.73, 2.68 and 2.55 ppm respectively. The two

sharp singlets at 3.50 and 2.36 ppm are attributable to two methyl groups on the nitrogen and carbon atoms of the heterocyclic ring. The two methyl groups of isobutyronitrile side chain are appeared as two sharp singlets at 1.37 and 1.29 ppm and the hydride chemical shift is obtained in the usual hydride field of σ - π vinyl complexes at -16.65 ppm.

5.1.4 Reaction of 2-Methylquinoxaline Complex, $\text{Os}_3(\text{CO})_9(\mu_3\text{-}\eta^2\text{-C}_8\text{H}_4(3\text{-CH}_3)\text{N}_2)$ ($\mu\text{-H}$) (66) with the Isobutyronitrile Carbanion.

Treatment of 2-methylquinoxaline complex (66) with a two-to-three fold excess of isobutyronitrile carbanion at -78°C followed by neutralization with trifluoroacetic acid provided a σ - π vinyl nucleophilic addition product, $\text{Os}_3(\text{CO})_9(\mu_3\text{-}\eta^3\text{-C}_8\text{H}_5(3\text{-CH}_3)(5\text{-C}(\text{CH}_3)_2\text{CN})\text{N}_2)(\mu\text{-H})$ (114) (Equation 5.3). After chromatographic separation this compound was isolated in a 62% yield. A trace amount of rearomatized product, $\text{Os}_3(\text{CO})_9(\mu_3\text{-}\eta^2\text{-C}_8\text{H}_3(3\text{-CH}_3)(5\text{-C}(\text{CH}_3)_2\text{CN})\text{N}_2)(\mu\text{-H})$ (115) was also obtained as a co-product as indicated from its ^1H NMR spectrum.

Compound (114) was characterized by IR, ^1H NMR and elemental analysis. ^1H NMR shows a series of multiplets for the carbocyclic protons. The multiplets at 4.06 and 2.74 ppm are due to C-7 and C-5 protons. The other two multiplets at 2.43 and 2.41 are for the C-6 methylene protons. The methyl group of the heterocyclic ring, C-2 proton and hydride are appeared as three singlets at 2.38, 8.34 and -16.88 ppm respectively.



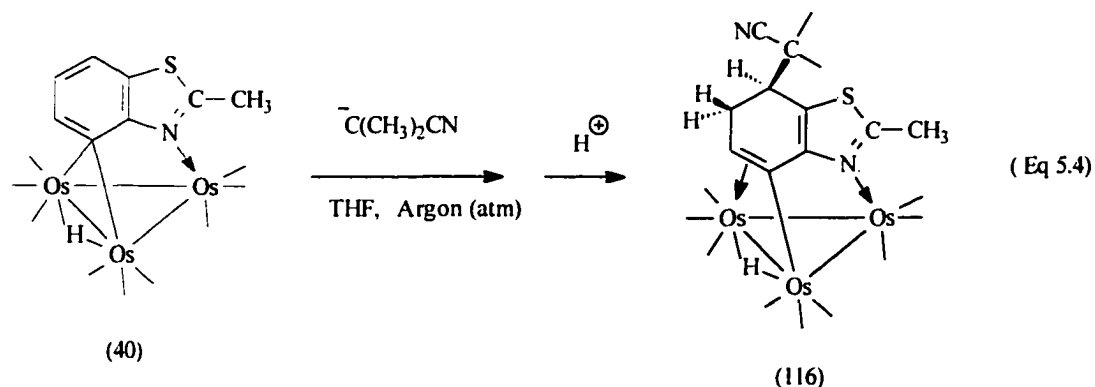
The two methyl groups of isobutyronitrile side chain are observed as two closely spaced singlets at 1.44 and 1.41 ppm.

^1H NMR of (115) shows a singlet and two doublets in the aromatic region at 9.06, 8.56 and 7.44 ppm attributable to C-2, C-7, C-6 protons respectively. Two sharp singlets of relative intensity 3 and 6 at 2.77 and 1.93 ppm can be assigned to the methyl groups of the heterocyclic ring and isobutyronitrile side chain respectively. Hydride is appeared at -12.32 ppm.

5.1.5 Reaction of 2-Methylbenzothiazole Complex, $\text{Os}_3(\text{CO})_9(\mu_3\text{-}\eta^2\text{-C}_7\text{H}_3(2\text{-CH}_3)\text{NS}) (\mu\text{-H})$ (40) with the Isobutyronitrile Carbanion.

The reaction of 2-methylbenzimidazole (40) with a two-to-three fold excess of carbanion followed by quenching with trifluoroacetic acid gave a nucleophilic addition

product, $\text{Os}_3(\text{CO})_9(\mu_3\text{-}\eta^3\text{-C}_7\text{H}_4(2\text{-CH}_3)(4\text{-C}(\text{CH}_3)_2\text{CN})\text{NS})(\mu\text{-H})$ (**116**) due to carbanion attack at 4-position of the carbocyclic ring (Equation 5.4). After chromatographic separation this compound was isolated in a 74% yield and characterized by IR, ^1H NMR and elemental analysis. In the ^1H NMR four separate multiplets are observed for the carbocyclic protons of the compound. The multiplets at 4.32, 2.83, 2.73 and 2.50 ppm can be fairly assigned to C-6, C-4 and C-5 protons. The methyl group of heterocyclic ring is appeared as a singlet at 2.67 ppm and the other two methyl groups of the isobutyronitrile side chain are also appeared as two closely spaced singlets at 1.36 and 1.34 ppm. The hydride chemical shift is obtained at -17.05, the typical high field region of hydride of $\sigma\text{-}\pi$ vinyl complexes.



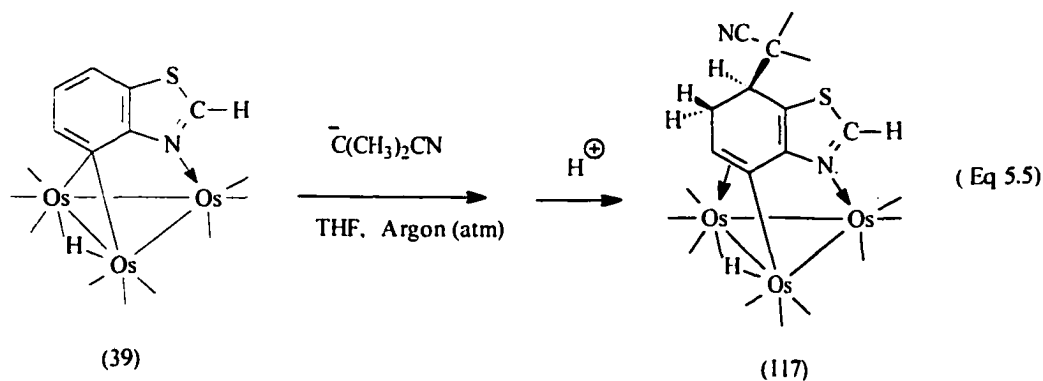
5.1.6 Reaction Benzothiazole Complex, $\text{Os}_3(\text{CO})_9(\mu_3\text{-}\eta^2\text{-C}_7\text{H}_4\text{NS})$

$(\mu\text{-H})$ (**39**) with the Isobutyronitrile Carbanion.

When benzothiazole complex (**39**) was treated with the less sterically demanding Et_3BH^- , the nucleophilic attack occurred at the C-2 position of the heterocyclic ring

(Scheme 4.6, chapter 4). Subsequent neutralization of the resulting anionic complex by trifluoroacetic acid yielded a dihydride complex.

With carbon based bulkier nucleophile benzothiazole undergoes nucleophilic attack at the 4-position of the carbocyclic ring. The C-2 atom of heterocyclic ring is not accessible for attack by bulkier nucleophile. Solid state structure of (117) reveals that C-2 position of the heterocycles is more sterically crowded by the metal carbonyl moiety. Thus, when compound 39 was reacted with a two-to-three fold excess of isobutyronitrile carbanion and quenched the resulting anion with trifluoroacetic acid a σ - π vinyl complex containing isobutyronitrile group at the 4-position was obtained. After chromatographic separation the nucleophilic addition product, $\text{Os}_3(\text{CO})_9(\mu_3\text{-}\eta^3\text{-C}_7\text{H}_5(4\text{-C}(\text{CH}_3)_2\text{CN})\text{NS})(\mu\text{-H})$ (117) was isolated in a 84% yield (Equation 5.5).



Compound (117) was characterized by IR, ^1H NMR and elemental analysis. In the ^1H NMR a pattern of chemical absorption peaks are observed for the carbocyclic protons similar to those of other σ - π complexes. The four multiplets at 4.45, 2.93, 2.83 and 2.49 are due to C-6, C-4 and C-5 protons. The C-2 atom of the heterocyclic ring

remains intact as evidenced from the spectroscopic data where C-2 proton is obtained as a singlet at 8.87 ppm. The two methyl groups of the isobutyronitrile side chain are appeared as two closely spaced singlets at 1.37 and 1.36 ppm and hydride is obtained at -16.93 ppm.

A solid state structural analysis was also carried out for this compound. The structure is shown in figure 5.2, selected distances and bond angles in table 5.2. The structure consists of a triangle of Os atoms with metal-metal bonds (Os(1)-Os(2) (2.80(5)Å), Os(1)-Os(3) (2.86(4)Å), Os(2)-Os(3)(2.91(5)Å). The hydride was located using the program HYDEX.²⁴ The hydride is tucked below the plane of the metal triangle along the doubly bridged Os(1)-Os(3) edge. The N(1)-C(1)(1.31(10)Å), C(5)-C(6)(1.40(11)Å) and C(2)-C(3)(1.36(4)Å) bond lengths are in the range of double bond (1.32-1.41Å) and the rest other bonds, for example, C(4)-C(5)(1.52(11)Å), C(3)-C(4)(1.56(10)Å) and C(2)-C(3)(1.51(10)Å) can be considered single bonds. The assignment of a σ interaction between Os(1)-C(6)(2.10(8)Å) and a π interaction between Os(3)-C(6)(2.24(7)Å) and Os(3)-C(5)(2.44(7)Å) is consistent with previous studies of σ - π interaction on triosmium clusters.⁵²

Table 5.2 Selected Bond Distances (Å) and Angles (°) for 117^a

| Distances | | | |
|-------------|----------|--------------------|-----------------------|
| Os(1)-Os(2) | 2.80(5) | C(5)-C(6) | 1.40(11) |
| Os(1)-Os(3) | 2.86(4) | C(4)-C(5) | 1.52(11) |
| Os(2)-Os(3) | 2.91(5) | C(3)-C(4) | 1.56(10) |
| Os(2)-N(1) | 2.16(6) | C(2)-C(3) | 1.51(10) |
| Os(3)-C(5) | 2.44(7) | C(2)-C(7) | 1.36(10) |
| Os(1)-C(6) | 2.10(8) | C(3)-C(8) | 1.55(11) |
| Os(3)-C(6) | 2.24(7) | C(6)-C(7) | 1.46(11) |
| C(1)-N(1) | 1.31(10) | C(7)-N(1) | 1.38(9) |
| C(1)-S(1) | 1.71(4) | Os-CO ^b | 1.92(9) |
| C(2)-S(1) | 1.72(8) | C-O | 1.13(10) ^b |

| Angles | | | |
|-------------------|-----------------------|------------------|-----------|
| Os(1)-Os(2)-Os(3) | 60.24(11) | Os(1)-Os(2)-N(1) | 85.50(17) |
| Os(1)-Os(3)-Os(2) | 58.20(11) | C(6)-C(5)-C(4) | 120.5(7) |
| Os(2)-Os(1)-Os(3) | 61.57(12) | C(3)-C(4)-C(5) | 114.8(6) |
| Os(1)-C(6)-C(5) | 124.8(6) | C(2)-C(3)-C(8) | 112.5(6) |
| Os(3)-C(6)-C(5) | 80.3(5) | C(2)-C(3)-C(4) | 105.6(6) |
| Os(3)-C(5)-C(6) | 65.2(4) | C(1)-N(1)-C(7) | 110.6(6) |
| Os-C-O | 176.1(8) ^b | C(5)-C(6)-C(7) | 113.0(7) |

a numbers in parentheses are estimated standard deviations.

b Average values.

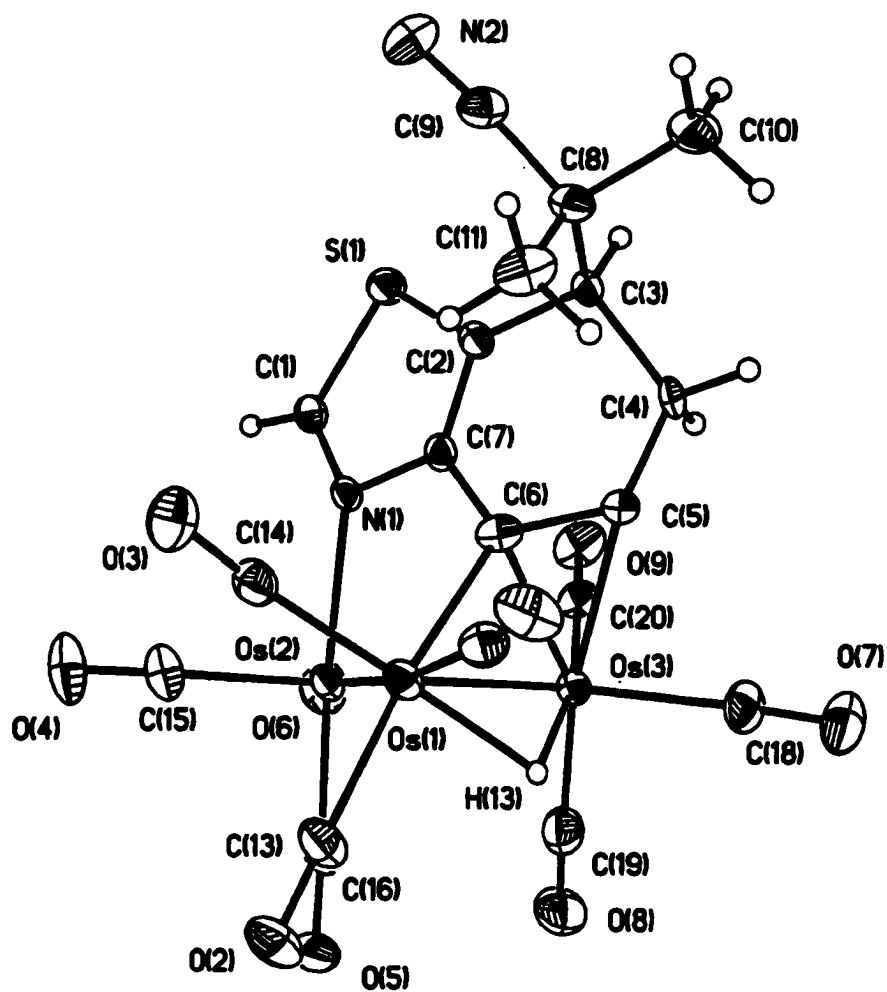
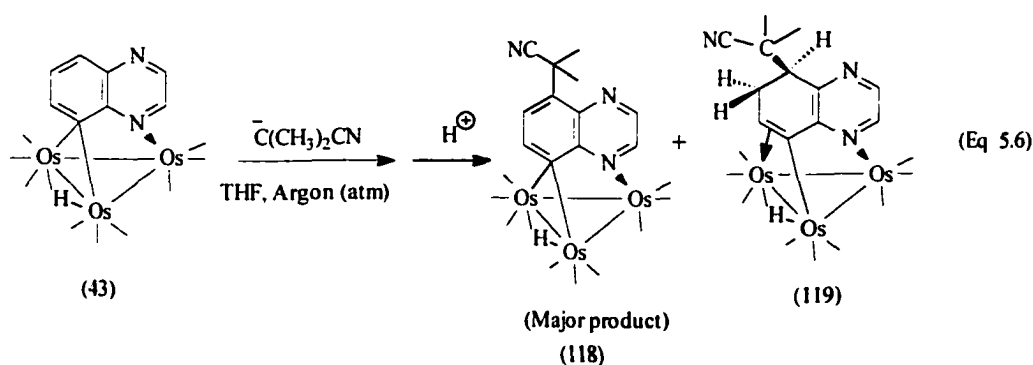


Figure 5.2 Solid state structure of $\text{Os}_3(\text{CO})_9(\mu_3\text{-}\eta^3\text{-C}_7\text{H}_5(4\text{-C}(\text{CH}_3)_2\text{CN})\text{NS})$
 ($\mu\text{-H}$) (117)

5.1.7 Reaction of Quinoxaline Complex, $\text{Os}_3(\text{CO})_9(\mu_3\text{-}\eta^2\text{-C}_8\text{H}_5\text{N}_2)$ ($\mu\text{-H}$) (43) with the Isobutyronitrile Carbanion.

The quinoxaline complex **43** underwent nucleophilic attack at the heterocyclic ring when reacted with H^- . Protonation of the anionic complex, for the most part, gave rearomatized product (starting material, scheme 4.1, chapter 4). But, with carbon based bulkier nucleophile nucleophilic attack occurs at the carbocyclic ring like that of benzothiazole complex. Thus, reaction of quinoxaline complex (**43**) with isobutyronitrile carbanion at -78°C gave rearomatized nucleophilic addition product, $\text{Os}_3(\text{CO})_9(\mu_3\text{-}\eta^2\text{-C}_8\text{H}_4\text{N}_2)(5\text{-C}(\text{CH}_3)_2\text{CN})(\mu\text{-H})$ (**118**) yield along with a small amount of $\sigma\text{-}\pi$ vinyl complex, $\text{Os}_3(\text{CO})_9(\mu_3\text{-}\eta^3\text{-C}_8\text{H}_6\text{N}_2)(5\text{-C}(\text{CH}_3)_2\text{CN})(\mu\text{-H})$ (**119**) yield as evidenced from their ^1H NMR spectra (Equation 5.6). These compounds could not be



isolated in pure form. Compounds **118** and **119** were formed in 23% and 6% yields respectively. ^1H NMR of (**118**) shows four separate doublets in the aromatic region at 9.21, 8.61, 8.55 and 7.46 ppm due to C-2, C-3, C-7 and C-6 protons. The two methyl

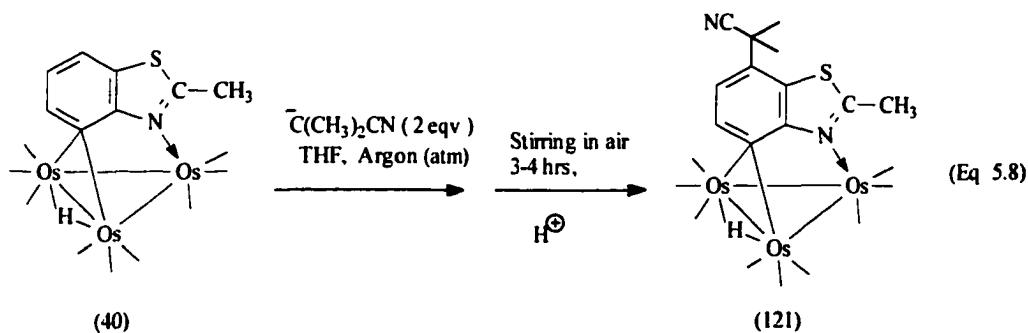
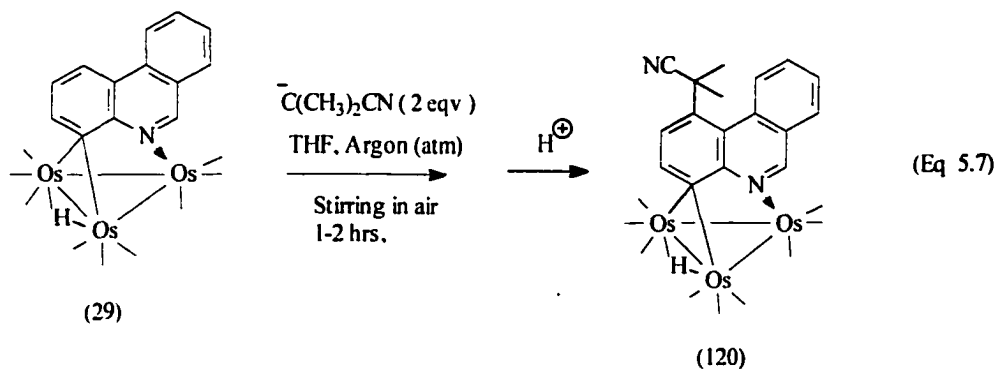
groups of isobutyronitrile side chain are appeared as a sharp singlet at 1.92 ppm and the hydride is seen at -12.32 ppm.

¹H NMR of (119) shows four multiplets in the aliphatic region at 4.06, 4.03, 2.79 and 2.45 ppm for the C-7, C-5 and C-6 protons and two doublets in the aromatic region at 8.48 and 8.21 ppm for the C-2 and C-3 protons respectively. The two methyl groups of isobutyronitrile side chain are observed as two sharp singlets at 1.43 and 1.40 ppm. The hydride is seen at -16.89 ppm.

5.2 Rearomatization of the Nucleophilic Addition Products.

Reactions of **32** and **71** with LiC(CH₃)₂CN gave green rearomatized complexes, **110** and **112** in 72% and 27% yields. Rearomatized products were also noted in the reaction of **43** and **66** with LiC(CH₃)₂CN. This similar type of rearomatization reaction with carbanion was also observed in the case of 6-methoxyquinoline complex.³ The facile oxidation (dehydrogenation) of the intermediate nucleophilic addition products arises from either the presence of a nitrogen lone pair in the heterocycle or a strongly π -electron donating group, such as 6-methoxy or an alkyl substituent in the carbocyclic ring. Rearomatization of the nucleophilic addition products of some quinoline complexes was realized either by reaction of the intermediate anion with trityl cation or DDQ/EtOH or by reaction of the σ - π vinyl complex with DBU and DDQ/EtOH.³ But the facile rearomatization of some of the nucleophilic addition products prompted us to develop a suitable method for other products. This has been achieved by stirring the

anions resulting from the addition of alkylating agent, $\text{LiC}(\text{CH}_3)_2\text{CN}$ to complexes for 1 to 2 hrs at 0°C in the air before quenching with acid. Thus, phenanthridine, 2-methylquinoxaline and 2,3-dimethylbenzimidazole complexes (**29**, **66**, and **71**) gave rearomatized products **120** [$\text{Os}_3(\text{CO})_9(\mu_3\text{-}\eta^2\text{-C}_{13}\text{H}_7(5\text{-C}(\text{CH}_3)_2\text{CN})\text{N})(\mu\text{-H})$] (Equation 5.7), **115** and **112** in 56, 42 and 71% yields respectively when isobutyronitrile carbanion was added at -78°C and the resulting anion was stirred for 1 to 2 hrs at 0°C before quenching with acid. 2-Methylbenzothiazole complex (**40**) also gave rearomatized product, $\text{Os}_3(\text{CO})_9(\mu_3\text{-}\eta^2\text{-C}_7\text{H}_2(2\text{-CH}_3)(4\text{-C}(\text{CH}_3)_2\text{CN})\text{NS})(\mu\text{-H})$ (**121**) (Equation 5.8) in 30% yield by the same method but required relatively longer hours of stirring (3 to 4 hrs). However, this method did not work for the benzothiazole complex (**39**).



5.3 Conclusions and Future work

The reactions of electron deficient benzoheterocycle complexes, $\text{Os}_3(\text{CO})_9(\mu_3\text{-}\eta^2\text{-benzoheterocycle-H})(\mu\text{-H})$ with a carbon based bulky nucleophile show that they all undergo regioselective nucleophilic attack at the C-4 (for benzothiazole, benzimidazole) or C-5 (phenanthridine, quinoxaline) position of the carbocyclic ring to give the

Table 5.3 Isolated nucleophilic addition product yields from the reaction of Benzo heterocycle complexes, $\text{Os}_3(\text{CO})_9(\mu_3\text{-}\eta^2\text{-L-H})(\mu\text{-H})$ with isobutyronitrile carbanion.

| L | σ,π -vinyl product (%) | Rearomatized product (%) |
|--|---------------------------------|--------------------------|
| Phenanthridine ^a | 79 | |
| Phenanthridine ^b | | 56 |
| 2-Methylbenzimidazole ^a | | 82 |
| 2-Methylbenzimidazole ^c | 69 | |
| 2,3-Dimethylbenzimidazole ^a | 56 | 27 |
| 2,3-Dimethylbenzimidazole ^b | | 71 |
| 2-Methylquinoxaline ^a | 62 | 4 |
| 2-Methylquinoxaline ^b | | 42 |
| 2-Methylbenzothiazole ^a | 74 | |
| 2-Methylbenzothiazole ^b | | 30 |
| Benzothiazole ^a | 84 | |
| Quinoxaline ^a | 6 | 23 |

a = anionic mixture was quenched with acid within 20 min.

b = anionic mixture on standing in the air.

c = excess carbanion was added.

nucleophilic addition products similar to those of quinoline complexes.³ Complexes without an alkyl group at the C-2 position of the heterocyclic ring underwent nucleophilic attack at the C-2 position with a small nucleophile such as hydride (Chapter 4) but with isobutyronitrile carbanion due to the steric effect attack occurs at the C-4 or C-5 position of the carbocyclic ring. The yields of the reactions of these complexes with isobutyronitrile carbanion are summarized in Table 5.3. The yields obtained for these complexes are very similar to those obtained from the reactions of quinoline complexes with a wide range of carbanions (Table 1.2, chapter 1).

It is noteworthy that some of these complexes give rearomatized nucleophilic addition products by facile air oxidation (dehydrogenation) of the intermediate anion (see Table 5.3). This facile rearomatization has also been achieved with other benzoheterocycle complexes thus, avoiding one extra step, the sequential reaction with DDQ and DBU leading to rearomatization.³

5.3.1 Cleavage of the Functionalized Benzoheterocycles from the Clusters.

In order for this synthetic method to be developed as a useful tool for the synthesis of novel benzoheterocycles, cleavage of the functionalized heterocycles from the clusters will be performed. Studies carried out in our laboratory show that quinoline, phenanthridine, and 5,6-benzoquinoline clusters undergo ligand cleavage at 70°C in acetonitrile under carbon monoxide atmosphere. Benzothiazole, benzimidazole and quinoxaline clusters require higher temperature to undergo cleavage from the clusters.^{2,53} Applying this synthetic method it should be possible to obtain free

rearomatized benzoheterocycles that are structurally novel and of interest for biomedical screening.

5.3.2 Reactions with other Carbanions.

The heterocyclic ligands of these complexes (Figure 4.1) have important biological applications.⁴⁻⁸ Modification of the ligands by adding different functionalities might bring extremely important biological applications in the design of new drugs. Considering this point we plan to interact these benzoheterocycles with other

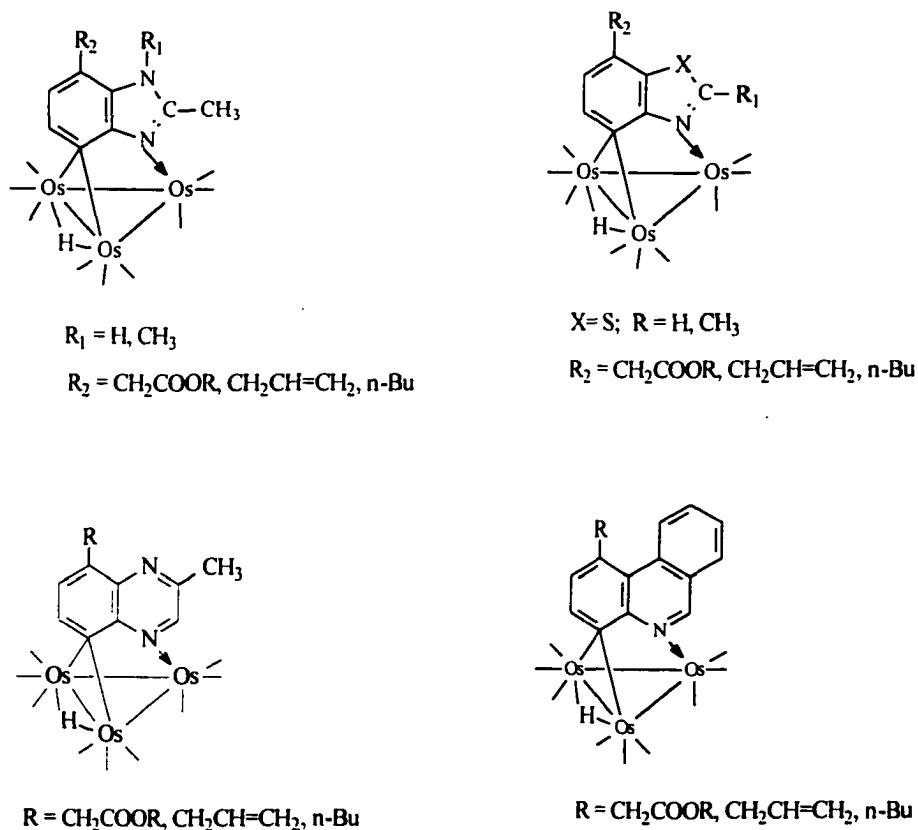


Figure 5.3

carbanions which are potentially useful for further synthetic elaboration. Thus, LiCH_2COOR , $\text{CH}_2=\text{CHCH}_2\text{MgBr}$ and Li n-Bu will be used in our developed synthetic method to make the following compounds with different functionalities which upon cleavage from the metal cluster will be used for biomedical screening (Figure 5.3).

5.4 Experimental Section

Materials and General Considerations

All reactions were carried out under an atmosphere of argon but were worked up in the air. Tetrahydrofuran was distilled from benzophenone ketyl. Methylene chloride and acetonitrile were distilled from calcium hydride.

Infrared spectra were recorded on a Thermo-Nicolet 633 FT IR Spectrometer and ^1H and ^{13}C NMR were recorded on a Varian Unity Plus 400 MHz. Elemental analyses were done by Schwarzkopf Microanalytical Labs, Woodside, New York. Chemical shifts are reported down field positive relative to Tetramethylsilane.

Trifluoroacetic acid, diisopropylamine and isobutyronitrile were purchased from Aldrich Chemical Co. The former compound was distilled from phosphorus pentoxide and the last two were distilled calcium hydride before use.

Isobutyronitrile carbanion was generated by deprotonation of its neutral precursor with lithium diisopropyl amide which was generated from diisopropyl amine and Li ⁿBu according to published procedures.¹⁰

Preparation of Isobutyronitrile Carbanion

Diisopropyl amine (0.28 mL, 2.2 mmol) was added in 15 mL THF taken in a 50 mL two-neck flask and fitted with a gas inlet tube evacuated and filled with argon. The mixture was cooled down to $-78\text{ }^{\circ}\text{C}$ and then n-BuLi in hexanes (1.60 mL, 2.1 mmol) was added to it. The reaction mixture was warmed to $0\text{ }^{\circ}\text{C}$ for 20 min., then cooled back it down to $-78\text{ }^{\circ}\text{C}$. After isobutyronitrile (0.22 mL, 2.2 mmol) was added to the cooled mixture, the solution was warmed again to $0\text{ }^{\circ}\text{C}$ for 20 min. The generated isobutyronitrile carbanion was then cooled back to $-78\text{ }^{\circ}\text{C}$ and used immediately.

Preparation of $\text{Os}_3(\text{CO})_9(\mu_3\text{-}\eta^3\text{-C}_{13}\text{H}_9(5\text{-C}(\text{CH}_3)_2\text{CN})\text{N})(\mu\text{-H})(109)$

Dark green crystals of $\text{Os}_3(\text{CO})_9(\mu_3\text{-}\eta^2\text{-C}_{13}\text{H}_8\text{N})(\mu\text{-H})(29)$ (100 mg, 0.10 mmol) was dissolved in 10 mL THF taken in a 25 mL two neck flask and fitted with a gas inlet tube evacuated and filled with argon. The solution was cooled to $-78\text{ }^{\circ}\text{C}$, at which time a 2.5 molar excess (2 mL) of the freshly prepared isobutyronitrile carbanion was added slowly by syringe. The color of the solution turned orange immediately. The reaction mixture was warmed to $0\text{ }^{\circ}\text{C}$, stirred for 20 min, cooled again to $-78\text{ }^{\circ}\text{C}$ and quenched with trifluoroacetic acid (21 μL , 0.11 mmol), a slight excess of the amount of carbanion used. At this stage, the solution changed to a light orange color as it warmed to room

temperature. The solution was then rotary evaporated and purified by thin layer chromatography on 0.1×20×20 cm silica gel plates using CH₂Cl₂/hexane (1:3) as eluent. An orange band containing the nucleophilic addition product (**109**) was obtained beneath the band of slight amount of unconsumed starting material. Isolation of the orange band gave compound **109** in a 79% yield.

Preparation of Os₃(CO)₉(μ₃-η²-C₇H₃(2-CH₃)(4-C(CH₃)₂CN)N₂)(μ-H)(110**) and Os₃(CO)₉(μ₃-η³-C₇H₅(2-CH₃)(4-C(CH₃)₂CN)N₂)(μ-H)(**111**).**

Compound **32** (100mg, 0.104 mmol) was dissolved in 10 mL dry THF and cooled to -78 °C. A two molar excess (1.8 mL, 2.3 mmol) of the freshly prepared isobutyronitrile carbanion was added slowly by syringe. The color of the solution turned orange immediately. The reaction mixture was warmed to 0 °C, stirred for 20 min, cooled again to -78 °C and quenched with 2.3 equivalent (relative to carbanion added) of trifluoroacetic acid (18 μL). After acid was added the color of the solution turned back to green. The mixture was allowed to warm to room temperature, rotary evaporated and purified by thin layer chromatography on silica gel using CH₂Cl₂/hexane (2:3) as eluent. Two bands were obtained. The isolated major green band provided a rearomatized nucleophilic addition product (**110**) in a 72% yield and the yellow orange band gave a σ-π-vinyl nucleophilic addition product (**111**) in a 16% yield.

Preparation of Os₃(CO)₉(μ₃-η²-C₇H₂(2-CH₃)(3-CH₃)(4-C(CH₃)₂CN)N₂)(μ-H)(112**) and Os₃(CO)₉(μ₃-η³-C₇H₄(2-CH₃)(3-CH₃)(4-C(CH₃)₂CN)N₂)(μ-H)(**113**).**

Green Crystals of $\text{Os}_3(\text{CO})_9(\mu_3\text{-}\eta^2\text{-C}_7\text{H}_3(2\text{-CH}_3)(3\text{-CH}_3)\text{N}_2(\mu\text{-H}))$ (**71**) (100mg, 0.10 mmol) were dissolved in 10 mL THF taken in a 25 mL two-neck flask and fitted with a gas inlet tube evacuated and filled with argon. The solution was cooled to $-78\text{ }^\circ\text{C}$ and a two molar excess of the freshly prepared isobutyronitrile carbanion (1.8 mL, 2.3 mmol) was added slowly. The color of the solution first turned amber, then orange after stirring for 15 min at $-78\text{ }^\circ\text{C}$. The solution was quenched with trifluoroacetic acid (18 μL , equivalent amount of carbanion added) and stirred for 10 min before warmed to $0\text{ }^\circ\text{C}$. The mixture was further stirred for 5 min at $0\text{ }^\circ\text{C}$ where a color change was observed from orange to yellow. The yellow solution then turned to green while standing in the air at room temperature. The reaction mixture was rotary evaporated and purified by thin layer chromatography on silica gel using CH_2Cl_2 /hexane as eluent in 2:3 ratio. Two bands were separated. The major green band gave rearomatized nucleophilic addition product (**112**) in 56% while the slower moving minor yellow band provided $\sigma\text{-}\pi$ vinyl nucleophilic addition product (**113**) in 27% yields.

Preparation of $\text{Os}_3(\text{CO})_9(\mu_3\text{-}\eta^3\text{-C}_8\text{H}_5(3\text{-CH}_3)(5\text{-C}(\text{CH}_3)_2\text{CN})\text{N}_2)(\mu\text{-H})(\text{114})$.

A solution of the carbanion of isobutyronitrile (1.8 mL, 2.3 mmol) was added dropwise to a solution of **66** (100 mg, 0.104 mmol) in dry THF (10 mL) at $-78\text{ }^\circ\text{C}$. A color change from green to dark brown was observed. The reaction solution was warmed to $0\text{ }^\circ\text{C}$, stirred for 20 min, cooled again to $-78\text{ }^\circ\text{C}$ and quenched with trifluoroacetic acid (18 μL , 2.3 mmol). The reddish reaction mixture was warmed to room temperature, rotary evaporated and purified by thin layer chromatography on

silica gel using $\text{CH}_2\text{Cl}_2/\text{hexane}$ (2:3) as eluent. One major orange band containing the nucleophilic addition product (**114**) was obtained in addition to a minor band of rearomatized product (**115**). Isolation the bands gave **114** in 62 % and **115** in 4 % yields.

Preparation of $\text{Os}_3(\text{CO})_9(\mu_3\text{-}\eta^3\text{-C}_7\text{H}_4(2\text{-CH}_3)(4\text{-C}(\text{CH}_3)_2\text{CN})\text{NS})(\mu\text{-H})$ (116**) and $\text{Os}_3(\text{CO})_9(\mu_3\text{-}\eta^3\text{-C}_7\text{H}_5(4\text{-C}(\text{CH}_3)_2\text{CN})\text{NS})(\mu\text{-H})$ (**117**).**

Compound **40** (100mg, 0.102 mmol) or Compound **39** (100mg, 0.104 mmol) was dissolved in 10 mL THF and cooled to -78°C , at which time a 2.5 molar excess of the freshly prepared isobutyronitrile carbanion (2 mL) was added slowly. The solution turned deep orange after stirring for 5 min at -78°C . The mixture was warmed to 0°C , stirred for 15 min, cooled again to -78°C and quenched with trifluoroacetic acid (20 μL , 2.5 mmol). When the color of the solution for compound **40** changed to yellow after stirring for 15 min, the mixture was allowed to warm to room temperature and rotary evaporated. The color remained unchanged for complex **39**. Purification of the crude product by thin layer chromatography on silica gel using $\text{CH}_2\text{Cl}_2/\text{hexane}$ (1:3) as eluent gave one major yellow band. Isolation of the band provided nucleophilic addition product (**116**) in a 74% yield. Crude mixture of **39** was purified by TLC using $\text{CH}_2\text{Cl}_2/\text{hexane}$ in 1:1 ratio. Isolated product (**117**) was obtained in 84% yield.

Preparation of $\text{Os}_3(\text{CO})_9(\mu_3\text{-}\eta^2\text{-C}_8\text{H}_4\text{N}_2)(5\text{-C}(\text{CH}_3)_2\text{CN})(\mu\text{-H})$ (118**) and $\text{Os}_3(\text{CO})_9(\mu_3\text{-}\eta^3\text{-C}_8\text{H}_6\text{N}_2)(5\text{-C}(\text{CH}_3)_2\text{CN})(\mu\text{-H})$ (**119**).**

Compounds (118) and (119) were synthesized by the same procedure as described for compound (114). The color of the solution turned pinked when 1.8 mL carbanion was added to 100 mg of 43 at $-78\text{ }^{\circ}\text{C}$ and again changed to purple after quenching with acid. Chromatographic separation on silica gel using $\text{CH}_2\text{Cl}_2/\text{hexane}/\text{THF}$ (6:3:1) gave two bands. The green band provided rearomatized product (118) in 23% while the orange band afforded a σ - π vinyl complex (119) in 6% yields.

X-Ray structures determination of 111 and 117

Crystals of 111 and 117 for X-ray examination were obtained from saturated solution in hexane/dichloromethane solvent system at $-10\text{ }^{\circ}\text{C}$. A suitable crystal was coated with Paratone N oil, suspended in a small fiber loop and placed in a cooled nitrogen gas stream at 100 K on a Bruker D8 SMART APEX CCD sealed tube diffractometer with graphite monochromated MoK_{α} (0.71073Å) radiation. Data were measured using a series of combinations of phi and omega scans with 10 second frame exposures and 0.3° frame widths. Data collection, indexing and initial cell refinements were all carried out using SMART³⁹ software. Frame integration and cell refinements were done using SAINT⁴⁰ software. The final cell parameters were determined from least-squares refinement on 4205 reflections. The SADABS⁴¹ program was used to carry out absorption corrections.

The structure was solved using direct methods and difference Fourier techniques (SHELXTL, V5.10).⁴² Hydrogen atoms were placed in their expected chemical positions using the HFIX command and were included in the final cycles of least squares with isotropic U_{ij} 's related to the atoms ridden upon. The C-H distances were

fixed at 0.93 Å (aromatic and amide), 0.98 Å (methane), 0.97 Å (methylene), or 0.96 Å (methyl). Hydride was positioned by using the HYDEX⁴⁶ program in the Win GX suite of programs.⁴³ All non-hydrogen atoms were refined anisotropically. Scattering factors and anomalous dispersion corrections are taken from the International table for X-ray crystallography⁵. Structure solution, refinement, graphics and generation of publications materials were performed by using SHELXTL, V5.10 software.

Analytical and spectroscopic data of complexes 109 through 121

Compound 109: Yield for **109**: 79 %. Anal Calcd. for C₂₆H₁₆N₂O₉Os₃: C, 29.16; H, 1.50; N, 2.62 %. Found: C, 29.02; H, 1.39; N, 2.54 %.

IR (ν CO) in CH₂Cl₂: 2080 m, 2049 s, 2027 s, 1992 s, br, 1967 w, br cm⁻¹ and (ν CN): 2305, s, cm⁻¹.

¹H-NMR of **109** at 400 MHz in CDCl₃: δ 9.42 (s, H(2)), 7.87(dd, 2H(9 and 12)), 7.80 (d of t, H(10)), 7.57 (d of t, H(11)), 4.08 (q, H(7)), 3.38 (d, H(5)), 2.87(m, H(6)), 2.29 (m, H(6)), 1.49(s, -CH₃), 1.45 (s, -CH₃) and -17.14 (s, hydride).

Compound 110: Yield for **110**: 72%. Anal Calcd. for C₂₁H₁₃N₃O₉Os₃: C, 24.68; H, 1.27; N, 4.11%. Found: C, 24.53; H, 1.34; N, 3.82%.

IR (ν CO) in CH₂Cl₂: 2074 m, 2047 s, 2015 s, 1988 s, br, 1944 w, br cm⁻¹ and (ν CN): 2301, s, cm⁻¹.

^1H NMR of **110** at 400 MHz in CDCl_3 : δ 9.68 (s, br, NH), 8.16 (d, H(6)), 6.82 (d, H(5)), 2.76 (s, $-\text{CH}_3$), 1.81 (s, 6H, $\text{C}(\text{CH}_3)_2\text{CN}$), -11.72 (s, hydride).

Compound **111**: Yield for **111**: 16%. Anal Calcd. for $\text{C}_{21}\text{H}_{15}\text{N}_3\text{O}_9\text{Os}_3$: C, 24.63; H, 1.47; N, 4.11%. Found: C, 24.55; H, 1.38; N, 3.92%.

IR (ν CO) in CH_2Cl_2 : 2078 m, 2054 s, 2044 s, 2020 s, 1992 m, br, 1967 w, br, 1942 w, br cm^{-1} and (ν CN): 2304, s, cm^{-1} .

^1H NMR of **111** at 400 MHz in CDCl_3 : δ 8.48 (s, br, NH), 4.46 (m, H(6)), 2.82 (m, H(4)), 2.62-2.58 (m, 2H(5)), 2.39 (s, $-\text{CH}_3$), 1.35 (s, $-\text{CH}_3$ of $\text{C}(\text{CH}_3)_2\text{CN}$), 1.25 (s, $-\text{CH}_3$ of $\text{C}(\text{CH}_3)_2\text{CN}$) and -16.58 (s, hydride).

Compound **112**: Yield for **112**: 56 %. Anal Calcd. for $\text{C}_{22}\text{H}_{15}\text{N}_3\text{O}_9\text{Os}_3$: C, 25.51; H, 1.45; N, 4.06%. Found: C, 25.28; H, 1.31; N, 4.13 %.

IR (ν CO) in CH_2Cl_2 : 2072 m, 2045 s, 2018 s, 1985 s, 1942 w, br cm^{-1} and (ν CN): 2302, s, cm^{-1} .

^1H NMR of **112** at 400 MHz in CDCl_3 : δ 8.15 (d, H(6)), 6.90 (d, H(5)), 4.29 (s, N- CH_3), 2.77 (s, C- CH_3), 1.89 (s, 6H ($\text{C}(\text{CH}_3)_2\text{CN}$)) and -11.71 (s, hydride).

Compound **113**: Yield for **113**: 27 %. Anal Calcd. for $\text{C}_{22}\text{H}_{17}\text{N}_3\text{O}_9\text{Os}_3$: C, 25.46; H, 1.64; N, 4.05%. Found: C, 25.27; H, 1.50; N, 3.96 %.

IR (ν CO) in CH_2Cl_2 : 2081m, 2044 s, 2022 s, 1986 s, br, 1953 w, br cm^{-1} and (ν CN): 2305, s, cm^{-1} .

^1H NMR of **113** at 400 MHz in CDCl_3 : δ 4.38 (dd, H(6)), 3.50 (s, N- CH_3), 2.73 (dd, H(4)), 2.68 (dd, H(5)), 2.55 (dd, H(5)), 2.36 (s, C- CH_3), 1.37 (s, CH_3 of $(\text{C}(\text{CH}_3)_2\text{CN})$), 1.29 (s, CH_3 of $(\text{C}(\text{CH}_3)_2\text{CN})$) and -16.65 (s, hydride).

Compound **114**: Yield for **114**: 62 %. Anal Calcd. for $\text{C}_{22}\text{H}_{15}\text{N}_3\text{O}_9\text{Os}_3$: C, 25.51; H, 1.45; N, 4.06 %. Found: C, 25.70; H, 1.36; N, 4.13 %.

IR (ν CO) in CH_2Cl_2 : 2079m, 2045 s, 2026 s, 1992 s, 1965w, br, 1941 w, br cm^{-1} and (ν CN): 2305, s, cm^{-1} .

^1H NMR of **114** at 400 MHz in CDCl_3 : δ 8.34 (s, H(2)), 4.06 (m, H(7)), 2.74 (m, H(5)), 2.43 (m, H(6)), 2.41 (m, H(6)), 2.38 (s, CH_3), 1.44 (s, CH_3 of $(\text{C}(\text{CH}_3)_2\text{CN})$), 1.41 (s, CH_3 of $(\text{C}(\text{CH}_3)_2\text{CN})$) and -16.88 (s, hydride).

Compound **115**: Yield for **115**: 4 %.

^1H NMR of **115** at 400 MHz in CDCl_3 : δ 9.06 (s, H(2)), 8.56 (d, H(7)), 7.44 (d, H(6)), 2.77 (s, CH_3), 1.93 (s, 6H $(\text{C}(\text{CH}_3)_2\text{CN})$), and -12.32 (s, hydride).

Compound **116**: Yield for **116**: 74 %. Anal Calcd. for $\text{C}_{21}\text{H}_{14}\text{N}_2\text{O}_9\text{SO}_3$: C, 24.23; H, 1.35; N, 2.69 %. Found: C, 24.23; H, 0.97; N, 2.48 %.

IR (ν CO) in CH_2Cl_2 : 2081m, 2057 s, 2026 s, 1990 s, 1968w, br, cm^{-1} and (ν CN): 2306, s, cm^{-1} .

^1H NMR of **116** at 400 MHz in CDCl_3 : δ 4.32 (m, H(6)), 2.83 (m, H(4)), 2.73 (m, H(5)), 2.50 (m, H(5)), 2.67 (s, CH_3), 1.36 (s, CH_3 of $(\text{C}(\text{CH}_3)_2\text{CN})$), 1.34 (s, CH_3 of $(\text{C}(\text{CH}_3)_2\text{CN})$) and -17.05 (s, hydride).

Compound 117: Yield for **117**: 84 %. Anal Calcd. for $C_{20}H_{12}N_2O_9SO_3$: C, 23.39; H, 1.17; N, 2.73 %. Found: C, 23.09; H, 0.85; N, 2.54 %.

IR (ν CO) in CH_2Cl_2 : 2080m, 2050 s, 2027 s, 1987 s, br, 1968w, br, cm^{-1} and (ν CN): 2305, s, cm^{-1} .

1H NMR of **117** at 400 MHz in $CDCl_3$: δ 8.87 (s, H(2)), 4.45 (m, H(6)), 2.93 (m, H(4)), 2.83 (m, H(5)), 2.49 (m, H(5)), 1.37 (s, CH_3 of $(C(CH_3)_2)CN$), 1.36 (s, CH_3 of $C(CH_3)_2CN$) and -16.93 (s, hydride).

Yield for 118: 23 %

1H NMR of **118** at 400 MHz in $CDCl_3$: δ 9.21 (d, H(2)), 8.61 (d, H(3)), 8.55 (d, H(7)), 7.46 (d, H(6)), 1.92 (s, 6H $(C(CH_3)_2)CN$), and -12.32 (s, hydride).

Yield for 119: 6 %

1H NMR of **119** at 400 MHz in $CDCl_3$: δ 8.48 (d, H(2)), 8.21 (d, H(3)), 4.06 (m, H(7)), 4.03 (m, H(5)), 2.79 (m, H(6)), 2.45 (m, H(6)), 1.43 (s, CH_3 of $(C(CH_3)_2)CN$), 1.40 (s, CH_3 of $C(CH_3)_2CN$) and -16.89 (s, hydride).

Yield for 120: 56 %

IR (ν CO) in CH_2Cl_2 : 2073 m, 2060 s, 2022 s, 1995s, 1961 w, 1947 w, br, cm^{-1} and (ν CN): 2302, s, cm^{-1} .

^1H NMR of **120** at 400 MHz in CDCl_3 : δ 9.88 (d, H(7)), 9.67 (s, H(2)), 8.53(d, H(6)), 7.88 (d, 2H(9 and 12)), 7.74(dd, H(10)), 7.12 (d, H(11)), 1.75 (s, 2X- CH_3) and -12.35 (s, hydride).

Yield for **121**: 30 %

IR (ν CO) in CH_2Cl_2 : 2078 m, 2055 s, 2021 s, 1996 s, 1958 w, 1942 w, br, cm^{-1} and (ν CN): 2303, s, cm^{-1} .

^1H NMR of **121** at 400 MHz in CDCl_3 : δ 8.60(d, H(6)), 7.08(d, H(5)), 3.07 (s, CH_3), 1.83 (s, 6H ($\text{C}(\text{CH}_3)_2\text{CN}$)) and 12.0 (s, hydride)

References

1. E. Rosenberg, E. Arica. Kolwaite, K.I. hardcastle, J. Ciurash. R. Duque, R.Gobetto, L. Milone, D. Osella, M. Botta, W. Dastru, A. Viale, J. Fiedler, "Mechanistic and Structural Studies of Electron Deficient Quinoline Triosmium Clusters," *Organometallics*, **1998**, *17*, 415.
2. Md. J. Abedin, B. Bergman, R Holmquist, R. Smith, E. Rosenberg, K.I. hardcastle, J. Roe, V. Vazquez, C. Roe, S. E. Kabir, B. Roy, S. Alam, K. A. Azam, R. Duque, "Electron Deficient Bonding of benzoheterocycles to Triosmium Clusters: Synthesis and Applications to Organic Chemistry," *Coord. Chem. Rev.*, **1999**, *190-192*, 975-1002.
3. B. Bergman, R Holmquist, R. Smith, E. Rosenberg, K.I. hardcastle, M. Visi, J. Ciurash. "Functionalizing Heterocycles by Electron Deficient Bonding of benzoheterocycles to Triosmium Clusters." *J. Amer. Chem. Soc.*, **1998**, *120*, 12818.
4. G. Traponi, M. Franco, A Lutrofa, G. Genchi, V. Iacobazzi, C.A. Ghiani, E. Maciocco, G. Liso, "Synthesis and Benzodiazapine Receptor Binding of Some Pyrimidobenzoxazoles and Benzimidazoles," *Eur. J. Med. Chem.*, **1997**, *32*, 83.
5. C.S. Schneider, J. Mierau, "Dopamine Autoreceptor Agonists: Resolution and Pharmacological Activity of 2,6-Diaminotetrahydrobenzothiazole and an Aminothiazole Analog of Apomorphine," *J. Med. Chem.*, **1987**, *30*, 494.

6. J.D. petke, H.K. Im, W.B. Im, D.P. Blakeman, E.J. Jacobson, B.J. Hamilton, D.B. Carter, "Characterization of Functional Interactions of Imidazoquinoxaline with Benzodiazepine- Gamma-Aminobutyric Acid A Receptors," *Mol. Pharmacol*, **1992**, *42*, 294.
7. O. Diouf, P. Depreux, D. Lesieur, J.H. Poupaert, D.H. Caignard. "Synthesis and Evaluation of New Piperazinylbenzothiazoles with High 5-HT1a and 5-HT3 Affinities," *Eur. J. Med. Chem.*, **1995**, *30*, 715.
8. R.D. Bartlett, C.S. Esslinger, C.M. Thompson, R.J. Bridges. "Substituted Quinolines as Inhibitors of L-Glutamate Transport into Synaptic Vesicles." *Neuropharmacology*, **1998**, *37*, 839.
9. A.V. Bar Din, B. Bergman, E. Rosenberg, R. Smith, W. Dastru, R.Gobetto, L. Milone, A. Viale, "The Solution Dynamics of Adduct Formation and Electronic Communication Between Ligand and Metal Core in Electron Deficient Quinoline Triosmium Clusters," *Polyhedron*, **1998**, *17*, 2975.
10. M.F. Semmelhack, G.R. Clark, D.C. Garcia, J.J. Harrison, Y. Thebtarnonth, W.A. Wuff, A.Yamashita, *Tetrahedron*, **1981**, *37*, 3957.
11. M.F. Semmelhack in, "*Comprehensive Organometallic Chemistry II*", eds. F.G.A. Stone, E. Abel, G. Wilkinson, Elsevier Science, Oxford, **1995**, *Vol. 12*, Chap. 9.1, P. 979.
12. N.F Masters, N. Mathew, G. Nechvatal, D.A. Widdowson, *Tetrahedron*, **1989**, *45*, 5955.
13. A.P. Kozikowski, K. Isobe, *J. Chem. Soc., Chem. Commun.*, **1978**, 1076
14. M.F. Semmelhack, J.L. Garcia, D. Cortes, R. Farina, R. Hong, B.K. Carpenter,

- Organometallics*, **1983**, *2*, 467.
15. L.A.P. KanMaguire, E.D. Honig, D.A.Sweigart, *Chem. Review*, **1994**, *84*, 525.
 16. S.E. Kabir, E. Rosenberg, J. Stetson, *Organometallics*, **1996**, *15*, 4473.
 17. R.H. Fish, J.J. Kim, J.L. Stewart, J.H. Busweller, R.K. Rosen, J.W. Dupon, *Organometallics*, **1986**, *5*, 2193.
 18. A. Eisenstadt, C.M. Gianomencio, M.F. Frederick, R.M., Laine, *Organometallics*, **1985**, *4*, 2033..
 19. S.E. Kabir, D.S. Kolwaite, E. Rosenberg, K.I. hardcastle, L.G. Scott, T. McPhillips, R.Duque, M.day, *Organometallics*, **1996**, *15*, 1979-1988.
 20. A. Nelson, *J. Amer. Chem. Soc.*, **1979**, 485.
 21. S.E. Kabir, D.S. Kolwaite, E. Rosenberg, K. Hardcastle, W. Cresswell, J. Grindstaff, *Organometallics*, **1995**, *14*, 3611.
 22. L.A.P. Kane.-Maguire, E.D. Honig, D.A. Sweigart, *Chem. Rev.*, **1994**, *84*, 525.
 23. (a) L.A. Bromley, S.G. Davies, C.L. Goodfellow, *Tet. Asymmetry*, **1991**, *2*, 139.
(b) S.G. Davies, T.J. Donohoe, M.A, Lister, *Tet. Asymmetry*, **1991**, *2*, 1089.
 24. M.F. Semmelhack, G.R. Clark, D.C. Garcia, J.J. Harrison, Y. Thebtarnonth, W.A. Wuff, A. Yamashita, *Tetrahedron*, **1981** *37*, 3957.
 25. S. Shouheng, L.K. Yeung, D.A. Sweigart, T.Y. Lee, S.S. Lee, Y.K. Chung, S.R. Switzer, R.D. Pike, *Organometallics*, **1995**, *14*, 2613.
 26. U.S. Gill, R.M. Moriarty, Y.Y. Ku, I.R. Butler, *J. Organometal. Chem.*, **1991**, *417*, 313.
 27. R.H. Fish, E. Baralt, H.S. Kim, *Organometallics*, **1991**, *10*, 1965.

28. J.A. Gladysz, G.A. Stark, A.M. Arif, *Organometallics*, **1994**, *13*, 4523.
29. G. Jones, "Quinolines" ed. Wiley Interscience, London (1977).
30. M.F. Semmelhack in, "Comprehensive Organometallic Chemistry II, eds. F.G.A. Stone, E. Abel, G. Wilkinson, Elsevier Science, Oxford, 1995, Vol. 12, Chap. 9.1, p981.
31. R. Smith, E. Rosenberg, K. I. Hardcastle, V. Vazquez, J. Roh, *Organometallics* **1999**, *18*, 3519.
32. F.A. Bovey, "NMR Data Tables for Organic Chemists," Wiley Interscience, New York, 1967.
33. J.P. Coleman, L.S. Hegedus, J.R. Norton, R.G. Fink, "Principles and Applications of Organotransition Metal Chemistry", University Science Books, Mill Valley, Ca, 1987, Chap 3, p96.
34. T. W. Green, P.G.M. Wuts, "Protective Group in Organic Synthesis," 2nd ed., Wiley Interscience, New York, (1991), P. 10, P. 227, P. 335.
35. Uhle, Jacobs, *J. Org. Chem.*, *10*, **1945**, 76, 82.
36. Sang Sup Jew, Jang IK Lee, Young sang Cho, Chae Ho Cook, *Soul Taehakkyo Yakhak Nonmunjip* **1986**, *11*, 67-9(Korean).
37. J. Lewis, P.J. Dyson, B.J. Alexander, B.F.G. Johnson, C.M. Martin, J.G.M. Nairn, E. Parsini, *J. Chem. Soc., Dalton Trans.*, **1993**, 981.
38. Michael C. Venuti, Brad E. Loe, Gordon H. Jones and John M. Young, "Topical Nonsteroidal Antipsoriatic Agent: 2,3-(Alkylidenedioxy) naphthalene Analogues of Lonapalene", *J. Med. Chem.*, 1988. **31**, 2132-36.
39. SMART Version 5.624, **2000**, Bruker AXS Inc. Analytical X-ray Systems, 5645 East

- Cheryl Parkway, Madison, WI 53711-5373.
40. SAINT version 6.02, **1999**, Bruker AXS Inc. Analytical X-ray Systems, 5645 East Cheryl Parkway, Madison, WI 53711-5373.
 41. SADABS version 2.03, **2001** George Sheldrick, University of Göttingen.
 42. SHELXTL V5.10, **2000**, Bruker AXS Inc. Analytical X-ray Systems, 5645 East Cheryl Parkway, Madison, WI 53711-5373.
 43. A. J. C. Wilson (ed), *International Tables of X-ray Crystallography, Volume C*, Kynoch, Academic Publishers, Dordrecht, **1992**, Tables 6.1.1.4 (pp 500-5020 and 4.2.6.8 (pp 219-222).
 44. E. Rosenberg, S.E. Kabir, K. I. Hardcastle, M. Day, E. Wolf, T. McPhillips, *Organometallics*, **1995**, *14*, 721.
 45. Rosenberg, E.; Kabir, S.E.; Hardcastle, K. I; Gobetto, R.; Milone, L.; Osella, D.; *Organometallics*, **1991**, *10*, 3550.
 46. A. G. Orpen, *J. Chem. Soc. Dalton Trans* **1980**, 2509
 47. E. Rosenberg, K.I. Hardcastle, S.E. Kabir, L. Milone, R. Gobetto, M. Botta, Nishimura, M. Yin *Organometallics*, **1995**, *14*, 3068.
 48. E. Rosenberg, S.E. Kabir, M. Day, K.I. Hardcastle, *Organometallics* **1994**, *13*, 4437.
 49. (a) A.R. Katritzky, A.J. Boulton, "Adv. Heterocycle chem.,"(1978), **22**, p.385.
(b) G. W.H. Cheeseman, "Adv. Heterocycle chem.," (1963), **2**, p.203.
(c) CA, **34**, 323⁶
(d) CA, **49**, 754
(e) CA, **47**, 4626c
(f) CA, **47**, 12366b

- (g) CA, **49**, 12449i
(h) N.G. Gaylord, *J. Amer. Chem. Soc.*, **1954**, *76*, 285.
50. (a) N.O.Cappel and W.C. Fernelius, *J. Org. Chem.*, **1940**, *5*, 40.
(b) F.R. Benson and W.L. Savell, *Chem. Revs.*, **1950**, *46*, 59.
(c) A.R. Katritzky, A.J. Boulton, "Adv. Heterocycle chem.,"(1971), *13*, p.390
(d) G. A. Russell and S.A. Weiner, *J. Org. Chem.*, **1966**, *31*, 248.
(e) H.Gilman and J. Eisch, *J. Amer. Chem. Soc.*, **1957**, *79*, 4423.
51. J.B. Keister, V. Frey, D. Zbinden, A.E. Merbach, *Organometallics* **1991**, *10*,
and references therein.
52. A.D. Clauss, M. Tachikawa, J.R. Shapely, C.G. Pierpont, *Inorg. Chem.*, **1981**, *20*,
1528.
53. Dalia Rokhsana, Edward Rosenberg, "Cleavage of the Functionalized
Benzoheterocycles from the Clusters", to be published.